50

INTERRUPTION OF SMALL INDUCTIVE CURRENTS

Working Group 13.02

Edited by S. Berneryd

December 1995

INTERRUPTION OF SMALL INDUCTIVE CURRENTS

Working Group 13.02

December 1995

CIGRE WG 13.02

INTERRUPTION

of

SMALL INDUCTIVE CURRENTS

Convener S. Berneryd (Sweden)

List of members

All Chapters:

D. Boyle (UK)
E. Colombo (Italy)
R.H. Harner (USA)
W.M.C. van den Heuvel (Netherlands)
M. Karttunen (Finland), Secretary
B.C. Papadias (Greece)
A.T. Roguski (Poland)
N.V. Shilin (USSR)
D.K. Sweeting (Australia)
S. Tominaga (Japan)

Part of the Chapters:

G. Bernard (France)
D. Birthwhistle (Australia)
A. Caccia Dominioni (Italy)
K. Fröhlich (Switzerland)
G. Gröber (Germany)
E. Hoffman (Germany)
H. Huber (Switzerland)
R. Jeanjean (France)
T. Laubst (Denmark)
J. Marty (Switzerland)
A. Mendés (France)
S. A. Morais (Brazil)
W. Onu (Romania)
J. Panek (USA)
V. Zajic (Canada)

Table of contents

INTERRUPTION
of
SMALL INDUCTIVE CURRENTS

prepared by
Working Group 13.02

edited by
S Berneryd

presented at the request of
Chairman of Study Committee 13
H. H. Schramm

PREFACE

CIGRE Working Group 13.02, Interruption of small inductive currents, was set up by Study Committee No. 13 in 1974. A reason to create a new Working Group was IEC's request given to CIGRE to give grounds for preparing an IEC-specification in the matter.

The WG 13.02 had the following subjects in its scope:

- study the behaviour of the switching device and its influence on overvoltages
- collect information about actual conditions
- study influence on the switching overvoltages of the load and source side networks
- propose substitute laboratory circuits for carrying out small inductive current switching tests.

The WG 13.02 has prepared a report containing Chapters on switching of high-voltage motors, no-load transformers, reactors and reactor-loaded transformers which have been published in Electra No. 72 to No. 138. Based on this IEC has issued the Technical Report IEC 1233 with test recommendations.

This brochure contains the Electra articles prepared by WG 13.02 and it aims at presenting the theoretical background to IEC 1233. The test circuits and test procedures prescribed in the IEC report differ somewhat from those proposed by 13.02. Since they are in principle equivalent, the IEC proposals have been adopted in this brochure. Also when new experience has been available, this brochure has taken this into account.

Chapter 1.

INTRODUCTION

The switching operations taking place in a network are numerous and of different kinds. They occur with manual switching during normal operation of the network as well as with automatic switching upon earth faults or short-circuits. Only a few of these switching operations cause high overvoltages.

The overvoltages arising from switching operations are not critical to a system as long as they do not surpass or approach the switching impulse withstand voltage (SIWL) of the equipment in the system. The critical value of the switching overvoltage thus depends on the SIWL which can be chosen from several values (IEC Publication 71-1). This choice is of economic importance, as the price of high voltage equipment is strongly influenced by the withstand voltage specified. This applies to the dielectric strength against atmospheric overvoltages as well as against switching overvoltages. In overhead systems where switching overvoltages as well as lightning overvoltages occur, these relations are interconnected. With medium voltages and particularly with motor insulation other considerations may be involved. The art of insulation coordination is used to find the optimal solution between the different overvoltage levels and the different withstand voltages of the equipment.

Usually the necessary dielectric strength of the equipment against atmospheric overvoltages, the lightning impulse withstand voltage, is determined by the protection level of the overvoltage protective device used. The protection level of the device is to a certain degree tied to the operating voltage of the system. The lightning impulse withstand voltage of the equipment is related to the switching impulse withstand voltage of the equipment.

So the choice of switching impulse withstand voltage also lies in a given range. If the switching overvoltages to be expected in a system are higher than the withstand level of the equipment, they have either to be reduced by surge arresters or other protective devices to values below this level or their development has to be limited to values below this level by modifying the switching operation (e.g. using breaking resistors), or the switching impulse withstand level of equipment has to be raised. The last method becomes very expensive especially at higher voltages. The first method, the reduction of overvoltages by protective devices, cannot for the time being be applied at all places, at any time and frequency. Thus the insulation coordination often requires that the switching overvoltages are kept below a certain level by limiting their development.

The interruption of small inductive currents is one of the switching operations which may lead to switching overvoltages. This operation takes place in switching off reactors, unloaded or reactor loaded transformers and motors. The current interrupted is small compared to the normal fault current of the system, it comprises the magnetizing current of transformers, the nominal current of reactors and the starting and the no-load current of motors. This operation is widely used at all voltage levels and can therefore be of economic importance.

Chapter 2

DEFINITIONS AND PHYSICAL PHENOMENA AT INTERRUPTION OF SMALL INDUCTIVE CURRENTS

2.1. General

The creation of overvoltages at switching of small inductive currents is complicated. It is not just the sudden forcing of a current to zero thereby releasing the energy in the load inductance that is important. The limited dielectric strength of the circuit-breaker contact gap, the ability of the circuit-breaker to interrupt high-frequency currents, the transfer of transients between phases - all these factors play an important role in the ultimate creation of the overvoltages. As a matter of fact even circuit-breakers with practically no current chopping tendency may create dangerous overvoltages.

The aim of this chapter is to clarify the picture and describe in some detail the physical phenomena involved. The arc model presented cannot explain all observations in connection with current chopping, but is regarded as the best available model. The behaviour of a multi-unit circuit-breaker is not fully understood -two theories giving different results are presented. They may give an estimated range of overvoltages for multi-unit circuit-breaker when the behaviour of one unit is known.

2.2. Definitions

For the purpose of this report the definitions of IEC 56 will apply. This holds in particular for the terms IEC 56 number:

3.105.46: re-ignition
3.105.47: restrike
3.105.12: breaking capacity
3.105.19: short-circuit breaking capacity
3.105.18: short-circuit making capacity
3.105.48: normal current
3.105.23: recovery voltage
3.105.24: transient recovery voltage
3.105.25: prospective transient recovery voltage (of a circuit and with respect to circuit-breaker)
3.101.19: power factor (of a circuit).

As an exception to this the definition of the term "overvoltage" will be taken from IEC 71-1 (1976) number 18 instead of IEC 56 number 3.101.13

The following additional definitions will apply in this report:

2.2.1. **Inductive current**: power-frequency current through a circuit-breaker drawn by an inductive circuit having a power factor 0.5 or less.

2.2.2. **Small inductive current**: inductive current having a steady state value considerably less than the rated short-circuit breaking current.

2.2.3. **Arc instability**: any abrupt change in the conductivity of the gas discharge between the contacts of a circuit-breaker, occurring away from the natural zero in the current loop and having its origin in the discharge characteristics and/or the quenching medium. (Arc instability may appear as a discontinuity and/or a high-frequency oscillation in the voltage across and/or in the current through the circuit-breaker).

2.2.4. **Instability oscillation**: arc instability appearing in the discharge current as a high-frequency oscillation with an increasing amplitude during at least a part of the oscillation.

2.2.5. **Current chopping**: an abrupt current interruption in the circuit-breaker away from the natural power-frequency current zero of the circuit connected to the circuit-breaker. (Current chopping may be originated by arc instability or by transients in the circuitry. The current interruption can be incomplete due to post arc conductivity).

2.2.6. **True current chopping**: current chopping originated by arc instability in the circuit-breaker discharge.

2.2.7. **Virtual current chopping**: current chopping originated by transients in (parts of) the circuit. (The transients may be originated by the previous history of the switching process and/or by reignition in another pole of the same circuit-breaker).

2.2.8. **Chopping current**: instantaneous value of the power-frequency current through the interrupting pole of the circuit-breaker at the moment of current chopping. This current may be different compared with the current through the main inductance.

2.2.9. **Chopping level**: maximum recorded value of the chopping current due to true current chopping in a specific circuit under rated voltage and normal operating ,D]d.

2.2.10. **First parallel oscillation**: oscillation occurring in the current through the circuit-breaker immediately after a reignition and having its energy sources in the capacitances of the direct vicinity of the circuit-breaker.

The frequency of the first parallel oscillation is in the Mhz-region. The discharge is a transient to a new (quasi) steady state or a new current zero. The capacitances involved are the inherent "stray" capacitances of the circuit-breaker pole and the few meters of conductors connected. The first parallel oscillation can only develop when a rapid transition from zero current to a low resistance gas discharge is possible and therefore often does not appear during a thermal reignition but rather during a dielectric breakdown. If occurring, the oscillation may be strongly damped by the transient discharge itself.

This oscillation can only be recorded by advanced measuring techniques but, due to a relatively high first current peak, it may disturb the recording of the succeeding lower frequency phenomena e.g. by zero line shifting in the cathode ray oscillograph.

2.2.11. **Second parallel oscillation**: oscillation in the current occurring after a reignition and having its energy sources in the capacitances of the supply side and load side networks connected to the circuit-breaker pole terminals.
The frequency of the second parallel oscillation is generally much lower than that of the first parallel oscillation. But the lumped inductances of the main circuit, such as transformer, reactor and generator coils, are not substantially involved in this phenomenon. This discharge has a (quasi) steady state character.

2.2.12. **Main circuit oscillation**: oscillation induced by one or more arc voltage discontinuities or reignitions and having its energy sources in the generators, capacitances and lumped inductances of the supply side and load side networks.
The frequency of the main circuit oscillation is generally much lower than that of the second parallel oscillation.

Note: Parallel oscillations and main circuit oscillation can be seen as current transients which may successively follow after a breakdown in the period between current zero and a new power-frequency current flow. The oscillations are often multi-frequency. They often cause current zeros and may consequently originate virtual current chopping.

2.2.13. **Supply side (or source side) oscillation**: oscillation of the supply side part of the main circuit after current chopping or natural current zero.

2.2.14. **Load side oscillation**: oscillation of the interrupted load side network after current chopping or natural current zero.

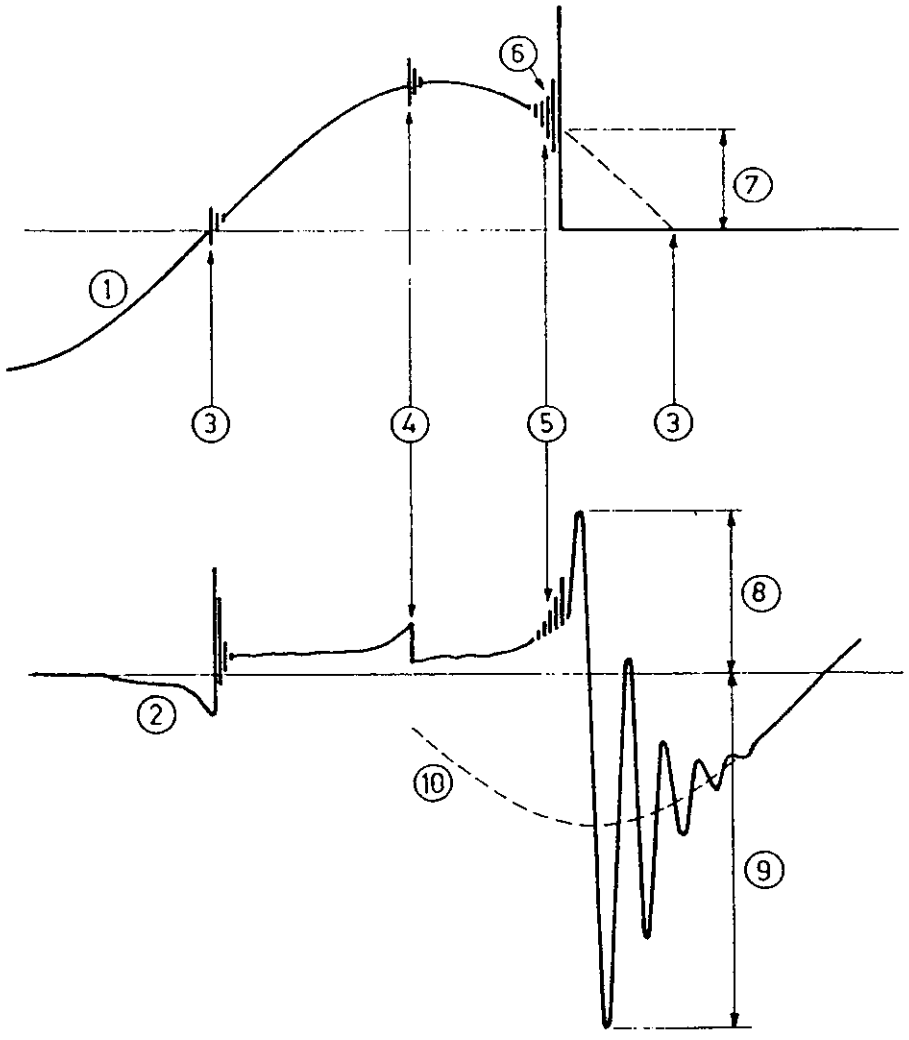

Figure 2.2.1 Definitions

1 current through circuit-breaker
2 voltage across circuit-breaker (u_a)
3 natural power frequency current zero
4 example of arc instability not leading to current chopping
5 example of arc instability leading to true current chopping
6 instability oscillation
7 chopping current (i_{ch})
8 suppression peak
9 recovery peak
10 supply voltage

2.2.15. Suppression peak: maximum in the transient voltage across the circuit-breaker, having the same polarity as the previous arc voltage and occurring before definite polarity change of the recovery voltage.

2.2.16 Recovery peak: maximum in the voltage across the circuit-breaker having a polarity opposite to the previous arc voltage polarity and occurring after definite polarity change of the recovery voltage.

Note: Suppression peak and recovery peak are not necessarily the absolute maxima in the transient recovery voltage. Previous breakdowns may have appeared at higher voltage values.

2.2.17. Voltage escalation: Increase in the amplitude of the prospective recovery voltage of the load circuit, produced by the accumulation of energy due to repeated reignitions.

Figure 2.2.1 shows current and voltages at an interruption and illustrates the definitions.

2.3. Phenomena of current chopping

2.3.1. Introduction

At interruption of small inductive currents, practically all circuit-breaker types will force the current to zero, "chop", at a time other than the natural current zero. For vacuum circuit-breakers the chopping is largely associated with instability of the last cathode spot, while for other circuit-breaker types, oil, air-blast and SF_6, current chopping is generally the result of an unstable interaction between the circuit-breaker arc and the circuit.

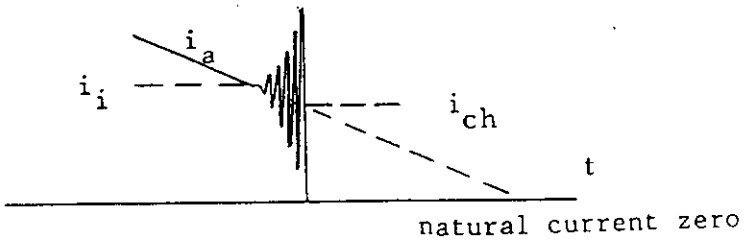

FIGURE 2.3.1 Schematic diagram of current chopping
i_a arc current
i_{ch} chopping current
i_i instability current

A typical current shape in this case is shown in Figure 2.3.1. From a certain current level i_i an instability oscillation develops, which leads to chopping at the (power frequency) current value i_{ch}. The frequency is usually so high (of the order of 100 kHz) and the amplitude of the oscillation rises so rapidly that the chopping can be regarded as instantaneous.

2.3.2. Theoretical model

The interaction between network and interrupter arc which leads to instability and current chopping was described by Rizk [1], who based his work on Mayr's arc model [2] and also on work by Weizel and Rompe [3] and Nöske [4]. The simplified model according to Rizk is presented below as it seems to explain the phenomena acceptably. More comprehensive theories exist, however [5], [6].

Assume a static characteristic of the circuit-breaker arc.

$$u_a i_a^{\alpha} = \eta \qquad (2.3.1)$$

where u_a is the arc voltage, i_a the arc current, α and η constants. The equation applies for d.c. and also for power-frequency current, while rapid current changes introduce deviations due to the thermal inertia of the arc. After a small deviation a new stationary condition is assumed to be approached exponentially with a time constant Θ. For such small deviations the arc can be replaced by the equivalent circuit shown in Figure 2.3.2.

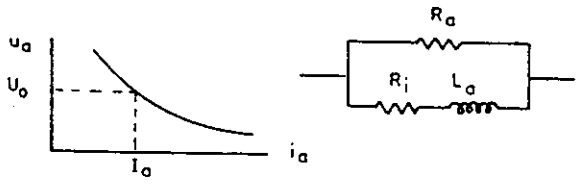

Figure 2.3.2
Arc characteristics and Rizk's equivalent circuit for small current deviations from steady state

In the equivalent circuit R_a is the static arc resistance at the current I_a prior to the disturbance.

$$R_a = \frac{U_a}{I_a} \qquad (2.3.2)$$

R_i and L_a are defined as

$$R_i = \frac{-\alpha R_a}{1+\alpha} \qquad (2.3.3)$$

$$L_a = \frac{\theta R_a}{1+\alpha} \qquad (2.3.4)$$

When considering interruption of small inductive currents the simplified equivalent circuit shown in Fig. 2.3.3. used by Baltensperger [7], [8] may be applied as a first approximation.

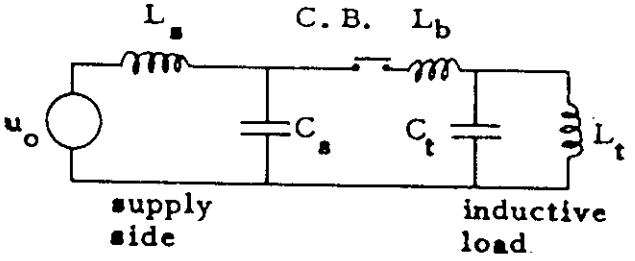

u_o = supply voltage (peak value)
L_s = supply inductance
L_t = load inductance
C_s = supply capacitance
C_t = load capacitance
L_b = stray inductance

FIGURE 2.3.3 Simplified single-phase equivalent circuit

The inductances L_s and L_t are large enough to prevent any rapid current changes, and therefore the external circuit, which interacts with the arc resulting in chopping of the current, is approximately a parallel capacitance C, equal to C_s and C_t in series. In many cases C_s is considerably larger than C_t, making C approximately equal to C_t.

Figure 2.3.4. shows the resulting circuit which determines the instability limit. The stray inductance L_b has been neglected.

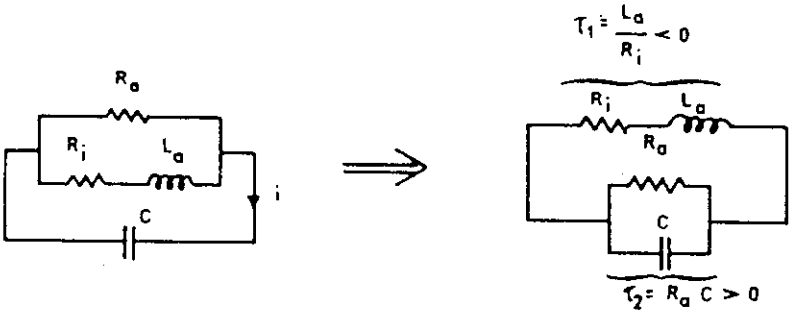

FIGURE 2.3.4 Circuit for determination of the instability limits of the arc

The differential equation for the current i (= the deviation from the steady state arc current I_a) in this circuit is

$$\frac{d^2i}{dt^2} + \left(\frac{1}{\tau_1}+\frac{1}{\tau_2}\right)\frac{di}{dt} + \omega_o^2 i = 0 \qquad (2.3.5)$$

with

$$\tau_1 = L_a/R_i; \quad \tau_2 = R_a C; \quad \omega_o^2 = \frac{R_a + R_i}{R_a} \cdot \frac{1}{L_a C} \qquad (2.3.6)$$

The solution is

$$i(t) = \hat{i} e^{-t/\tau} \cdot \cos(\omega_i t + \phi) \qquad (2.3.7)$$

with

$$1/\tau = \frac{1}{2}(1/\tau_1 + 1/\tau_2); \quad \omega_i = \sqrt{(\omega_o^2 - 1/\tau^2)} \qquad (2.3.8)$$

ϕ is the phase angle and $\hat{i}$ is the current amplitude, both depending on initial conditions.

If $1/\tau_1 + 1/\tau_2 < 0$, the damping factor $1/\tau$ is negative. This means that a current amplitude will increase

$$\alpha R_a > \theta \qquad (2.3.9)$$

with time instead of damp out. This is the case for
The angular frequency ω_i corresponding to the instability limit is found from $1/\tau = 0$, i.e. $\omega_i = \omega_0$ and with the help of Eqs. (2.3.6), (2.3.3) and (2.3.4).

$$\omega_i = \frac{\sqrt{\alpha}}{\theta} \qquad (2.3.10)$$

Thus, when interrupting a small inductive current, the circuit will become unstable when the arc resistance has reached such a value that Eq. (2.3.9) is fulfilled. Equations (2.3.1) and (2.3.2) yield

$$R_a = \eta I_a^{-(\alpha+1)} \qquad (2.3.11)$$

Equations (2.3.9) and (2.3.11) together determine the current value i_i at which the instability oscillation will start. From test results so far published or otherwise known, it seems that in most cases the instability oscillation develops so rapidly that there are only moderate differences between the actual values of i_i and the chopping current i_{ch}. For instance, it was found in [9] that the ratio i_i/i_{ch} for an air-blast circuit-breaker was in most cases between 1.4 and 1.0. The chopping current i_{ch} is thus approximately

$$i_{ch}^{\alpha+1} = \frac{\alpha \eta C}{\theta} \qquad (2.3.12)$$

Experiments, [1, 9...13], have shown that for both air-blast, oil and SF_6 circuit-breakers the chopping current is approximately proportional to the square root of the capacitance C across the circuit-breaker terminals provided that the stray inductance (L_b in Figure 2.3.3) is low.

$$i_{ch} \sim \sqrt{C} \qquad (2.3.13)$$

With large values of L_b there are indications that a linear relationship, $i_c \sim C$, may be approached [9].

It may be seen from Eq. (2.3.12) that the theory is in accordance with the experimental results in the special case of $\alpha = 1$. This case was in fact suggested by Mayr [2]. With $\alpha = 1$ Equation (2.3.12) simplifies to

$$i_{ch} = \sqrt{\frac{\eta C}{\theta}} \qquad (2.3.14)$$

In addition to using the model described above it is possible, by means of computer, to simulate current chopping by direct use of a dynamic arc model. Mayr's model [2] with constant arc parameters may be used, but better results are obtained with an arc model with variable parameters [14]. With such a model, used together with an appropriate circuit, instability oscillations and current chopping are obtained which are in good accordance with real test recordings. Further experimental results, e.g. the dependence of i_{ch} on $\sqrt{C}$ (Equation (2.3.13)) may also be reproduced [5].

The characteristic value $i_{ch}/\sqrt{C}$ is called "the chopping number", λ.
Typical values of $\lambda = i_{ch}/\sqrt{C}$ for single unit circuit-breakers are (with i_{ch} in Amperes, C in Farads)

oil-minimum	(7...10) x 10^4
SF_6	(4...17) x 10^4
air-blast	(15..20) x 10^4

Thus, with a load capacitance C = 10 nF, the mean values of the chopping currents of the various circuit-breaker types will typically be from 4 to 20 A.

The behaviour of the vacuum circuit-breaker differs from the others in that the chopping occurs instantaneously without any instability oscillations although other types of oscillation may sometimes be observed [15, 16]. The chopping current is to a high degree determined by the contact material and is typically 2...10 A for circuit-breakers and may be as low as 0.1 A for vacuum contactors. It is fairly independent of the circuit parameters, but a slight increase with parallel capacitance has been observed [17, 18].

2.3.3. Overvoltage generated

The current chopping results in overvoltages in the circuit. As long as the chopping level of the circuit-breaker is higher than the peak value of the breaking current, the latter, of course, determines the maximum current that can be chopped. When the peak value of the breaking current exceeds the chopping level, the chopping current is fairly independent of the breaking current [19, 20].

The overvoltage factor of the inductive load in a single phase circuit is mainly determined by the chopping current i_{ch}, the capacitance C_t and inductance L_t of the load.

Figure 2.3.5 b shows the most frequent case with current chopping before the natural current zero. The voltage across the load increases to a first maximum, the suppression peak, with amplitude u_m, and thereafter oscillates with a frequency given by the circuit data (typically 0.5 to 10 kHz). The overvoltage is caused by the release of the magnetic energy stored in the load inductance at the moment of current chopping. It is usually fully justified to regard the current chopping as an instantaneous current step. Only if the forcing to zero takes place during more than a quarter of a cycle of the natural frequency of the load, will there be any noticeable decrease in overvoltage amplitude [21].

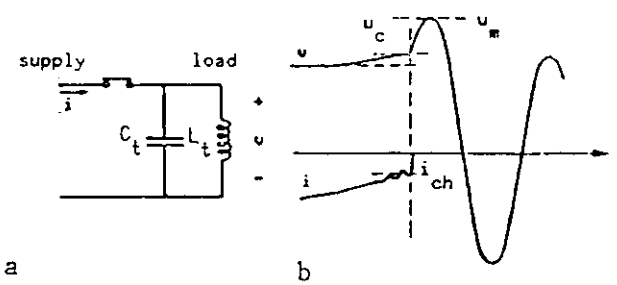

FIGURE 2.3.5
Overvoltages at current chopping

a - equivalent circuit
b - chopping before natural current-zero

As the stored magnetic energy, e.g. in case of a no-load transformer, is not always fully converted into electrostatic energy it is convenient to introduce the magnetic efficiency, η_m, defined as the ratio

between the magnetic energy gained from the load during demagnetization to the magnetic energy applied during magnetization [22]. It must, however, be understood that η_m is not a constant but depends in a complex way on the following factors [23]:

- non-linearity of the magnetic material
- degree of magnetization
- natural frequency of load circuit

With the definitions above the following relationship applies:

$$\frac{1}{2} C_t u_m^2 = \frac{1}{2} C_t u_c^2 + \frac{1}{2} L_t i_{ch}^2 \eta_m \qquad (2.3.15)$$

As the inductance L_t the high-frequency inductance should, strictly, be used but several investigations have shown that for reactors the high frequency inductance only differs from the power-frequency inductance by a few percent. In case where a true inductance value does not exist, as for no-load transformers, L_t should be regarded as an equivalent inductance of the load, the value of which makes $1/2\ L_t i_{ch}^2$ equal to the energy applied during magnetization.

In Eq. (2.3.15) losses have not been taken into account. This is a considerable approximation but may, however, be justified, as the influence on the peak value, u_m, of the suppression peak can be assumed to be fairly small.

With

$$k_a = \frac{u_m}{u_o} \qquad (2.3.16)$$

$$k_c = \frac{u_c}{u_o} \qquad (2.3.17)$$

where u_0 is the peak value of the power-frequency voltages. Equation (2.3.15) may be transformed to

$$k_a = \sqrt{k_c^2 + \left(\frac{i_{ch}}{u_o}\right)^2 \cdot \frac{L_t}{C_t} \eta_m} \qquad (2.3.18)$$

If the current chopping occurs at a moment when the supply voltage is close to its maximum, which is normally the case when critical cases are studied (chopping level is considerably lower than breaking current peak value) and if further the arc voltage is neglected (which is almost always justifiable) then u_c is close to u_0 and $k_c \approx 1$. Eq. (2.3.18) then simplifies to

$$k_a = \sqrt{1 + \left(\frac{i_{ch}}{u_o}\right)^2 \cdot \frac{L_t}{C_t} \eta_m} \qquad (2.3.19)$$

The value of η_m is close to unity in case of motors, reactors and reactor-loaded transformers, while modern no-load transformers have η_m of the order 0.2 to 0.5. This reduces considerably the overvoltages at steady state magnetizing current chopping [23]. At interruption of magnetizing inrush currents the value of η_m is larger and somewhat higher overvoltages may be generated.

Three phase loads make conditions more complicated. The following cases may be distinguished:

A. Earthed neutral on the supply and load side with no mutual inductance between phases on the load side. The above equations apply to each of the three phases in turn.

B. Earthed neutral on the supply and load side with mutual inductance between phases on the load side. In this case power frequency voltage in the first and second phases to clear might not be zero after interruption. Figure 2.3.6 shows an equivalent scheme which can be used in this case, for each of the three phases in turn.

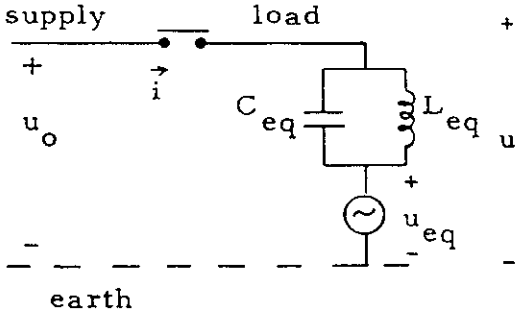

FIGURE 2.3.6
Equivalent network to be used for phases in case of loads with mutual inductance between phases and/or unearthed neutral

In Figure 2.3.6 u_{eq} is the remaining power frequency voltage in the phase after interruption, while L_{eq} and C_{eq} are equivalent inductance and capacitance values of that phase. u_{eq} might be estimated from the positive, negative and zero sequence impedances of the network, or determined from test oscillograms. L_{eq} might also be approximated from

$$L_{eq} = \frac{|\overline{U_o} - \overline{U_{eq}}|}{\omega I}$$

where
U_o supply voltage phasor
U_{eq} phasor of u^{eq}
I phase current before interruption
ω power angular frequency

C_{eq} may be obtained from the oscillation of the load after interruption.

Figure 2.3.7 shows an example of interruption in a phase with remaining voltage, and also indicates how the definitions of suppression peak voltage u_m and the initial voltage must be modified. Note that u_ℓ, the momentary value of u_{eq} at interruption, may be either positive or negative.

With the generalized definitions of u_m and u_c (or k_a and k_c) and by use of proper values of L_{eq} and C_{eq} instead of L_1 and C_1 equations 2.3.15 and 2.3.18 may still be used. Since k_c will no longer necessarily be close to unity, equation 2.3.19, on the other hand, cannot be applied.

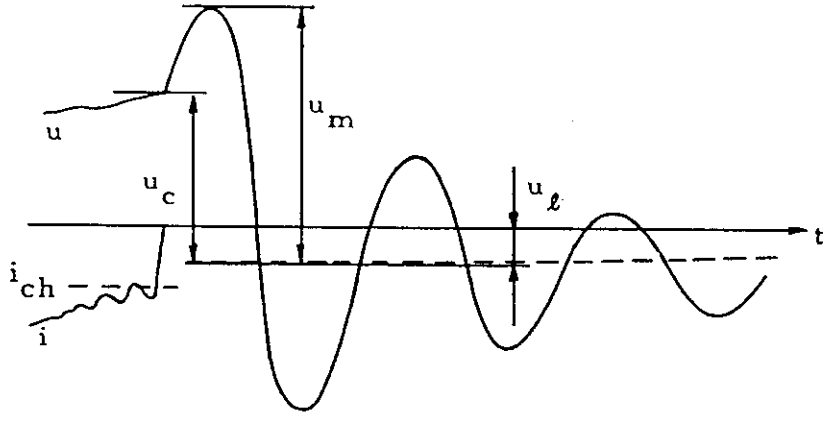

FIGURE 2.3.7
Example of interruption in phase with remaining voltage.

C. Unearthed neutral on the load side. The load will in principle behave as in case B and the same equations apply. The last two phases will clear simultaneously. If there is no mutual inductance between phases, and the supply side neutral is earthed, u_{eq} of the first phase to clear will be

1/2 of the supply voltage and with reversed polarity. u_{eq} of the last two phases will be zero. Therefore in the important case of an unearthed load with no mutual inductance between phases L_{eq} = 3/2 L_t in the first phase to clear and L_{eq} = L_t in each of the two other phases.

2.3.4. Multi-unit circuit-breakers

At constant breaking current and a fixed number of breaking units, the mean value i_{cm} of the chopping current of a certain circuit-breaker is (except for vacuum circuit-breakers) more or less proportional to the square root of the capacitance C seen from the circuit-breaker terminals. Two different theories of the dependence on the chopping current of the number of breaking units are available [10, 11].

In [11] the arc losses of the individual breaking units are assumed to vary stochastically leading to the following relationships

$$\frac{i''_{cm}}{\sqrt{n''C''}} = \frac{i'_{cm}}{\sqrt{n'C'}} \qquad (2.3.20)$$

$$\frac{i''_{c2\%}}{\sqrt{n''C''}} = \sqrt{\left(\frac{i''_{cm}}{\sqrt{n''C''}}\right)^2 + \sqrt{\frac{n'}{n''}\left(\frac{i'_{c2\%}}{\sqrt{n'C'}}\right)^2 - \left(\frac{i'_{cm}}{\sqrt{n'C'}}\right)^2}} \qquad (2.3.21)$$

where
- i'_{cm} – chopping current, mean value
- $i'_{c2\%}$ – chopping current, 2%-value
- C', C" – capacitances
- i''_{cm} – chopping current, mean value
- $i''_{c2\%}$ – chopping current, 2%-value

In [10] a different statistical approach is used, leading to a slower increase of i_{cm} with n than given by Eq.(2.3.20). This theory is based on the assumption that a multi-unit circuit-breaker will not be unstable and chop the current until all units independently have become unstable, the instability limit of each unit being a statistical variable. This assumption was confirmed by experience.

With this method the probability p" in the n"-unit case of obtaining a certain value of the ratio $i_{cr}/\sqrt{n}C$ or above is

$$p'' = (p')^{n''/n'} \qquad (2.3.22)$$

where p' is the corresponding probability in the n'-unit case.

The nature of the interaction between series connected breaking units and the influence on the chopping current is still not understood in detail. Further research is needed in this area, and the equations given in this paragraph should be taken as guidelines only.

2.4. Virtual current chopping

Transient currents superimposed on the power-frequency current may cause the total current to pass through zero. If this is experienced by a circuit-breaker the contacts of which are already under the arcing conditions, the circuit-breaker may clear the circuit before the power-frequency current zero. Some circuit-breakers have the ability to interrupt these very high rates of decrease of current. Such a rapid interruption virtually appears to other parts of the circuit (particularly those not coupled to the transient current) as if power-frequency current is chopped.

Note that with this type of "chopping" the current zero is not forced on the circuit by the instabilities of arc as described in Chapter 2.3. Really, this is not the phenomenon of true chopping, it is rather a normal interruption under fast transient conditions. However, the circuit transients which lead to such

an interruption may be typically originated by a reignition in another pole of the same circuit-breaker. This kind of interruption, generally associated with three-phase circuits, is called virtual current chopping.

Of course, the principle, of the phenomena remains the same if the current zero is originated by reignition in another or the same pole of the circuit-breaker. However, if the interruption is originated by reignition in the same circuit-breaker pole, the phenomenon has a general tendency to be repetitive. Several reignitions and clearances are normally experienced in fast sequence. Therefore such a phenomenon, which is self-generating in a single-phase circuit, is known as repetitive reignitions. It is treated separately in Clause 2.5. As opposed to the train of transients experienced during repetitive reignitions, the virtual chopping can be a single "shot" phenomenon where the currents in all three phases are interrupted simultaneously. Virtual chopping can be followed by repetitive reignitions. In fact it can be the cause which would trigger a complicated sequence of events.

The basic phenomenon of virtual current chopping can be briefly illustrated using a simplified circuit in Fig. 2.4.1. Here a three-phase source of internal emf E and impedance Z_s supplies a load Z_L via a circuit-breaker. The diagram shows also a capacitance to earth C_e on the load side of the circuit-breaker. This could be either the capacitance of the cable, or a surge capacitance for motor or transformer protection, or only the stray capacitance of the load circuit.

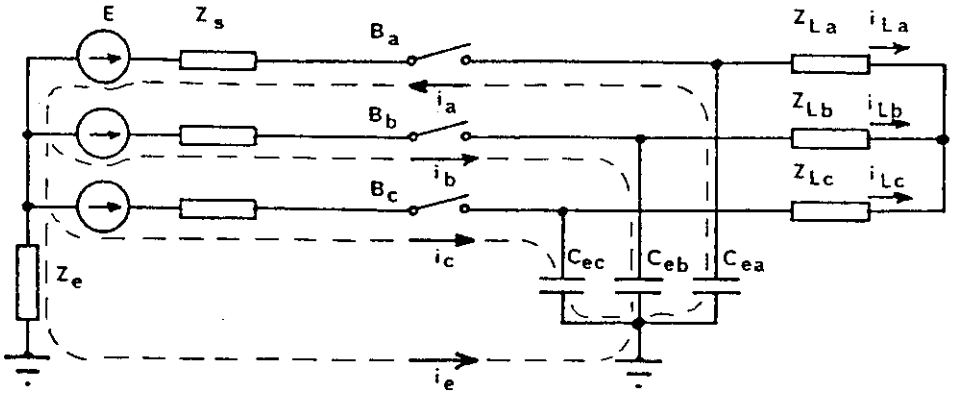

FIGURE 2.4.1 Simplified equivalent circuit of a motor or transformer installation

Let us assume that the three-phase load currents i_{La}, i_{Lb}, i_{Lc} are being interrupted by the circuit-breaker B and that the contacts in all three poles part at the time t_k with respect to the current wave (see Fig. 2.4.2). The pole B_a is the first pole to interrupt as it sees a current zero at time t_1. The voltage across its contacts begins to recover while the other poles are still arcing and waiting for their respective current zeros. The pole B_a may not be able to support its recovery voltage (e.g. due to short contact gap) and a reignition can occur at the time t_2.

This reignition will cause the capacitance C_e to charge to the system voltage. The charging process causes a transient current i_a to flow through the breaker pole B_a, the components of the reignition current i_b and i_c will return through the poles B_b and B_c, and some portion of the current will also flow through the earth return. The sum of the reignition current and the load current may pass through zero, e.g. as pictured at the time t_3 for the current in the phase c. The pole B_c may clear the current at that instant. This, from the viewpoint of the load, would look like chopping of the load current at its instantaneous value i_{vc}. Should the load be inductive, the stored inductive energy may give rise either to overvoltage by charging the capacitance C_{ec}, or to the process of repetitive reignitions as described in Chapter 2.5.

It should be noted that the current zeros appear approximately at the same time in all the three poles of the circuit-breaker. The circuit-breaker can actually clear the current in all the phases practically at the same time. Therefore this phenomenon is sometimes also called "simultaneous interruption". Such simultaneous interruption could give rise to a complicated sequence of voltage transients including repetitive reignitions in all the three phases.

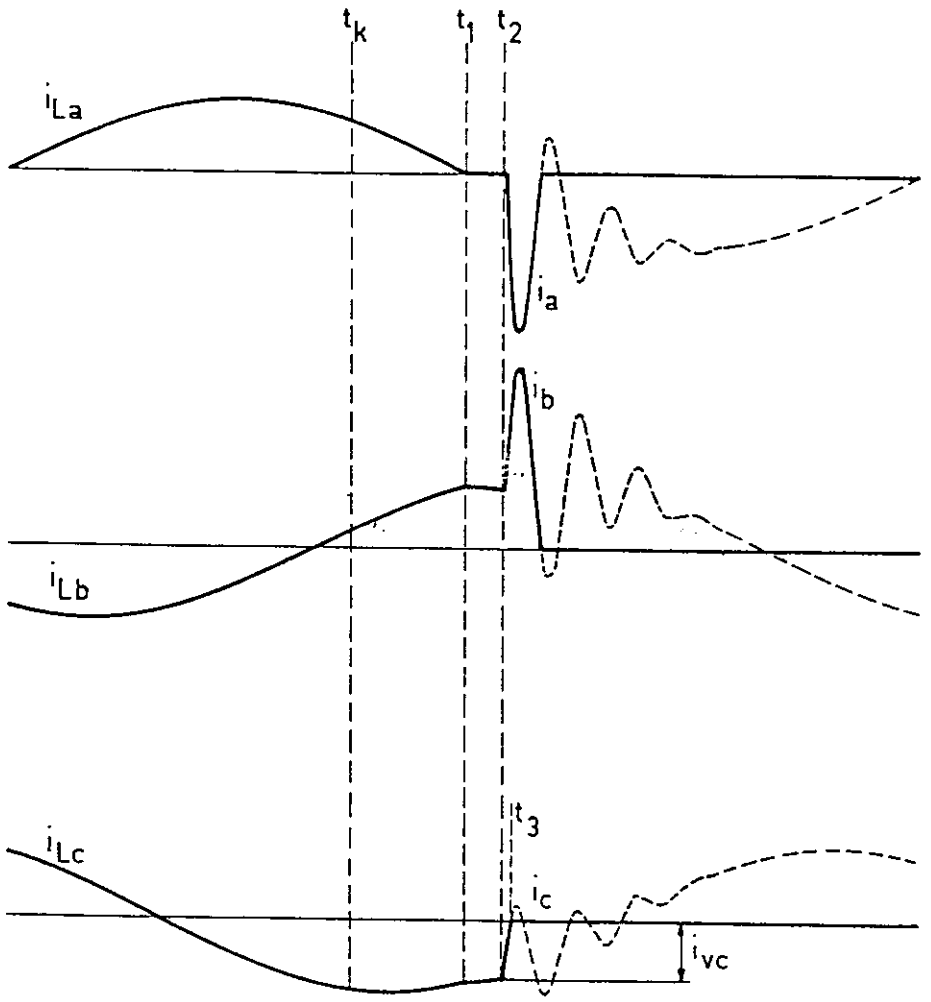

FIGURE 2.4.2 Currents during interruption with virtual current chopping. (The dotted lines show the circuit-breaker currents, if pole B_c does not interrupt in the high-frequency current zeroes.)

It should be realized that the instantaneous value of the load current which is virtually chopped can be much higher than the chopping level of the circuit-breaker. It would depend mainly on the amplitude of the reignition current which in turn is given by the restriking voltage, the surge impedances at both sides of the circuit-breaker, the mutual coupling between the phases and the mode of earthing. For example, should there be a power factor compensation capacitor bank C on the bus bars of the source side, the reignition current would be limited only by the short bus bars between C and C_e. If the neutral of the bank is unearthed, which is the usual case with medium voltage systems, half of the reignition current would return through each of the other poles, thus determining the maximum possible value of the virtually chopped current. For such a virtual chopping the circuit-breaker must have the capability of clearing the high rate of fall of current to zero.

It should be noted that the virtual chopping in practical circuits is very limited. Not only the circuit parameters have to be in a very limited range, but there are also very limiting constraints on the moment of contact partition and the value of voltage at which the reignition occurs. For example, a relatively high value of capacitance C_e is needed to obtain sufficiently high reignition current for virtual chopping. However, with the increase of the capacitance the frequency of the recovery voltage slows down which in turn makes a reignition unlikely. Further the circuit-breaker must be able to interrupt high-frequency currents. Thus, from the practical viewpoint, the virtual chopping is limited only to some specific circuits. It has been observed and reported for vacuum switching devices when switching medium voltage motors [24, 25] and arc furnace transformers [26], in both cases only within a certain range of ratings. Various protective measures have been reported and can be applied, if desirable.

2.5 Reignitions

2.5.1. Introduction

After current interruption the voltage across the inductive load starts to oscillate, as described in 2.3.3. If, during this oscillation, the momentary withstand voltage of the interrupter is exceeded, the circuit-breaker reignites. A rapidly oscillating current will start to flow through the circuit-breaker, initiated by the difference between the voltages of the source and the load side of the circuit. Such reignitions may repeat several times.

The phenomena during reignitions can be illustrated from the simplified single phase equivalent circuit diagram, Fig. 2.5.1, in which all network elements shown are regarded lumped and linear. Damping elements are omitted for the sake of simplicity. However they are of basic importance for the overvoltages actually obtained.

As shown in Fig. 2.5.1 the source-side as well as the load-side circuit is considered a parallel LC-circuit. When no current flows through the circuit-breaker, i.e. after a current interruption with or without chopping, the source-side and the load-side oscillate practically independently with oscillation frequencies, respectively:

$$f_s = \frac{1}{2\pi\sqrt{L_s C_s}} \quad and \quad f_t = \frac{1}{2\pi\sqrt{L_t C_t}}$$

In actual cases the oscillations are damped, the source-side oscillation due to a rather large value of the resistance of the source network at high frequencies and the load-side oscillation due to losses of the load.

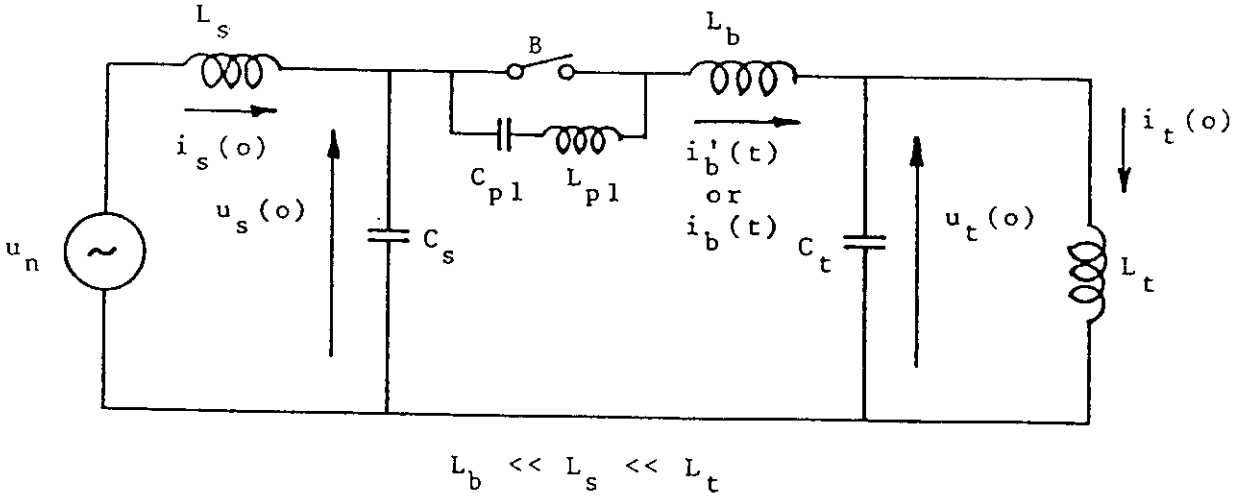

FIGURE 2.5.1 Simplified single-phase equivalent circuit diagram (in practical cases damping should be considered)

The inductance L_s can be derived from the short-circuit current at the position of the circuit-breaker B, and the load inductance L_t from the load current. The capacitances C_s and C_t represent all distributed capacitances to earth of the source and the load respectively.

In the direct vicinity of the circuit-breaker a circuit comprising a capacitance C_{pl} and an inductance L_{p1} exists C_{p1} represents the inherent parallel-capacitance of the circuit-breaker plus the capacitance to earth of both circuit-breaker terminals and the conductors connected. L_{p1} is the equivalent inductance in the circuit of "first parallel oscillation". It may physically be found in series with the circuit-breaker or in series with grading capacitors parallel to the breaking units or may be a combination of both.

The connections between the source-side and the load-side circuit form a circuit with an equivalent inductance L_b.

Detailed investigations demand the C_{pl} – L_{pl} – B (circuit-breaker) circuit to be considered both when current chopping occurs and immediately after reignitions [27]. To get an overall idea of the phenomena during reignitions, however, the oscillation, denoted "first parallel oscillation", in this circuit can be disregarded. The first parallel oscillation has a very high frequency

$$f_{p1} = \frac{1}{2\pi\sqrt{L_{p1}C_{p1}}}$$

and the current through the circuit-breaker often becomes high too, > 100 A, so the current may cross zero without causing the discharge in the circuit-breaker to cease.

Besides the "first parallel oscillation" a reignition in the circuit-breaker is followed by two kinds of oscillation:

A. "Second parallel oscillation" during which the voltage across the capacitances C_s and C_t are equalized and

B. "Main circuit oscillation" during which the total circuit is involved.

Current interruption in the circuit-breaker may occur at natural zero-crossing during the second parallel oscillation as well as the main circuit oscillation depending on the character of the circuit-breaker and the current slope at zero-crossing.

Although the different oscillations all start at the moment of the reignition it is appropriate to consider each oscillation separately because the three oscillation-frequencies differ by at least one order of magnitude.

One or more of the oscillations may be prevented from development. The second parallel oscillation, for instance, can develop after the first parallel oscillation provided the conductivity of the discharge path through the circuit-breaker remains sufficiently high. In the same way the main circuit oscillation can develop only when current interruption does not take place during the second parallel oscillation.

Reignitions cause energy exchanges in the network. The energy content on the load-side of the circuit-breaker is of special interest, because this energy is responsible for the prospective peak-voltage across the capacitance C_t, i.e. the prospective peak-voltage to earth on the load-side of the circuit-breaker after each interruption.

High overvoltages may occur in cases with consecutive reignitions where each reignition increases the prospective peak-voltage of the load oscillation by increasing the stored energy. This situation is called voltage escalation, and it may occur with circuit-breakers able to interrupt currents with high rate-of-change at zero passage.

2.5.2. Single reignition

Apart from the first parallel oscillation during which the capacitance C_{p1} immediately after a reignition is discharged through the circuit-breaker B, Figure 2.5.1, a potential difference $u_s(o) - u_t(o)$ across the circuit-breaker causes a second parallel oscillation to equalize these voltages. The flux-linkages in the inductances L_s and L_t remain nearly constant and the oscillation-frequency therefore is

$$f_{p2} = \frac{1}{2\pi}\sqrt{\frac{C_t + C_s}{L_b C_s C_t}}$$

The current $i'_b(t)$ of the second parallel oscillation is given as Eq. (2.5.1) in the Table 2.5.1 and its general shape shown in Fig. 2.5.2a. $i'_b(t)$ may be interrupted at a natural zero-crossing, but if no current interruption takes place until the oscillation has damped out a common quasi-stationary voltage u(t') across C_s and C_t results. u(t') is shown as Eq. (2.5.2) in Table 2.5.1.

When the second parallel oscillation has ceased without current interruption the main circuit oscillation develops. For this oscillation the complete network is involved. During the main circuit oscillation the voltages across C_t and C_s are assumed equal, i.e. the arc-voltage in the circuit-breaker and the inductance L_b are disregarded. The oscillation-frequency.

$$f_m = \frac{1}{2\pi}\sqrt{\frac{L_s + L_t}{L_s L_t (C_s + C_t)}}$$

or

$$f_m = \frac{1}{2\pi}\frac{1}{\sqrt{L_s (C_s + C_t)}}$$

if L_s is assumed negligible compared with L_t. The current $i_b(t)$ passing the circuit-breaker is given as Eq. (2.5.3) in Table 2.5.1, and an example of its possible shape is shown in Figure 2.5.2b. Eq. (2.5.3) shows that $i_b(t)$ does not always have a natural zero-crossing, for instance when $C_s \gg C_t$. Under such circumstances the discharge-current may continue until the main circuit oscillation has damped out and renewed current chopping takes place.

Oscillations following a single reignition are indicated in Fig. 2.5.3 and Fig. 2.5.4. The figures are examples only to illustrate the phenomena.

More thorough investigations are carried out in [27].

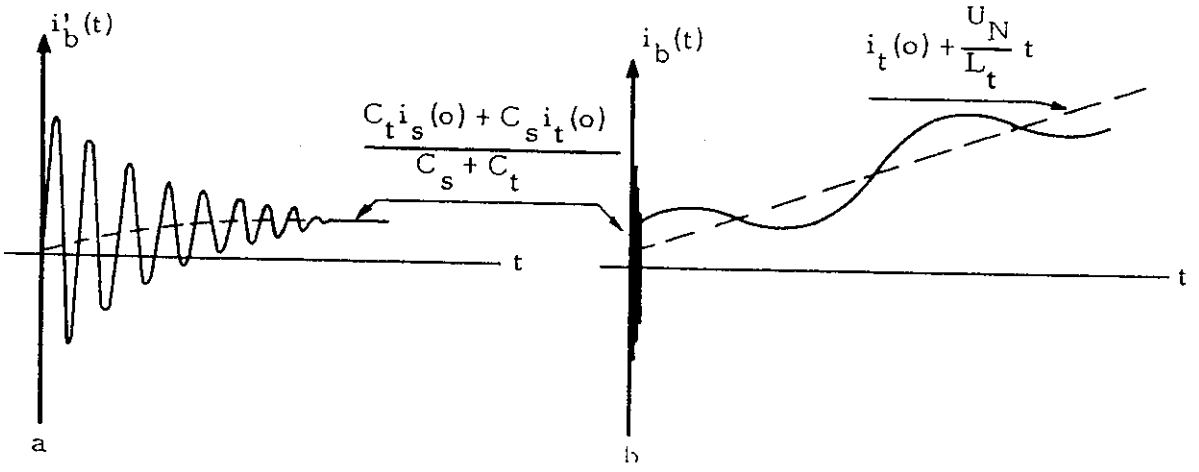

FIGURE 2.5.2 a) General shape of $i'_b(t)$
b) Possible shape of $i_b(t)$ with no zero crossing.

In Figure 2.5.3 a reignition takes place near the recovery peak. Only the second parallel oscillation is shown. The current $i_b(t)$ is assumed to have several zero crossings in which interruption may occur before the transient oscillation has damped out. If no interruptions take place (as assumed in the figure) further zero crossings may occur if a main circuit oscillation (not shown in the figure) of sufficient amplitude develops.

In Figure 2.5.4 a reignition takes place near the suppression peak. The current $i_b(t)$ has a start in the opposite direction compared with Figure 2.5.3 and zero crossing during the transient oscillations must follow. i_t is usually close to zero at the moment of reignition and only a very small part of $i_b(t)$ flows through L_t. No high overvoltages result in this case.

An example of reignitions even before the suppression peak is shown in Figure 2.5.5. Current flow following the reignitions is not assumed.

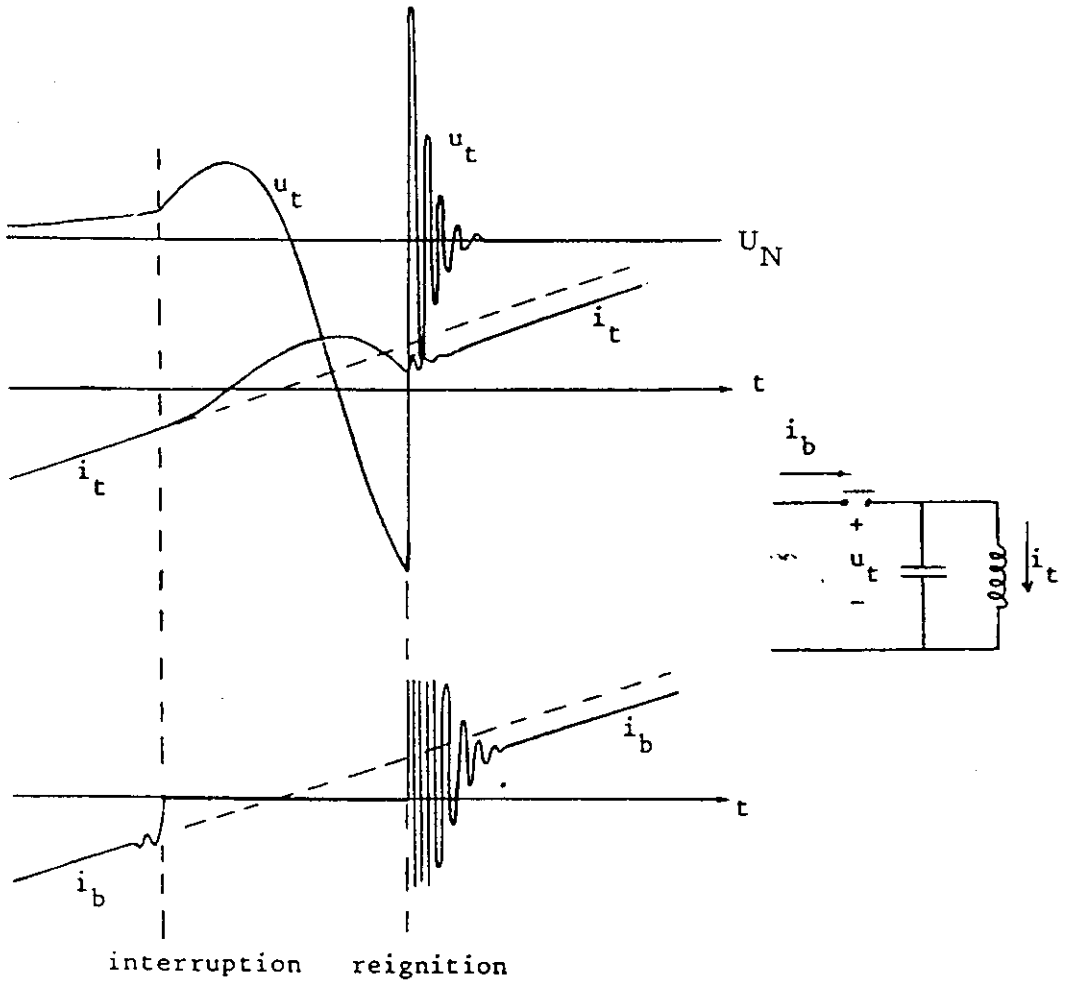

FIGURE 2.5.3 Reignition near recovery peak leading to new current loop.

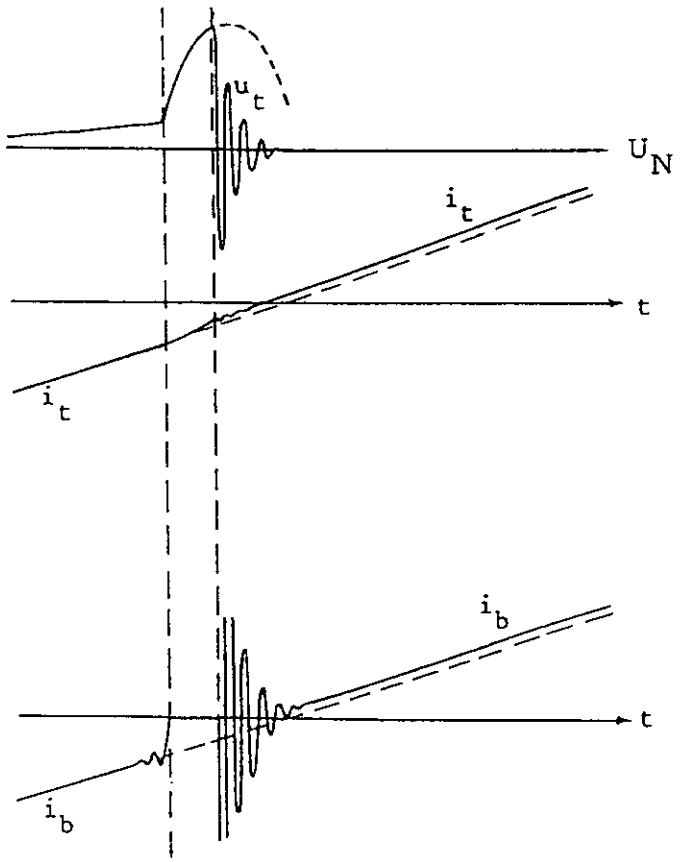

FIGURE 2.5.4 Reignition near suppression peak leading to new current loop.

2.5.3. Repeated reignitions - Voltage escalation

As previously indicated several reignitions may occur before final arc-extinction. Each reignition follows the pattern mentioned in 2.5.2. but the initial conditions in the network and in the circuit-breaker differ from one reignition to the next.

The energy content on the load-side of the circuit-breaker changes during a reignition and thus the total energy W_t left on the load-side when the restriking current interrupts differs from the energy just before the reignition.

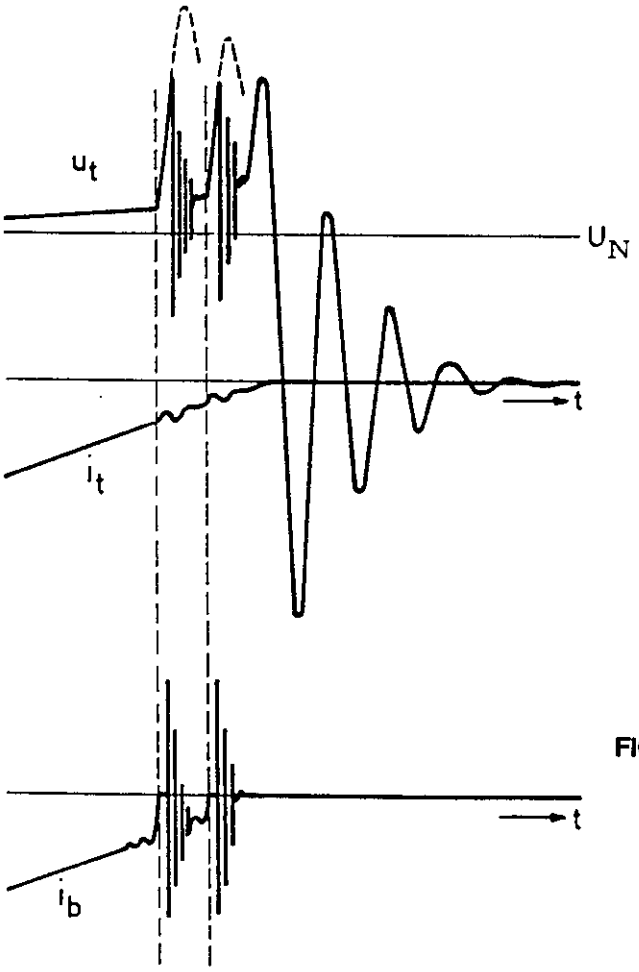

FIGURE 2.5.5 Reignitions before suppression peak not leading to new current flow.

The prospective peak-voltage across C_t when the load-side oscillates freely is proportional to $\sqrt{W_t}$ and appears at the times when W_t is fully converted into electrostatic energy. Reignitions, however, may prevent the prospective peak-voltage from being attained. If repetitive reignitions cause increased W_t and consequently increased prospective peak-voltage the phenomenon is denoted voltage-escalation and is observed as an increase of the rate-of-rise in the voltage across C_t following each arc-extinction. The voltage-escalation must not be confused with the increase in the actual voltage across C_t just before each consecutive reignition (the reignition voltage) which is solely due to the increase in the dielectric recovery strength across the contacts in the circuit- breaker.

Voltage escalation is often observed during interrupting procedures especially when arc-extinction takes place at the first current zero of the second parallel oscillation, and the phenomenon is not related to current chopping.

In Figure 2.5.6 an example is shown just to illustrate the phenomenon. It is based on the equivalent circuit diagram Figure 2.5.1. Figure 2.5.6 shows the voltage u_t across C_t, the current i_t and the current i_b through the circuit-breaker after a current chopping at t = 0 followed by two consecutive reignitions.

The existence of voltage escalation could also be defined by $i_{t2max} > i_{t1max}$ as this means increasing energy W_t, where i_{t1max} is the maximum value of the load oscillation current before the first reignition and i_{t2max} the maximum value after the first reignition.

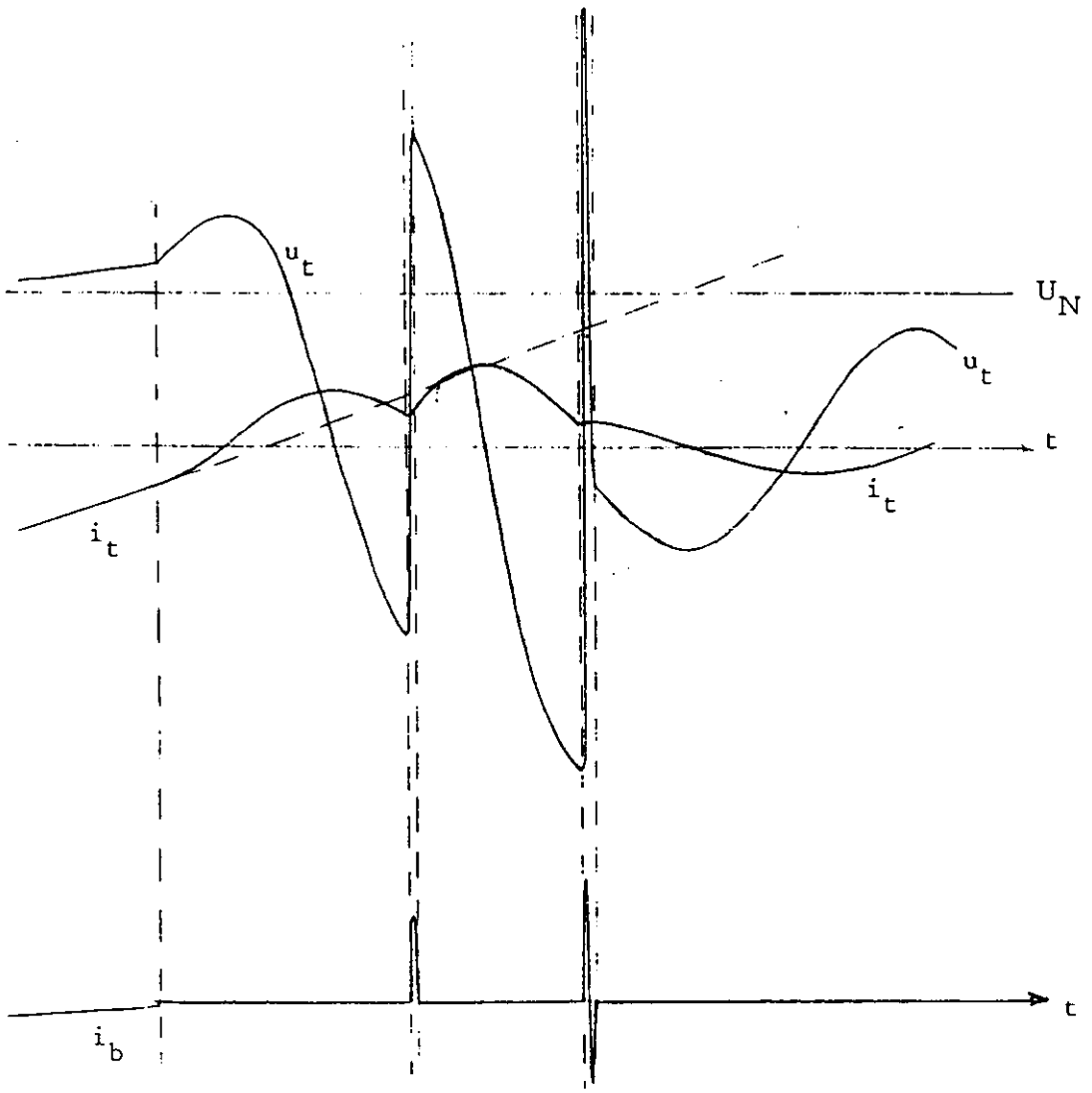

FIGURE 2.5.6 Interruption with two reignitions and voltage escalation.
Note: i_b and i_t are not drawn to the same scale.

2.5.4. Energy exchange

The total energy content on the load-side of the circuit-breaker immediately following an interruption can be expressed as $W_t = W_{t,stat} + W_{t,magn}$ with $W_{t,stat}$ and $W_{t,magn}$ as given in Eq. (2.5.4), Table 2.5.1. If damping is neglected W_t remains constant until reignition, but the oscillation with the frequency f_t causes alternation between the electromagnetic energy $W_{t,magn}$ and the electrostatic energy $W_{t,stat}$.

When reignitions take place energy exchange with the supply-side starts following the pattern mentioned in 2.5.1.

During the first parallel oscillation only the electrostatic energy in C_p1 is released and energy exchange between the load-side and the source-side does not take place.

During the second parallel oscillation the flux linkages in L_s and L_t are assumed constant and energy exchange takes place only between C_s and C_t.

During the main circuit oscillation all network elements are involved and the energy exchange, therefore, comprises both electromagnetic and electrostatic energy.

The energy stored in the load-side after interruption of the restriking current normally differs from the energy stored just before the reignition. If the energy steadily increases voltage escalation is present as mentioned in Sub-clause 2.5.3. The risk of voltage escalation occurring increases when the ratio between the capacitances C_s and C_t is large.

TABLE 2.5.1

Eq. No.	
(2.5.1)	$i'_b(t) \approx [u_s(o) - u_t(o)] \sqrt{\frac{C_s C_t}{L_b (C_s + C_t)}}\, e^{-\frac{t}{T}} \sin \omega_{p2} t + \frac{C_t i_s(o) + C_s i_t(o)}{C_s + C_t} [1 - e^{-\frac{t}{T}} \cos \omega_{p2} t]$ $u_s(o)$, $u_t(o)$, $i_s(o)$ et/*and* $i_t(o)$ selon la figure 2.5.1 au moment du réallumage – *according to Figure 2.5.1 at the moment of reignition.* T = constante de temps correspondant à l'amortissement réel – *time constant for the actual damping.* $\omega_{p2} = 2\pi f_{p2}$
(2.5.2)	$u(t') \approx \frac{u_s(o) C_s + u_t(o) C_t}{C_s + C_t} + \frac{[i_s(o) - i_t(o)] t'}{C_s + C_t}$
(2.5.3)	$i_b(t) \approx \frac{U_N}{L_t} + \frac{U_N - u(t')}{L_s \omega_m} \frac{C_t}{C_s + C_t} \sin \omega_m t + i_t(o) + \frac{C_t}{C_s + C_t} [i_s(o) - i_t(o)] \cos \omega_m t$ U_N = Tension de la source (supposée constante) – *supply voltage (assumed constant)* $\omega_m = 2\pi f_m$ *Remarque* : on a négligé l'amortissement Note : *Damping is neglected*
(2.5.4)	$W_t = W_{t,stat} + W_{t,magn}$ $W_{t,stat} = 1/2\, u'_t(o)^2\, C_t$ Energie électrostatique – *electrostatic energy* $W_{t,magn} = 1/2\, i'_t(o)^2\, L_t$ Energie électromagnétique – *electromagnetic energy* $u'_t(o)$ = tension aux bornes de C_t } au moment de l'interruption du *at moments of current interruption* $i'_t(o)$ = courant traversant L_t } courant dans le disjoncteur B *in the circuit-breaker B*

2.5.5. Influence of network and circuit-breaker parameters

The network parameters and the circuit-breaker characteristics influence the interrupting procedure in a very complicated manner. For that reason it is only possible to give some general tendencies to illustrate the significance of parameter-variations.

In Table 2.5.2 the ranges of the frequencies involved are stated. For the circuit elements L_{p1}, C_{p1} and L_b the following representative values are assumed:

L_{p1} ≈ 2.....10 μH
C_{p1} ≈ 100...50000 pF
L_b ≈ 0.1...1 mH

The supply-side inductance L_s is normally small compared with the load-inductance L_t. At the same time the capacitance C_s on the supply-side most often is large in comparison with the load-side capacitance C_t. The voltage on the supply-side of the circuit-breaker is, therefore, nearly unaffected by the transient phenomena during the interruption.

Frequency		*Frequency range*
	f_s	1..... *20 kHz*
	f_t	0,5.... *5 MHz**
First parallel osc.,	f_{p1}	*1..... 10 MHz.*
Second parallel osc., f_{p2}	f_{p2}	*100 ... 500 kHz*
Main circuit osc.,	f_m	*5..... 20 kHz*

TABLE 2.5.2.
Frequencies during reignitions.

(*) This phenomenon may be aperiodic e.g. in case of no-load transformer switching.

The actual large ratio between C_s and C_t means that

a) the voltage u_t across C_t, during the second parallel oscillation, oscillates around the voltage across C_s just before the reignition.

b) the current slope at zero-crossing during the second parallel oscillation is determined by C_t and L_b rather than C_s.

c) the main circuit oscillation current $i_b(t)$ often has no zero-crossing

High overvoltage and a great number of reignitions are to be expected if the circuit-breaker has a high ability to extinguish the arc-current during or even before the second parallel oscillation. This tendency is especially pronounced at negligible damping in the second parallel oscillation. Damping, including surge impedances of cable-sections acting as resistances, has crucial influence on the conditions, but not necessarily in a simple way, because damping decreases the current slope at zero-crossing, which means that the current interruption is facilitated. A reduction of the overvoltages, however, is a consequence.

Increasing C_t reduces the second parallel frequency f_{p2} and the load-side frequency f_t. The number of reignitions and the resulting overvoltages may decrease, but, as shown in 2.3, the chopping current depends on the actual size of C_t, resulting in chopping overvoltages that are more or less independent of the C_t-value for most circuit-breaker types.

2.6. Interaction between phases

In a 3-phase network the phenomena may be much more complicated than in a single-phase case due to the interaction between the phases [28, 31]. Only in rare cases where the interphase coupling is negligible, the three phases may be treated separately. The interphase coupling, that may be magnetic or capacitive or a combination of both, may result in two different classes of phenomena:

A - Cases where the interruption process in one phase is influenced by events in another phase, i.e.

(i) induced current chopping
(ii) induced reignition

B - Cases where the overvoltages in one phase are influenced by events in another phase without further reignitions. The energy transfer may be due to:

(i) chopping overvoltages
(ii) reignition transients

The different cases will be described in the following sections.

2.6.1. Induced current chopping

An interruption of the current before the power frequency current zero may be caused by transients induced from other phases. The induced high frequency current creates a current zero in which interruption takes place. Virtual current chopping described in 2.4 is a specific example of induced current chopping where the current zero is induced by a restrike in another pole.

2.6.2. Induced reignitions

Any transfer of energy from one phase to another after interruption may lead to increased voltages across an open breaker pole. This may result in a reignition of that pole, and the whole interruption process could be drastically changed. It is, however, more or less impossible to analyze this case. It is further of statistical nature. It is therefore regarded sufficient to limit the discussion to the first step - induced overvoltages due to interphase coupling.

2.6.3. Induced overvoltages due to switching in other phases

The induced overvoltages could be transferred by magnetic and/or capacitive coupling. The kind of coupling may have different importance depending on the nature of the transient. Normally the chopping overvoltage (with load-side oscillation frequency ≈ 0.5 – 5 Khz) of one phase is transferred to the other phases mainly by magnetic coupling.

The first steep transient at reignition is normally transferred to the other phases by capacitive coupling but magnetic coupling may "take over" later.

Besides these obvious transient effects another type of energy transfer can be observed during the load side oscillation after the successful interruption of at least two phases.

2.6.3.1. Transfer of chopping overvoltages

The chopping in one phase can produce an overvoltage by coupling to another phase that has already cleared. The transferred overvoltage is superimposed on the voltage of the phase which has cleared. The magnitude of the transferred overvoltages depends on the type of circuit, the kind of interphase coupling, the relative clearing times and the chopping level of the breaker. Especially in circuits with strong magnetic coupling considerable transfer of energy can be observed. E.g., switching on the HV side of a transformer loaded with a tertiary connected reactor has resulted in coupled overvoltages in the first phase-to-clear, exceeding its own chopping overvoltages, when the last phase clears [29], even in the case of single phase units [20].

Also when switching a directly connected reactor with 3-legged core a considerable energy transfer is observed. Figure 2.6.1 shows the load side oscillations when switching a 132 kV, 55 MVAr 3-legged reactor. See further Chapter 4.

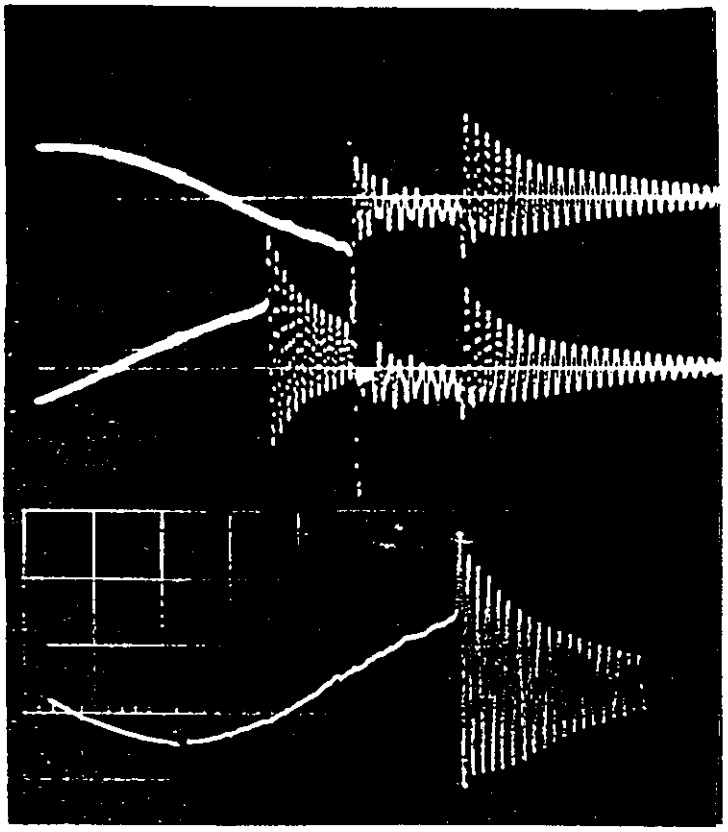

FIGURE 2.6.1 Load side voltages at switching a 35 MVAr, 132 kV, reactor.

Besides the possibility to create virtual current chopping a reignition in one phase may induce overvoltages in other phases which may be superimposed to prevailing voltages and thus give rise to a considerable enhancement of the overvoltage amplitude. The steep voltage wave created at a

reignition is primarily transferred to the other phases by capacitive coupling. The process may be illustrated by an oscillogram from [29] shown in Figure 2.6.2. Field tests have given similar results when switching a transformer with a reactor loaded tertiary. See further Chapter 6.

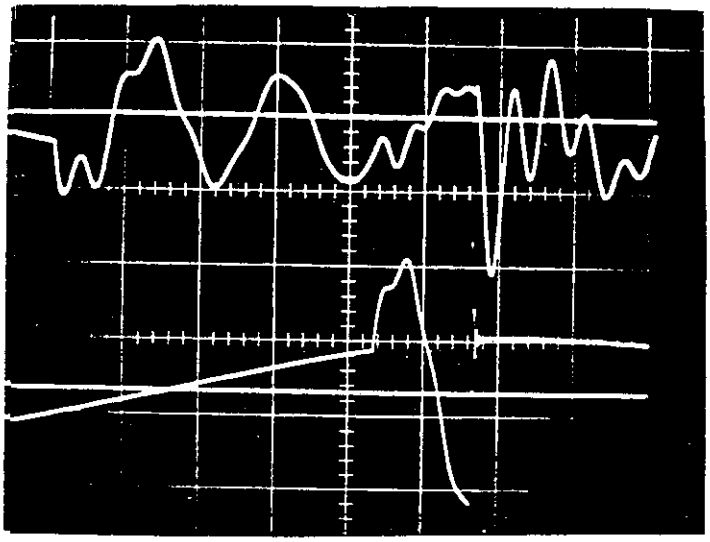

Upper beam - second pole-to-clear
1 div. = 1.35 p.u.

Lower beam - last pole-to-clear with reignition
1 div. = 1.35 p.u.

Timebase = 1 ms/div.

FIGURE 2.6.2 Interphase coupling effects following a circuit-breaker reignition (30 MVAr load, TNA study).

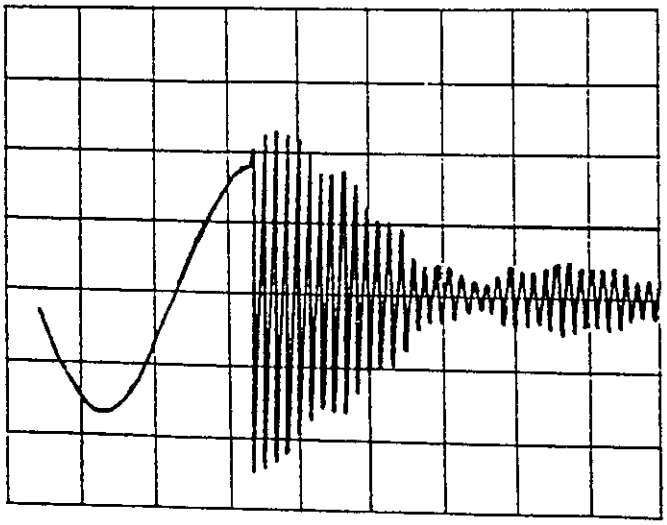

FIGURE 2.6.3.
Switching a 200 MVAr, 420 kV reactor. Load side voltage of last phase-to-clear

2.6.4. Transfer during load side oscillation

During the load side oscillations after the interruption an energy transfer can take place that results in higher overvoltages than determined by the chopping level. In Figure 2.6.1 such energy transfer obviously takes place in the interval when two of the phases have cleared. In Figure 2.6.3 an oscillogram from a field test with switching of a 420 kV, 200 Mvar reactor of the 5-legged core type shows energy transfer that leads to some enhancement of the load oscillation amplitude in the last phase-to-clear [30]. The first phase-to-clear shows a uniformly decaying oscillation amplitude, but as soon as the second phase clears the energy transfer starts. See further Chapter 4.

2.7 REFERENCES IN CHAPTER 2

[1] F.A.M Rizk. – Interruption of small inductive currents with air-blast circuit-breakers, Thesis, Gothenburg, 1963.

[2] O. Mayr. – Beiträge zur Theorie des statischen und des dynamischen Lichtbogens, Archif für Elektrotechnik (1943), p. 588...608.

[3] W. Weizel, R. Rompe. – Theorie elektriescher Lichtbögen und Funken, Leipzig 1949.

[4] H. Nöske. – Zum Stabilitätsproblem beim Abschalten kleiner induktiver Ströme mittels Hochspannungsschalter, Diss. TU Berlin 1955.

[5] C.E. Sölver. – Simulation of the current chopping phenomena at interruption of small inductive currents by means of a generalized arc model, CIGRE 13-79 (WG 13.02) 08 IWD.

[6] W.M.C van den Heuvel. – Current chopping in SF_6 T.H. Report 80-E-107; T.H. Eindhoven 1980.

[7] P. Baltensperger. – Form und Grösse der Uberspannungen beim Schalten kleiner induktiver sowie kapazitiven Ströme in Hochspannungsnetzen, Brown Boveri Mitt. 47 (1960): 4, p. 195...224.

[8] P. Baltensperger, P. Schmidt. – Lichtbogenstrom und Uber-Spannungen beim Abschalten kleiner induktiver Ströme in Hochspannungsnetzen, Bull. SEV 46 (1955), p. 1...13.

[9] G.E. Gardner, R.J. Urwin. – Arc instability and current chopping in an air-blast interrupter, Proc. IEE 124 (1977) 7, p. 619...627.

[10] G.E. Gardner, R.J. Urwin. – Performance and testing of multi-unit circuit-breakers switching low inductive currents, Proc. IEE 125 (1978) 3, p. 230...236.

[11] S. Berneryd, C.E. Sölver, L. Ahlgren, R. Eriksson. – Switching of shunt reactors – comparison between field and laboratory tests, CIGRE 1976, Report 13-04.

[12] M. Murano, S. Yanabu, H. Ohashi, H. Ishizuka, T. Okazaki. – Current chopping phenomena of medium voltage circuit-breakers IEEE Trans. PAS-96 (1977) 1, p. 143...149.

[13] G.C. Damstra. – Current chopping and overvoltages in relation to system parameters, CIGRE 1964, Report 120.

[14] A. Hochrainer. – Eine regelungstechnische Betrachtung des elektrischen Lichtbogens, ETZ-A 92 (1971) 6, p. 367...371.

[15] Y. Ozaki, Y. Honaga. – Tests on current interruption with 24 kV vacuum circuit-breakers, IEEE Paper No. 71 CP 557-PWR.

[16] F. Froncek, H. Markiewicz, Z. Zalucki. – Strom- und Spannungsverläufe des Vacuumlichtbogens in der Nähe des Stromnulldurchganges, ETZ-A 99 (1978) 6, p. 549...552.

[17] G.C. Damstra. – Influence of circuit parameters on current chopping and overvoltages in inductive MV circuits, CIGRE 1976, Report 13-8.

[18] F.A. Holmes. – An empirical study of current chopping by vacuum arc, IEEE Paper C 74 088-1. Winter Power Meeting 1974.

[19] A.F.B. Young. – Some researches on current chopping in high voltage circuit-breakers, Proc. IEE 100 (1953), p. 337...361.

[20] R. Thaler, Th. Heinemann, J. Marty. – Overvoltages during interruption of small inductive currents in laboratory and in network, CIGRE 1964, Report 117.

[21] T.H. Lee. – The effect of current chopping in circuit breakers on networks and transformers, AIEE Transaction 79 (1960), p. 535...544.

[22] P. Joss. – Switching operations and switching phenomena in electrical power supply systems, Bulletin Oerlikon (1966) Nr. 367, p. 10...16.

[23] E.J. Touhy, J. Panek. – Chopping of transformer magnetizing currents. Part 1: Single phase transformers, IEEE Trans. PAS-97 (1978) 1, p. 261...268.

[24] M. Murano, T. Fujii, H. Nishikawa, S. Nishiwaki, M. Okawa. – Three-phase simultaneous interruption in interrupting inductive current using vacuum switches, IEEE Trans. PAS-93 (1974) 1, p. 272...280.

[25] Y. Murai, T. Nitta, T. Takami, T. Itoh. – Protection of motor from switching surge by vacuum switch, IEEE Trans. PAS-93 (1974) 5, p. 1472...1477.

[26] J. Panek, K.G. Fehrle. – Overvoltage phenomena associated with virtual current chopping in three phase circuits, IEEE Trans. PAS-94 (1975) 4, p. 1317...1325.

[27] W.M.C. van den Heuvel. – Interruption of small inductive currents in A.C. circuits, Thesis, Eindhoven, 1966.

[28] A.N. Greenwood. – Electrical transients in power systems, Wiley, 1971.

[29] B.S. Leyman. – 275 kV switching of a supergrid transformer having a reactor loaded tertiary, CERI, Report RD/L/N 224/71.

[30] R. Eriksson, S. Berneryd. A. Ericsson. – Laboratory and field tests with a 420 kV SF_6 puffer breaker for a gas-insulated substation, IEE Conf. on HV Switchgear, Publ. 182(1979).

[31] Th. Heinemann. – Uberspannungen beim dreiphasigen Ausschalten von leerlaufenden oder induktiv belasteten Transformatoren. ETZ-A 86 (1965); 4, p. 97...102.

Chapter 3:

HIGH-VOLTAGE MOTORS

The Electra Report was published in two parts – Chapter 3A and 3B, where 3B contained mainly enlargements and a few amendments. They are merged in this brochure.

3.1. High-voltage motor and equivalent circuit

3.1.1. General

Normal high-voltage a.c. motors cover the ranges 2 kV...14 kV,
100 kW...40 MW. The motors are classified to following types:

- Asynchronous squirrel-cage motors, direct starting. I_{start} = 6...7 x rated current of the motor, cosφ = 0.15...0.20. Large motors (i.e. > 10 MW) may be started with special means to reduce the current, if it is necessary due to the characteristics of the supply.

- Asynchronous slip-ring motors, $I_{start} < 6 \times I_{rated}$. The actual value of the current may be chosen according to the requirements.

- Synchronous motors. Motors are often started by means of a squirrel-cage rotor, I_{start} = 3...5 x I_{rated}, cos φ = 0.25...0.30. Large motors (i.e. > 5 MW) are often started by means of a start-transformer to reduce the current.

There is a trend towards more common use of direct starting at the higher motor ratings.

From the circuit-breaker point of view the direct started asynchronous motor is the most important category. These motors are numerous. Also most measured overvoltages are observed when breaking the starting current of asynchronous motors.

In normal motor applications the supply is strong enough so that its short circuit impedance has no influence on the phenomena during the switching-off. The voltage drop in the supply circuit is normally lower than 10 % during the starting period.

Other supply side conditions may have a considerable influence on the overvoltage generation such as long cables, power factor compensation capacitors.

The cable between the circuit-breaker and the motor has a great influence on the natural frequency of the circuit and on travelling waves. Cable lengths vary very much in practical situations, the range being from a few meters to 1 000 meters. For high-frequency oscillations the distances from the circuit-breaker to the first discontinuities are important as well as the nature of the discontinuities, especially their capacitances. Therefore, it is difficult to chose a typical situation.

3.1.2. Equivalent circuit of motor during current interruption and generation of overvoltages

Breaking of the starting current and breaking of the current of a running motor, loaded of unloaded, are typical duties for circuit-breakers as motor-starters.

The characteristic features of these duties are:

1) Starting current

- high current (I = 6...7 x motor rated current)

- low power factor (cos $\varphi \approx 0.1...0.2$)
- infrequent operation
- due to the higher interrupted current the chopping current can attain high values
- the arcing time for some switching devices may be longer than when the motor is running
- according to practical experience the overvoltages when breaking the starting current are usually higher than when no-load or load-current is to be broken. In addition to possible higher chopping currents this is caused also by reignitions, which usually are much more numerous when starting current is interrupted.

2) No-load current

- the no-load current of a small HV motor may be lower than the chopping current level of the circuit-breaker
- the power-frequency recovery-voltage is very small compared to the case of breaking the starting current. As the rotor is running a voltage is induced in the stator with a frequency equal to the power frequency during the first periods.
- reignitions are not likely as the recovery voltage is low
- low power factor (cos $\varphi \approx 0.1$).

3) Load current

- high power factor (cos $\varphi \geq 0.9$)
- power-frequency recovery voltage is low
- low overvoltages, no reignitions.

Switching off a running motor is important when the mechanical and electrical wear of the circuit-breaker is discussed, because the number of these operations may be high. As regards overvoltages and breaking capacity, the interruption of the starting current is usually the more severe operation.

For all breaking operations the same equivalent circuit applies, see Figure 3.1.1. Typical oscillograms are shown in Figure 3.1.2. At the moment when current chopping occurs the currents and voltage in the motor are as shown in Figure 3.1.1.

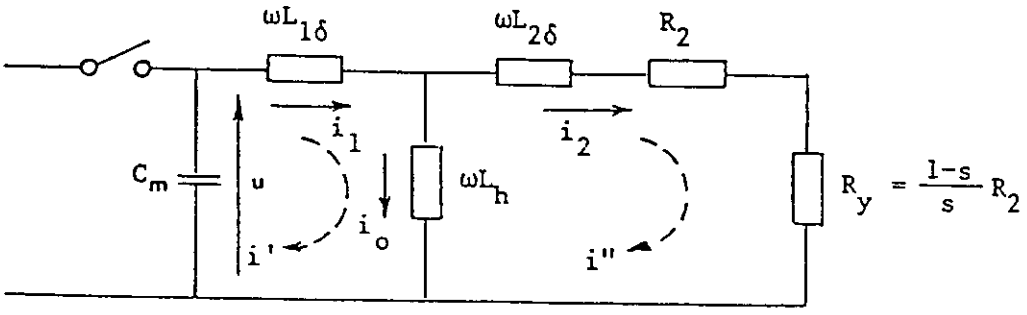

FIGURE 3.1.1 Single phase equivalent circuit of an asynchronous motor.
All impedances are transferred to the stator side of the motor.

C_m	Cable capacitance plus effective earth capacitance at the motor terminal.
$L_{1\delta}$	Stator leakage inductance.
$L_{2\delta}$	Rotor leakage inductance referred to the primary.
R_2	Rotor resistance referred to the primary.
S	Slip
L_h	Main inductance.
R_y	Resistance equivalent to the power of the motor.
u	Voltage at the motor terminal (at the moment of current chopping $u = u_c$).
i_1,i_2 and i_o	Currents at the moment of current chopping (referred to the primary).
i' and i"	Transient currents following the current chopping.

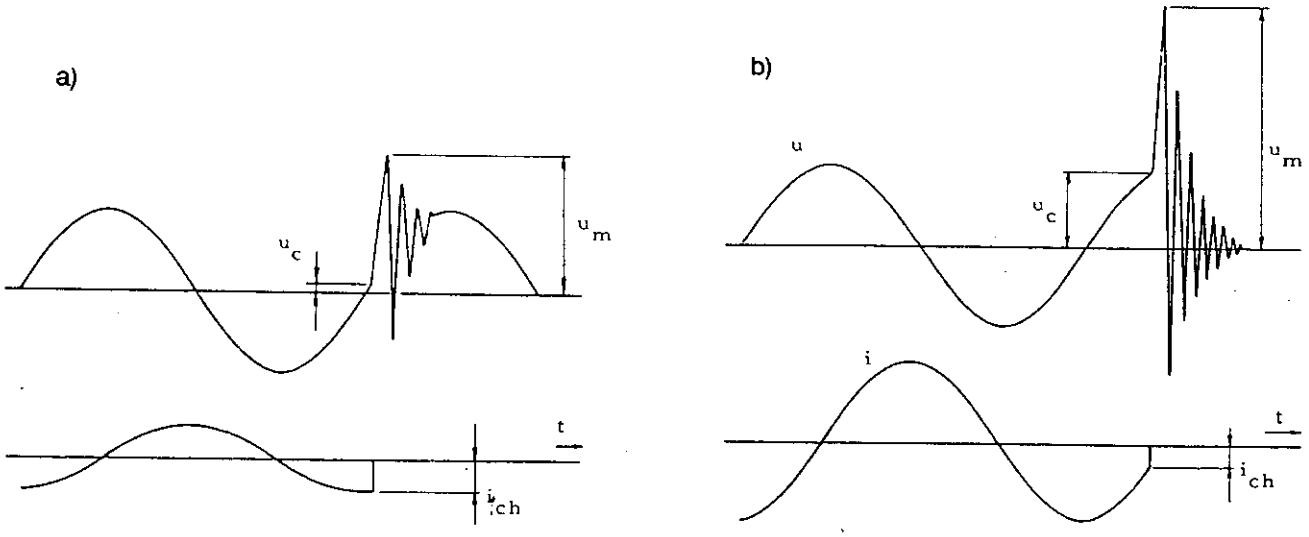

FIGURE 3.1.2 Typical oscillograms.
i_{ch} = chopping current.

a) Switching off a running motor at no-load. A power frequency voltage is included in the stator and the over-voltage U_m is usually low due to the low chopping current limited by the low peak current.
b) Breaking of the starting current. The over-voltage may be high due to the possible higher chopping current.

If damping is neglected the currents i' and i" are calculated as

$$i' = i_1 \cos \nu t + u_c C_m \nu \sin \nu t \qquad (3.1.1)$$

$$i'' = \frac{1}{1 + \frac{L_{2\delta}}{L_h}} i' - \frac{1}{1 + \frac{L_{2\delta}}{L_h}} i_1 + i_2 \qquad (3.1.2)$$

where

$$\nu = \sqrt{\frac{1 + \frac{L_{2\delta}}{L_h}}{C_m \left[L_{1\delta} + L_{2\delta} + \frac{L_{1\delta} L_{2\delta}}{L_h} \right]}} = \frac{1}{\sqrt{C_m \left[L_{1\delta} + L_{2\delta} \right]}} \qquad (3.1.3)$$

In fact i' is damped out quickly, and from Eq. (3.1.2.) it appears that i" will reach the value

$$i'' = -\frac{1}{1 + \frac{L_{2\delta}}{L_h}} i_1 + i_2 \qquad (3.1.4)$$

At the moment of current chopping the current through the main inductance L_h is

$$i_0 = i_1 - i_2$$

If a running motor is switched off the main flux when i' disappears has approximately the same value as the value at the moment of current chopping.

This flux is damped with a time constant

$$T = \frac{L_h + L_{2\delta}}{R_2 + R_y}$$

and because the rotor is still running a voltage is induced in the stator with a frequency determined by the running speed, that is a frequency equal to the power frequency during the first periods but decreasing due to damping in the mechanical system.

If the motor is switched off during the start ($s \approx 1$) the starting current is high and has a low power factor because the resistance on the rotor side is low and the current is determined approximately by $L_{1\delta}$ and $L_{2\delta}$ only. After the damping of i' no voltage is induced in the stator because there is no main flux.

The magnetic energy at the moment of current chopping is

$$W_m' = \frac{1}{2}[L_{1\delta} i_1^2 + L_h (i_1 - i_2)^2 + L_{2\delta} i_2^2] \qquad (3.1.5)$$

When i' has disappeared the magnetic energy is

$$W_m'' = \frac{1}{2}(L_h + L_{2\delta})\, i''^2 \qquad (3.1.6)$$

The difference $\Delta W_m = W_m' - W_m''$ is available for overvoltages

$$W_m = \frac{1}{2}\left(L_{1\delta} + \frac{L_h L_{2\delta}}{L_h + L_{2\delta}}\right) i_1^2 \approx \frac{1}{2}(L_{1\delta} + L_{2\delta})\, i_1^2 \qquad (3.1.7)$$

The peak value of the voltage u in Figure 3.1.1 may be calculated from the Eq. (3.1.8), when damping is disregarded.

$$u_m = \sqrt{u_c^2 + (i_{ch} Z_m)^2} \qquad (3.1.8)$$

where U_c is the voltage before current chopping, i_{ch} the chopping current, and

$$Z_m = \sqrt{\frac{L_m}{C_m}}$$

$$L_m = L_{1\delta} + L_{2\delta}$$

The limitation of voltages by the dielectric strength of the circuit-breaker is not taken into account. Also such high-frequency phenomena, which would require the use of distributed parameters and travelling waves are disregarded.

The frequency of the oscillation is nearly the same both when the starting current and when the current of a running motor is interrupted.

$$f = \frac{1}{2\pi}\sqrt{\frac{1}{L_m C_m}} \qquad (3.1.9)$$

3.1.3. Switching-on (energizing) of a motor

Overvoltage problems may arise also when energizing a motor.

In the first pole to close (or prestrike) the surge wave injected into the motor may approach the peak value of the phase-to-neutral voltage at least if the source is rigid (large capacitor or many cables connected). As the motor normally is cable connected the surge wave may then be almost doubled because of the reflections at the motor terminal.

The voltage appearing at the motor terminals, u_m, will be

$$u_m = u_s \frac{2Z_i}{Z_c + Z_i}$$

where u_s = incident surge amplitude
Z_c = surge impedance of the cable
Z_i = surge impedance of the motor (see 3.2.3)

Typical values are:

Z_i = 0.5 ... 8 kΩ (Table 3.2.2 and Figure 3.2.1)
Z_c = 20 ... 50 Ω

giving $u_m \approx 2\ u_s$.

Due to damping and other effects the actual values are lower. Typical measured surge enhancement factors are 1.5 ... 1.8 times the prestrike voltage [26].

The three phases are usually not energized simultaneously, but a certain spread in time (up to a few milliseconds) will exist due to differences in the contact travel or prestrike conditions. The surge from the first pole to close will cause an oscillation in the motor winding and the open ends of the windings of the other two phases will also show an oscillating voltage. Assuming that the first pole prestrikes at maximum voltage across the contacts, the peak voltage across the second and third poles of the switch may approach a value of 2.0 ... 2.3 (= 0.5 + 1.5 ... 1.8) times the peak phase-to-neutral voltage [28, 39]. If any of those poles then close or prestrike, a surge wave of the same magnitude will be injected. Also this wave may be enhanced by reflections at the motor terminal by a factor 1.5 ... 1.8 theoretically resulting in a maximum swing of 3.0 ... 4.1 p.u.

Note. Theoretically a somewhat larger swing can appear if the first pole closes or prestrikes 30 electrical degrees after the peak voltage [29], but the probability of this may be regarded as low.

In the calculations it has been assumed that the motor is energized at stand-still. Theoretically still higher transients can be achieved if the motor is running close to full speed. Out-of-phase conditions may then occur. This case may appear when switching from one source to another or at a reclosing after a temporary fault on the feeder.

Switches that are able to interrupt high frequency currents (e.g. vacuum circuit-breakers, vacuum contactors) may sometimes cause repetitive high frequency transients due to reignitions at switching-on. The phenomenon is equivalent with the voltage escalation described in Chapter 2, Clause 2.5.3 but will usually not result in escalation since the amplitude of the transient normally is limited by the breakdown of the contact gap that is continuously decreasing contrary to the increasing gap at interruption. However, due to the spread in dielectric strength it is possible for the prestrike magnitudes to attain values higher than the initial gap breakdown voltage [25, 26, 40]. E.g. whiskers on the contact surface may cause a breakdown after which the breakdown voltage may be increased as the whiskers are burned off. Figure 3.1.3 shows increasing prestrike voltages during the five first breakdowns indicating voltage conditioning (whisker burn-off?).

Contact speed and contact material have great influence on prestrike behaviour of vacuum switches.

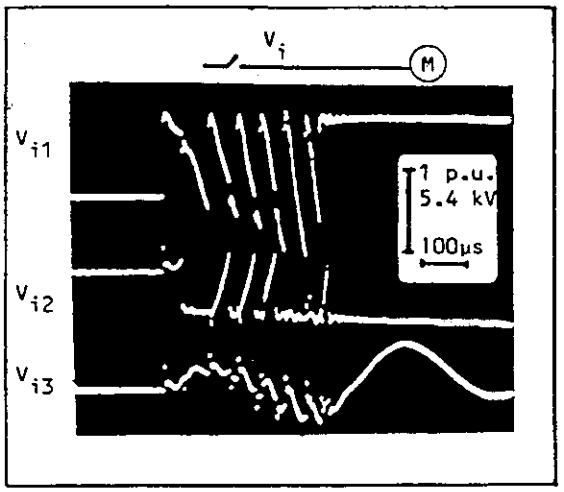

Figure 3.1.3
Example of voltage escalation during switching-on of a 185 kW, 6.6 kV motor with a vacuum breaker [39].
V_{i1}, V_{i2} and V_{i3} are the phase-to-earth voltages at the terminal of the breaker.

The amplitude and rate-of-rise of the overvoltages at switching-on are influenced by the surge characteristics of the motor, the connecting cable and the supply network, while the type of switch seems to have no influence on normal prestrikes (without repetitive reignitions) [57].

The time to peak of the overvoltages has been shown to increase slightly with the length of the cable between the switch and the motor [24, 52] while the initial rate-of-rise is unaffected by the cable length. Belted cables seem to give higher rate-of-rise than coaxial type [52].

A high surge impedance of the supply reduces the amplitude (and rate-of-rise) of the surge, while lumped source side capacitances close to the switch (e.g. compensation capacitors or a large number of cables connected to the supply bus) enhances the overvoltages.

Peak-to-peak voltage excursions up to 15 kV (3 p.u.) in 0.5 μs have been measured at switching-on of 6 kV motors according to reference [6]. Transients of up to 3.5 p.u. with front times as short as 0.2 μs are mentioned in reference [43]. In reference [57] a switching-on of a 5400 kW, 11 kV motor is presented that illustrates the enhanced transient in the second or third pole to close, due to the oscillations excited when the first pole closes. See Figure 3.1.4.

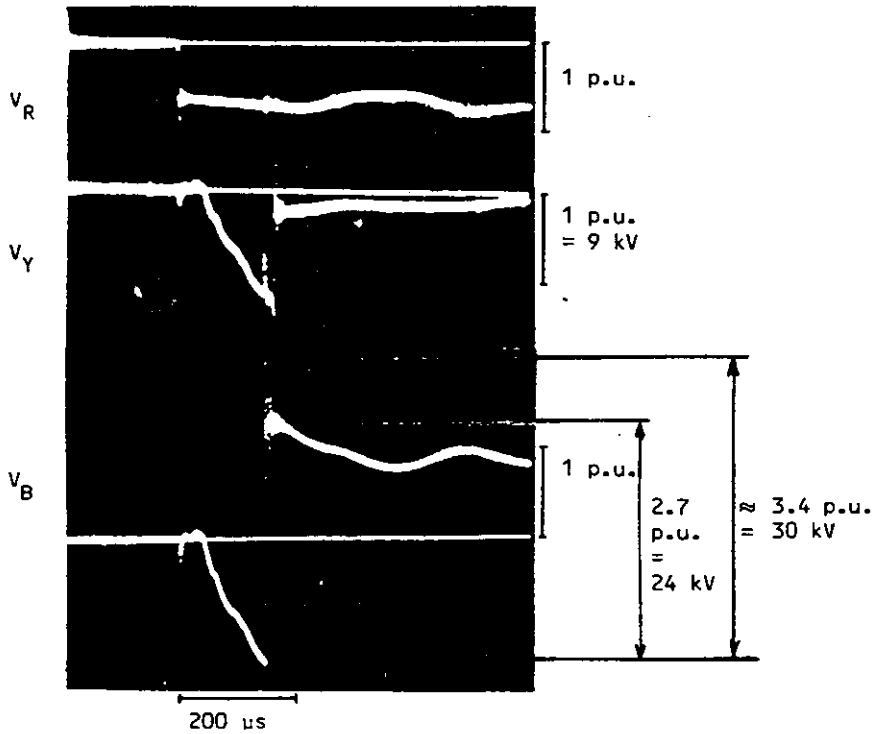

FIGURE 3.1.4 Switching-on of a 5 400 kW, 11 kV synchronous motor, with an SF_6 contactor.

A peak-to-peak excursion of at least 3.4 p.u. is shown (probably closer to 4 p.u. since the maximum overswing may not have been sampled).

Repetitive prestrike transients, in the worst case, can be considered to involve 20 to 30 major strikes, with swings occasionally above 3.0 per unit and rise times of 0.2 to 1.0 μs [26, 39].

When conditions for enhanced prestrike transients due to voltage escalation exist, then similar overvoltage enhancing phenomena may occur at interruption of motor starting currents. Precautions taken to prevent motor damages at interruption are also effective at switching-on.

It should be noted that motor failures observed at switching-on also may be the result of an insulation damage caused by overvoltages at a preceding interruption. However, there are several evidences that switching-on operations have caused motor failures [39, 43].

When interruptions of starting currents and stalled motors are avoided, the closing transients will represent the most severe case for the motor. Frequent operations will produce transients at switching-on that may give a statistical risk of excessive overvoltages as well as successive degrading of the insulation eventually leading to breakdown.

3.2. RANGES OF PARAMETERS

In the following a summary of published information about typical parameters when breaking the current of asynchronous motors is given. Parameters may be classified in three categories.

3.2.1. Power frequency characteristics of motor

voltage	2 kV...14 kV
power	100 kW...40MW
starting current	6...7 x motor rated current
no-load current	$\approx$ 0.3 x motor rated current
cos φ of the starting current	0.1...0.2
cos φ of the no-load current	$\approx$ 0.1
cos φ of the load current	0.7...0.9

3.2.2. Parameters associated with natural frequency of motor

A summary of measured values available is shown in Table 3.2.1. Unless the cables are very long the range of the frequency is 2...20 kHz. The highest values are observed for lower rated voltages. The amplitude factor γ is approximately 1.8.

Because of the relatively small capacitance of the motors, very short cables between the motor and the circuit-breaker have a great influence on the frequency of the transients.

3.2.3. Parameters associated with steep waves

The surge impedances and travelling times are essential for high frequency phenomena.

The surge impedance of the motor is calculated using the equation

$$Z_i = \sqrt{\frac{L_i}{C_i}}$$

where

L_i stray inductance of the winding
C_i capacitance to earth of slot portion of the winding

TABLE 3.2.1
The natural frequency of H.V. asynchronous motors

Tension nominale *Rated voltage* kV	Puissance nominale *Rated power* kW	Intensité de démarrage *Starting current* A	Capacité phase-terre du câble entre le disjoncteur et le moteur *Phase-earth capacitance of the cable between the circuit-br. and motor* μF	Longueur du câble *Length of the cable* m	Fréquence naturelle *Natural frequency* kHz		Référence
					1er pôle qui s'ouvre *1st pole to clear*	2e et 3e pôles qui s'ouvrent *2nd and 3rd poles to clear*	
3	110			0	15		[2]
				515	2		
	155		0		22		[3]
			0.01		10		
3	160	240		56	7.6	8.6	[4]
	110	133...140		551	2.1		
	110	140...164		165	4.3	4.4	
	92	145...158		470	2.3	2.3	
4		100 ; 240			4... 10		[5]
6	175	130	0.02	70	3		[6]
	210	100	0		11		
			0.02	70	3		
			0.16	350	1		
6	310	180	0.005	10	5	6	[6]
			0.14	300	1	2	
6	370		0		10		[3]
			0.01		6.6		
			0.1		2.3		
6	520	240	0	0	10	13	[6]
			0.02	70	5	5	
			0.11	250	2...3	2...3	
			0.16	350	2	2	
6	210	138...151		340	1.6...1.7	1.5	[4]
	210	141...151		120	2.3	2.13	
	2 500						
	synchron.	915		43	7.0	8.7	
7	150	100	0		10	13	[6]
			0.005	10	5	6	
			0.140	300	1	1	
7		100 ; 240				2...5	[5]
7		40...2 000		*not known*	2.4		[7]
12		80...4 000		*non connu*	2.4		
7		100...1 000		*no cables*	4...10		[8]
12		100...1 000		*pas de câbles*	4... 10		

Here the subindex "i" means "input" to emphasize that for high-frequency phenomena only the part of the winding near the terminal has an influence. Z_i is in principle not the same as Z_m in clause 3.1.2. It is important to note that Z_i is much higher than the surge impedance of the cable. The absolute magnitude of Z_i is not very important, the motor acts nearly as an open circuit for incoming steep waves. It seems also that measured values of Z_i and Z_m do not differ much from each other, see [2, 9]. A summary of surge impedance values is given in Table 3.2.2 and in Figure 3.2.1 [9].

TABLE 3.2.2
Typical ranges of surge impedance [2, 9]

Puissance nominale du moteur *Motor rating* kW	Tension du moteur *Motor voltage* kV	Impédance de choc (Z_m) *Surge impedance* (Z_m) kΩ
100	3 6	2...4 3...8
1 000	3 6 10	0.5...1 0.9...2 3

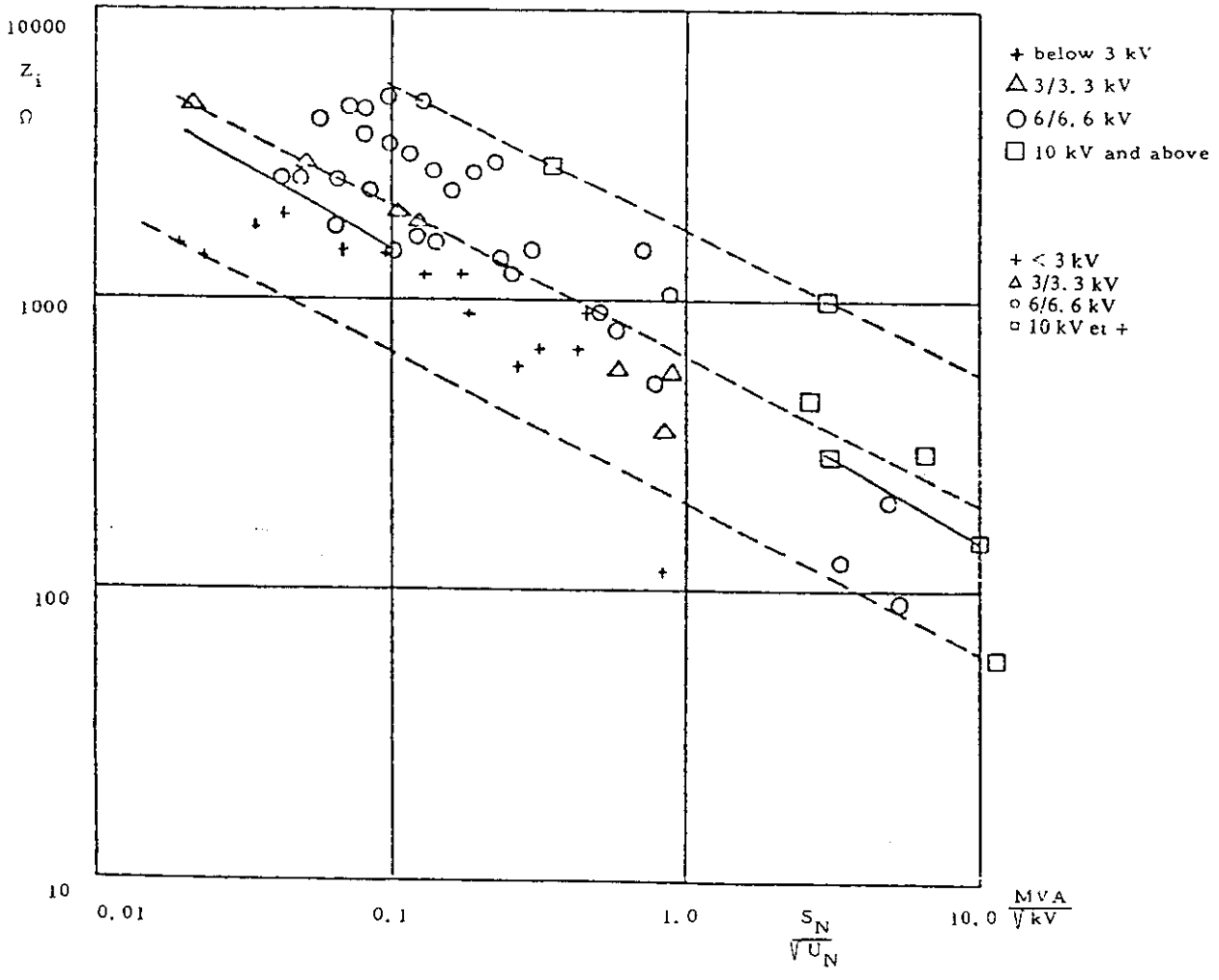

FIGURE 3.2.1 Surge impedance of rotating machines [9]

3.3. Interaction with circuit-breaker

The theory of different interactions with the circuit-breaker and the motor is the same as for all other cases of small inductive current switching, see Chapter 2.

3.4. Limitation of overvoltages and steep wave fronts

A low chopping current is most important, when low overvoltages are aimed at. The peak value of overvoltages may sometimes be limited by the low rate-of-rise of the dielectric strength of the circuit-breaker. However, in certain circumstances this may cause voltage escalation (Chapter 2, clause 2.5.3). The rate-of-rise of the incoming waves depends mainly on the following factors:

- system voltage
- characteristics of the cables (the length and surge impedance)
- lumped capacitances in the network
- reignition characteristics of the circuit-breaker.

The overvoltages may stress the motor insulation in two manners, the peak voltage stresses the phase-to-earth insulation, the steepness of the voltage wave may stress the insulation between turns. In general the following means of protection exist:

1) Surge capacitors connected phase-to-earth at the motor terminals mainly to control the steepness of the overvoltages.

2) Surge arresters of conventional or MO-type connected phase-to-earth to limit the phase-to-earth overvoltages. Some types may not fully protect the motor against steep waves [10, 21].

3) Both surge capacitors and surge arresters at the motor terminals may be necessary for complete overvoltages protection [18] including lightning overvoltages.

4) RC-circuit connected phase-to-earth [11] (typically 100 Ω, 0.1...0.2 μF) either
   a) at the circuit-breaker
   b) at the motor terminals

5) The circuit-breaker is equipped with breaking resistors typically some 100 Ω or non-linear resistance inserted by interruption in the main break for 20...30 ms [12].

6) Saturating series reactor at the circuit-breaker terminals [21].

7) An RC-circuit with the resistor parallelled by a MO-varistor (ZORK-suppressor)[40, 57] connected:
   a) at the motor terminals
   b) at the circuit-breaker if the cable is short(< 15 m)[40].

To get an idea of typical overvoltages when switching off a motor, a summary of values is given in Table 3.4.1.

Figures 3.4.1 and 3.4.2 [6] are based on 500 tests with a 12 kV oil-minimum circuit-breaker, when interrupting motor starting currents. They show the general tendency, i.e. that the highest overvoltages are observed when the motor is relatively small and the cable length is about 100 m. For other circuit-breakers different curves may be obtained.

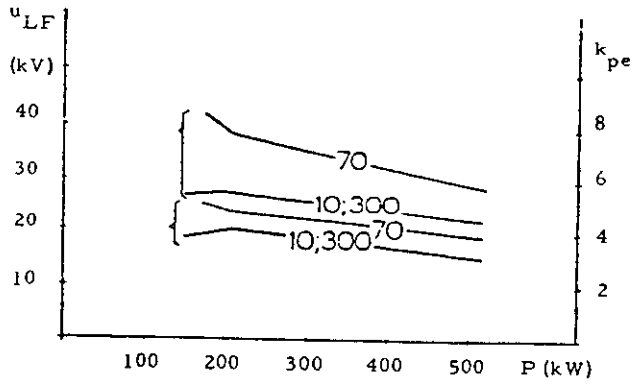

FIGURE 3.4.1 Phase-to-earth overvoltage when interrupting motor starting currents.
u_{LF} overvoltage
k_{pe} overvoltage factor referred to the peak value of the rated motor phase-to-earth voltage (√2/3 x 6 kV)
10, 70 and 300 are cable lengths in meters (from circuit-breaker to motors)

a) 98 % (50%+ 2σ) probability values.
b) Mean values

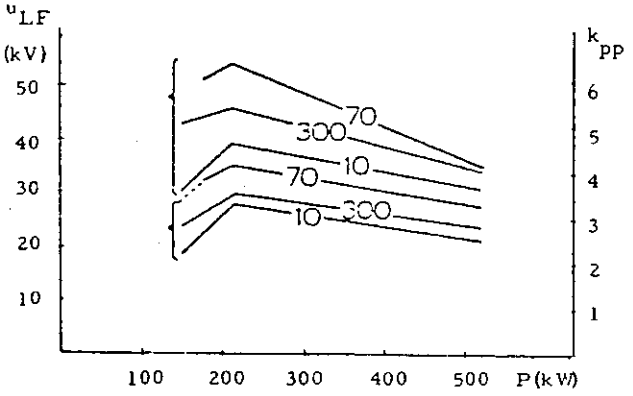

FIGURE 3.4.2 Phase-to-phase overvoltage when interrupting motor starting currents

k_{pp} overvoltage factor referred to the peak value of the rated motor voltage (√2 x 6 kV).
The other symbols are given in Figure 3.4.1.

TABLE 3.4.1

Summary of phase-to-earth overvoltages when switching off a motor.

The overvoltage factors are referred to the peak values of the rated motor phase-to-earth voltages (√2/3 U). Values only indicate the order of magnitude and should not be generally used.
In practical applications overvoltage protection may be applied to limit the overvoltages.

U kV	P kW	Longueur de câble m (+ capacit. addition.) *Cable length* *m* *(+ add. capacit.)*	Nombre d'essais *Number* *of tests*	Conditions *S* : démarrage *R* : en marche *Condition* *S : start* *R : running*	Disjoncteur *Circuit-breaker*	Facteur de surtension maximum *max. overvolt.* *factor*	Référence *Reference*
3	110	165 551	14 9 10 6	*R* *S* *R* *S*	à faible volume d'huile *oil minimum*	2.3 3.7 1.4 4.3	[4]
3	92	470	12 8	*R* *S*	à l'huile *oil*	1.5 4.8	[4]
3	160	56	4	*S*	à air comprimé *air blast*	6.8	[4]
3	90	70 + 0.2 μF + 4 μF	4 4 4	*S* *S* *S*	à air comprimé (sans résistance) *air blast* *(without resistor)*	7.8 6.8 4.1	[13]
3	90	70 + 0.2 μF + 4 μF	16 4 4	*S* *S* *S*	à air comprimé (avec une résistance de 200 Ω) *air blast* *(+ 200 Ω resistor)*	3.4 3.9 3.2	[13]
3	75	100 + 0.01 μF + 0.05 μF		*S* *S* *S*	interrupteur à vide *vacuum switch*	6.0 5.0 3.8	[14]
6	175	70	20 71	*R* *S*	à faible volume d'huile *oil minimum*	2.8 9.8	[6]
6	210	120 340	15 11 17 6	*R* *S* *R* *S*	à faible volume d'huile *oil minimum*	1.4 3.5 2.8 3.5	[14]
6	210	70 0 70 350	10 20 34 20	*R* *S* *S* *S*	à faible volume d'huile *oil minimum*	2.8 5.5 8.3 5.9	[6]
6	310	10 300	21 22 11	*R* *S* *S*	à faible volume d'huile *oil minimum*	2.8 4.6 4.9	[6]
6	520	70 0 70 250 350	9 26 50 21 35	*R* *S* *S* *S* *S*	à faible volume d'huile *oil minimum*	2.2 5.1 6.7 4.9 4.2	[6]
6	210	340	44 16	*R* *S*	à air comprimé *air blast*	3.8 7.2	[4]

TABLE 3.4.1 (continued)

U kV	P kW	Longueur de câble m (+ capacit. addition.) *Cable length* *m* *(+ add. capacit.)*	Nombre d'essais *Number* *of tests*	Conditions *S*: démarrage *R*: en marche *Condition* *S: start* *R: running*	Disjoncteur *Circuit-breaker*	Facteur de surtension maximum *max. overvolt.* *factor*	Référence *Reference*
6	2500	43	6	*S*	à air comprimé *air blast*	2.7	[4]
6	110	100	10	*S*	interrupteur à vide *vacuum switch*	5.1	[13]
7	150	140	20 28	*R* *S*	à faible volume d'huile *oil minimum*	2.8 5.2	[6]
7	155	170 + 0.25 μF + 0.85 μF	20 45 7	*S* *S* *S*	à faible volume d'huile *oil minimum*	4.7 5.0 3.2	[13]
7	220	108 + 0.2 μF	25 10	*S* *S*	à faible volume d'huile *oil minimum*	4.1 3.9	[13]
7	155	184 (C = 0.1....0.85 μF)	24	*S*	magn. dans l'air *magn. air*	2.1	[13]

3.5. Surge voltage withstand of motors

3.5.1 Surge voltage distribution

The voltage stress caused by the natural oscillation of the motor (frequency < 20 kHz) is distributed evenly in the coils of the winding in the same way as the power-frequency stress is distributed.

Switching-on and arc reignitions generate steep fronted surges which may have a rise-time of less than a microsecond. When a steep fronted surge penetrates the winding significant stresses appear only over a portion of the winding at the same time. The length (l) of this portion may be calculated, if the rise-time (τ) and the mean velocity (v) of the surge are known: $l = v\tau$. For steeper surges fewer turns share all the voltage and the interturn stress is higher.

Figure 3.5.1 shows an example of the influence of winding length and front time on the relative stress of the line-end coil [50].

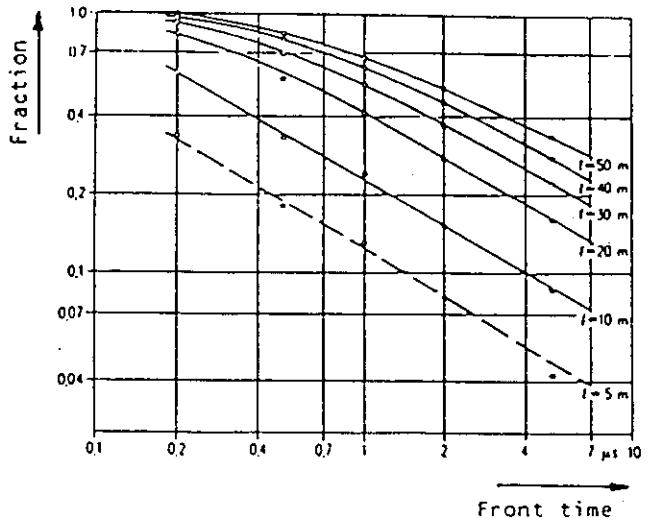

Figure 3.5.1
Fraction of incident voltage appearing across entrance coil as function of impulse front time for different conductor lengths,l, of the coil [50].

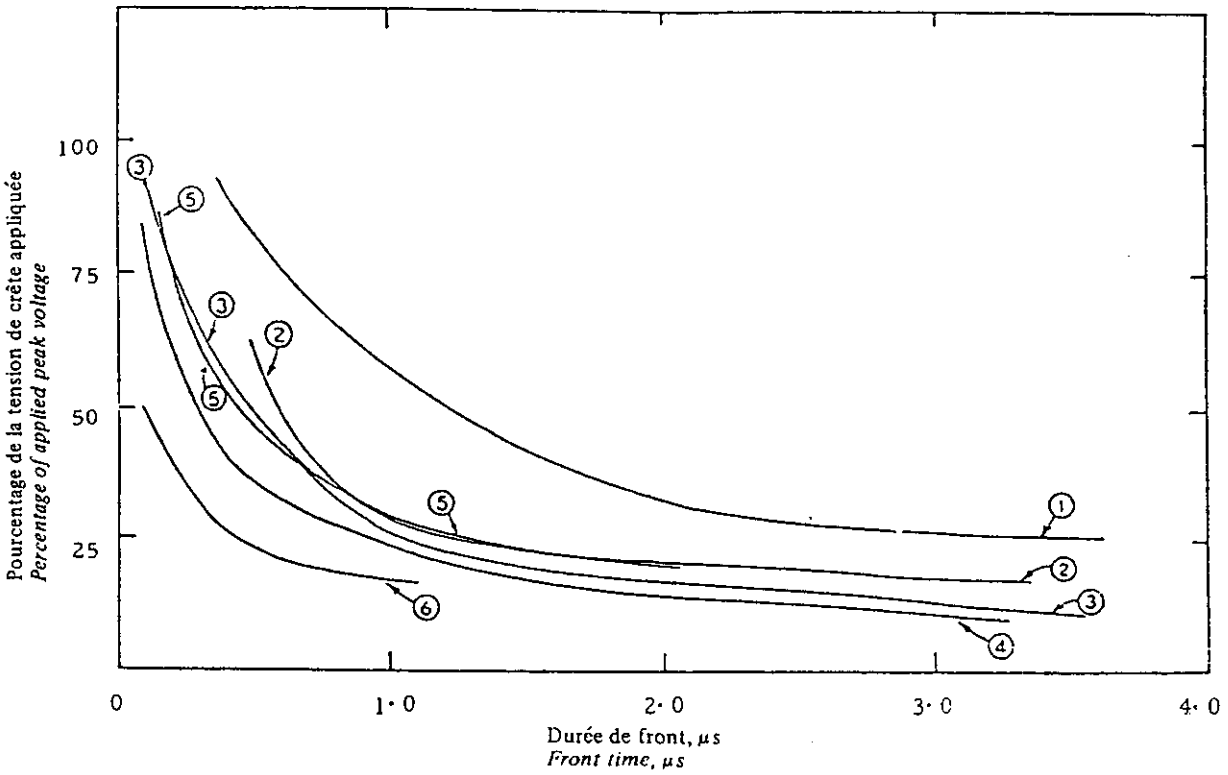

FIGURE 3.5.2 Comparison of peak line end coil voltages as a function of front time [15]

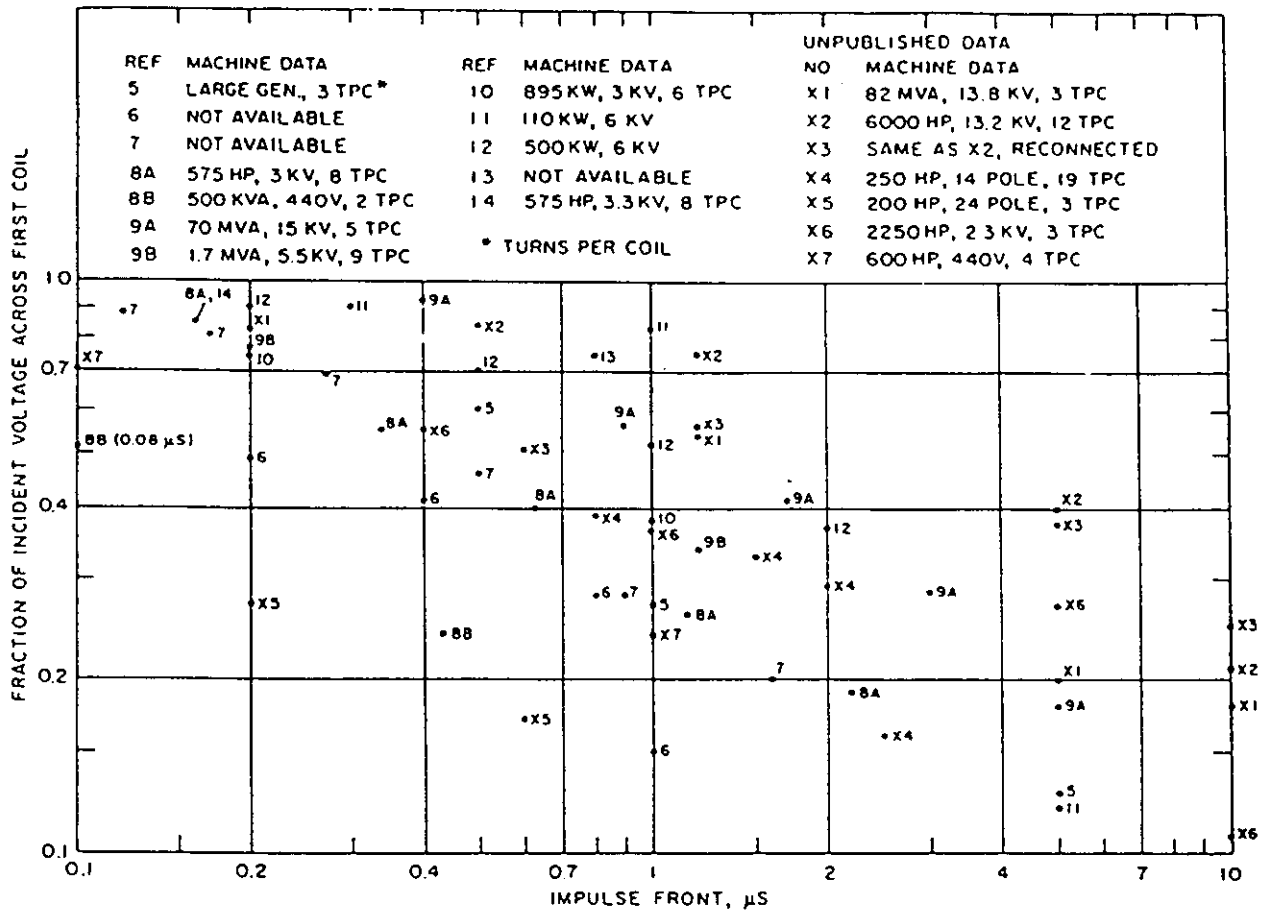

FIGURE 3.5.3 First coil voltage vs. impulse front [41]

The front of the surge becomes less steep, when it penetrates the winding, due to eddy currents and reflections from the discontinuities of the surge impedance of the winding. The interturn voltage stress is therefore highest in the line-end coil of the winding.

Figures 3.5.2 and 3.5.3 summarizes published measurements of surge voltage distributions. There is a tremendous spread in the data due to the wide range of pertinent variables represented. However, the conclusion can be drawn that the peak voltage across the line-end coil may be as high as 70 to 90 % of the total voltage across the winding at front times of 0.2 μs.

Within a coil a fairly even distribution is reported [28, 51] even though at extremely short front times (< 0.5 μs) a certain nonlinearity has been found. Figure 3.5.4 from reference [28] shows that the larger interturn voltages then are developed towards the inner end of the line-end coil. A similar result is also reported in reference [55].

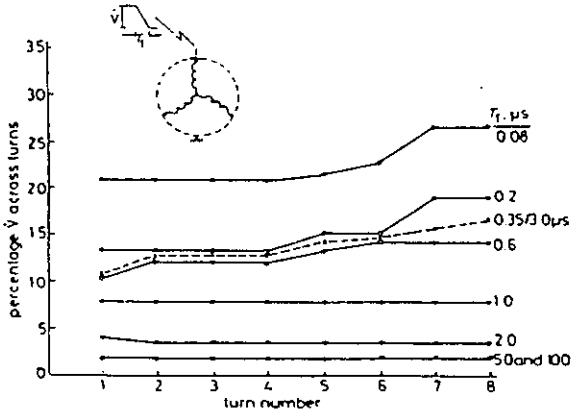

FIGURE 3.5.4 Line-end coil interturn voltages /28/

3.5.2 Surge voltage withstand testing

While the IEC standard, Publication 34-1 [44], requires routine tests with one minute power frequency voltage of (2U+1 kV), the testing of the ability of motor insulation to withstand steep voltage surges is not standardized, although discussions are going on within IEC [45, 46, 54] and IEEE [41, 56].

The power frequency testing stresses the insulation to earth (main insulation). Besides the routine testing at (2U+1) kV an IEC TC 2 Working Group (WG 15) is considering type tests on two representative coils by rising the power frequency voltage with 1 kV/s up to a break down voltage of not less than 2(2U+1 kV) [46, 54]. This test is regarded as a substitute for an impulse withstand test of the main insulation.

The power frequency tests stress the interturn insulation only moderately. Special tests to prove the interturn insulation has been under discussion for many years and several proposals have been published. Tests with separate coils or specially prepared single turns have been suggested. Some of the proposals are as follows:

- Working group 15 of IEC TC 2 proposes type tests with highfrequency oscillation voltage across the terminals of two separate (representative) coils [54], with an amplitude of 7.2, 14.4 and 24 kV for motors with rated voltage of 3.0, 6.0 and 10 kV respectively (corresponding to k = 2.9 p.u). The proposal is based on the assumption that 50 % of the total voltage appears across the entrance coil (for the standard 1.2/50 μs impulse). The total winding is supposed to be stressed with k = 6 p.u.

- High-frequency oscillation routine tests of separate coils are proposed by an IEEE working group for trial use [47]. The test amplitude is suggested to be equal to the rated voltage, U, but with a minimum of 0.35 kV per turn.

- Surge testing with various impulse shapes of separate coils as well as complete motors has been discussed. E.g. in Europe proposals have appeared to test new motors with a standard 1.2/50 μs impulse of amplitude (4U+5 kV) [41]. Other proposals have favoured shorter front

times (0.2 to 0.35 μs) and – for practical reasons – also short wave-tail durations of a few μs [28]. When testing separate coils the amplitude should be 70 to 90 % of the withstand level for the complete motor.

- Power frequency testing of the interturn insulation using cut windings or special test coils, with r.m.s. voltages of 2.1, 3.2 and 4.7 kV for 3.3, 6.6 and 11 kV motors respectively according to UK-requirements (CEGB). The German standard VDE 0530 requires a similar test at somewhat lower voltages.

- Impulse testing of the interturn insulation with a 0.25/0.8 μs surge of amplitude (U+1.25 kV), corresponding to 25 % of a required total motor withstand of (4U+5 kV). This is based on the assumptions that the line-end coil is stressed by the full surge voltage, that the distribution within the coil is linear and that the number of turns per coil is > 4. The amplitudes for 3.3, 6.6 and 11 kV motors are thus 4.5, 7.8 and 12.3 kV respectively [48].

Table 3.5.1 summarizes the test values in some existing and proposed tests.

Routine tests with oscillating voltages have been discussed but no general rules for the peak values and frequency are proposed [46, 54].

3.5.3 Surge voltage withstand

The surge voltage withstand of the main insulation (to earth) is deemed to be 1.25 times the crest value of the 1 minute power frequency test voltage, i.e. 1.8 times the r.m.s.-value [45, 46, 54].

Based on present routine testing of a complete motor with (2U+1 kV) the minimum surge voltage withstand figures of the main insulation will therefore be 5.0, 4.7 and 4.5 p.u. for 3.3, 6.6 and 11 kV motors respectively.

TABLE 3.5.1
Summary of power frequency and surge voltage withstand tests.

	System voltage U 3.3 kV		6.6 kV		11 kV	
	Test voltage kV	*Voltage ampl. p.u.*	*Test voltage kV*	*Voltage ampl. p.u.*	*Test voltage kV*	*Voltage ampl. p.u.*
Power frequency type test, rms value						
Earth insulation withstand voltage of two representative coils, proposal of IEC TC 2 WG 15 [54]:						
2 (2U + 1 kV) rising with 1 kV/sec	15.2	8.0	28.4	7.5	46	7.2
Interturn insulation withstand voltage (1 min), per turn						
(Spec. VDE 0530): (U/3)	*1.1*	*0.6*	*2.2*	*0.6*	*3.7*	*0.6*
(CEGB spec.): (U/3 + 1 kV)	*2.1*	*1.1*	*3.2*	*0.8*	*4.7*	*0.7*
Power frequency routine test, rms value						
Earth and interphase insulation withstand voltage (1 min)						
IEC 34-1: (2U + 1 kV)	7.6	4.0	14.2	3.7	23	3.6
Surge voltage type test (proposals), peak value						
Earth and interturn insulation withstand voltage, complete motor:						
(4U + 5 kV), 1.2/50 µsec.	18	6.7	31	5.8	49	5.5
Interturn insulation withstand voltage, complete coil:						
(2U + 10 kV), 0.3/3 µsec.	16.6	6.2	23.2	4.3	32	3.6
Interturn insulation withstand voltage, per turn:						
0.25 (4 U + 5 kV), 0.25/0.8 µsec.	4.5	1.7	7.8	1.5	12.3	1.4
High frequency oscillating volage type test, peak value						
Interturn insulation withstand voltage, complete coil, proposal of IEC TC 2 WG 15						
[54], (*)	7.2	2.9	14.4	2.9	24	2.9
High frequency oscillating voltage routine test, peak value						
Interturn insulation withstand voltage, complete coil, IEEE Std. 522-1977 [47]:						
U kV (min 0.35 kV/turn)	3.3	1.2	6.6	1	11	1.2

(*) The values are based on rated voltages 3.0, 6.0 and 10 kV respectively.

By the type testing proposed by IEC TC 2 WG 15 with rising power frequency voltage the insulation to earth is stressed by crest voltages of 21 kV, 40 kV and 65 kV for 3.3, 6.6 and 11 kV motors respectively corresponding to 7.8 ... 7.2 p.u. overvoltage factor.

An IEEE working group has presented a minimum impulse voltage withstand envelope as a function of the front time considered appropriate for a.c. rotating machines of recent design valid also for aged motors operating within their rated temperature limits [41].

For wave fronts equal to or longer than 5 μs the withstand voltage should be:

$$V = 1.25 \sqrt{2} (2U+1 \text{ kV})$$

and for front times in the interval 0.2 to 5 μs the withstand value decreases linearly with the front time down to a value of $2\sqrt{(2/3)}*U$ at 0.2 μs. See Figure 3.5.5.

In Europe the acceptable impulse voltage level nas been discussed frequently [9, 42, 48, 49, 50, 51, 53, 54]. The surge amplitude mostly considered has been (4U+5 kV), i.e. 6.8, 5.8 and 5.5 p.u. for 3.3, 6.6 and 11 kV motors respectively [41, 49]. Front times of 1.2 μs have usually been considered, but also shorter times seem to be accepted at least in special cases [50].

It must be observed that these withstand levels are restricted to motors in new and cold condition. High winding temperatures and ageing may result in a considerably decreased voltage withstand.

The Working Group has asked some of the main motor manufacturers to give a safe surge withstand value at different front times.

Figure 3.5.5 presents the result of the enquiry for 6.6 kV motors. Answers from five motor manufacturers are within the hatched area. The IEEE envelope falls below this, but it should then be remembered that the envelope is also taking ageing into account.

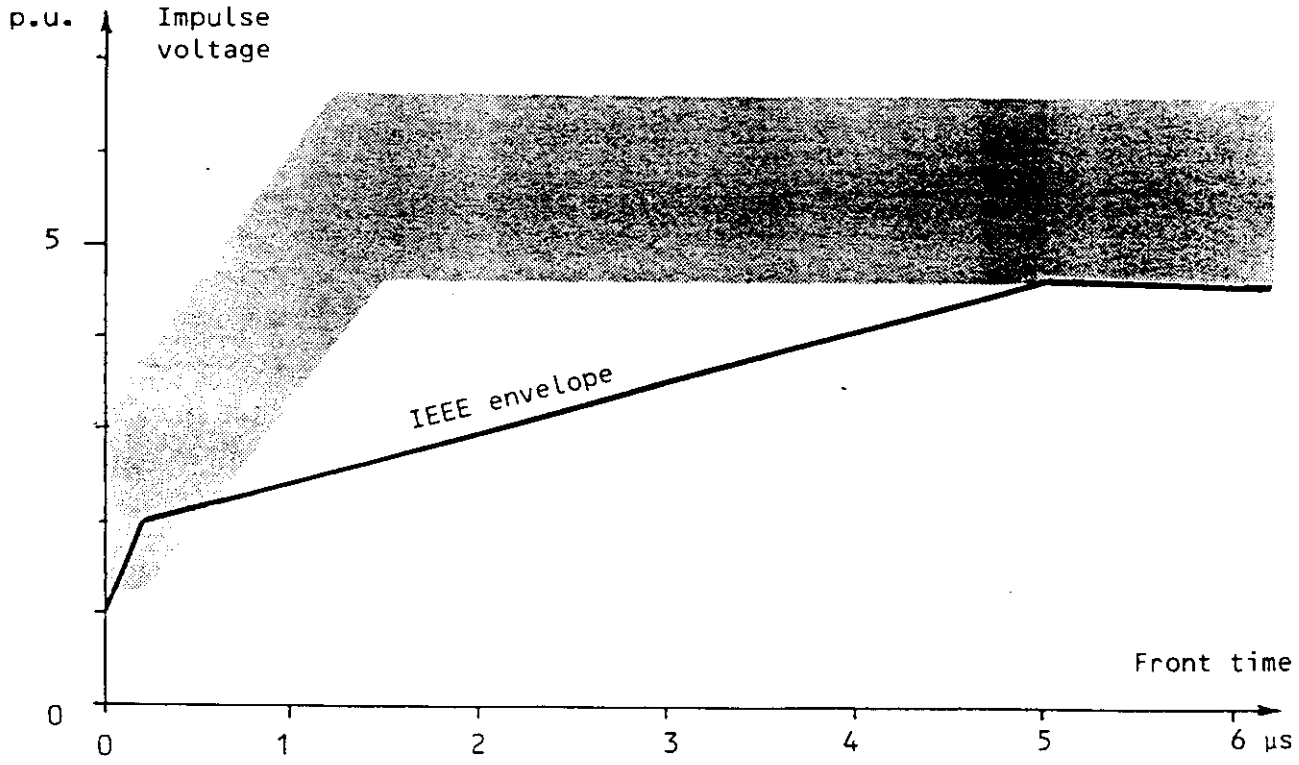

FIGURE 3.5.5 Impulse withstand levels of 6.6 kV motors.

Several investigations [1, 6, 26, 28, 29, 39, 43] show nevertheless that transients with magnitudes above the IEEE-curve with wave fronts < 1 μs may occur at normal switching-on. To overcome this in the U:S.A. the use of surge capacitors at the motor terminals is very common and this will reduce the steepness considerably and may explain the generally good operational experience.

Many motor manufacturers also claim a surge voltage withstand, which is at least 3 p.u. at 0.2 ... 0.5 μs front time. This covers the maximum stresses that seem to be expected at normal energization in the majority of cases according to clause 3.1.3 and may explain the relatively few failures in other countries, where surge capacitors normally are not used.

Surge arresters are deemed to have a minor influence on closing transients since the amplitude to earth is normally below the protection level (although the swing is larger). Other overvoltage limitation methods may or may not be effective. See clause 3.4.

The hatched area covers the withstand values given by 5 manufacturers. The IEEE envelope according to ref. [41]

3.6. TESTING

3.6.1. Testing objective

Testing can be done with any of a number of different objectives. In this report the specific and general objectives are distinguished:

Specific:

To investigate the performance of the circuit-breaker for a specific motor installation in the field.

General:

To investigate the performance of the circuit-breaker over a wide range of motor ratings and in various installations.

To investigate the performance of the circuit-breaker means:

a) To confirm the ability of a circuit-breaker to switch motors.

b) To establish the switching overvoltage performance of the circuit-breaker when switching motors.

This report concentrates mainly on objective b) and in this respect it may apply also to switching devices other than circuit-breakers, e.g. high-voltage switches and contactors.

3.6.2. Test criteria

The circuit-breaker must be able to execute the prescribed motor switching operation within the specified time, without damage of excessive wear and without external hazards like dangerous exhausts, flames, etc.

At the moment it is not possible to establish the criteria for the switching overvoltage performance. This is because there is no rated lightning and/or switching impulse withstand voltage prescribed by standards for motors, nor is there enough information about the withstand strength and deterioration of motor insulation, when subjected to repetitive switching overvoltage waveshapes. Therefore, it should be left to the user and/or manufacturer to judge test results with respect to the equipment in question. When interpreting test results, attention should be paid particularly to:

a) Low frequency maximum overvoltages, at the motor terminals (u_{LF} in Figure 3.6.1). This is the maximum voltage attained by complete half cycle voltage excursions at the natural frequency of the motor, with the cable connected. The order of magnitude is 1 to 20 Khz, see Table 3.2.1.

This value could approximately be referred to the motor 1 min power-frequency withstand voltage.

b) Maximum overvoltages, at the motor terminals (u_p in Figure 3.6.1). This is the maximum voltage attained, regardless of frequency or duration. The maximum overvoltage could be referred to values between 1 min power-frequency withstand and impulse strength of motor.

c) Maximum peak to peak voltage excursion at a reignition (u_s in Fig. 3.6.1). This value could be referred to the level of interturn insulation of the motor.

d) Initial voltage (u_c in Fig. 3.6.1).

e) Suppression peak voltage (u_m in Fig. 3.6.1). From u_c and u_m information can be gained of the chopping behaviour of the breaker under test.

When evaluating overvoltages at a complete three phase interruption u_{LF}, u_p and u_s should be used to denote the highest value of each type of the entire interruption process in all three phases. On the other hand, u_1, u_c and u_m, which are mainly used for determination of chopping currents, should be evaluated separately for each interrupting attempt. In this case the final interruption in each phase is normally of most interest.

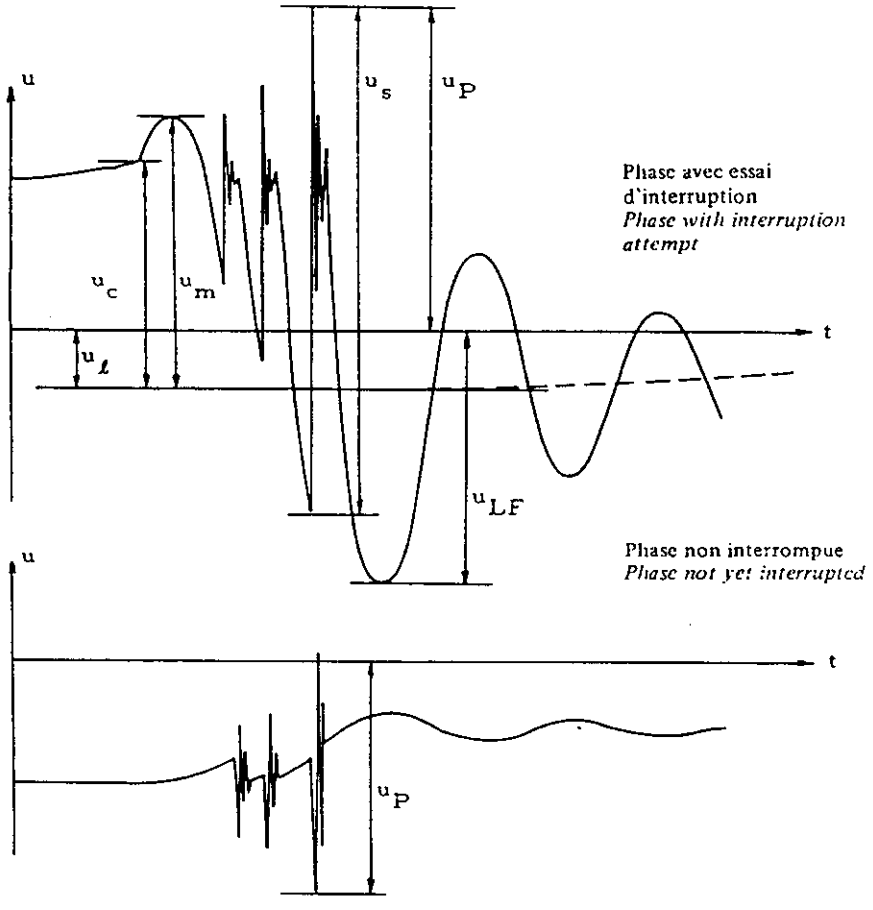

FIGURE 3.6.1 Illustration of load side voltages

u_1 Instantaneous value of the remaining power frequency voltage.
u_c Initial voltage.
u_m Suppression peak voltage.
u_{LF} Low frequency overvoltage (to earth).
u_p Maximum overvoltage (to earth).
u_s Maximum peak-to-peak voltage excursion at reignition.

3.6.3. Test conditions

In summary the motor switching overvoltages depend on:

A – Motor:

* Motor type and characteristics

* Power-frequency parameters like operating voltage, current, power factor, leakage inductances.

* Transient parameters, particularly natural frequencies, surge impedance, input capacitances.

* Motor operating conditions like no-load, starting, load.

B – Electrical system (configuration and parameters)

* The motor side of the circuit-breaker, particularly the length, type and parameters of the connections between the circuit-breaker and the motor (e.g. cable surge impedance, attenuation) any capacitances to earth, power factor compensating capacitors and mutual coupling between phases.

* Source side of the circuit-breaker, particularly power factor compensation capacitors, capacitances-to-earth and between phases close to the breaker and mutual coupling between phases, number of parallel cables. The phenomena seem to be relatively insensitive to the configuration of the system further away from the circuit-breaker, also to the short-circuit current of the system.

* Mode of system earthing and earthing of the load side.

C – Circuit-breaker

* Type of the circuit-breaker, particularly its characteristics on chopping levels, dielectric recovery, restriking behaviour and their statistical variations.

* Specific operating conditions as instant of contact separation with respect to the current wave.

This summary does not intend to list all the possible items which could influence the overvoltages, however, it attempts to list the important ones, and/or indicate the area which should receive attention.

It is noted that a change of conditions described in any of the above paragraphs could lead to a substantial change in overvoltage. Moreover, it is noted that a voltage shape, measured during any particular test, may differ from that obtained at some other test under the same test conditions. The statistical variations of the circuit-breaker performance call for statistical evaluation and description of the overvoltage.

3.7. TEST CIRCUITS

3.7.1. Field tests

The enumeration of critical test conditions in 3.6.3 indicates that only testing in the field can produce conditions which will allow the full assessment of the ability of a certain circuit-breaker in the specific condition. The test circuit is fully defined by the installation itself: one should take care that the circuit will not substantially be changed by connection of measuring and protective devices (e.g., the capacitance of the capacitive dividers should be smaller by an order of magnitude than other adjacent capacitances).

The test results, even though reliable for that specific installation, should be extended to other installations only with the utmost caution.

3.7.2. Laboratory tests

3.7.2.1. Specific tests

The laboratory test circuit should represent the actual installation as closely as possible. Namely, it should be a three-phase circuit which includes the proper length and type of actual cables from the circuit-breaker to the motor. A substitute circuit for cable representation (e.g. π or τ sections) should be used only cautiously. The circuit should include motor surge protective capacitors, if any. The capacitances connected on the source side of the circuit-breaker should be estimated and adequately represented. For some tests, even the distance between those capacitances and the circuit-breaker (some tens of meters representing the inductances of the order of tens of μH) may be important.

If the actual motor cannot be used for the test, a laboratory substitute circuit could be a useful approximation.

Motor substitute circuit:

Figure 3.7.1 suggests a diagram of a substitute circuit for a three-phase asynchronous motor. This diagram is intended to represent the motor under starting conditions. The power-frequency impedance is represented by the linear inductance L and resistance R for each phase. The values of L and R are calculated from the test voltage, required starting current and associated power factor. The natural frequency and damping of the circuit, for both first-pole and last-pole-to-clear, are adjusted by means of capacitances C_p to earth and parallel resistance R_p.

Their values are adjusted to give the natural frequency and its damping for the simulated motor. Exact calculations are complicated due to the stray capacitances and resistance of the reactor L. This representation is adequate for both the first-pole and last-pole-to-clear transients. The surge impedance of the motor is not represented in any larger detail than that given by the parameters L, C_p, R, R_p. Mutual coupling between phases is neglected.

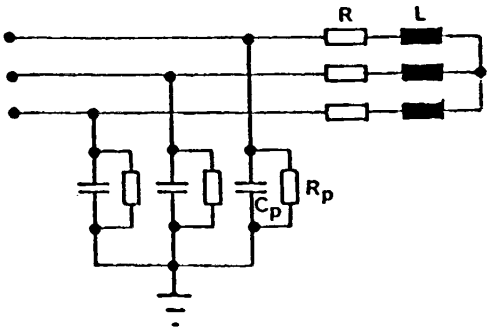

FIGURE 3.7.1 Motor substitute circuit.
L and R are calculated to give the specified current and power factor.

C_p and R_p are adjusted to give the specified frequency and damping.
R_p can alternatively be connected across the motorinductance R-L

The substitute circuit does not represent a running motor, because there is no back electromotive force.

The best test circuit is the actual motor circuit. However it is considered that the substitute circuit suggested will be useful.

3.7.2.2. General tests

It remains uncertain that a test procedure can be formulated to give reliable data for general use. This difficulty stems from the variations in performance of different types of circuit-breaker as well as from the large spread of different motor parameters and variations in their installations. Little knowledge has been accumulated to recognize the simplifications which would be generally acceptable without rendering the extrapolation of test results questionable. Therefore, the test circuit for general test purpose must be understood only as a means of providing limited information. This information may for some circuit-breakers assist in making calculations and in the exercise of judgement on the performance of the circuit-breaker in other applications. With this intention the parameters of the test

circuit should be varied to cover a wide range of applications as well as to expose the tested circuit-breaker to different stresses.

Figure 3.7.2 suggests a diagram of a test circuit for general test purposes.

The diagram is divided into sections representing the supply source, substation busbars, circuit-breaker, connection, and motor substitute circuit. The sections are specified below. The diagram does not show the measuring elements (e.g. capacitive dividers) and overvoltage protective elements which may be desirable to protect the circuit from switching overvoltage hazards.

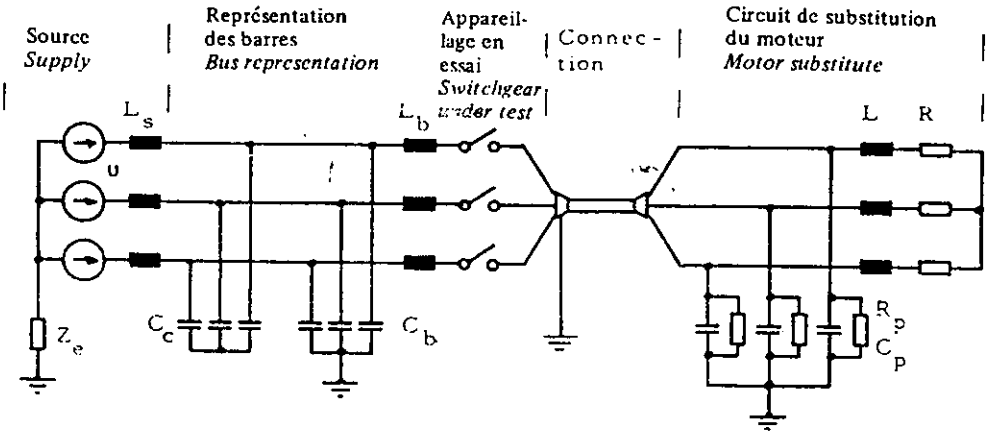

FIGURE 3.7.2 General test circuit

Z_e Earthing impedance
L_s Source inductance
U Source voltage (phase-to-phase)
C_s Bus capacitance
L_{b1} ≤ 2 μH
L_{b2} Inductance of the connections between circuit-breaker and motor
L Load inductance
R Load resistance
C_p Load parallel capacitance
R_p Load parallel resistance

The sections are specified as follows:

a) Supply source:

- Z_e impedance high enough to limit line-to-earth current to less than test current (can be infinite)
- U highest system voltage
- L_s $\omega L_s \leq 0.1\ \omega L$, but not lower than that corresponding to the rated s.c. current of the tested circuit-breaker
- C_s 0.03 to 0.05 μF for supply circuit A
  1.5 to 2.0 for supply circuit B
- L_{b1} ≤ 2 μH, stray inductance of capacitor connections

b) Bus representation:

- L_{b2} ≤ 5 μH, stray inductance of connections
- Bus representation formed by three bars of 5 to 7 m length, spaced at a distance appropriate for the rated voltage

In some cases reignitions with corresponding overvoltage generation occur in quite limited ranges of contact separation instant. More information about the overvoltages may then be obtained by performing additional tests in the critical range.

3.7.4. Measurements

By oscillograph or other suitable recording techniques at least the following quantities should be recorded:

- Power-frequency voltage
- Power-frequency current
- Phase-to-earth voltage, at the motor terminals, in all three phases, with slow and fast resolutions

In general testing it may further be valuable to measure the phase-to-earth voltage at the source side terminal of the tested breaker and/or the voltage across the circuit-breaker as well as the current through the circuit-breaker. These measurements should preferably make use of high speed recording technique.

Besides these recorded quantities the test report should include a thorough description of the circuit including the following details:

- Main dimensions of the bus, connections to the breaker and the type of L_b (lumped or distributed)

- The characteristics of the cable
  - Length
  - Rated values
  - Type - radial field (screened) or non-radial field (belted)
  - Main insulation dielectric - XLPE, paper/oil etc.
  - Earthing
  - Capacitances
  - Surge impedance

3.7.5 Switching-on (energizing) tests

Since the test circuit in Figure 3.7.2 is judged to be an acceptable representation of actual conditions in case of reignitions, it should also be useful when studying the overvoltage transients that may occur at closing the circuit. The influence of the circuit-breaker, the connection and the supply network characteristics may be investigated, while the absolute magnitude of the overvoltage should be treated cautiously.

The same number of tests may be used as when opening the circuit. Sometimes a higher number of tests may be needed, because the range in the point-on-wave control during which high overvoltages may occur, can be rather narrow.

3.8. RESULT EVALUATION

From the recorded quantities the following characteristics should be evaluated:

A - Overvoltage characteristics

The overvoltages at the motor terminals in each phase (see 3.6.2 Fig. 3.6.1):

* u_p maximum overvoltage
* u_{LF} low frequency maximum overvoltage
* u_s maximum peak to peak voltage excursion at reignition

C_{eq} total capacitance of phase under consideration

ω_{eq} angular frequency of the voltage oscillation after current interruption in phase under consideration

L_t load inductance per phase

This calculation neglects the damping of the circuit, but is anyway regarded as a reasonable approximation.

Attempts should be made to establish relationships between the chopping current, the circuit capacitances, and the breaking current.

The shape of the current through the breaker at reignitions, and thus the critical current rate of change at which a new interruption will occur, can only be recorded with fast measurement systems. If possible relations between the critical rate of change of current, the arcing time, and/or the contact distance should be determined.

The rise of dielectric strength between breaker contacts should preferably be determined from direct measurements of reignition voltage between the breaker contacts as a function of time after the interruption/chopping of the current. Alternatively the dielectric strength characteristic may be obtained by means of the source and load side voltage measurements, but great care must be exercised in this case since not only the load voltage but also the source voltage may vary rapidly during reignition processes. It should be attempted to relate the recorded curves of rise of dielectric strength to breaking current, arcing time and/or contact distance.

If the rise of dielectric strength between the circuit-breaker contacts does not depend on the current the dielectric recovery characteristic of the circuit-breaker may be determined separately by measuring the no-load characteristic with d.c. voltage applied through a resistance [23].

For certain interrupter types a few of the tests in a test series, due to reignitions, may give appreciably higher overvoltages than others. In such cases the number of tests giving reignitions should be stated.

For switching-on tests the steepness of the wavefronts should be given. The number of prestrikes during the test should be recorded. It may further be valuable to identify any correlation between overvoltage amplitude and number of prestrikes.

3.9. RESULT EXTRAPOLATION

The results obtained refer strictly to the tested circuit. Other interpretations of the results could be misleading. On the other hand, the test results offer some insight in the performance of the tested circuit-breaker. Based on this, the circuit-breaker performance in other circuits could be estimated.

3.9.1. Computer analysis

There exist a number of transient analysis computer programs which can be gainfully used to assess the circuit-breaker performance in a given installation. It is necessary to consider the following characteristics when modelling the breaker:

- the dependence of chopping level on load capacitance, current through the breaker and its rate-of-change (frequency of current oscillations).
- the ability to interrupt the current in dependence of rate-of-change of current and rate-of-rise of recovery voltage.
- the dependence of dielectric recovery on arc current, arcing time, contact separation and voltage wave shape.

The statistical variation of these characteristics should be taken into account.

c) Switchgear under test:

- includes possible overvoltage protection devices if they belong to the standard switching equipment

d) Connection:

- Cable, 100 ± 10 m, screened, Z_0 = 30 to 50 Ω. (Radial field cable is recommended to be used in the tests. The belted type may give different overvoltages [52].

e) Motor substitute, see 3.7.2.1 and Figure 3.7.1

- L load circuit 1: 100 ± 10 A
  load circuit 2: 300 ± 30 A
- R $\cos \phi \leq 0.2$
- C_p frequency 10 to 15 kHz
- R_p amplitude factor 1.6 to 1.8

Notes 1 The source impedance shall not be lower than that corresponding to the rated short-circuit breaking current of the tested circuit-breaker.

2 A high ohmic earthing impedance is permissible so that the supply voltage is defined with respect to earth. The resistance value must be high enough to limit a prospective line to earth fault current to a value below the test current. Use of such earthing resistance should be stated in the test report.

3 The switchgear under test includes the tested circuit-breaker with all its associated equipment including possible overvoltage protection devices if they belong to the standard switching equipment.

4 Testing at a current of 10 A representing the no-load conditions may occasionally be of interest depending on the type of the circuit-breaker. However, no substitute circuit for a motor can be suggested at the time being. The motor substitutes No. 1 and 2 do not represent the situation when a motor running at no-load is switched off, because the power-frequency recovery voltage in this case is very small compared to the case of breaking the starting current. The substitute circuit does not take into account the fact, that because the rotor is running, a voltage is induced in the stator with a frequency equal to the power frequency during the first periods.

3.7.3. Test series

For practical reasons only a limited number of test series should be mandatory. The following is thought to be a possible procedure:

TABLE 3.7.1

Test duty	Supply circuit	Motor substitute circuit
1	A	1
2	A	2
3	B	1
4	B	2

Each test duty should consist of at least 20 tests, differing in point-on-wave of contact separation by 9° el. (This is to avoid that the same phase angle at contact separation is repeated in the three phases). If the point-on-wave control of contact separation cannot be achieved, a total of 40 tests in each test duty is suggested with random circuit-breaker trip signal.

For each test series the above quantities should be evaluated for

- maximum value
- mean value
- standard deviation, σ - value

The frequencies of voltage oscillations should be evaluated.

B – Breaker characteristics

It is recommended that particularly for the general tests the following breaker characteristics are evaluated:

- chopping current
- rate of change of current at which the breaker is able to interrupt (after reignition)
- rise of dielectric strength between breaker contacts after interruption.

These characteristics may serve as a basis for estimates of the breaker performance in other circuits (see 3.9.1).

The chopping current should, if possible, be determined from current measurements. If this is not done, approximate values of the chopping current may, however, be deduced from the peak value of the suppression peak and the voltage across the load before current extinction, together with the frequency of the voltage oscillation following current interruption. In Chapter 2 , clause 2.3.3 the following factors were defined:

$$k_a = \frac{u_m}{u_o}$$

$$k_c = \frac{u_c}{u_o}$$

where

u_m the suppression voltage peak value
u_c the initial voltage at the moment of current chopping and
u_o the peak value (phase-to-earth) of the power frequency voltage

Figure 3.6.1 shows how u_m and u_c are defined.

The chopping current is then (from 2.3.3. Equation 2.3.18 with $\eta_m = 1$, unearthed load, no mutual inductance between phases:

$$i_{ch} = u_o\sqrt{\frac{C_{eq}}{L_{eq}}}\sqrt{k_a^2 - k_c^2} = \frac{u_o}{\omega_{eq} L_{eq}}\sqrt{k_a^2 - k_c^2}$$

where

L_{eq} is the equivalent inductance in the phase about to clear namely:
L_{eq} = 1.5 L_t for first phase to clear
L_{eq} = L_t for second and third phases to clear

and

3.10 REFERENCES in Chapter 3

[1] W. Pucher. – Överspänningar vid in– och urkoppling av högspända asynkronmotorer. Elteknik 6 (1963) 8, p. 139...146.

[2] W. Andrä, P.G. Sperling. – Beanspruchung der Wicklungsisolierung beim Schalten elektrischer Maschinen. Siemens Zeitschrift 49 (1975) 10, p. 672...677.

[3] Unpublished information (Oy Strömberg Ab).

[4] W. Andrä. – Unpublished information.

[5] IEC 17A (Secr.) 124, June 1972, Table 1.

[6] M. Karttunen, P. Paloniemi. – Use of the oil–minimum circuit–breaker as a high–voltage motor switch (in Finnish). Voima ja Valo 36 (1963) 12, p. 333...338. (A summary of test results: Proceedings CIGRE 1964, Discussion Gr. 13, p. 430...431).

[7] Comment on IEC 17A (Secr.) 81, Dec. 1967, 17A (Switzerland)66.

[8] Comment on IEC 17A (Secr.) 81, Dec. 1967 17A (Germany) 60.

[9] T.D. Smith. – Machine winding design with respect to vacuum contactors. L.S. Engineering Bulletin 13 (1975) 2, p. 14...18.

[10] W. Jakszt, K. Reichelt, G. Schiele. – 3 EF 1 Surge absorber for the protection of motors in industrial cable systems. Siemens Review 14 (1978) 2, p. 83...86.

[11] M. Murano, T. Fujii, H. Nishikawa, S. Nishiwaki, M. Okawa. – Voltage escalation in interrupting inductive current by vacuum switches. IEEE Trans. PAS–93 (1974) 1, p. 264...271.

[12] K.H. Hinterthür, D. Hoffmann, P. Huhn. – Mark worth, E.: Special switching problems in industrial circuits and their solution by the use of non–linear damping resistors. International Conference on Electricity Distribution 23...27 May 1977, London. Part 1: Contributions. Paper No. 6.4. IEE Conference Publ. No. 151 CIRED.

[13] K. Norbäck, J.K. Jakobsen, E. Thorstensson, W. Pucher. – Switching surges in connection with high voltage induction motors. CIGRE 1964, Report 116.

[14] I. Kano, T. Hakamada, Y. Kurosawa, H. Sugawara. – Switching surge phenomena in induction motor windings and their endurance. Hitachi Review 24 (1975) 5, p. 225...232.

[15] P.G. Parrot. – Surge voltage distribution in line–end coils of high voltage motor windings. ERA Report No. 5224 (1967).

[16] A.T. Roguski. – Hochleistungsschalter als Ursache und Begrenzungsmittel für Uberspannungen. Elektrie 19 (1965) 10, p. 429...434.

[17] C.E. Sölver. – Influences of reignition on overvoltages at switching of small inductive currents. To be published.

[18] IEEE Recommended practice for electric power distribution for industrial plants. IEEE Std 141–1976.

[19] F.A. Holmes. – An empirical study of current chopping by vacuum ars. IEEE Paper C–74–088–11, 1974.

[20] T. Itoh, Y. Murai, T. Ohkura, T. Takami. – Voltage escalation in the switching of the motor control circuit by the vacuum contactor. Trans. PAS-91, No. 5, P. 1897, 1972.

[21] G.C. Damstra. – Influence of circuit parameters on current chopping and overvoltages in inductive MV circuit. CIGRE 1976, Report 13-08.

[22] Y. Murai, T. Nitti, T. Takami, T. Itoh. – Protection of motor from switching surge by vacuum switch. IEEE Trans. PAS-93 (1974), p. 1472...1477.

[23] A. Hochrainer. – Investigation of the recovery of dielectric strength in alternating current breakers. CIGRE 1954, Report No. 112.

[24] J.P. Speedy. – The characteristics and application of vacuum switching devices. The South African Institute of Electrical Engineers – Symposium on the application of vacuum contactors and vacuum circuit breakers, 18 October 1978, p. A1...A13.

[25] R.W. Blower, K.J. Cornick, M.P. Reece. – The use of vacuum switchgear for the control of motors and transformers in industrial systems. IEE Conf. Publ. 168, 1978, p. 5...10.

[26] PRETORIUS, R.E. and ERIKSSON, A.J.
Field studies of switching surge generation in high-voltage vacuum contactor controlled motors – results of extensive practical investigations
IEE Conference Publication 210, 1982, p 54-64

[27] PRETORIUS, R.E.
Optimized surge suppression on high voltage vacuum contactor controlled motors
IEE Conference Publication 210, 1982, p 65-70

[28] CORNICK, K.J. and THOMPSON, T.R.
Steep-fronted switching voltage transients and their distribution in motor windings
Part 1: System measurements of steep-fronted switching voltage transients
Part 2: Distribution of steep-fronted switching voltage transients in motor windings
IEE Proc. Vol. 129, Pt. B, No. 2, March 1982

[29] FOURMARIER, M.P.
Sur les surtensions a front raide auxquelles peuvent ètre soumis les moteurs triphas#s raccordés a un réseau de cables lors de l'enclenchement et du déclenchement
Soc. Franc. é1. Bull. 7 sér. 3(1953), p 447-454

[30] RICHTERS, J.J., LIPPERTS, J.H.F.G., SCHNELLEKENS, H., COPPOOLSE, W., KLAASSEN, A.C., DE KONIG, B.N. and NOORDHUIS, B
Experiences related to the development of vacuum interrupters CIGRE 1982, Report 13-13

[31] MALLER, V.N. and THAKER, T.M.
Switching surge studies on high voltage motors with minimum oil circuit-breaker and vacuum contactor

[32] SLAMECKA, E. et al
Colloquium of Study Committee 13(Switching Equipment) Helsinki (Finland), September 1981
Electra No. 80, January 1982, p 25-41

[33] KARTTUNEN, M. and KEMPPAINEN
Experiences of a test circuit for switching of small inductive currents
Second CIGRE SC 13 Colloquium 1981 in Helsinki CIGRE 13-81(SC)15

[34] Berneryd, S. and Sölver, C.E.
Substitute test circuit for motor switching – Comparison tests.
Second CIGRE SC 13 Colloquium 1981 in Helsinki CIGRE 13-81(SC)17

The characteristics may be more or less important for different kinds of circuit-breakers. They are often given as input parameters as they otherwise will make the breaker model very complicated.

The tests described in the previous section can provide meaningful data for at least an approximate assessment of the circuit-breaker characteristics.

The computer study must adequately represent the system configuration. For some breakers even representation of small capacitances close to the breaker may be necessary. Estimation and representation of damping often presents problems, but its omission tends to give unrealistically high values of overvoltage.

3.9.2. Other estimation possibilities

Besides the thorough analysis according to Section 3.9.1, there are some possibilities to make coarse estimations of the circuit-breaker performance in other circuits.

When estimating the overvoltages it is necessary to distinguish between:

- overvoltages due to current chopping
- overvoltages due to reignitions

When the overvoltages are determined solely by current chopping (no reignitions occur) the highest overvoltage is usually observed at the suppression peak (see Fig. 3.1.2). For relatively high overvoltages ($k > 2$ p.u.) a rough estimate of the maximum amplitude is given by:

$$u_m \approx i_{ch,max} \cdot Z_m$$

where

$i_{ch,max}$ is the maximum expected chopping level in the actual case (dependent on load capacitance) and
Z_m the surge impedance of the motor defined by Equation 3.1.8.

(This equation is an approximation of Equation 3.1.8)

This crude method may give an idea of the maximum overvoltages especially in cases of such low currents that chopping may occur at current maximum.

A better estimate may be possible by considering the theory in Chapter 2, clause 2.3 if the breaker characteristics are sufficiently known from the general testing. The difficulty arises, however, when reignitions cannot be neglected. Reignitions may result in a limitation of the overvoltages [16] as well as in a considerable increase in overvoltage amplitude [11, 20]. Simplified estimation procedures taking reignitions into account have been suggested [17] but as long as they have not been proved by experience the method of thorough computer analysis seems to be the only safe estimation method.

[50] MEYER, H. and POLLMEIER, F.J.
Transiente Beanspruchungen der Spulenwindungsisolierung von elektrischen Maschinen mit Leistungen Uber 1 MW Siemens Energietechnik 3(1981):11-12, p 347-352

[51] SCHOPPER, E.
Stossspannungsbeanspruchungen als Kriterium fUr die Auslegung der Isolation rotierender elektrischer Maschinen E und M, 100(1983):5, p 200-205

[52] CORNICK, K.J and DAVENPORT, J.L.
The influence of switching transients on industrial motors CIRED 1983, report b.10

[53] ZWICKNAGEL, W.
Zur Stossspannungsfestigkeit von Hochspannungsmotoren und deren Prüfung
E und M 100(1983):5, p 206-212

[54] Revised proposal prepared by WG 15 relating to impulse voltage withstand and test levels of insulating systems of form-wound stator coils for rotating a.c. machines with rated voltage 3 kV and above
IEC Doucment 2(Secretariat)611, June 1983

[55] CHRISTIANSEN, K.A. and PEDERSEN, A.
An experimental study of impulse voltage phenomena in a large AC motor
IEEE Proceedings of the EIC, 1968, p 148-150

[56] NAILEN, R.L.
Transient surges and motor protection
IEEE Trans. Ind. Appl. IA-15(1979):6, p 606-610

[57] Eriksson & Pretorius
A study of switching surge generation in HV motor installations - including interturn insulation and surge suppression requirements

[58] Luxa, A.
Messtechnische und rechnerische Untersuchung von multiplen Wiederzündungen beim schalten von Motoren mit Vakuumschaltern.
Diss. TU Berlin, 1987.

Chapter 4:

REACTOR SWITCHING

4.1 Introduction

In high voltage systems it is often necessary to compensate the capacitive reactive power by shunt reactors. Shunt reactors are either directly connected to the substation bus, to a transmission line or connected to the system through delta tertiary windings of transformers. Although in the latter case the reactors are usually switched at the medium voltage side the need can arise to interrupt the reactive current on the high voltage side of the otherwise unloaded transformer (dealt with in Chapter 6, Reactor Loaded Transformers).

Shunt reactors are usually built with transformer-type windings on an iron core with air-gaps, although coreless reactors at medium voltage are also frequently used. In general, they are star-connected with ratios X0/X1 in the range 0.3-2, or infinity with an unearthed reactor neutral. The neutrals of m.v. reactors are often left unearthed to avoid additional zero-sequence current flow in case of faults at the m.v. installation, whereas the neutrals of the reactors directly connected to transmission lines are almost always directly earthed, although they may be earthed through a fourth reactor leg, installed between the neutral and earth.

Many shunt reactors are switched frequently, even daily. Overvoltages may occur due to current chopping, reignitions, or both. High voltage reactors are generally protected by surge arresters.

Even though this study is mainly directed to circuit-breakers, it is understood that the general philosophy is also applicable to other switching devices such as high voltage switches.

Other overvoltage aspects, which may be associated with reactor applications (for example the overvoltage caused by near resonance phenomena, coupling to parallel lines or neighbouring conductors and stuck breaker pole conditions) are not discussed although they may be important from the overvoltage protection viewpoint. Further the switching of a reactor combined with a long cable or line is not considered in this report.

4.2 Typical network configurations and reactor ratings

4.2.1 High-voltage reactors - rated voltage $\geq$ 72.5 kV

Typical high voltage reactor and network characteristics may be summarized as follows.

4.2.1.1 Reactor ratings

The vast majority of the installed shunt reactors are in the 30-300 MVA (three-phase) range. The largest single-phase units at present (1985) in existence have capacities of about 125 MVA, i.e. 375 MVA as a three-phase group.

The table below summarizes typical reactor data at different rated voltages obtained in a survey conducted by WG 13.02 [1].

4.2.1.2 Open-air substations

The supply system to which the reactors are connected usually consists of a double busbar arrangement with a number of bays ranging from four to eleven. Ring-bus and breaker-and-a-half arrangements are also common in some countries.

[35] KOSTELECKY, L.
Utilisation d'un circuit équivalent pour la vérification du pouvoir de coupure des disjoncteurs pendant la coupure des moteurs asynchrones h.t.
Second CIGRE SC 13 Colloquium 1981 in Helsinki, CIGRE 13-81(CE)19

[36] DAMSTRA, G.C.
Virtual chopping phenomena switching three phase inductive currents
Second CIGRE SC 13 Colloquium 1981 in Helsinki, CIGRE 13-81(SC)21

[37] BALAN, G.H and ONU, V.
Switching of small inductive currents. Main problems determining circuit-breaker test conditions
Second CIGRE SC 13 Colloquium 1981 in Helsinki, CIGRE 13-81(SC)22

[38] SWEETING, D.K., BIRD, A.N., FRITH, J.S., GASCOIGNE, A.E., HAYDON, S.C., WARING, H. and WILSON, T.
Switching induced failures of h.v. motors. Survey of Australian experience
Second CIGRE SC 13 Colloquium 1981 in Helsinki, CIGRE 13-81(SC)28

[39] PRETORIUS, R.E.
The suppression of internal overvoltage surges in industrial high voltage systems
Journal of the SAICMEE, Vol. 54, No. 7, July 1981, p 938-956

[40] PRETORIUS, R.E.
Field study of switching surges in the 11 kV system of Western Deep Levels Limited (South)

[41] IEEE WORKING GROUP PROGRESS REPORT
Impulse voltage strength of a.c. rotating machines IEEE Trans. PAS, Vol. 100, No. 8, August 1981, p 4041-4053

[42] SCHWARZ, K.K.
Performance requirements and test methods for high-voltage a.c.motor insulati#
Proc. IEE, Vol. 116, No. 10, October 1969, p 1735-1743

[43] CORNICK, K.J.
Private communication

[44] IEC Recommendation Publ. 34-1 7th edition 1969, Rotating Electrical Machines, Part I, Including Amendment No. 1, 1977.

[45] Progress report of Preparatory Working Group 15 - Insulation coordination
IEC Document 2(Secr)565, August 1980

[46] Proposal prepared by WG 15 relating to voltage test levels of insulation systems of form-wound stator coils for rotating a.c. machines with rated voltage 3 kV and above IEC Document 2(Secr)592, April 1982

[47] IEEE Guide for Testing Turn-to-Turn Insulation on Form-Wound Coils for Alternating-Current Rotating Electric Machines - For Trial Use
IEEE Std 522 - 1977

[48] OUYANG, M.
Switching surge strength of non-exposed equipment IEC paper TC 28[WG 2, 1968

[49] KRÄNKEL, D. and SCHULER, R.
Kontrolle der Windungsfestigkeit bei Spulenwicklungen rotierender Hochspannungsmaschinen
Brown Boveri Mitt. (1970):4, p 191-196

TABLE 4.2.1
High voltage reactor ratings

Rated voltage of reactor kV	Rated power of reactor, three-phase MVA	Rated current A	Total losses three-phase kW
735	330	259	289
550	133-300	140-315	489-552
525	50-135	55-149	135-439
460	100	126	315
400	50-200	72-289	150-540
380	100	152	400
362	60	96	180
300	35	67	212
275	25-100	53-210	47-310
230	10-180	25-442	48-301
154	60	225	216
132	15-63	101-290	66-276
115	25	126	n.a.
77	20-40	90-300	150-300

n.a. not available

The supply system neutral is usually solidly earthed, with exception at the lower voltages ($\leq$ 123 kV) where in some countries they are earthed through a reactance or resistance or resonant-earthed.

Use of a four-leg arrangement at EHV is also rather common in some countries to ease secondary arc current extinction at single phase fault switching [2, 3]. The fourth reactor between the neutral and earth has a reactance of 15 to 50 percent of the phase values.

The connection from the circuit-breaker to the line or busbar is usually by an overhead line from 10 to 100 m long with inductance and capacitance values of about 1 μH/m and 10 pF/m respectively.

The usual connection from the circuit-breaker to the reactor is by an over-head line of a length not exceeding 150 m and inductance and capacitance values of about 1 μH/m and 10 pF/m.

The total effective surge impedance is typically in the range 250 to 280 ohms for the non-homopolar modes (positive and negative sequences) and 300 to 500 ohms for the homopolar mode (zero sequence).

Cable connections with a capacitance value usually in the 200-400 pF/m range with surge impedances of 30-50 ohm and wave velocities of 110-160 m/μs may also exist, although not so frequently.

A capacitance of a few hundred pF due to lumped capacitances may also be found along the connections on both the source and load side. A lumped capacitance of several nanofarads could be present in cases with capacitive voltage transformers.

4.2.1.3 Metal-enclosed substations

Gas-insulated substations have characteristics that differ greatly from open-air installations. It may be more important to deal with them than conventional stations in the event of reactor switching, because there may be no overvoltage protection between breaker and reactor.

The lay-out of GIS substations differ, but the following covers the majority of cases [4]:

- The supply system usually consists of a double busbar arrangement, with three to eight bays. However, single or breaker-and-a-half arrangements may also be used with up to twelve bays.

- The single-phase enclosed coaxial bus-duct is most prevalent, with a surge impedance in the 55-100 ohms range. Values of about 60 ohm with a capacitance of about 60 pF/m are typical.

- The wave velocity in the GIS is close to that of light, i.e. 300 m/μs.

- Three-phase common enclosed bus-ducts are also used, with a value for the self and the mutual surge impedances, in the case of a symmetrical arrangement, in the 70-130 ohms and 10-30 ohms ranges, respectively.

- The circuit-breaker is usually connected to the reactor by a bus duct 8 to 30 m long and an interconnecting cable or line 3 to 30 m or 1 to 50 m long, respectively. Cable connections with a length of some 100 m may also be used, although not so frequently.

- The bus duct connecting the circuit-breaker to the supply bus bar is usually 3 to 15 m long.

- The cables usually have a surge impedance of 30-50 ohms and a wave velocity of 110-160 m/μs.

- The circuit-breaker can be represented by its capacitance to the enclosure and grading capacitors across the interrupter units (if any).

- GIS-open air bushings are of different types:

  * SF6-insulated, with very low capacitance of 25 to 150 pF (increasing with the voltage rating)
  * Oil-paper insulated, with a capacitance of 100 to 1000 pF
  * Epoxy insulated, with a capacitance of 100 to 1000 pF

- SF6-oil bushings have capacitances in the 190 to 550 pF range. The higher values are representative for the higher voltages.

- Examples of equivalent circuits of inductive potential transformers are given in Figure 4.2.1. They are valid within 100 kHz to some MHz. Also for this range of frequency only a capacitance of 100 ... 200 pF, sometimes shunted by a damping resistor of 5 ... 10 kohm, may be taken as the equivalent circuit.

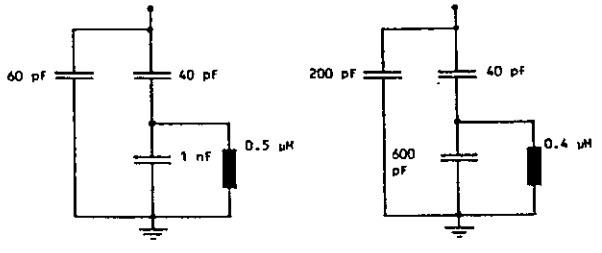

FIGURE 4.2.1
Equivalent circuit of inductive potential transformer

a) SF6-impregnated laminated foil insulation, U > 145 kV
b) Epoxy resin insulation, U ≤ 145 kV

TABLE 4.2.2

Tension de service *Operating voltage* U/kV	Capacité *Capacitance* C/nF
145	16
245	8-11
362	8
420	4-7
550	5
800	2-3.5

- The capacitance of capacitive potential transformers is relatively large and should be taken into consideration. Table 4.2.2 gives representative values for different system voltages.

- The influence of further elements, such as disconnectors in the closed position and current transformers, can usually be ignored.

4.2.2 Medium voltage reactors – < 72.5 kV

M.V. reactors are usually connected to the tertiary winding of a transformer or, in rare cases, directly to a substation bus. The principal difference between a bus-connected and a tertiary-connected reactor is that the short circuit current on the tertiary side of a large high-voltage transformer is usually much higher than on a bus of a m.v. network. Therefore a more powerful breaker is needed and this may influence the chopping level.

The rated voltage of m.v. reactors ranges from 10 to 66 kV, the rated power from 10 to 100 MVA corresponding to rated currents from 50 to 2000 A. Table 4.2.3 gives the main data of m.v. reactors based on information collected in the course of the enquiry on actual system conditions [1].

TABLE 4.2.3
Medium voltage reactor rating

Tension assignée *Rated voltage* kV	Puissance triphasée de dimensionnement de la réactance *Rated power three-phase* MVA	Courant assigné *Rated current* A	Puissance de pertes totale en triphasé *Total losses three phase* kW
> 36 – ≤ 60	20 – 30	190 – 290	90 – 140
> 24 – ≤ 36	50 – 100	750 – 1500	150 – 300
> 17.5 – ≤ 24	35 – 80	1000 – 2300	100 – 300
> 12 – ≤ 17.5	40 – 70	1400 – 3100	150 – 200
≤ 12	10 – 20	500 – 1100	70 – 190

4.3 Reactor switching phenomena

Interruption behaviour of reactors depends on a number of factors such as:

- Construction (single-phase units, three-phase units, with three or five legs, gapped or coreless)
- Star or delta connection
- Connection to the line (directly, through a tertiary winding, via overhead line or cable, type of cable)
- Method of earthing of the neutral
- Type of circuit-breaker
- Rated power

Overvoltages may occur due to current chopping and/or to reignitions.

4.3.1 Reactor characteristics

Shunt reactors are often star connected with small interphase coupling (single phase units or 3-phase units with five iron legs or shell type cores) and solidly earthed neutral. Other reactor connections are, however, also used.

Interruption in each consecutive phase will initiate transient oscillations. For iron-core reactors the frequency is typically a few kHz while it may reach 50 kHz for air-core reactors. For each interrupting phase in turn an equivalent parallel RLC-network may be defined which can be used for simulation of the interruption process.

The components R, L and C of such equivalent networks may be obtained from corresponding positive and zero sequence values for the reactor. Frequency dependence must be considered so these values must, at least in principle, be recorded at the same frequency as will occur at disconnection of the reactor. A low voltage DC-chop method which can be used to obtain adequate data is described in [5]. Measurements by means of a current ramp are also possible.

The positive sequence values of the inductance at a frequency of a few kHz will typically be 5–10 % lower than the corresponding power frequency values [6, 7]. This will probably also be true for the zero sequence values. A good approximation may thus be obtained by use of the power frequency values.

Positive and zero sequence power frequency capacitance and resistance values are generally not known. Even if they were known espécially the parallel resistance values would be of quite limited use since they represent losses in both winding and iron and are thus strongly frequency dependent.

In the case of star connected reactor without inductive or capacitive inter-phase coupling and with solidly earthed neutral, the phases are independent (positive and zero sequence components are equal) and can be treated separately. In this case the representation of the reactor is quite simple: Each phase can be represented by a parallel RLC-network, either with all components obtained from low voltage current injection or chop tests, or with L obtained from the power frequency reactor rating and thereafter C and R from frequency and damping of an interruption test recording.

The effective equivalent capacitance of a reactor depends on frequency and is typically of the order of some 2000–5000 pF for the phenomena under consideration.

As examples of data, Table 4.3.1 gives values for ten different reactors of various types and ratings.

The gapped iron cores used in shunt reactors can typically be considered linear up to about 1.3 p.u. voltage at power frequency. When dealing with transient oscillation frequencies, of the order of kHz, the cores may be considered unsaturated.

4.3.2. Single phase type interruption without reignitions

Reactors without capacitive or magnetic interphase coupling and with solidly earthed neutral may be regarded as single phase units and each phase approximately represented by the equivalent circuit in Figure 4.3.1.

If damping is neglected the reactor may be represented by a parallel circuit of L_t and C_t having a natural frequency ω_t. Damping could be taken into account by a parallel resistance R.

The load side capacitance, C_t, and source side capacitance, C_s, are the effective high frequency capacitances both seen from the breaker terminals. C_t may be somewhat smaller than the low frequency capacitance because a part of the latter one comes from the distributed winding capacitances of the reactor. But often, as a reasonable approximation, C_t can be assumed to be equal to the low frequency capacitance.

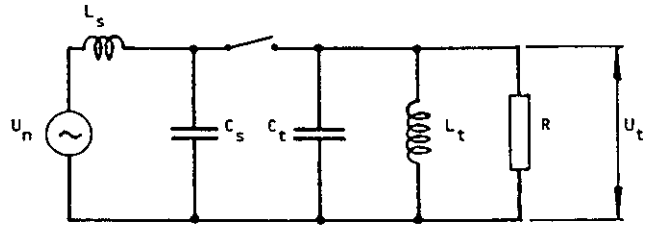

FIGURE 4.3.1 - Single-phase equivalent circuit

TABLE 4.3.1
Examples of reactor characteristics

	Réactance n° *Reactor No.*									
	1	2	3	4	5	6	7	8	9	10
Tension assignée *Rated voltage* kV	13.8	14.6	115	132	235	235	275	400	550	735
Puissance assignée tri-phasée *Rated power three-phase* MVA	30	34.1	25	55	120	180	100	200	133	330
Fréquence assignée *Rated frequency* Hz	60	60	60	50	60	60	50	50	60	60
Type de noyau *Type of core*	sans fer *Coreless*	cuirassé *Shell*	sans fer *Coreless*	trois colonnes *3-leg*	trois colonnes *3-leg*	cinq colonnes *5-leg*	sans fer *Coreless*	cuirassé *Shell*	sans fer *Coreless*	cuirassé (2) *Shell(2)*
Couplage *Type of connection*	étoile *star*	étoile *star*	delta *delta*	étoile *star*	étoile *star*	étoile *star*	étoile *star*	étoile *star*	étoile *star*	étoile *star*
Neutre à la terre *Neutral earthed*	non/*no*	oui/*yes*	-	oui/*yes*	oui/*yes*	oui/*yes*	oui/*yes*	oui/*yes*	oui/*yes*	oui/*yes*
Rapport X_0/X_1 (fréquence industrielle) *Ratio X_0/X_1 (power frequency)*	∞	≈ 1	∞	0.4	≠ 1	≈ 1	≈ 1	1.0	≈ 1	≈ 1
Fréq.ind.,inductance L_1 H/phase *Power freq.inductance L_1 H/phase*	0.017	0.017	1.40	1.0	1.22	0.81	2.42	2.55	6.03	4.34
HF inductance L_1 *High freq.inductance L_1* H/phase	-	-	-	≈ 1.0	-	-	2.20	2.4	-	-
Capacité nF/phase *Capacitance nF/phase*	2.1	10.1	2.9	1.3	1.2	2.3	2.95	1.9	2.5	4.05
Fréquence propre *Natural frequency* 1) kHz	27.0	12.3	2.5	4.2	4.1	3.7	2.0	2.3	1.3	1.2
Amortissement,rapport entre crêtes successives 1) *Damping,consec.peak ratio*	0.75	0.88	0.99	0.9	0.80	0.99	0.96	0.93	0.96	0.97

1) Première phase coupée/*First phase to clear*
2) Trois unités monophasées/*Three single phase units*

The small short-circuit inductance of the source side, L_s, will be neglected in this section.

After interrupting each pole a single frequency load side oscillation occurs, independent of the momentary situation in the other phases. The recovery voltage across the interrupted reactor phase after a current chopping at t=0 is given by (see e.g. Appendix 4):

$$u_t(t) = e^{-\frac{1}{\tau}} u_m \cos(\omega_t + \psi) \qquad (4.3.1)$$

Here τ is determined by the actual damping and Ψ by the initial conditions respectively.

Neglecting damping the amplitude u_m is given by

$$u_m = \sqrt{u_c^2 + (i_{ch}\omega_t L_t)^2} \qquad (4.3.2)$$

where u_c = instantaneous value of voltage at t = 0
i_{ch} = instantaneous value of current at t = 0 (chopping current)

The damping of a reactor current is very small. Therefore the highest overvoltage across the load after current chopping (the suppression peak) is close to u_m.

Equation (4.3.2) can be rewritten as an expression for the maximum possible per unit chopping overvoltage, $k_a = u_m/u_o$ (eq. 2.3.16 in Chapter 2):

$$k_a = \sqrt{k_c^2 + \frac{3 i_{ch}^2}{2\omega C_t Q}} \quad p.u. \qquad (4.3.3)$$

where $k_c = u_c/u_o$ (Eq. 2.3.17),
u_o is the amplitude of the phase-to-earth voltage
ω is the angular power frequency
Q is the total power of the three phase reactor bank, i.e.:

$$Q = \frac{3 u_o^2}{2\omega L_t}$$

Since the chopping normally occurs close to the crest of the phase-to-earth voltage, $k_c \approx 1.0$, and:

$$k_a \doteq \sqrt{1 + \frac{3 i_{ch}^2}{2\omega C_t Q}} \quad p.u. \qquad (4.3.4)$$

Curves indicating k_a vs. chopping current i_{ch} are given in Appendix 4 for a number of Q and C_t-values.

Vacuum breakers have a more or less constant current chopping level which is only weakly affected by C_t. So for a certain vacuum breaker the chopping overvoltage is a function of the product C_tQ.

For many other breakers the chopping behaviour can be characterized by a chopping number, κ:

$$\kappa = i_{ch}/\sqrt{C_p} \qquad (4.3.5)$$

(See section 2.3.2 and equ. (2.3.13) in Chapter 2)

Here C_p is the effective h.f. capacitance seen in parallel to the breaker terminals including, of course, any grading capacitors across the breaker. So for Figure 4.3.1:

$$C_p = \frac{C_s C_t}{C_s + C_t}$$

Practical κ-values, in A/√F, for one breaker unit range from approximately $1 \cdot 10^4$ (for certain m.v. SF6-breakers) to $60 \cdot 10^4$ (for some EHV air-blast breakers).

If a reduced chopping number κ_r is defined by

$$\kappa_r = \kappa \sqrt{\frac{C_p}{C_t}} = \kappa \sqrt{\frac{C_s}{C_s + C_t}} \qquad (4.3.6)$$

the overvoltage factor is

$$k_a = \sqrt{1 + \frac{3\kappa_r^2}{2\omega Q}} \qquad (4.3.7)$$

Overvoltage factors k_a vs κ_r are plotted in Figure 4.3.2 with Q as a parameter, for a main frequency of 50 Hz.

In case of an "infinite" bus ("Infinite" means here only: having a much lower impedance to the h.f. oscillations than the load side) we can assume that $C_s >> C_t$ and therefore

$$C_p \sim C_t$$

an approximation which leads to $\kappa_r = \kappa$ in eq. (4.3.7) and Figure 4.3.2.

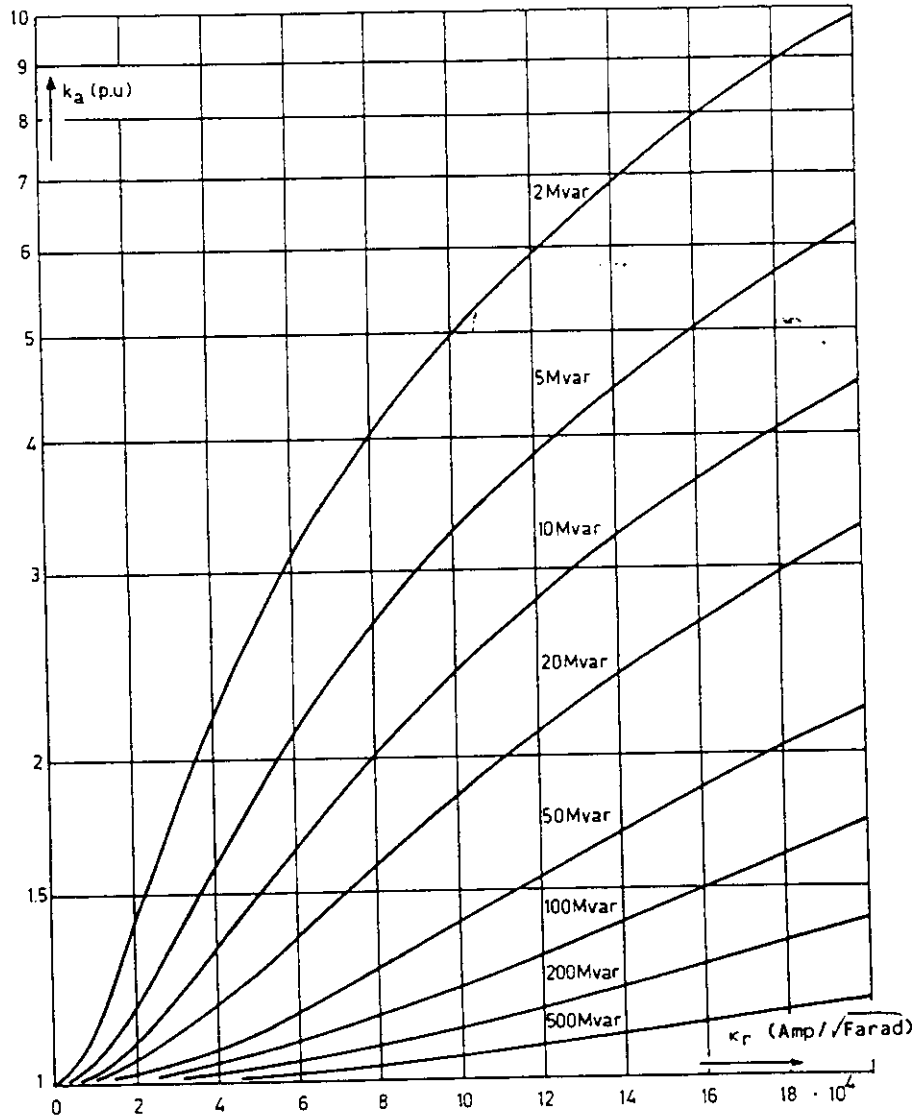

FIGURE 4.3.2 Overvoltage factors k_a vs the reduced chopping number κ_r for a number of inductive power magnitudes. Power frequency is 50 Hz

In case of a reactor connected to a tertiary winding, C_p may be appreciably smaller than C_t. So κ_r will be smaller than κ and the overvoltage lower than in the case of an infinite bus.

The plots of Figure 4.3.2 may also be used for 60 Hz networks when instead of the real Q a reduced power Q_r = 5/6 Q is taken into account.

From eq. (4.3.7) and Figure 4.3.2 it can be seen that neither the incidental chopping value i_{ch} nor the parallel capacitance C_t are significant parameters behind the maximum possible chopping overvoltages. In the first place the overvoltages are expressed in terms of only the reduced chopping number κ_r and the reactor power Q.

Figure 4.3.2 indicates clearly in which situations high overvoltages from current chopping will certainly ***not*** be generated. On the other hand, this figure cannot be used to predict the occurence of extremely

high overvoltages because many breakers tend to smooth out such extrema by reignitions. However, high overvoltages may also occur even without current chopping due to reignitions only.

4.3.3 Reignition phenomena

4.3.3.1 Overvoltages at single reignitions

Reignition phenomena associated with switching of small inductive currents are described in detail in Chapter 2, Section 2.5, giving the basic theory as well as description of the relationships between the various circuit parameters. The transient defined as the "second-parallel-oscillation" is that which may impose overvoltages across the inductive component being switched. The "first-parallel-oscillation" and the "main-circuit-oscillation" are not of particular significance regarding overvoltages.

The tendency for reignitions to occur under reactor switching is not uncommon. All circuit-breakers exhibit this characteristic more or less. The frequency of occurrence and voltage magnitudes at which reignitions occur are a characteristic of the circuit-breaker. The nature and relative magnitude of the overvoltages produced, however, are a circuit phenomenon and not necessarily dependent upon the characteristics of the switching device.

There is a reasonable probability that reignitions may occur near the recovery voltage peak. At this point in time, the instantaneous transient voltage across the reactor may be approximately 1 p.u. of a given polarity, assuming chopping has not occurred, whereas the instantaneous source voltage may be 1 p.u. of the opposite polarity. The voltage across the circuit-breaker therefore is approximately 2 p.u. If a reignition occurs at this time, the instantaneous reactor terminal voltage will change very rapidly towards the instantaneous source voltage. The reactor transient voltage will over-swing beyond 1 p.u. due to the oscillatory nature of the circuit and may reach an opposite polarity peak of greater than 2 p.u. but less than 3 p.u [11, 12]. See Figure 4.3.3.a. (A more detailed description is given in Figure 2.5.3 of Chapter 2.)

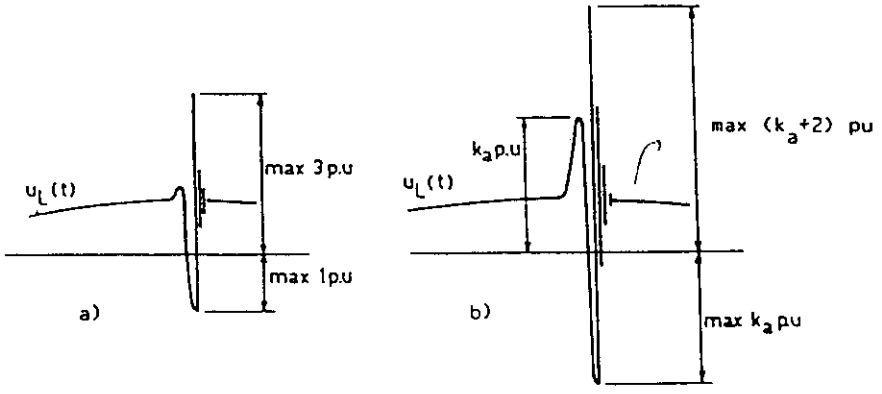

FIGURE 4.3.3 Maximum reignition voltages essentially without (a) and with (b) current chopping

During this transient oscillation, the net change in reactor terminal voltage can be greater than 3 p.u. This net change in voltage occurs in a very short time, on the order of microseconds, and is dependent upon the bus configurations on either side of the circuit-breaker, including a multiplicity of reflection points typical of a high voltage substation. For h.v. shunt reactors, the rate-of-change of voltage across the reactor may be on the order of 1000 kV per microsecond.

Current chopping may accentuate the voltages produced by reignitions. The maximum transient recovery voltage across the circuit-breaker increases so that reignitions may occur at a higher voltage across the reactor. If a reignition occurs at the recovery peak voltage, the maximum overvoltage may approach a value k = (k_a+ 2) p.u., where k_a is the chopping overvoltage in p.u. See Figure 4.3.3.b.

The above description of the reignition phenomena is strongly simplified. It does not take e.g. damping of the second parallel oscillation into account. Furthermore it assumes that the source side capacitance

C_s is infinite in relation to the load side capacitance C_t, i.e. $C_s >> C_t$. If this is not valid, charge redistribution will reduce the first overvoltage peak to

$$k = 1 + (k_a + 1)\left(\frac{C_s - C_t}{C_s + C_t}\right) \qquad (4.3.8)$$

However, the situation is often more complicated by the fact that one or more lines and/or cables are connected to the source side busbars. In the first instant they react as their surge impedances and contribute to C_s with only a part of their low frequency capacitance.

The result is that the overvoltages are restricted to

$$k = 1 + \beta(k_a + 1) \quad p.u. \qquad (4.3.9)$$

where β can be regarded as an equivalent damping of the first reignition transient taking charge redistribution into account. For example, if k_a = 2.0 p.u. and β = 0.5 (which is a normal value [11, 12]), the maximum overvoltage will be k_{max} = 2.5 p.u.. Without any current chopping, i.e. k_a = 1, and with β = 0.5, a reignition overvoltage of k_{max} = 2.0 p.u. may occur. Since reignitions cannot be excluded in any kind of circuit-breaker or high voltage switch, an overvoltage level of about 2.0 p.u. may be expected at reactor switching irrespective of the switching device if no special mean for limitation is applied.

For reactors which are not solidly earthed higher reignition voltages may occur. E.g. for a reactor with isolated neutral reignition overvoltages with $k_{max} = 1 + \beta(k_a + 2)$ p.u. are anticipated. Also the use of a fourth reactor between star point and earth may lead to some enhancement of the overvoltages at reignition (see Appendix 4).

Figures 4.3.4 to 4.3.6 illustrate the influence of charge redistribution. The first reignition transient shows much more "damping" than what could be expected from the decaying oscillation that follows.

Field measurements of the transient overvoltages produced at the reactor terminals caused by single reignitions and without chopping of the switching device, indicate that the transient voltages are extremely high in frequency (200 to 500 kHz) and can reach peak values of the order of 2.0 p.u. [11, 12]. Figures 4.3.4 and 4.3.5 show results from switching a 500 kV, 180 MVA reactor.

4.3.3.2 Multiple reignitions

Overvoltages resulting from multiple reignitions may be higher than that for a single reignition. To cause a voltage escalation as described in Chapter 2, Sub-clauses 2.5.3 and 2.5.4, the energy stored in the load side after interruption of the restriking current has to be higher than the energy stored just before the reignition. The following conditions increase the risk of voltage escalation:

a) the ratio C_s/C_t is large, i.e. the source side capacitance is much higher than the load side capacitance (the surge impedance of a long bus between C_s and the breaker, may influence this condition)

b) the high frequency current is interrupted by the breaker at the first or an early uneven high frequency current zero

c) the interruption of the reignition current occurs after the prospective current zero of the load current. Compare Figure 2.5.6 of Chapter 2.

Condition *b)* exists mainly in vacuum circuit-breakers and vacuum switches resulting in a considerable risk of generating trains of overvoltage transients with amplitudes that may increase to very high values. The situation is similar to the switching of high voltage motors described in Chapter 3.

Other type of h.v. breakers are usually not able to interrupt high frequency current. Even though they may reignite more than once, the repetition frequency is usually low. This characteristic in conjunction

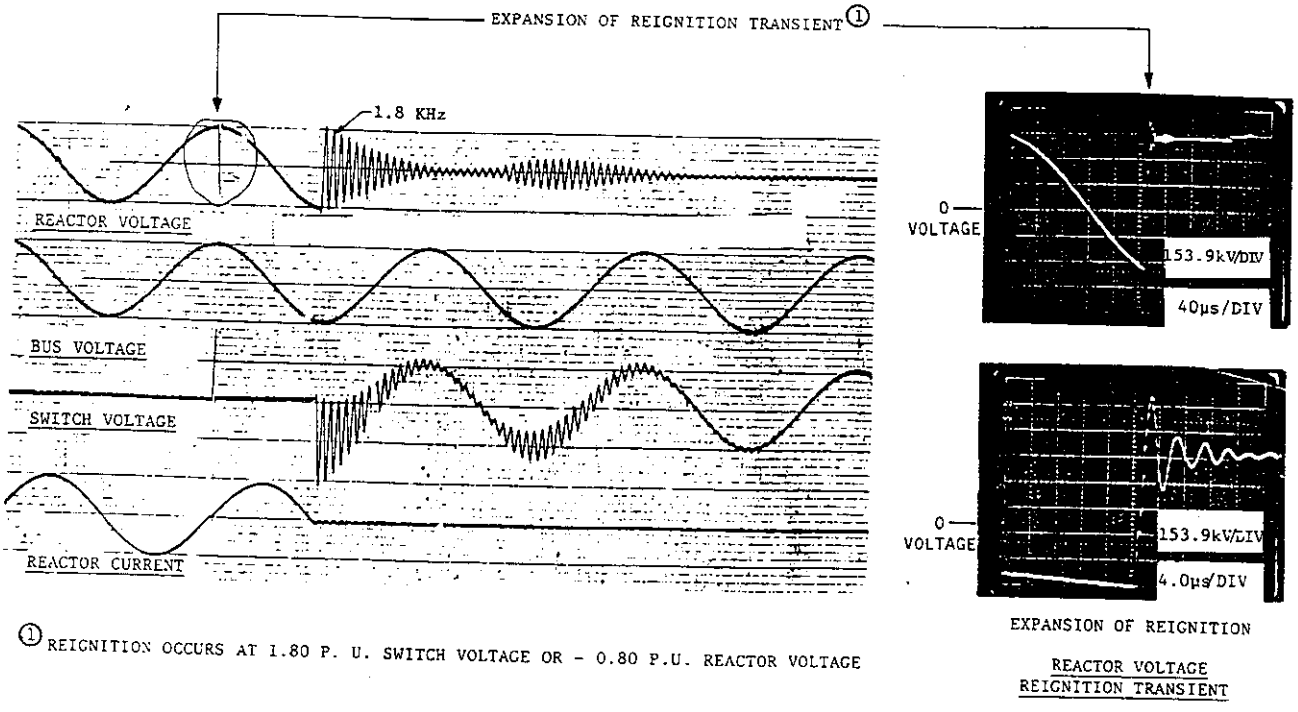

① REIGNITION OCCURS AT 1.80 P. U. SWITCH VOLTAGE OR - 0.80 P.U. REACTOR VOLTAGE

FIGURE 4.3.4 500 kV 180 MVA shunt reactor switching tests.
Typical oscillograms showing transient phenomena for a single reignition.

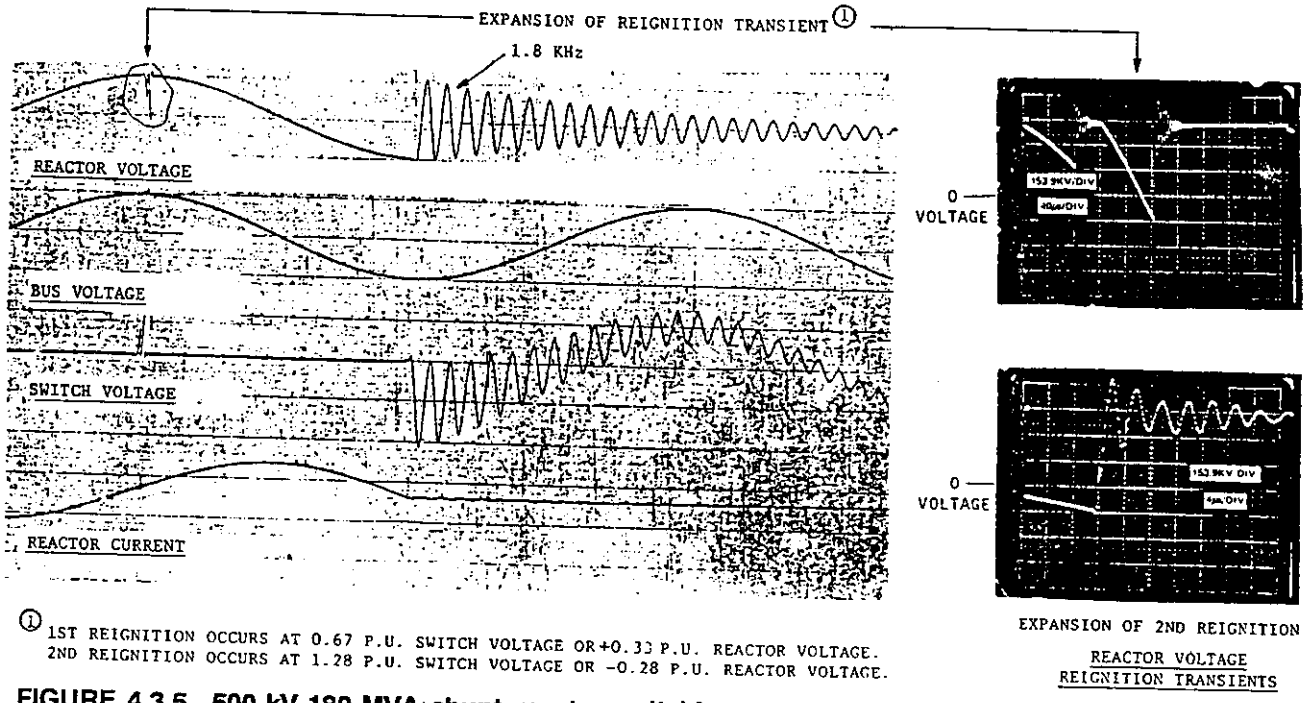

① 1ST REIGNITION OCCURS AT 0.67 P.U. SWITCH VOLTAGE OR +0.33 P.U. REACTOR VOLTAGE.
2ND REIGNITION OCCURS AT 1.28 P.U. SWITCH VOLTAGE OR -0.28 P.U. REACTOR VOLTAGE.

FIGURE 4.3.5 500 kV 180 MVA shunt reactor switching tests.
Typical oscillograms showing transient phenomena for a double reignition.

with low chopping level makes on the other hand condition *c)* somewhat probable in typical h.v. breakers. This can be seen in Figure 4.3.5 where an energy increase of the load side oscillation after the first reignition has occured is shown by the higher rate-of-rise of the recovery voltage. However, the enhancement of the overvoltage amplitude due to this phenomenon is judged to be marginal.

4.3.3.3 Computer modelling

Results from the field tests mentioned in Sub-clause 4.3.3.1 have been used as a reference when developing computer analysis methods for calculation of the reignition overvoltages [11, 12]. The

computer studies show an acceptable agreement with the field tests and the result for a wide variety of station configurations indicates that maximum overvoltages of up to 2.1 p.u. [11] and 2.3 p.u. [12] can be expected when the switch reignites at the recovery voltage peak (without chopping). The times to crest voltage were on the order of 1 to 4 μs.

Calculation of reignition overvoltages by use of a digital computer requires that the substation bus configuration and connected apparatus are properly modelled. The substation elements have to be modelled such that travelling-wave phenomena are accurately represented, at least up to a point of a major discontinuity.

A three-phase computer model must be used. The reactor terminal voltage is dependent upon the capacitive and inductive coupling between phases, the positive and zero sequence components, and travelling wave velocities. A single-phase model will not permit an accurate representation of these parameters. Reignition transient frequencies are on the order of 200 kHz to several MHz. Therefore, it is necessary to use high-frequency models for the resistive, inductive and capacitive line and bus components.

A typical reignition transient calculated by using a complete three-phase model is shown in Figure 4.3.6. Included is a comparison to the measured transient from a direct test. It can be observed that the general waveform, amplitude and time to first peak, of the calculated transient are similar to the measured transient [11].

The use of a complete substation model becomes quite tedious and time consuming particularly when setting up a three-phase model. A number of attempts has been made to simplify the model. It was concluded that an accurate model is necessary for the direct connections between the circuit-breaker and the reactor, and to a distance of approximately 500-1000 meters on the source side of the circuit-breaker. A relatively simple model beyond this point seems to be adequate.

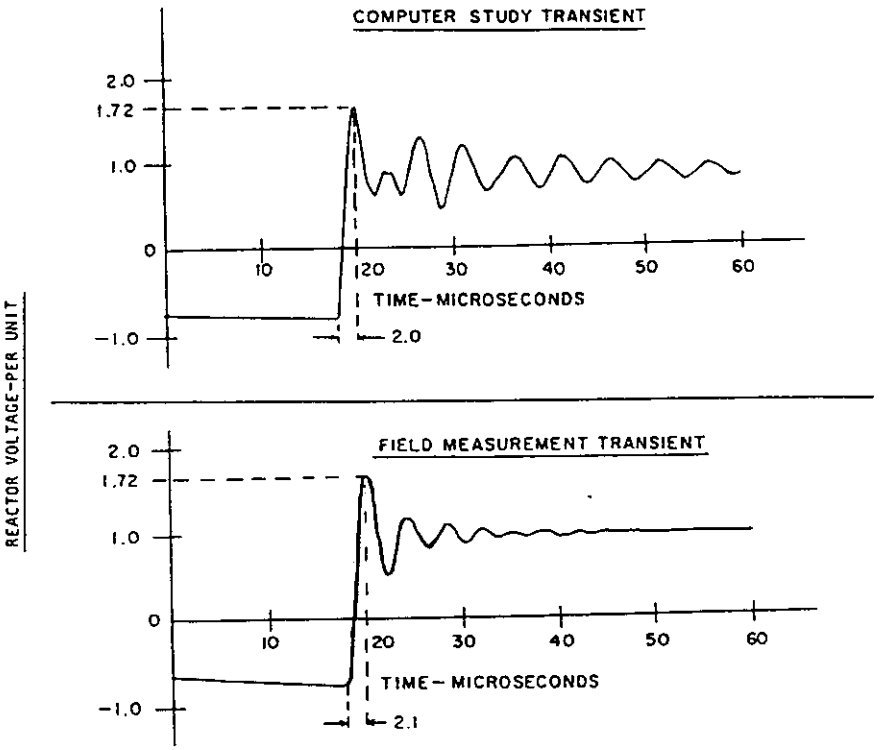

Complete 3 Ø model used for computer study, 500 kV substation, 180 MVAr reactor.

Reignition occurs at 1.8 p.u. switch voltage or -0.8 p.u. reactor voltage.

FIGURE 4.3.6 Comparison of reignition transients from computer study and field measurement Complete 3-phase model used for computer study, 500 kV substation, 180 MVA reactor. Reignition occurs at 1.8 p.u. switch voltage or – 0.8 p.u. reactor voltage

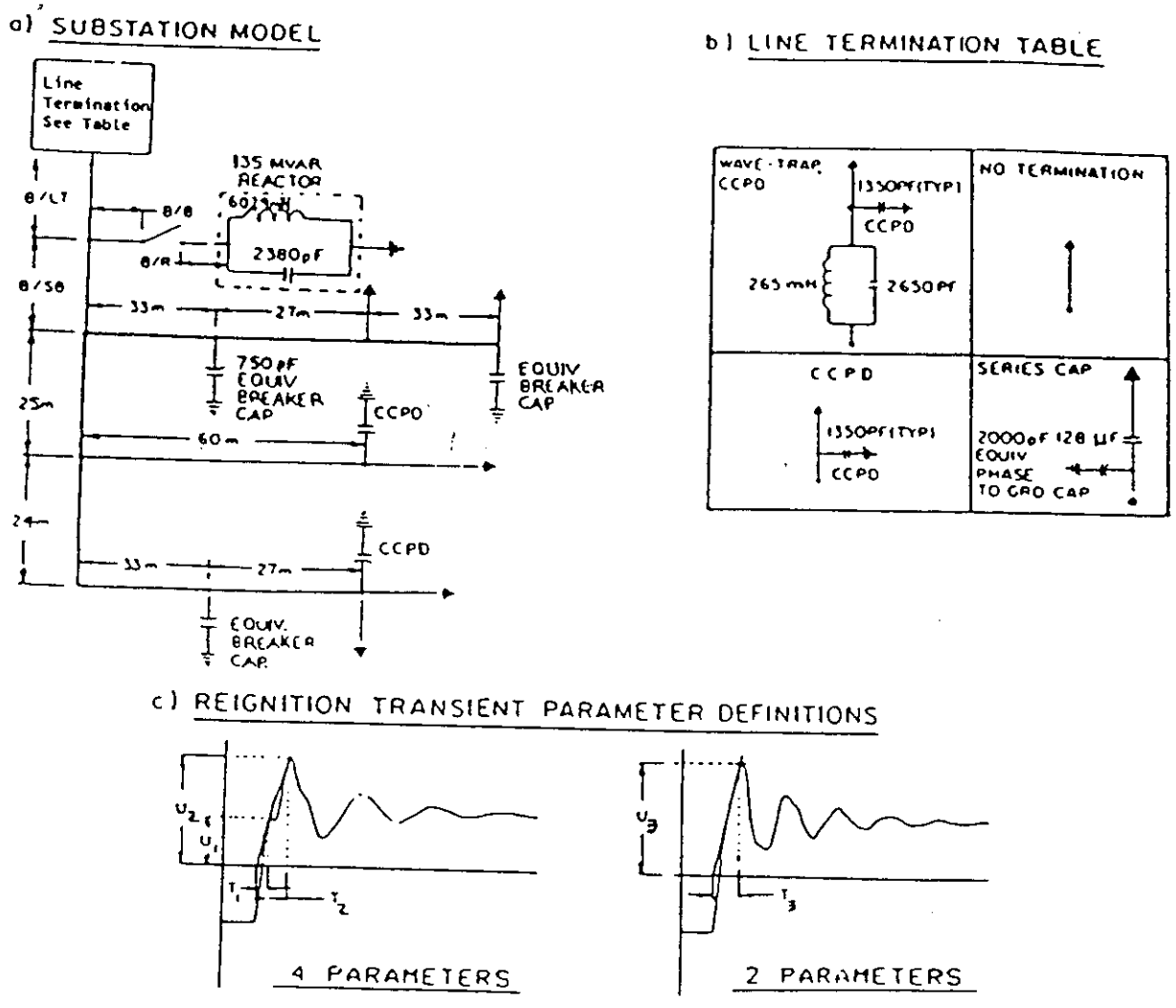

FIGURE 4.3.7 500 kV station configurations – General computer study of influence of station configuration on reignition transients.

Such a simple model has been used to study a variety of station and bus configurations. The three-phase model used and a few bus configurations studied are shown in figure 4.3.7. The calculated reignition transient parameters tabulated in Table 4.3.2 suggest several broad trends regarding overvoltage magnitudes as dependent upon station layout:

- Long bus connections between the breaker and the reactor will yield higher overvoltages
- Long bus connections on the source side of the breaker to a major discontinuity may cause higher or lower voltages. The result is dependent upon the specific bus configuration and the presence of an outgoing line [11, 14].
- Transmission line connections in the immediate vicinity of the reactor, as for line connected EHV shunt reactors, will decrease the overvoltage, particularly if a direct connection is made (e.g. no wave traps, series capacitors, coupling capacitors etc.).

Interphase coupling may create enhanced overvoltages in the other phases. This phenomenon is described in Chapter 2, Clause 2.4. Three-phase switching effects are treated in Section 4.3.4.

TABLE 4.3.2

Reignition transient parameters as a function of bus lengths and transmission line terminations

Case No	Line termination	Bus lengths				Reignition transients			
						First peak		Max peak	
		Breaker to bus	Breaker to reactor	Bus connection to substation bus	Bus connection to line termination	U_1	T_1	U_2 or U_3	T_2
		m	m	m	m	p.u.	μsec	p.u.	μsec
A(1)		6	9	180	-	-	-	1.84	2.14
B(1)	No line	27	9	180	-	-	-	1.86	2.28
C(1)		6	15	180	-	-	-	1.87	2.18
D(1)		6	9	90	-	1.77	1.54	2.02	1.94
A(2)		6	9	180	90	1.14	.98	1.58	2.90
B(2)	Wave-trap	27	9	180	90	1.21	1.04	1.70	3.00
C(2)		6	15	180	90	1.14	1.00	1.64	2.20
D(2)	CCPD	6	9	90	90	1.47	1.02	1.67	2.80
E(2)		6	9	180	5	.61	.46	1.72	2.10
A(3)	No ter-	6	9	180	90	.82	.80	1.48	1.90
B(3)	mination	27	9	180	90	1.00	1.00	1.53	2.30
C(3)		6	15	180	90	.84	.80	1.52	2.10
D(3)		6	9	90	90	1.29	1.20	1.44	1.60
A(4)	CCPD	6	9	180	90	-	-	1.29	1.00
A(5)	Series capacitor	6	9	180	90	-	-	1.38	1.03

4.3.4 Three-phase switching phenomena

4.3.4.1 Influence of reactor type

In a 3-phase network the phenomena may be much more complicated than in a single-phase case due to the interaction between the phases. The different types of interaction were described in Chapter 2.6. The types of interaction which may occur at reactor switching are highly dependent on the reactor type and its X_0/X_1-ratio.

In Table 4.3.3 the normal cases are presented. The second order influence could usually be neglected in assessing the expected overvoltage level.

Directly connected shunt reactors in high voltage networks are usually covered by case 1 and 2 in the Table.

Reactors connected to a tertiary m.v. winding of a transformer are often unearthed (case 3). Switching by a m.v. circuit-breaker may therefore give quite a complicated situation. Capacitive interphase coupling also increases the complexity.

4.3.4.2 Earthed reactors with $X_0/X_1 = 1$

This case may usually be treated as three single phase consecutive interruptions with negligible interaction between the phases. This is not even strictly true for the case with three single phase reactors, since there may still be a capacitive coupling between the connections of the phases. But the

influence on the maximum overvoltage amplitude could be disregarded when the line-to-line capacitances are small compared to the earth capacitances.

In a 5-1egged reactor or a shell-type reactor a certain inductive coupling between phases may exist. Energy transfer between phases may then take place. There is, however, no evidence that such an energy transfer has resulted in a noteworthy increase of the overvoltages. Figure 4.3.8 shows this kind of energy transfer taking place during the decay of load side oscillations [7].

All experience gained so far support the view, that this case may be treated as three consecutive single phase interruptions.

TABLE 4.3.3
Interaction between phases for different reactors
(without significant capacitive interphase coupling)

Reactor type	Possible interaction	
	First order influence	Second order influence
CASE 1 Earthed reactor with: $\frac{X_o}{X_1} = 1$ i Single phase reactor ii 5-legged reactor iii Shell type reactor		Transfer of reignition transients Transfer of chopping overvoltages
CASE 2 Earthed reactor with: $\frac{X_o}{X_1} \neq 1$ i 3-legged reactor ii Reactor earthed neutral ("4-legged reactors")	Transfer of chopping overvoltages	Transfer of reignition trtansientss
CASE 3 Unearthed reactors $\frac{X_o}{X_1} = \infty$ Any type of core	Transfer of chopping overvoltages Transfer of reignition transients	Common d.c. voltage shift

NOTE With strong capacitive interphase coupling, e.g. through connecting cables, transfer of all voltage and current transients is possible.

4.3.4.3 Earthed reactors with $X_0/X_1 \neq 1$

The common case is the three-legged reactor, which typically has $X_0/X_1 \approx 0.3$ to 0.5 due to the mutual inductance, M, between the phases. Corresponding values are $M/L_0 \approx 0.7$ to 0.3.

The coupling does not influence the chopping overvoltage to earth of the first phase-to-clear but reduces the recovery voltage. (See Figur 4.3.9.)

The suppression peak due to chopping at the second and third pole clearance will also be uninfluenced by the coupling, but energy transfer may give somewhat higher overvoltages during the load oscillation that follows (see Appendix 4).

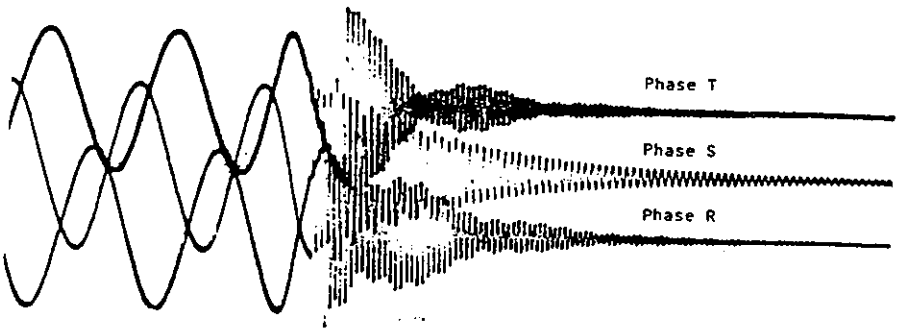

Figure 4.3.8 Switching a 200 MVA, 420 kV reactor, load-side voltages, phase to earth [7].

One example of an interruption is given in Figure 4.3.9 (the same as Figure 2.6.1 in Chapter 2). The first phase to interrupt (S) shows, as expected, a pronounced chopping overvoltage followed by decaying load side oscillation as in a single phase case.

The second phase (R) to interrupt also produces a chopping overvoltage of the same order. This is transferred to the S-phase by inductive coupling. The overvoltage in both phases then collapses probably due to a reignition. After this the oscillating energy runs forth and back between the two phases. In other tests with the same reactor without reignitions the oscillating energy decays normally from the chopping peak, but with the energy swinging between the phases in the same manner.

When the third phase (T) interrupts, new transfer of energy to the R and S-phases occurs.

This recording case demonstrates a transfer of chopping overvoltages giving rise to load oscillations of almost the same amplitude as the chopping itself but still without any enhancement of the overvoltage level.

Use of an inductance between reactor neutral and earth also results in $X_0/X_1 \neq 1$ and a pronounced coupling between the phases. With a reactor between neutral and earth the ratio X_0/X_1 usually lies between 1.5 and 2.5. In this case the recovery voltage across the breaker is increased and the arrangement may therefore result in higher reignition overvoltages in comparison with the neutral earthed (see Appendix 4).

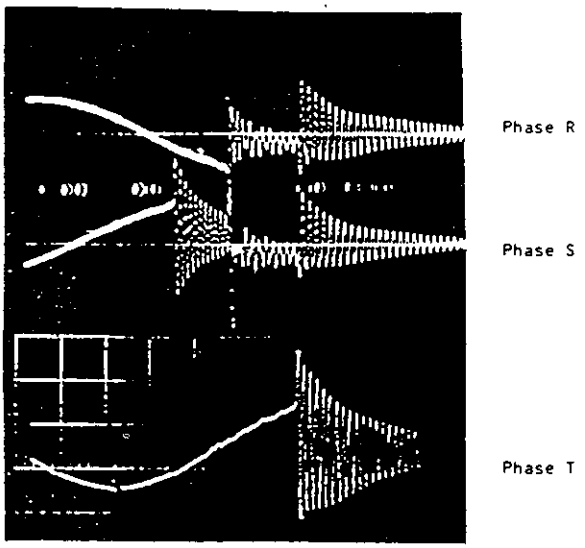

Figure 4.3.9 Switching a 55 MVAr, 132 kV reactor, load side voltages, phase to earth, [15].
Time scale 2 ms/div.

4.3.4.4 Earthed reactors with capacitive interphase coupling

M.V. reactors connected through a cable with large line-to-line capacitances have a strong capacitive interphase coupling. Therefore transfer of all voltage and current transients is possible.

Usually the second and the third pole interrupt before the energy in the previously interrupted phase(s) is damped out. Then the total energy which swings through the interrupted network (in a double-frequency mode) is larger than without interphase coupling. Therefore also higher overvoltages are possible depending on the incidental conditions at the moment of second or third pole clearance (see Appendix 4).

4.3.4.5 Unearthed reactors

In some cases the reactors are not earthed or not solidly earthed at their common neutral. Then some typical differences with the foregoing cases make the occurring overvoltage pattern still more complicated [16]:

- After the first pole has cleared, the potential of the star connection jumps to a value which can reach half the source phase voltage. Therefore the transient recovery voltage to earth is superimposed on a power frequency sinusoidal voltage wave with an amplitude of up to 0.5 p.u.

- At the moment of last pole clearance the load-side capacitances are charged to certain voltages to earth. Then the interrupted circuit is completely separated from earth and therefore obtains a d.c. voltage level with respect to earth, which is an average of all the capacitance voltages before. The transient recovery voltages to earth in the three phases are superimposed on this d.c. level. The latter will disappear slowly in an unearthed system even in the presence of an inductive potential transformer. Particularly high d.c. voltage levels with respect to earth are possible due to the fact that a certain time lag may occur between current chopping in the second and the last pole to clear. Figure 4.3.10 shows a typical oscillogram of such a situation.

- After interruption of the second and the last phase a reignition in one of these phases may occur. This results in a stepwise voltage change in the relevant phase, leading to high frequency swinging of all capacitor charges in the load-side circuit ("second parallel oscillation", see Chapter 2, Clause 2.5.1). Therefore h.f. overvoltages are possible, superimposed on a maximum of the load-side oscillation of the non-reignited phases, which in its turn is superimposed on a high d.c. level. Typical oscillograms of such situations are given in Figures 4.3.11 and 4.3.12.

  Note: This transfer of reignition voltage is not specific for the unearthed reactor. It may also occur after last pole clearance of an earthed reactor, provided some capacitive interphase coupling is active. But in those cases the induced h.f. voltages are not superimposed on a high recovery voltage as it is in the unearthed situation.

4.3.5 Summary of results from field tests

To give an idea of the magnitude of overvoltages by switching off reactors, some measured values have been collected and presented in Table 4.3.2. The Table contains results from three-phase field tests only.

The values only indicate the order of magnitude and should be used with care because there is an important influence of network parameters on the overvoltage created.

It is not always known if the overvoltages were due to current chopping or reignitions. In some cases their values have been limited by surge arrester operation.

The overvoltages given are all phase-to-earth. Phase-to-phase overvoltages may sometimes be important. E.g. if overvoltages are generated due to induced chopping (see Chapter 2, Clause 2.6.1) they will have opposite polarity in two phases. In three-phase enclosed GIS systems this will result in enhanced stresses of phase-to-phase insulation.

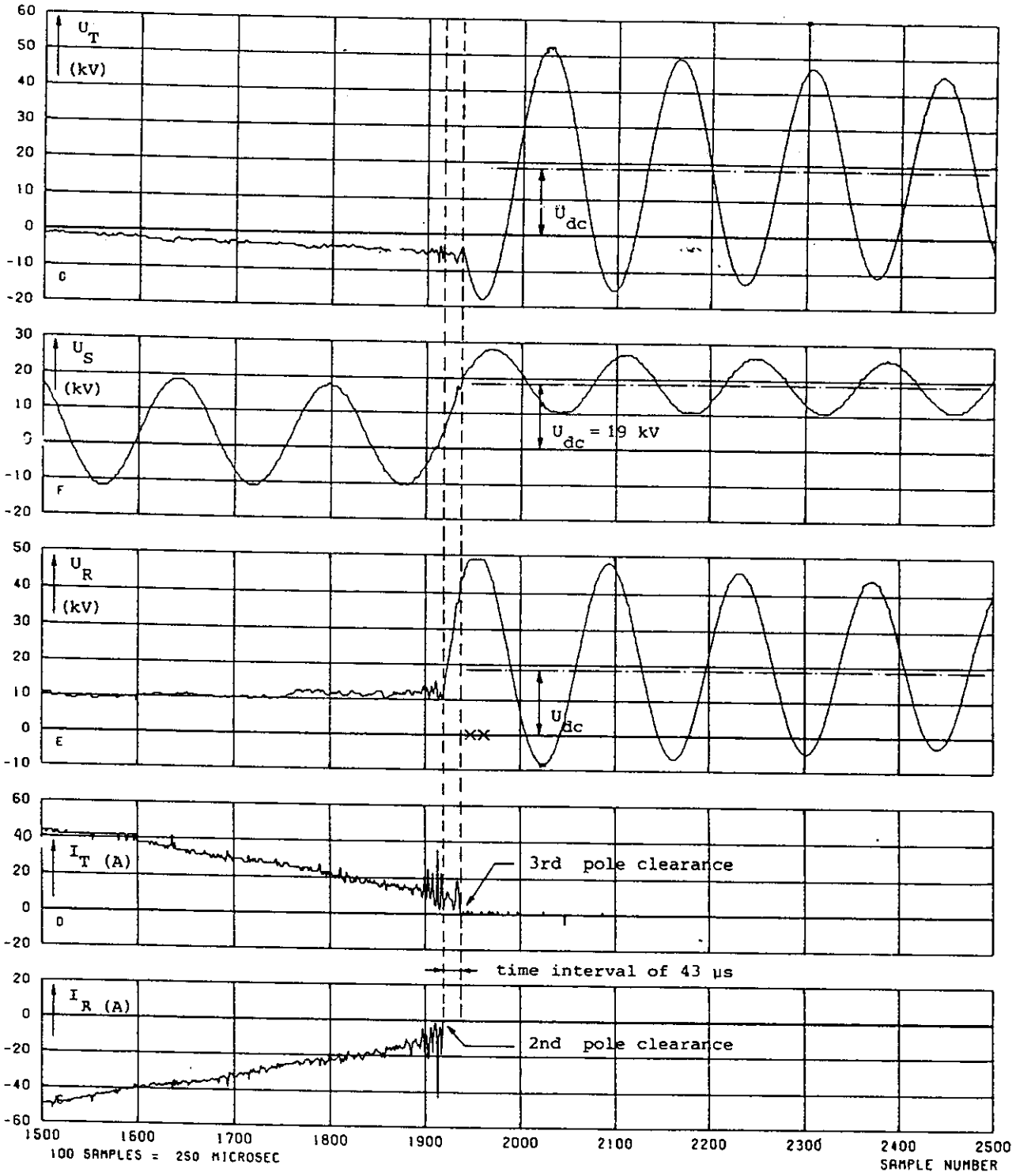

FIGURE 4.3.10 Typical oscillogram of current chopping with time-lag between second and third pole clearance, leading to high d.c. level in unearthed interrupted circuit. U_T, U_R and U_S are phase-to-earth voltages.

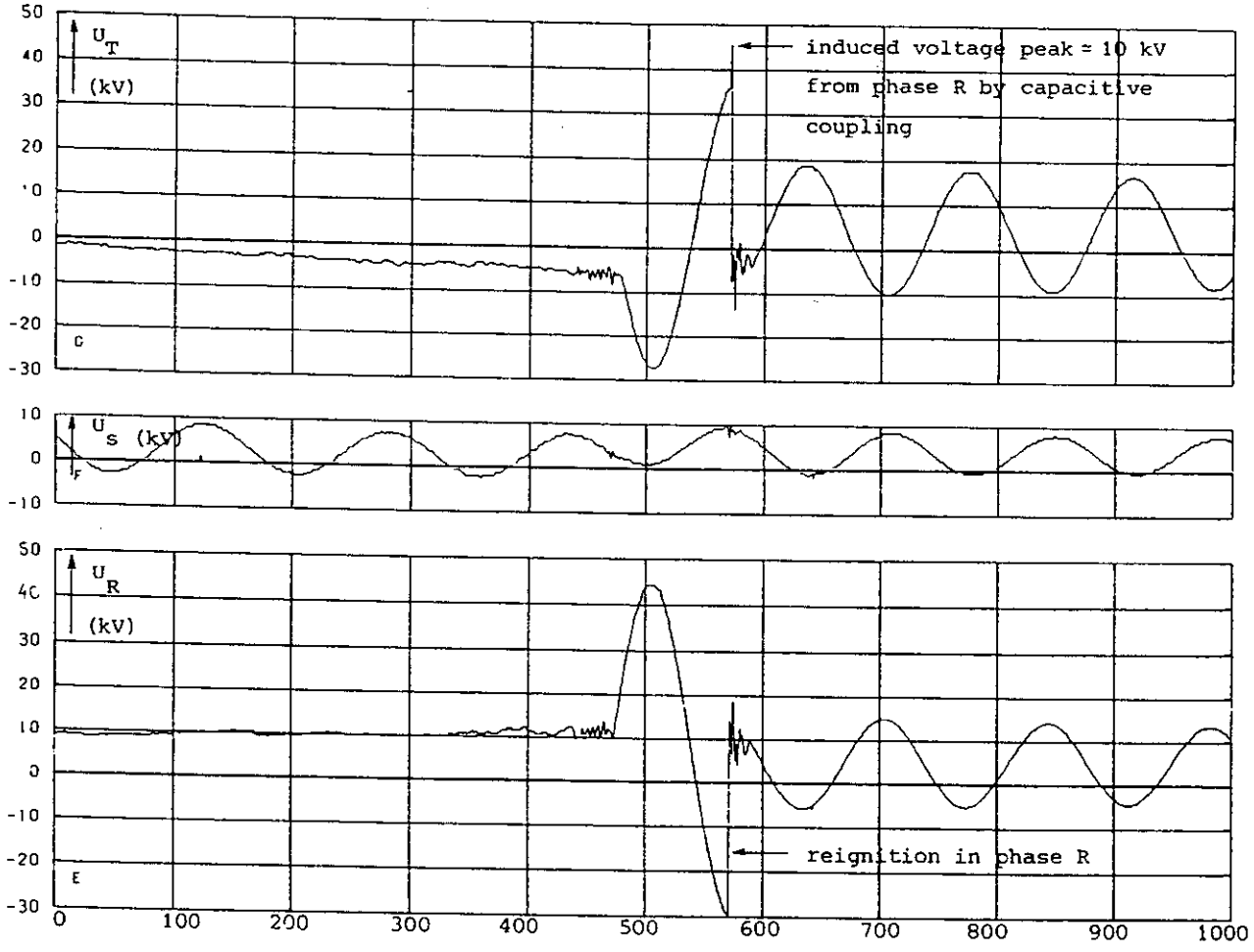

FIGURE 4.3.11 Typical oscillogram of h.f. peak voltage (in phase T) introduced by a reignition in another phase (phase R). (In phase S a similar peak voltage must have existed but it is out of the figure).
U_T, U_S and U_R are phase-to-earth voltages. 100 samples = 100 μsec.

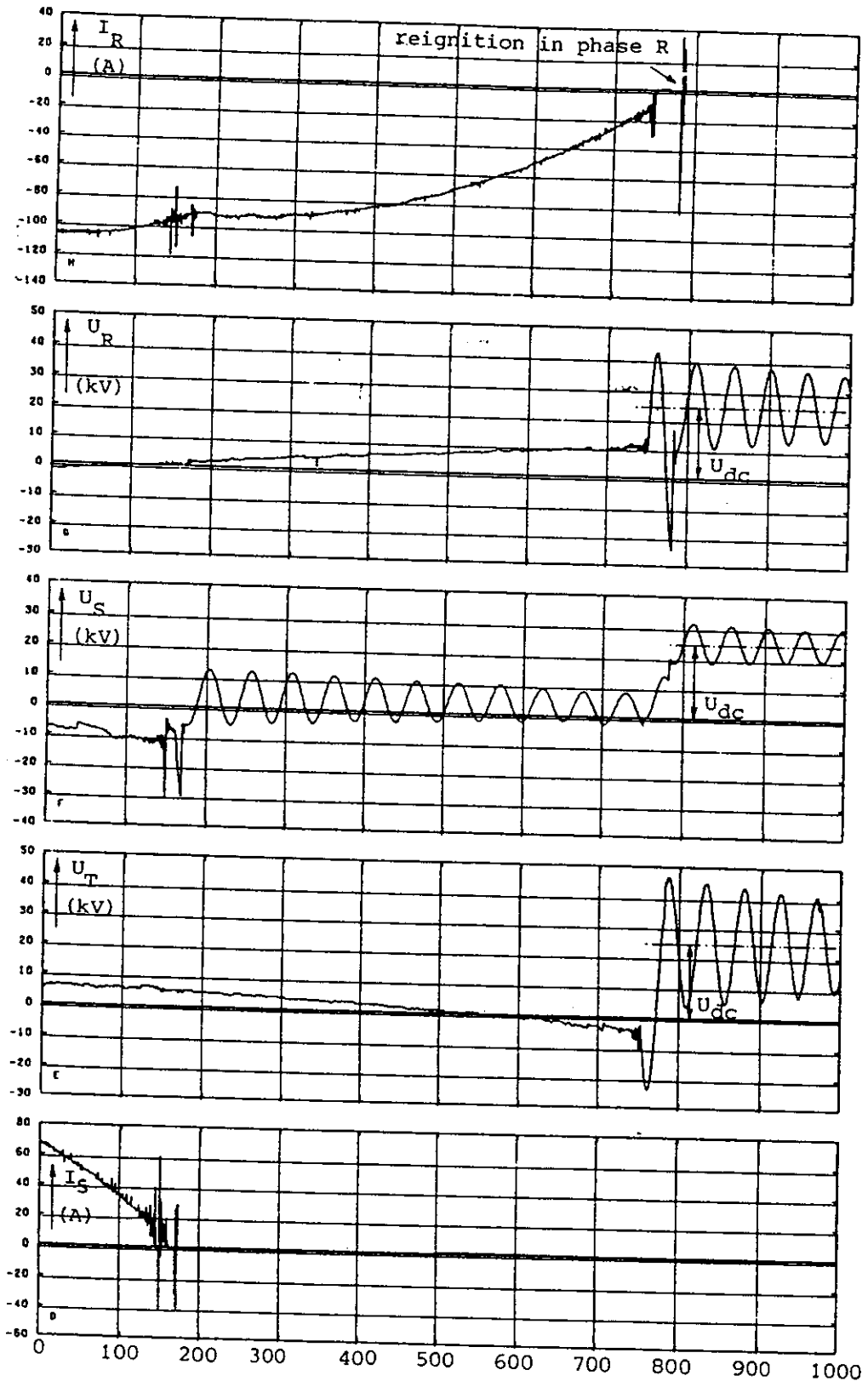

FIGURE 4.3.12 Reignition in phase R was not followed by a reignition in another phase. Therefore the current must chop again, introducing a new and high d.c. level.
U_R, U_S and U_T are phase-to-earth voltages. 100 samples ≈ 100 μsec.

TABLE 4.3.4

Summary of measured overvoltages on reactor disconnection.

The overvoltage factors are referred to the peak values of the rated reactor phase-to-earth voltages (√(2/3)U)

Rated voltage kV	Reactor power (three-phase) MVA	State of the reactor neutral	Extinguishing medium	No. of opening operations	Breaking current A r.m.s.	Natural frequency kHz	Max overvoltage factor	Ref
13	40	Free	SF_6 6)	7	1770	1.8 5)	2.3	23
13	40	"	" 6)	5	170	25.0	1.0	23
16	60	"	Air	9	2200	15.0	2.1 1)	18
				7	2200	8.4 2)	2.2 1)	18
30	60	"	Oil	40	1030	13.0	2.65	19
				10	1030	8.5 3)	2.55	19
30	45	"	"	4	770	Not known	2.5	24
30	50	"	Air	10	950		2.6	24
30	60	"	SF_6	10	1105		2.0	24
30	35	"	Oil	16	635	4.0	2.85	21
30	100	"	SF_6	12	1800	13.00	2.85	22
132	15	Direct earthed	Oil	15	67	1.3	3.14	17
132	55	"	"	4	240	4.2	2.4	15
420	200	"	"	10	290	2.3	1.55 1)	7
				17	290	2.3	2.26	7
400	50	"	Air	7	216	1.3	2.2	20
500	60 11)	"	"	36	198	1.3	2.2	20
500	60 11)	"	"	83	198	1.3	>2.2 10)	20
500	135 11)	"	SF_6 6)	13	154	1.3	1.3	23
500	180 11)	"	" 6)	38	208	1.8	>1.7 4)	23
750	330 11)	"	Air	32	242	0.8	>2.0 10)	20
765	274 11)	"	SF_6 6)	2	207	1.1	1.07	23
765	165 11)	"	Air	10	134	1.06	1.6 7)	25
765	165 11)	"	"	10	134	1.06	1.3 8)	25
765	165 11)	"	"	10	134	1.06	1.52 9)	25

1) Circuit-breaker with high-ohmic breaking resistors, 30 kohms/phase
2) Parallel capacitance of 15 nF
3) Parallel capacitance of 3 nF
4) Max overvoltage may be limited by arrester operation
5) Parallel capacitance of 680 nF
6) High voltage switch
7) With opening resistor 1080 ohms/phase
8) With opening resistor 4000 ohms/phase
9) With opening resistor 8000 ohms/phase
10) Max overvoltage is limited by surge arrester. Prospective values are estimated to 3.0–3.5 p.u. from chopped current
11) Single phase units

4.4 Switching stress and overvoltage limitation

4.4.1 General

If there is a risk of dangerous overvoltages, the insulation level may be chosen higher, or measures must be taken to limit the overvoltages.

4.4.2 Overvoltage levels

The overvoltages produced by switching small inductive currents can have very different wave shapes. It is therefore difficult to assess the degree of danger in relation to the insulation levels defined in IEC Publication 71-1 [26].

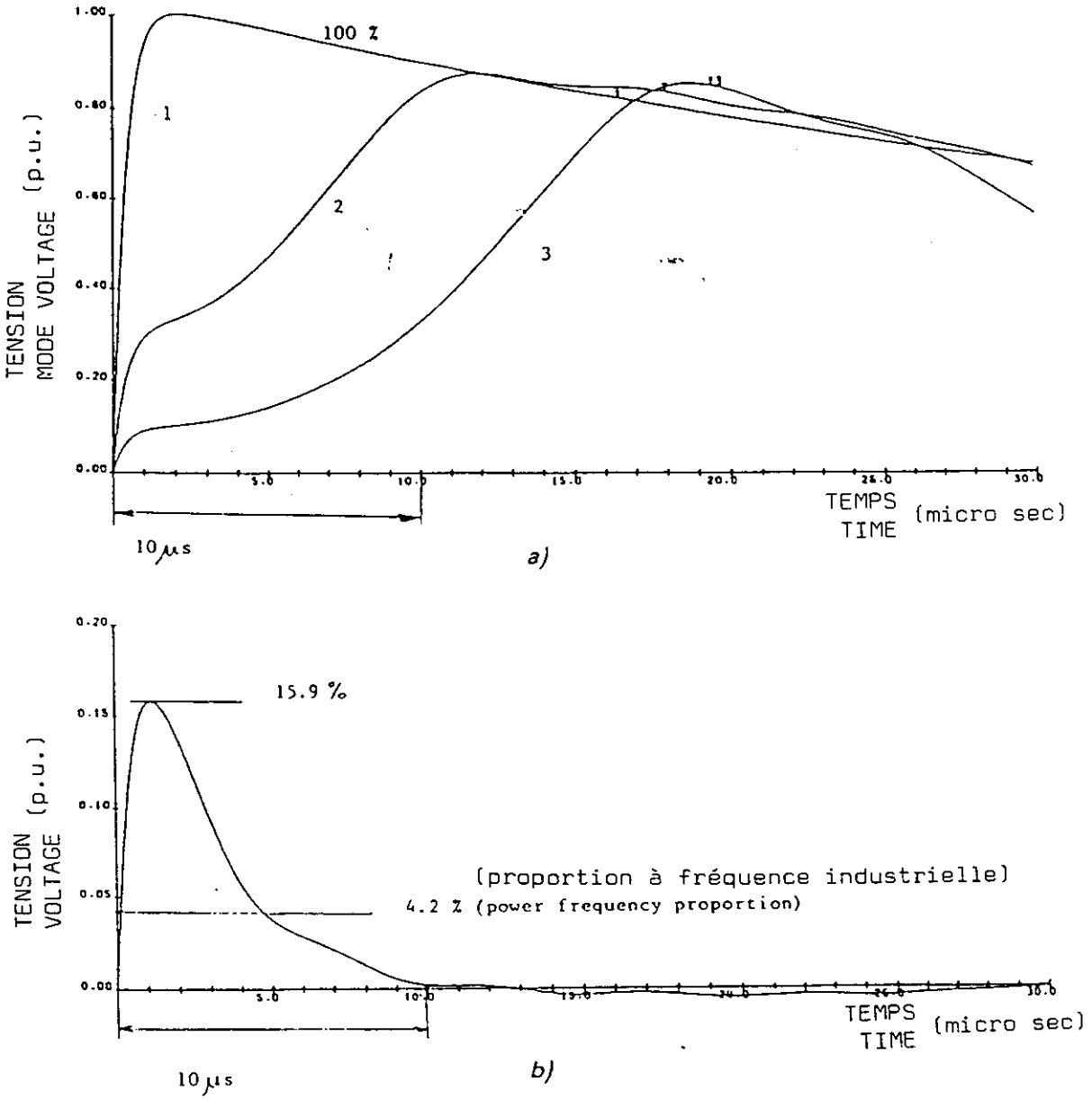

FIGURE 4.4.1 Voltage distribution along the winding of a star-connected, neutral earthed 150 MVA, 275 kV reactor with an applied lightning impulse (1.2/50 µsec)

Fig. a) Curve 1: Voltage at the terminal (100% of the winding)
2: Voltage at 75% of the winding
3: Voltage at 50% of the winding

Fig. b) Voltage across first two sections

The clean chopping overvoltages (without reignitions) may be compared with the standard SIWL (250/2500 µs) test wave shape, which gives some guidance for EHV circuit-breakers. For lower rated voltages the LIWL may serve as a guide-line [27, 28, 29].

The character of the stresses imposed on the reactor by reignitions are similar to those in the standard LIWL (1.2/50 μs) test. It should then be observed that it is the peak-to-peak voltage excursion across the reactor and the non-uniform voltage distribution within the reactor at steep transients that stresses the winding at reignitions. An example of the distribution of a 1.2/50 μs lightning impulse is shown in fig. 4.4.1. The stress between the beginning of the first section (disc) of the winding and the end of the second section is given in fig. 4.4.1.b) and is shown to be nearly 16 percent of the impulse amplitude. This should be compared to the fraction of the steady state power frequency voltage which is 4.2 percent between the same points.

4.4.3 Measures to limit switching overvoltages

4.4.3.1 Opening resistors

Opening resistors may be used to effectively limit the overvoltages caused by small inductive current switching. The resistor is connected in parallel with the main interrupter and an auxiliary interrupter has to be added to break the resistor current in a subsequent current zero.

To reduce the overvoltage amplitudes one can distinguish between two cathegories of resistors having different ranges of resistance values:

- resistance values of the order 10 - 50 kohms per phase
- resistance values of the order 1 - 5 kohms per phase

Note: Low ohmic opening resistors are used for damping the TRV of short-circuit interruptions. Resistance values for this purpose are several hundred ohms (for line circuit-breakers) down to a few ohms (for generator circuit-breakers). The values are too low to be suitable for reactor switching. See Fig. 4.4.4.

The resistor influences the overvoltages generated by the main break interruption in several ways.

- The positive resistance parallel with the arc reduces the chopping level (see Clause 2.3 of Chapter 2).

- For large resistance values ($R > Z_0$, where $Z_0 = \sqrt{L/C}$) the recovery voltage is produced by the LCR-circuit, where R determines the degree of damping.

- For medium resistance values ($R < Z_0$) the magnetic energy on the load side is dissipated through the resistor, causing a voltage drop, which at most can be $i_{ch} \cdot R$.

The damping effect of resistors having high resistance values is illustrated by the recording in Fig 4.4.2 showing the voltages at the terminal of a 275 kV, 150 MVA reactor produced by an air-blast breaker (with high chopping level) equipped with an opening resistor (15.8 kΩ) and by an SF_6-breaker (with low chopping level) without resistor [36]. (It should be observed that the interruption of the resistor current is not shown in Fig 4.4.2.a.)

Further results from the test series with the air-blast circuit-breaker are presented in Fig 4.4.3. The anticipated overvoltages without the opening resistor have been calculated from the chopping level.

The resistor current is usually interrupted by an auxiliary break after one or more loops of current. In case of a high resistance value, this small current is almost resistive and no overvoltages are expected upon its interruption. The auxiliary interrupter can be a simple switch in this case.

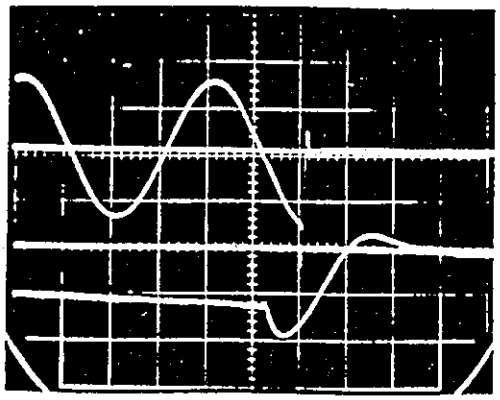

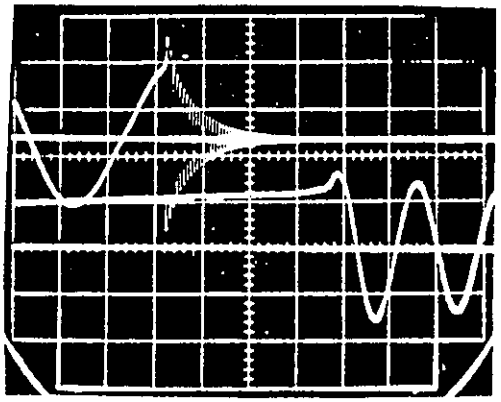

FIGURE 4.4.2 Typical oscillograms of reactor overvoltage waveforms

a) Air-blast circuit-breaker (with resistor)
Top: 157 kV/div, 5 msec/div
Bottom: 206 kV/div, 200 μsec/div

b) Puffer-type SF_6 circuit-breaker (without resistor)
Top: 157 kV/div, 5 msec/div
Bottom: 206 kV/div, 200 μsec/div.

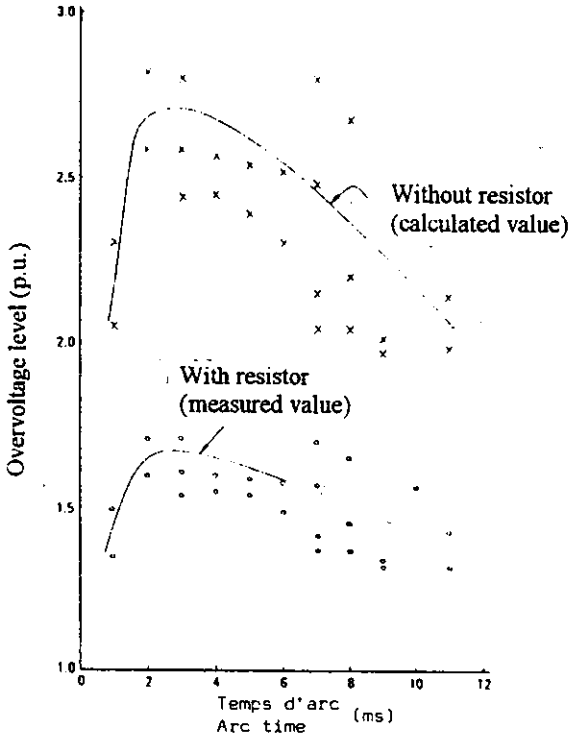

FIGURE 4.4.3 Example of the effect of resistor (15.8 kΩ) in air-blast circuit breaker [36]

With high resistance values reductions of overvoltages reported are:

- from k_{max} = 2.8 p.u. to k_{max} = 1.7 p.u. (with 15.8 kΩ per phase) [36]
- from k_{max} = 2.26 p.u. to k_{max} = 1.55 p.u. (with 30 kΩ per phase) [7]

To achieve still more effective reduction, which may be necessary for breakers with very high chopping level (e.g. heavy duty air-blast circuit-breakers) in EHV and UHV networks, medium resistance values are used. In this case the auxiliary break has to interrupt higher currents and may therefore generate overvoltages due to current chopping. They are usually low for the following reasons:

- The chopping level in the auxiliary interrupter is in itself lower than in the main interupter.

- The resistance in the circuit provides a positive damping reducing the chopping level.

- The current and voltage are much more in phase and thus the recovery voltage is limited.

The overvoltage created by both main and auxiliary interrupters are dependent upon the resistance magnitude as follows:

- In the main interrupter, the higher the resistance the higher the overvoltage because the smaller damping effect of the resistor.

- In the auxiliary interrupter, the higher the resistance the lower the overvoltage.

As a result the resistance value shall be a compromise dictated by the two successive interruptions.

The effect is shown in Fig 4.4.4 [25].

A certain overvoltage reduction would be achieved if the main and auxiliary breaks interrupt the current at the same zero. But to get the full advantage the timing of the contact parting of the main and auxiliary breaks should be such that the auxiliary break is still closed upon the interruption of the main break. The "insertion time", usually defined as the time difference between the contact partings of the main and auxiliary breaks respectively, should be larger than the maximum arcing time of the main break. The current loop through the resistor will in all practical cases also be several times the time constant of the LR-circuit.

Besides the use of linear opening resistors [7, 25, 31, 32, 36] also non-linear resistors may be used [33]. It has even been proposed to use ZnO-resistors without any auxiliary break to reduce reignition transients, i.e. to introduce a surge arrester connected in parallel to the breaker. See section 4.4.3.3.

Reignition overvoltages are also limited by opening resistors. With resistors of a value in the range of the load surge impedance or lower, the recovery voltage will be heavily damped thereby considerably reducing the probability of reignitions. See Fig 4.4.2.a. Should a reignition occur the overvoltage is expected to be less than 2 p.u. even with negligible damping of the second parallel oscillation. This is obvious from a comparison of figures 4.4.2.a and 4.3.3. The voltage excursion - peak-to-peak - will also be reduced to values less than 2 p.u.

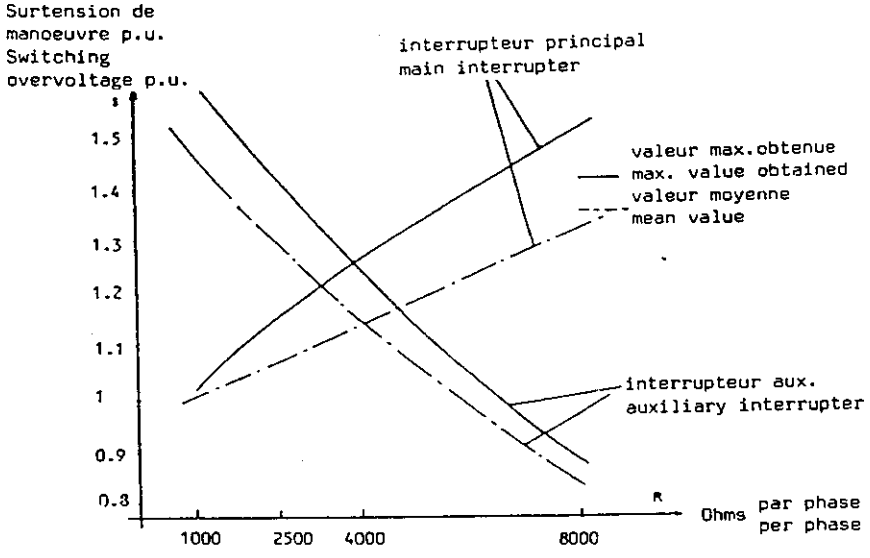

FIGURE 4.4.4 Measured overvoltages produced by the main interrupter and auxiliary interrupter when switching a 735 kV, 165 MVA reactor bank with an air-blast breaker [25]

4.4.3.2 Spark gaps

Spark gaps have been widely used in the past to limit overvoltages especially at moderate rated voltages, but they have several disadvantages which have reduced their use in modern systems:

- Erratic sparkover voltage
- Long and erratic time delay to breakdown
- Strong dependence on wave shape
- Dependence on ambient conditions
- Risk of creating an evolving fault
- Imposing a short circuit condition on the network
- Creating chopped waves

Spark gaps are not recommended as a measure to reduce switching overvoltages [34]. Encapsulated spark gaps (in SF_6) have been introduced lately, but their suitability to limit switching surges remains to be investigated.

4.4.3.3 Surge arresters

Two basic types of surge arresters are available today:

- Non-linear resistor type with passive or active spark gaps
- Metal oxide varistor type without spark gaps (ZnO-arresters)

Knowing the approximate statistical distribution of overvoltages (calculated from breaker characteristics deduced from general tests) the probability and/or frequency of arrester operations may be estimated.

Due to the relatively low discharge energy, a high number of arrester operations may be permitted. Therefore the arrester is a very suitable device to limit overvoltages at interruption of small inductive currents. The gapless metal oxide arresters with their low protection level are especially well suited since they reduce the (cumulative) dielectric stress applied to the reactor [12].

As noted in Sub-clause 4.3.3 reignition transients can still achieve peak-to-peak excursions much higher than the arrester level - theoretically up to twice the arrester operating level. Figures 4.5.3 and 4.3.7 together with the data in Table 4.3.2. (noting that $u_s = U_2 + 1$ or $u_s = U_3 + 1$) illustrate that a voltage excursion of greater than 3 p.u. may be anticipated, even without any chopping by the switch.

As mentioned in Section 4.4.3.1 it has been suggested to arrange ZnO arresters in parallel with the circuit-breaker to reduce the peak-to-peak excursion and steepness of reignition transients as well as the number of reignitions. This may be an interesting alternative to opening resistors with an auxiliary break. However, to limit the reignition overvoltages to values < 2.0 p.u., the protection level of the arrester has to be decreased to 1.5 p.u. or lower. This may still be feasible, but the need for an arrester to earth between the breaker and the reactor will remain unchanged.

4.4.3.4 Use of capacitors as voltage limiter

Adding of lumped shunt capacitances to the reactor has a complicated influence on the generation as well as on the limitation of overvoltages.

For a given amount of released energy in the interrupted load circuit, the voltage amplitude decreases (Eq. 4.3.2) and the time to crest increases. But - except for vacuum breakers - the amplitude reducing effect is neutralized by a higher chopping level. The overvoltage factor given by Eq. 4.3.7 is only slightly dependent upon the load side capacitance C_t. If the supply side capacitance C_s is much greater than C_t, the overvoltage is practically independent of C_t.

An added capacitance may reduce both the steepness and amplitude of the voltage transients caused by reignitions (see e.g. eq. 4.3.8 in Sub-clause 4.3.3). A large load side capacitance increases the energy involved in the second parallel oscillation and the h.f. current magnitude associated with the reignition. This may influence the risk for virtual current chopping in a similar way as reported in

reference [39] of Chapter 3 for high voltage motor circuits [13]. (The widespread successful use of surge capacitors in motor circuits is due to the sensitivity of motors to steep transients. The steepness of wave fronts at energization and reignition is reduced very effectively by the capacitors.)

4.5 Testing

4.5.1 General

In the scope of WG 13.02 it is stated that substitute laboratory circuits for small inductive current switching tests should be proposed. The analysis in the preceeding Clauses of this Chapter shows that it is impossible to model an actual network situation correctly in all respects in a laboratory. In spite of this, a substitute test circuit will be proposed. It is believed that tests in this circuit will give valuable information that could be used in estimations of the overvoltage risk in actual networks.

The main purpose of any tests representing reactor switching is to establish the risk of creating dangerous overvoltages.

If the breaking ability as such or the coordination of the dielectric strength of the contact gap at reignitions for some reason is doubted and has to be verified by tests, the general tests described below may be chosen as they are intended to cover interruption of different kinds of inductive load. They may also be used to test the breaking capability of other switching devices than circuit-breakers, e.g. high voltage switches.

4.5.2 Field tests

Field tests in the actual network is the only way to achieve full assessment of the performance of a certain circuit-breaker in that specific situation.

Care must be taken that the circuit is not noticeably modified by the measuring equipment used. Specially the capacitance of voltage dividers must be low compared to the capacitances of the circuit. Furthermore one should take care that the circuit will not be substantially changed by abnormal connection of the supply network (the substation) and by protective devices.

In addition to the tests suggested in Subclause 4.5.4., it might also be valuable to perform some closing tests to determine the severity of the switching transients upon closing for the actual installation.

The test results, even though reliable for that specific installation, can be extended to other installations only with the utmost care.

4.5.3 Laboratory tests

Laboratory tests may be performed either to obtain general information about the circuit-breaker behaviour (general tests) or with the aim of reproducing the conditions in a certain reactor installation as closely as possible (specific tests).

The general tests may be used for assessment of the chopping performance and reignition level of the circuit-breaker when used in other circuits. The absolute overvoltage level in another circuit may, however, be quite different. The tests may also be used to provide data on breaker parameters intended for more thorough computer calculations.

The specific tests are necessary when a closer prediction of overvoltages in a certain installation is required. However, the accuracy of the result is very dependant on how precise the modelling of the actual circuit components – the reactor, the supply network, the connections – can be made in the laboratory.

4.5.3.1 General tests, h.v. reactor circuit

Figure 4.5.1 suggests a single-phase test circuit which may be used for determination of the general properties such as the chopping level and the reignition characteristic of circuit-breakers when switching

h.v. reactors, > 72.5 kV. The circuit could be used for testing of a full circuit-breaker pole if the laboratory resources make it possible. Alternatively, tests could be performed on a part of a pole or on a single breaking unit.

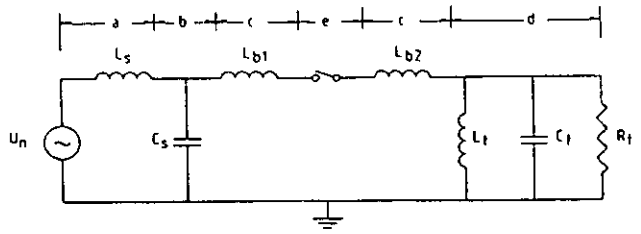

FIGURE 4.5.1 Basic lay-out of test circuit

The characteristics of the various parts of the circuit are discussed below (refer to the lettering in Figure 4.5.1):

a) Supply network

The test circuit supply network will normally consist of a generator and a transformer. The inductance L_s should be less than 10 % of the load inductance L_t. L_s must, however, be chosen large enough to limit the short-circuit current of the circuit to a value not exceeding the rated breaking current of the circuit-breaker under test.

b) Supply side capacitance C_s

The supply capacitance C_s represents a network that may consist of several lines and/or cables. The effective capacitance may be rather large and values of $C_s > 10\ C_t$, where C_t is the total load capacitance, are representative.

Note: No further modelling of the TRV of the supply is necessary.

c) Connecting leads

The total inductance, $L_b = L_{b1} + L_{b2}$, is determined by the required natural frequency of the $C_s - L_b - C_t$ loop, i.e. the circuit of the second parallel oscillation after a reignition. The added inductance, if any, may be arbitrarily divided between the supply and the load side.

The capacitances of the supply and load side leads are considered to be included in C_s and C_t, respectively.

Even though the damping of the second parallel oscillation may influence the tendency of multiple reignitions to occur by changing the current rate of change at current zero, it seems difficult to prescribe a damping factor. Experience indicates an overswing of $\geq$ 50 per cent of the peak-to-peak voltage excursion on the load side after a reignition (see Figures 4.3.5 and 4.3.6 and Table 4.3.2, all indicating that $\beta \approx 0.4$ to 0.5 in eq. 4.3.9). This may be taken as a guideline.

d) Inductive load

The load should preferably consist of a directly connected reactor. When a suitable reactor is not available a transformer, loaded on its secondary side by a reactor, may be used. The transformer should be operated within the nonsaturated part of its magnetizing curve and its leakage inductance should be low, preferably less than 10 % of the total load inductance L_t.

The natural frequency of the load may be adjusted by means of a lumped capacitance, connected in the direct vicinity of the reactor or on the h.v. terminals of the transformer. The total capacitance C_t of the load consists of the sum of the stray capacitance, reactor capacitance and the additional lumped capacitance.

The damping of the load is represented by the equivalent parallel resistance R_t. The consecutive peak ratio of the damped oscillation should not be below 0.9. The consecutive peak ratio (CPR) is defined as the ratio of two consecutive peaks of the same polarity. The relationship to the damping factor $\alpha = 1/\tau$ in equ. 4.3.1 is: $1/\tau = -(\omega/2\pi) \cdot \ln(CPR)$.

Note: Use of a reactor loaded transformer to represent the load may introduce an additional oscillation, associated with the oscillatory behaviour of the transformer network. Such an oscillation may change the test results from those which would be obtained in a circuit with a load consisting of a reactor only, e.g. by introducing additional current zeros. Often several separate transformer units are combined with the high-voltage windings in series. If the low voltage windings are in parallel the oscillation may be significant, thus this connection should be avoided if possible.

If a serial connection of the l.v. windings or if one single phase transformer is employed, the oscillation may be negligible and a representative result can be expected.

e) Breaker under test

The breaker under test should include any grading capacitors and opening resistors.

The pressure of the extinguishing medium as well as the operating pressure should have rated values. The reasons are:

- the tests aim at a statistical distribution of overvoltages. The breaker conditions should therefore be the most probable ones, i.e. rated conditons;
- pressures above the rated levels may result in higher chopping overvoltages but lower reignition overvoltages (due to fewer reignitions);
- pressures below the rated values may result in lower chopping overvoltages but higher reignition overvoltages (due to larger number of reignitions).

The tests should be performed with the following power frequency voltage of the supply circuit after interruption:

- for full pole testing: $U_n/\sqrt{3}$ where U_n is the rated voltage of the circuit-breaker.
- for unit testing: $\alpha U_n/N\sqrt{3}$ where N is the number of breaking units in a full breaker pole and α is a correction factor, $\alpha > 1.0$, that takes uneven voltage division into account.

Note: Since the supply side voltage usually can be assumed to be stiff (large capacitance) the load side oscillation will be distributed between the units in the same ratio as the TRV at short-circuit tests (with opposite terminal connection). An increased test voltage to represent the most highly stressed unit is required mainly to demonstrate the reignition characteristics of the circuit-breaker.

f) Test duties

For simulation of the conditions in normal h.v. reactor installations, $\geq$ 72.5 kV, tests should be performed with the following parameter combinations:

A. Current: 100 A
Natural load frequency, f_L: 0.8-2.3 kHz, preferably $f_L = k_f\sqrt{(l/U)}$ (where $k_f = 72.8 \cdot 10^3$ for 50 Hz)
Natural frequency of C_s-L_b-C_t-loop: 150-200 kHz

B. Current: 300 A
Natural load frequency, f_L: 1.4-4.0 kHz, preferably $f_L = k_f\sqrt{(l/U)}$
Natural frequency of C_s-L_b-C_t-loop: 150-200 kHz

The preferred natural load frequency f_L is given by:

$$f_L = k_f\sqrt{\frac{I}{U}} = \sqrt{\omega\frac{\sqrt{3}}{4\pi^2 C_t}}\sqrt{\frac{I}{U}} \qquad (4.5.1)$$

where I = test current
U = rated voltage of circuit-breaker
ω = angular frequency of main voltage
C_t = effective capacitance parallel to the reactor winding

The value of the factor k_f (= $72.8 \cdot 10^3$ for 50 Hz and = $78.6 \cdot 10^3$ for 60 Hz) corresponds to an effective load capacitance of 2.6 nF which is judged representative for reactors in the HV range.

Note 1: The highest chopping overvoltages are usually produced at low breaking currents (see Eq. 4.3.7 in section 4.3.2). Therefore it may be necessary to perform test A at the lower limit of the current range, for which the circuit-breaker will be applied as a reactor switch (or to make an extra test series at that current).

Note 2: Further test duties may be needed to determine basic circuit-breaker data for calculations.

It should be observed that the recommendations *a)* through *f)* are to a certain extent determined by what is judged to be achievable in a normal testing station. They do not cover all actual installations. For example:

- values $C_s/C_t < 10$ may exist. This will result in a higher amplitude of the main circuit oscillation which may influence the number of reignitions. With values of $C_s/C_t > 10$ when $L_s < 0.1$ L_t, the supply side will not significantly influence the recovery voltage.

- the effective load capacitance may be considerable less than 2.6 nF, e.g. for air-cored reactors, resulting in higher load frequencies

- the load natural frequency may influence the number of reignitions. A high frequency may limit the chopping overvoltage due to reignitions occurring before the suppression peak is reached. Reignition overvoltages may on the other hand be increased due to a larger number of reignitions at voltages approaching the recovery peak.

- the second parallel oscillation frequency may influence the probability of a new interruption after a reignition and thereby the risk of voltage escalation.

If the switch is to be applied in a situation that differs considerably from the conditions under *a)* through *f)*, the neccessity of specific tests with the actual conditions should be considered.

4.5.3.2 Specific tests, h.v. reactor circuit

Generally, for a specific test, the laboratory circuit should represent the actual installation as closely as possible. Thus, ideally, the actual reactor in a three-phase circuit should be used, and the actual circuit should be modelled as detailed as possible. Quite often, however, limitations of the test plant make comprehensive simulation of an actual installation impossible. In such cases simplification is necessary, and the following points may then be observed:

- In case the actual reactor is directly earthed and has uncoupled phases, the current chopping and related overvoltages in the three phases are independent. It should thus be possible to model these phenomena properly in a single-phase circuit. However, since a certain capacitive coupling between phases always will exist, a three-phase model will yield improved accuracy when reignitions, with the associated high frequency transients, are involved. Therefore, especially in case of three-phase metal enclosed circuit-breakers, three-phase testing is to be preferred.

- In cases with strong interphase coupling where $X_0/X_1 \neq 1$ only three-phase modelling can give a realistic result. The cases are: unearthed reactors, 3-1egged reactors and cases with a fourth reactor between neutral (starpoint) and earth (see sub-clause 4.3.4).

- Unit testing considerably increases the difficulty of relating the laboratory test results to the actual installation. Nevertheless limited available test voltage will often make unit testing the only alternative.

- Quite often the laboratory cannot realize a real reactor load even at unit tests, but has to resort to a load consisting of a reactor-loaded transformer. It is then important that the natural frequencies are not significanly altered by the transformer.

In addition to reproducing correct values of power frequency current and voltage the laboratory circuit should primarily be modelled to reproduce as correctly as possible

- The source side impedance
- The source and load side connections to the test breaker, length and surge impedance
- The natural oscillation frequency and damping of the load
- The oscillation frequency of current through the circuit-breaker at reignitions (the second parallel oscillation)
- The coupling between the phases

4.5.3.3 General test, m.v. reactor circuit

M.V. reactors, < 72.5 kV, are normally unearthed and connected to transformer tertiaries. During switching there is strong interaction between the phases and for realistic simulation of the conditions it is therefore necessary to make three-phase tests. General tests should normally not be recommended for m.v. reactor switching. Specific tests will generally give more reliable results. However, when some guidance on circuit-breaker behaviour is required, a test circuit according to Figure 4.5.2 may be used for determination of the chopping performance and reignition level of a circuit-breaker when switching m.v. reactors.

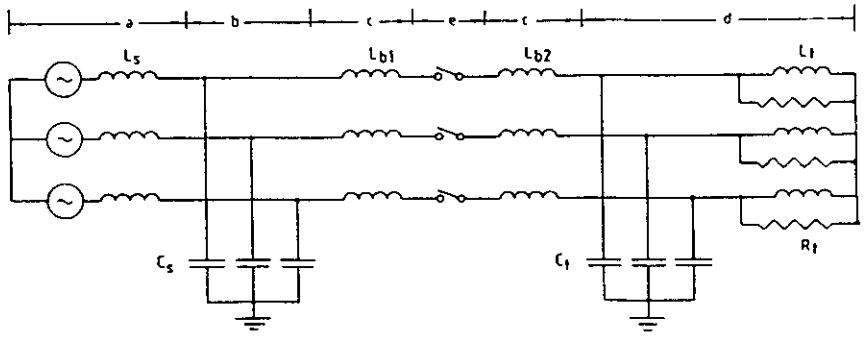

FIGURE 4.5.2 Basic lay-out of three-phase m.v. circuit for genera[test purposes

The various parts of the circuit may be commented as follows (refer to the notation in Figure 4.5.2):

a) Supply network

Same as for HV circuit, see 4.5.3.1.*a*)

b) Supply side capacitance C_s

See 4.5.3.1.*b*

c) Connecting leads

See 4.5.3.1.*c*)

d) Inductive load

The inductive load should consist of single-phase units and be unearthed. The single-phase units should preferably consist of reactors. Otherwise the requirements are the same as for the HV circuit in 4.5.3.1.*d*).

e) Breaker under test

The breaker under test should include any equipment normally fitted to the breaker, like surge suppressors.

All operating characteristics (pressure, operating voltage, etc.) should have rated values. See subclause 4.5.3.1.*e*).

f) Test duties

The tests should be performed with a power frequency voltage at the supply side after interruption equal to the rated voltage of the tested circuit-breaker.

For simulation of the conditions in normal m.v. reactor installations, tests are recommended to be performed with parameter combinations according to Table 4.5.1:

TABLE 4.5.1
Test duties for general testing - m.v. reactor circuits

Rated voltage kV	Test duty	Current A	Natural load frequency 1) kHz	Natural frequency of C_s-L_b-C_t-loop kHz
12 - 36	A B	500 1500	9 - 11 2), 4) 18 - 22 2), 4)	150 - 200 150 - 200
>36 - 72.5	A B	200 500	1.8 - 2.2 3), 4) 3.6 - 4.4 3), 4)	

1) For the first phase to clear
2) These values are based on practical values for coreless reactors with an effective load capacitance of 1.2 to 2 nF (including phase-to-phase capacitances of reactors as well as connections). Considerably higher frequencies are not uncommon in installations with air-cored reactor units and short connections.
3) These values are based on practical values for gapped iron-core reactors with an effective capacitance of 3 to 4 nF (including phase-to-phase capacitances).
4) When the actual effective load side capacitance is known, a load frequency f_L given by Eq. 4.5.1 in 4.5.3.1 would make the test to better represent the specific case.

Note 1: The highest chopping overvoltages are usually produced at low breaking currents (see Eq. 4.3.7 in section 4.3.2). Therefore it may be necessary to perform test A at the lower limit of the current range, for which the circuit-breaker will be applied as a reactor switch (or to make an extra test series at that current).

Note 2: Further test duties may be needed to determine basic circuit-breaker data for calculations.

It is obvious that a test circuit according to the recommendations *a)* through *e)* may differ considerably from most actual installations. Tests performed in the circuit should result in giving an estimation of the breaker characteristics and a basis for comparison of different circuit-breakers. To get a more representative result specific tests should usually be considered.

The common case with cable connections on the supply and/or load side differ drastically from the test conditions recommended. In such cases it might be better to use the substitute test circuit for h.v. motor switching proposed in Chapter 3.

4.5.3.4 Specific tests, m.v. reactor circuit

The supply circuit should be modelled as detailed as possible and the actual reactor should preferably be used. In general care should especially be taken to model appropriately:

- The impedance and winding arrangement of the supply (e.g. star–delta connected transformer, neutral point earthing).
- The type (e.g. bus, line or cable), length, and surge impedance of the connections between supply, circuit–breaker and reactor.
- The oscillation frequency of current through the cicuit–breaker at reignitions (the second parallel oscillation).
- If a substitute for the actual reactor is used:
  - * The winding arrangement and earthing conditions of the load.
  - * The natural oscillation frequency and damping of the load.

4.5.4 Test series and measurements

The required test procedure depends greatly on the purpose of the tests. This may be split into two cathegories, which could be further divided according to the specific object of the test:

A. Proving the interrupting ability of the breaker (or switch)

A1) to prove the ability of the breaker (or switch) to interrupt reactor currents.

A2) to prove that reignitions are not harmful to the breaker.

B. Investigation of the breaker's behaviour mainly in respect of overvoltage production

B1) to achieve an estimation of the maximum chopping current.

B2) to study the statistical distribution of the chopping current (and maybe a possible dependence on arcing time).

B3) to investigate the reignition probability or determine the range in point–on–wave setting with reignitions.

B4) to get an estimation of the dielectric strength characteristic of the contact gap.

To cover item A1) and B1) it is recommended that, for both general and specific tests, a test serie should consist of 20 breaking tests, differing in point–on–wave of the breaker trip signal by 18° el for single phase tests and 9° el for three–phase tests. The reason for the latter being to prevent a repetition of the same tripping phase angles in the three phases that takes place at the normally used point––on–wave steps of 15° and 30° el.

To investigate the breaker characteristics (mean value, standard deviation) with some degree of statistical significance, it is necessary to increase the number of tests considerably. To cover item B2) a sufficient number as determined by the desired confidence level has to be carried out with contact parting evenly spread over 360° el. At least 60 single–phase or 40 three–phase tests are deemed to be required to give an acceptable estimation of the 2σ–value.

To determine the range of arcing times where reignitions occur (item B3) it is recommended to run 40 tests with 9° el change in point–on–wave setting of trip instant. This tests series will also provide data such that an estimation of the dielectric strength characteristic (item B4) may be made.

To cover item A2) tests should be performed wherein the maximum number of reignitions are caused to occur. E.g. after a coarse determination of the reignition range with 20 tests to cover item A1) and B1) a further 20 tests with settings evenly distributed within the reignition range(s) should be made. Alternatively the test to cover item B3) may be extended to contain a sufficient number of reignitions.

If point-on-wave control for the moment of contact separation cannot be arranged, twice the above numbers are suggested with a random circuitbreaker trip signal.

The above recommendations are summarized in Table 4.5.2.

TABLE 4.5.2
Summary of test recommendations

	Single-phase tests		Three-phase tests	
	Number of tests	Point-on-wave steps Electrical degrees	Number of tests	Point-on-wave steps Electrical degrees
A. Proving the breaker ability A1) To interrupt reactor currents	20	18	20	9
A2) To withstand reignitions (in addition to the tests under A1)	20	$\Theta_R/20$ 1)	20	$\Theta_R/20$ 1)
B. Investigation of overvoltage characteristics B1) Estimation of chopping current	20	18	20	9
B2) Statistical distribution of chopping current	N($\geq$ 60)	360/N	N ($\geq$ 40)	360/N
B3) Determine range of reignitions	40	9	40	9
B4) Estimation of dielectric strength of contact gap	40	9	40	9

Notes – 1: Θ_R = reignition range(s), i.e. point-on-wave steps in which reignitions occur.
2: Test data from tests under B3) may be used.

By oscillographs or other suitable recording techniques, the following quantities should be recorded (in all three phases if applicable):

a) Recordings with moderate bandwidth and time resolution (suitable for power frequency phenomena):

- Supply side voltage, phase-to-earth
- Load side voltage, phase-to-earth
- Load side neutral point voltage to earth (in case of unearthed reactors)
- Current through the circuit-breaker
- Current in the opening coil of the breaker
- Travel of moving contacts (if practicable)

b) Recordings with bandwidth and time resolution high enough to record correctly transient voltages, even in case of reignitions:

- Load side voltage, phase-to-earth, at the terminals of the load reactor (or the transformer primary in case of reactor loaded transformers)
- Current through the circuit-breaker
- Voltage across the circuit-breaker

Note: If surge arresters used to protect equipment are connected to the test circuit, current through the arresters should be recorded with a fast time resolution since counters may not operate for short current pulses.

4.5.5 Result evaluation

4.5.5.1 Overvoltage characteristics

Several overvoltage characteristics may be measured from records of the load side voltage, the most important being:

- u_{m1} suppression peak voltage to earth (for evaluation of i_{ch})
- u_{m2} maximum peak voltage to earth of load oscillation following interruption
- u_p maximum overvoltage to earth
- u_s maximum peak-to-peak voltage excursion at reignitions

The voltages are identified in Figure 4.5.3 for a typical single phase test circuit representative of a h.v. reactor which typically has an earthed neutral. A similar example for interruption in a three-phase circuit with unearthed neutral is given in Figure 3.6.1. of Chapter 3.

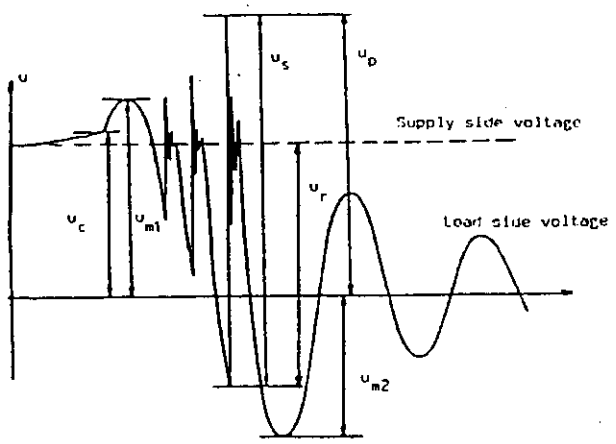

FIGURE 4.5.3
Illustration of transient voltages

u_c Initial voltage
u_{m1} Suppression peak voltage to earth
u_{m2} Recovery peak voltage to earth
u_p Maximum overvoltge to earth
u_s Maximum peak-to-peak voltage excursion at reignitions
u_r Reignition voltage across breaker

The highest peak value of the load side oscillation is usually u_{m1} at single-phase testing. Only in case of voltage escalation it may happen that u_{m2} is higher than u_{m1}. In the statistical treatment the highest of the values should be taken as u_m.

For each test series, it is recommended that at least for u_m and u_p a statistical analysis should be made. The following values should then be determined:

- maximum recorded value
- mean value
- an estimated value of the standard deviation (e.g. by using normal distribution charts).

In addition the number of tests in a test series at which significant reignitions have occured may be stated and, if possible, the point-on-wave range of trip settings which result in reignitions.

4.5.5.2 Chopping current characteristics

It is recommended that particularly for the general tests the circuit-breaker chopping level should be evaluated.

The chopping current should, if possible, be determined from current measurements with sufficient frequency response. The current should be measured close to the circuit-breaker to avoid errors due to currents through stray capacitances. This can be done using fibre optic telemetry techniques.

In case of current instability oscillations before the final chop, the equivalent chopping current can usually be estimated as shown in Fig. 2.3.1 of Chapter 2.

If the current measurements give uncertain values of the chopping current, approximate, but usually sufficiently correct, values of the chopping current may be determined from measurements of the peak value of the suppression peak and the voltage across the load before current extinction. The chopping current is then (from Eq. 4.3.2 or Eq. 2.3.18 of Chapter 2):

$$i_{ch} = u_o \sqrt{\frac{C_t}{L_t}(k_a^2 - k_c^2)} \qquad 4.5.1$$

where u_o = peak value of the power frequency voltage
C_t = total load capacitance
L_t = total load inductance
$k_a = u_m/u_o$, where u_m is the suppression voltage peak value
$k_c = u_c/u_o$, where u_c is the initial voltage at the moment of current chopping.

In order to give precise results, this calculation must be corrected for the damping effect of the circuit but since the consecutive peak ratio is > 0.9 this correction is normally negligible.

It can normally be assumed that $k_c \approx 1.0$. For h.v. breakers, this will result in a negligible error.

For each test series the

- mean value and
- standard deviation

of the chopping current should be determined if possible. For most breakers the chopping number, κ_r, according to Eqs. 4.3.5 and 4.3.6 may be evaluated and used as a convenient characteristic in further calculations (exception: vacuum-breakers).

For certain breakers a correlation between chopping current and arcing time exists. But since one usually can assume that the trip-angle in actual operation is random, the estimation of probable maximum overvoltage (e.g. the 2σ -value), will take any dependence of chopping level on arcing time into account by the value of standard deviation derived from a test with evenly distributed point-on-wave settings over a cycle.

4.5.5.3 Dielectric strength characteristics

The rise of dielectric strength may be determined from direct measurements of reignition voltages u_r (see Figure 4.5.3) between the breaker contacts as a function of time after current zero and – if relevant with the arcing time as parameter.

4.5.6 Result applicability

The results obtained are applicable only to the tested circuit. However, they can also give information of the characteristics of the tested circuit-breaker. Based on this, the breaker performance in other circuits could be estimated. The main difficulties involved in such an estimation are:

a) Extrapolation to breakers with a different number of breaking units
b) Extrapolation from single phase to three-phase circuits
c) Influence of the source side network
d) Influence of the characteristics of the load

If the overvoltages due to current chopping dominate over overvoltages caused by reignitions (i.e. the suppression peak voltage u_m gives the maximum overvoltage value) crude extrapolation of the test results to other circuits is possible by using the Eq. 2.3.18 of Chapter 2 or Eqs. 4.3.2 to 4.3.7 of this Chapter.

In extrapolating to other numbers of breaking units (item a) the chopping characteristic, κ, is preferably used. The relation is simple:

$$\frac{\kappa_1}{\sqrt{N_1}} = \frac{\kappa_2}{\sqrt{N_2}}$$

where κ_1 is achieved with N_1 units and
κ_2 is achieved with N_2 units

This simple relationship has been shown to give a slightly too high chopping number when extrapolating to a larger number of breaking units [7, 38]. A theoretical study supports this [39]. However, the error is small compared to other uncertainties in the procedure and since it gives a conservative estimation in the normal extrapolation from single unit tests, the simple relationship is recommended to be used in such extrapolations.

To overcome the difficulty to apply single-phase test results to a three-phase circuit some general conclusions presented in Clause 4.3.4 may be used. For earthed reactors with weak interphase coupling, three-phase interruption may be treated as three single phase interruptions when chopping overvoltages are considered. In cases with strong coupling between the phases or for unearthed reactors, the interaction between phases makes overvoltage prediction by simple calculation doubtful even though some indication of the level can be achieved.

The overvoltages due to reignitions are very dependent upon the source side network and the load characteristics. For example, long bus connections tend to increase the overvoltages. Also, transmission line connections in the immediate vicinity of the reactor on the source side will tend to decrease the overvoltages, particularly if a direct connection is made (that is, without wave traps or series capacitors). Therefore overvoltages due to reignitions cannot be extrapolated to other situations with any acceptable degree of accuracy. The only possibility seems to be a thorough computer analysis as described in Clause 4.3.3.3.

4.6 Conclusions

Interruption of reactor currents may create overvoltages of two types:

- Chopping overvoltages having magnitudes and time durations approximately corresponding to switching surges.
- Reignition overvoltages having time durations similar to lightning surges but having typically lower crest voltages.

4.6.1 Expected chopping overvoltages

The chopping overvoltages can be estimated with acceptable accuracy from breaker characteristics and reactor size. The diagram in Figure 4.3.2 shows that chopping overvoltages for reactors with earthed neutral are below 2.0 p.u. for normal h.v. reactor sizes if they are switched with modern circuit-breakers, that usually have low chopping levels ($\kappa < 20 \cdot 10^4$). Higher chopping overvoltages may occur for relatively small reactors (smaller than 20 MVA). Overvoltages may be mitigated by reignitions especially when the natural frequency is high as for medium voltage air-core reactors.

For reactors with isolated or impedance earthed neutral somewhat higher chopping overvoltages may be expected due to the first-phase-to-clear effect. This may result in a higher recovery peak (theoretically up to 1 p.u. extra). In isolated reactors a dc-voltage shift may occur after second and third pole clearance which will also increase all transient voltages to earth (see Appendix 5).

In cases with strong interphase coupling - capacitive and/or inductive - the oscillating energy of the load side may be increased in any phase on the load side but the influence on the maximum chopping overvoltages seems to be marginal.

4.6.2 Expected reignition overvoltages

The reignition phenomenon can limit or enhance the maximum overvoltages at switching. However, some conclusions can be drawn:

- All kinds of circuit-breakers and high voltage switches are expected to reignite for a certain range - smaller or larger - of contact separation instants just before a current zero.

- Circuit-breakers and even switches with very low chopping tendency are expected to generate reignition overvoltages of about 2.0 p.u. with a peak-to-peak excursion normally less than 3.0 p.u. but in certain cases up to 3.5 p.u. The front time may be in the range 1 to 4 μs.

- Current chopping preceding a reignition may give rise to higher reignition overvoltages. The highest overvoltages may be estimated from the following expression:

  $k = 1 + \beta(k_a + p)$ p.u.

  where
  μ = an equivalent damping factor < 1, normally $\approx$ 0.5 or less
  k_a = p.u. maximum chopping overvoltage
  p = 1 for earthed reactors
  p = 2 for unearthed reactors;

  For the normal case of k_a < 2 p.u., the maximum reignition overvoltage is expected to be k < 2.5 p.u. and k < 3.0 p.u. for earthed and unearthed reactors, respectively.

  The corresponding peak-to-peak excursions would then be < 4.2 p.u. and < 5.6 p.u. resp. (with $\beta \approx 0.4$).

  For breakers with the chopping level increasing with arcing time reignitions are not likely to occur for long arcing times (= large contact separation). In such cases estimation of the reignition transients should be based on k_a-values for short arcing times only.

- Vacuum circuit-breakers and vacuum contactors may show repeated reignitions with increasing amplitude (voltage escalation) and have therefore to be treated with special care. Other types of modern high voltage circuit-breakers (air-blast, SF_6, oil) normally reignite once or at most a few times and then without voltage escalation.

- In cases with capacitive interphase coupling reignition transients may be transferred between the phases. This may result in increased maximum overvoltages due to superposition. However, this is a stochastical phenomenon and the probability to achieve more than marginal enhancement is rather low.

For a more accurate estimation of the influence of reignitions on overvoltages - enhancement or limitation - either field tests or a thorough computer modelling of the network is necessary. For a computer analysis also knowledge of the breaker characteristics is essential. The general tests recommended in this report can supply this knowledge.

4.6.3 Application considerations

The estimations of normal maximum overvoltage values due to chopping and reignitions may allow some general application considerations:

4.6.3.1 Rated voltage ≤ 300 kV

For rated voltages ≤ 300 kV the normal withstand levels are so high that the overvoltages produced due to chopping and/or reignitions are not dangerous for the reactor insulation. Even in cases of isolated neutral or cases with strong interphase coupling, the risk should be small, especially as those configurations are mostly used at lower rated voltages where the relative impulse withstand is high. However, one or more of the following conditions may create exceptions:

- reactor size < 20 MVA
- high chopping level (chopping number $\kappa > 20 \cdot 10^4$), e.g. heavy duty air-blast breakers
- vacuum circuit-breakers or vacuum switches due to risk of voltage escalation.

Surge arresters are normally used to protect reactor installations. Due to the low energy that has to be dissipated they may be operated frequently without difficulty. Therefore installing surge arresters may in many cases make the need for closer study of the possible overvoltage level unnecessary.

Only in the case of vacuum circuit-breakers it may be necessary to use special protection means of the same kind as for motor switching described in Chapter 3.

4.6.3.2 Rated voltage > 300 kV

For rated voltages > 300 kV the relative withstand level is lower and overvoltages > 2.0 p.u. may not be accepted.

Earthed reactors are predominantly used and the overvoltages are usually low. Unacceptable chopping overvoltages may be produced only if:

- reactor size < 50 MVA
- chopping number $\kappa > 15 \cdot 10^4$.

Protection by surge arresters is usually applied and is quite sufficient to limit the chopping overvoltges, which have relatively low frequencies. Opening resistors are also commonly used, especially with heavy duty air-blast circuit-breakers.

Even with optimized surge arrester protection (ZnO arrester with protection level ≈ 2.0 p.u.) reignition transients with peak-to-peak excursions of > 3.0 p.u. are possible. The insulation and winding techniques used in modern reactors are apparently adequate to withstand the fast reignition transients since the operational experience is extremely good.

However, sometimes special precautions to limit the peak-to-peak excursion and/or the front steepness of the reignition transients, may be judged necessary especially at the highest rated voltages. The following methods are possible:

- opening resistors
- ZnO arresters parallel with the breaker
- high capacitance to earth between breaker and reactor

4.6.4 Validity of testing

Laboratory testing of circuit-breakers for reactor switching duty cannot fully reproduce the conditions in service. Laboratory tests are often performed using single-phase circuits and with single units of the circuit-breakers. Such tests do not take into account three-phase effects, influence of series connected units and other circuit differences. In spite of this, tests carried out in accordance with the recommendations in this report will provide information which may be used to predict approximately the performance in any potential field circuit and allow a judgement of the feasability of the application.

For a more accurate determination of the overvoltage level a field test in the actual installation is the only safe method.

4.7 References in Chapter 4

[1] E. COLOMBO and G. SANTAGOSTINO
Results of the enquiries on network conditions when switching magnetizing and small inductive currents and transf. and shunt reactor saturation characteristics Electra No.94, May 1984

[2] N. KNUDSEN
Single phase switching of transmission lines using reactors for extinction of the secondary arc. CIGRE Report No. 310, 1962

[3] A.J. FAKHERI, J. GRZAN, B.R. SHPERLING, B.J. WARE The use of reactor switches in single phase switching Cigre Report 13-06, 1980

[4] W. BOECK and K. PETTERSSON
Fundamentals and specific data of metal-enclosed substations for the insulation coordination CIGRE Report 23-03, 1978

[5] CEGB: LV injection testing, notes for seminar jointly organized by system technical branch, planning department, HQ and CERL, 1974

[6] B. JONES
The performance of 275 kV air-blast circuit-breakers when switching 100 MVAr shunt reactors C.E.R.L. Laboratory Note No. RD/L/N 3/68, 1968

[7] S. BERNERYD et al
Switching of shunt reactors - comparison between field and laboratory tests
CIGRE Report 13-04, 1976

[10] S.M. POPOV, V.S. RASHKES
Switching surges on 500 kV reactor transformer due reactor switching-off by air-blast cirucit-breaker. VV-400 Elektricheskie Stanzii, 1969, (No. 9) (In Russian)

[11] T.A. BELLEI
Analysis of overvoltages produced during switching of high voltage shunt reactors
Document CIGRE 13-82(WG 11.02)16 IWD

[12] S.H. SARKINEN et al
High frequency switching surges in EHV shunt reactor installation with reduced insulation levels
Paper No. F 78 659-5, IEEE PES Summer Meeting 1978

[14] C.E. SÖLVER
The Stackbo shunt reactor - overvoltages at field tests and normal service switching
Document CIGRE 11-78(WG 134.02)24 IWD

[15] Unpublished information (ECNSW, Australia, 1975)

[16] V.M.C. VAN DEN HEUVEL
Overvoltages after current chopping in a three-phase inductive circuit with isolated neutral
IEEE Trans. on PAS, 100(1981), p. 4795-4801

[17] Unpublished information (C.E.R.L., United Kingdom, 1972)

[18] Unpublished information (FKH, Switzerland, 1965)

[19] Unpublished information (FGH Mannheim, Germany, 1977/

[20] A.N. KOMAROV et al
La coupure des courants inductifs des reactances shunt à EHT. CIGRE Report 13-06, 1978

[21] H. PATRUNKY et al
Switching of transformers, reactors and long transmission lines. Field tests in German 420 kV networks CIGRE Report 13-08, 1980

[22] E. HOFFMAN and B. STÖSSER
Schaltversuche mit unbelasteten und induktive belasteten 380 kV Transformatoren Elektrizitätswirtschaft 79 Jg. (1980) Heft 8

[23] Unpublished information (S & C Electric Company, U.S.A.)

[24] E. HOFFMANN et al
Schaltversuche mit unbelasteten und induktiv belasteten 220 kV - und 380 kV - Transformatoren

[25] E. THURIES, PHAM VAN DOAN, R. JEANJEAN, D. DUFOURNET Coupure des faibles courants inductifs en réseau et en station d'essais limitation des surtensions Report 13-81(SC)25 presented at CIGRE SC 13 Colloquium in Helsinki, September 1981

[26] IEC Publication 71-1, Insulation co-ordination Part 1: Terms, definitions, principles and rules (1976)

[27] B SALVAGE et al
The electric strength of oil-impregnated, paper-lapped conductors for transformer windings International High Voltage Symposium, ZUrich 9-13 Sept. 1975

[28] M OUYANG et al
Switching impulse and lightning impulse strengths of oilimmersed insulation structures and relevance to service and test voltage requirements of transformers. CIGRE 12-01, 1970

[29] E T NORRIS
Transformer switching surge strength
Electrical Review (1965):12, February, p. 239-240

[30] IEC Publication 56: High-voltage alternating current circuit-breakers

[31] P BALTENSPERGER
Form und Grösse der Ueberspannungen beim Schalten kleiner induktiver sowie kapazitiver Ströme in Hochspannungsnetzen. Brown Boveri-Mitteilung 47(1960):4, p. 195-224

[32] B JONES
The switching of transformers. CERL 1967, Report RD/L/R 1477

[33] K HINTERHTHUR and B SCHEMMANN
Damping the switchig overvoltages of MV circuit-breakers by non-linear damping resistors. Teschnische Mitteilungen, AEG-Telefunken 65(1975):H 1/2, p 46-50

[34] IEC Publication 71-2, Insulation co-ordination Part 2: Application Guide (1976)

[36] A. KOBAYASHI et al.
Interrupting test of 275 kV reactor and its evaluation in three kinds of gas-blast cb. IEEE-report 85SM371.0

[38] G E GARDNER, R J URWIN
Performance and testing of multi-unit circuit breakers switching low inductive currents. Proc. IEE 125(1978):3, p. 230-236.

[39] D ANDERSSON
Current instability and chopping with arcs in series. Proc. IEE 132(1985):4, p. 224-228.

Chapter 5:

SWITCHING OF UNLOADED TRANSFORMERS

5.1 Introduction

Unloaded transformers require a small no-load magnetizing current. For a given transformer rating the magnitude of the no-load current depends on the size and quality of the transformer core. The extensive application of cold-rolled, grain-oriented iron sheets, has reduced the magnitude of no-load currents to values lower than 0.2 % of the transformer rated current, in the largest units.

The range of transformers considered is from medium voltage power transformers switched at 3.3 kV to large-power transformers at the highest rated voltages.

The main consideration is given to modern power transformers having cold-rolled grain-oriented steel (CROS) cores, but older transformers using hot-rolled steel (HRS) are also considered.

Experience shows that significant overvoltages are not typically generated by the interruption of the steady-state no-load current of a modern transformer, even if the interrupting device should be able to chop the current at its maximum value. However, in the case of interruption of the inrush current of a transformer the actual switching device determines the maximum chopping level, since the inrush current has an amplitude many times the steady-state value. Therefore under certain conditions overvoltage generation may have to be considered if inrush currents are interrupted.

High-voltage transformers are not switched frequently in service and the interruption of inrush currents, in particular, is rare since this necessitates interruption within a few seconds after switch-on, e.g. due to a low setting of the overcurrent protection level, which should be avoided.

The possibility of excitation of part winding resonance phenomena due to repetitive reignitions has been discussed, but the probability is judged to be negligible [1, 2].

Even though this study is mainly directed to circuit-breakers, it is understood that the general philosophy is also applicable to other switching devices, for example h.v. switches.

5.2 Typical network configurations and transformer characteristics

This section is mainly based on the results of an enquiry carried out by WG 13.02. The detailed result is presented in Electra No. 94 [3].

5.2.1 High voltage networks > 72.5 kV

In the great majority of the cases reported, the busbars on both sides of the transformers have several bays connected. The lay-out of the supply system, to which the transformers are connected shows great variations. The most recurrent arrangements appear to be both a single and a double busbar system, with three to eight bays [3]. For higher voltages ring-bus and breaker-and-a-half schemes are common.

The general layout and arrangement of connections etc., is the same as described in Chapter 4 in sub-clause:

- 4.2.1.2 for open-air substations
- 4.2.1.3 for metal-enclosed substations (GIS)

5.2.2 Medium-voltage networks

There are substantial differences between industrial, urban and rural distribution networks. Disconnections of unloaded transformers are normally carried out from the higher voltage level. Switching of 12-24 kV distribution transformers is very often performed by switches.

The neutrals of m.v. systems may be isolated, solidly earthed, resistance earthed or resonant earthed.

Capacitor-banks may be connected to the bus-bars and influence the equivalent supply-side capacitances of the transformer circuit-breaker.
In outdoor installations the connections from the circuit-breaker to the higher voltage side of the transformers very often are short (<5 m), this means that only small line inductances and capacitances have to be considered between the circuit-breaker and the transformer, but supplementary capacitance from current transformers may be present. The connections from the circuit-breaker to the bus-bars are also rather short (5-10 m), but the equivalent supply side capacitance may be influenced by voltage transformers and the actual bus-bar configuration.

Open indoor installations differ only slightly from the outdoor installations. The connections between the transformer and the circuit- breaker may contain higher capacitances due to cables or bushings and the equivalent bus-bar capacitance is increased compared to the overhead line bus-bars.

Metal-enclosed installations represent a compact concept in which the circuit-breakers are connected directly to the bus-bars, which have relatively high equivalent capacitance. The cable lengths between the transformer and the switchgear may be considerable, e.g. > 50 m.

In industrial networks transformer circuit-breakers are normally concentrated in a limited number of switchboards whereas the transformers are placed close to the loads. Considerable cable distances (several hundreds of meters) are not unusual. In some cases one transformer circuit-breaker may switch several transformers.

An extremely large number of switching operations is executed in supply circuits feeding arc furnace transformers. Usually such transformers are provided with tap-changers or series reactors of variable inductance. Small inductive currents of transformers under no-load conditions, supplied through variable reactors, may be interrupted 20-40 times per day.

Another special case is switching of generator transformers. When switching a generator transformer by a generator circuit-breaker, the current in the no-load condition would be in the range of 10-50 Amperes, but during routine operations, and even in the case of a failure operation, an unloaded condition is extremely unlikely.

Usually air-blast generator circuit-breakers are shunted by low ohmic damping resistors in series with an auxiliary interrupter, therefore small inductive currents will not be interrupted in the main chamber but by the auxiliary switch which has a much lower breaking capacity. It chops current at a level within the range of normal air blast distribution circuit-breakers at the medium voltage level. Therefore air blast, generator circuit-breakers with damping resistors behave in the same way as medium voltage distribution circuit-breakers. Some air blast generator circuit-breakers may be equipped with voltage dependent resistors across the last gap to interrupt. Furthermore, the m.v. side of the transformer is usually protected by surge arresters and additional capacitance.

For the more modern SF6 self-blast generator circuit-breakers experience shows that because of its arc characteristics this breaker type causes less overvoltages than medium voltage air blast breakers without opening resistors.

It is concluded that generator circuit-breakers switching small inductive currents do not produce dangerous overvoltages and thus this type of breakers need no special consideration.

5.2.3 High-voltage transformers - rated voltage > 72.5 kV

In the majority of cases, the transformers are three-phase units though banks of single-phase units are common at the highest voltages. Typical values of the steady state no-load current related to the rated power and voltage of the transformers are as shown in Table 5.2.1. The maximum values of the no-load current are not necessarily related to the higher values of the rated power. The maximum values given for 1.1 U_N are likewise not necessarily related to the higher values of U_N.

Typical values of the steady state no-load current for voltages other than the rated value and the corresponding values of no- load losses are given in Figs. 5.2.1.a and 5.2.1.b respectively.

The inrush currents of transformers during energization are usually very high, up to ten times the peak value of rated current or more, and high peak currents may persist for times exceeding 10 seconds in the largest transformers.

Table 5.2.1 **Typical values of no-load current for HV transformers** (values are based on information collected by WG 13.02, but transformers outside the range in this table are known to exist) [3].

Rated Voltage of Transformer U_N	Three Phase Rated Power of Transformer	No-Load Steady State Current (r.m.s.)			
		Amperes		% of rated current	
kV	MVA	U_N	1.1 U_N	U_N	1.1 U_N
700	510	0.4	1.1	0.09	0.27
550	300-600	0.4-0.5	1.4-1.5	0.08-0.13	0.22-0.46
525	560-1275	0.3-1.6	0.4-3.3	0.05-0.25	0.06-0.5
512.5	240	0.4	1.0	0.13	0.37
500	400-1000	0.5-0.9	1.2-3.0	0.05-0.19	0.10-0.65
430	735	2.7	10.8	0.27	1.1
420	250-725	1.1-6.0	2.1-13.0	0.31-0.6	0.6-1.3
415	1020	3.1	n.a.	0.22	n.a.
410	330-750	0.8-2.5	2.2-10.0	0.08-0.33	0.21-1.01
400	200-1000	0.5-4.2	1.0-7.4	0.09-0.76	0.3-1.50
345	560	0.47	0.6	0.05	0.06
286	510	0.9	2.8	0.09	0.27
275	240-1000	1.1-2.5	2.1*)	0.05-0.5	0.1
245	330	0.33	7.8	0.33	1.0
230	100-1000	0.3-4.8	1.0-7.5	0.08-0.4	0.22-1.28
225	75-250	0.2-0.9	0.4-2.6	0.09-0.18	0.17-0.41
220	40-160	0.2-0.8	3.0	0.09-0.3	0.66
160	100-250	1.4-2.0	5.4	0.22-0.39	0.6
155	75	0.3	0.5	0.11	0.17
150	16-250	0.1-1.9	0.2-1.4*)	0.09-1.23	0.17-1.6
145	160-750	1.1-2.4	3.1-6.3	0.08-0.18	0.21-0.49
135	40-500	0.5-5.1	1.8-12.8	0.08-0.40	0.2-1.1
132	240	4.2-12.6	12.5 *)	0.4-1.2	1.1
130	16-250	0.4-5.6	0.8-4.6*)	0.09-1.25	0.41-1.22
127	25-40	0.7-1.0	1.1-2.4	0.36-0.85	0.9-1.6
120	350	1.7	n.a.	0.1	n.a.

*) Values for 1.1 U_N are not available for all transformers and are not necessarily consistent with values for 1.0 U_N.

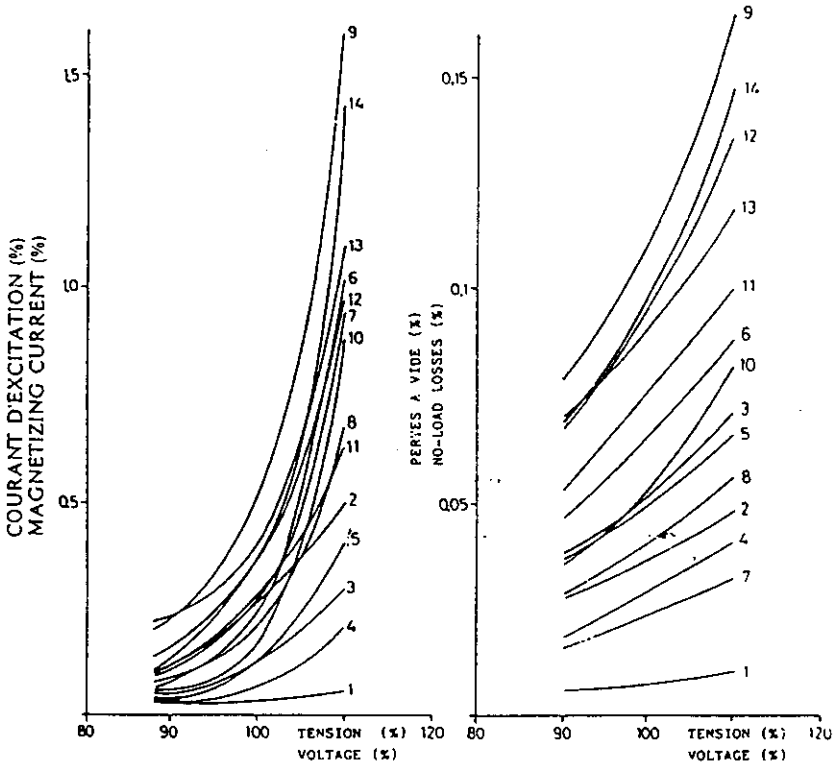

5.2.1.a) 5.2.1.b)

Courbe Curve	Type	Tension assignée Rated voltage kV U1	U2	U3	MVA triphasée nominale Three phase MVA rating P1	P2	P3	Connexion de l'enroulement Winding connection W1	W2	W3
1	A	525	345	13.8	560	560	186	Y	Y	Δ
2	A	525	230	13.8	200	200	66	Y	Y	Δ
3	A	410	135	20.0	500	500	250	Y	Y	Δ
4	A	410	145		750	750		Y	Y	
5	A	400	150	30.0	250	250	60	Y	Y	Δ
6	T	410	17.5		700	700		Y	Δ	
7	T	432	23.5		735	735		Y	Δ	
8	A	230	135	15.0	160	160	75	Y	Y	Δ
9	T	150	21.6		16	16		Y	Y	
10	T	135	58		100	100		Y	Y	
11	T	130	23		40	40		Y	Y	
12	T	127	21.6		25	25		Y	Y	
13	T	127	16.2		25	25		Y	Y	
14	T	127	10.8		25	25		Y	Y	

T = Transformateur
Transformer

A = Autotransformateur
Autotransformer

Fig 5.2.1 **a) Transformers excitation current (r.m.s. value);**
b) Transformer No-load losses in percentage of base MVA [3]

5.2.4 Medium voltage transformers

Medium voltage (m.v.) distribution or industrial networks show numerous variations. The transformers are usually three-phase but single phase transformers are common at the smaller rated powers. Typical values of the steady state no-load current related to the rated power voltage of the transformers are as shown in Table 5.2.3.

Table 5.2.3 **Typical values of no-load currents for m.v. transformers**
(Values are based on information collected by WG 13.02 [3])

Rated voltage of Transformer U_N kV	Three Phase Rated Power of Transformer MVA	No Load Steady State Current (r.m.s.) Amperes		% of rated current	
		U_N	1.1 U_N	U_N	1.1 U_N
66	90	1.4	2.8	0.18	0.36
33	90	3.5	6.3	0.22	0.4
33	60	1.6	3.2	0.15	0.30
33	20	0.7	1.4	0.20	0.40
20	2	0.40	–	0.7	–
20	1	0.20	–	0.7	–
20	0.63	0.33	–	1.8	–
20	0.10	0.08	–	2.9	–
17.5	10–50	4.3–32.0	10.0–38.0	–	–
12	10–40	2.8–13.0	8.0–19.0	–	–
11	30	7.9	15.8	0.5	1.0
11	1.25	0.50	0.72	0.70	1.1
11	0.8	0.34	0.50	0.8	1.2
3.3	1.25	1.6	2.6	0.74	1.2

5.2.5 Transformer core characteristics

Sections 5.2.3 and 5.2.4 give typical values of no-load r.m.s. currents for a range of transformers. Due to the non-linear B-H characteristic of the core material the current contains a substantial amount of harmonics as illustrated by Figure 5.2.2.

The ratio $\hat{i}/I_{r.m.s.}$ may be of the order of 2.0 to 2.5 for a transformer having cold-rolled grain-oriented steel (CROS) core as used in modern transformers having a maximum flux density at rated voltage in the range 1.5 to 1.9 Tesla. In older type of transformers using hot-rolled steel cores the magnetizing current is higher and the ratio $\hat{i}/I_{r.m.s.}$ is less. The maximum flux density is also lower, about 1.3 to 1.5 Tesla.

Due to asymmetries of the magnetic circuits in three-phase transformers the no-load currents in the three phases are generally different.

The extreme non-linearity of modern core material is illustrated in Figure 5.2.3.
However, in an actual transformer the B-H characteristic may be different from this, e.g. due to inevitable air-gaps in joints.

The actual B-H or B-i characteristic is normally not available. Instead the r.m.s. value of excitation current is measured. From this it is possible to calculate the instantaneous current as a function of instantaneous flux linkage (or voltage) by a method suggested by Talukdar el.al. [5]. By using a slightly modified method Boyle has calculated B-i characteristics from normal excitation measurements on a wide variety of transformers. The method is presented in Appendix 1.

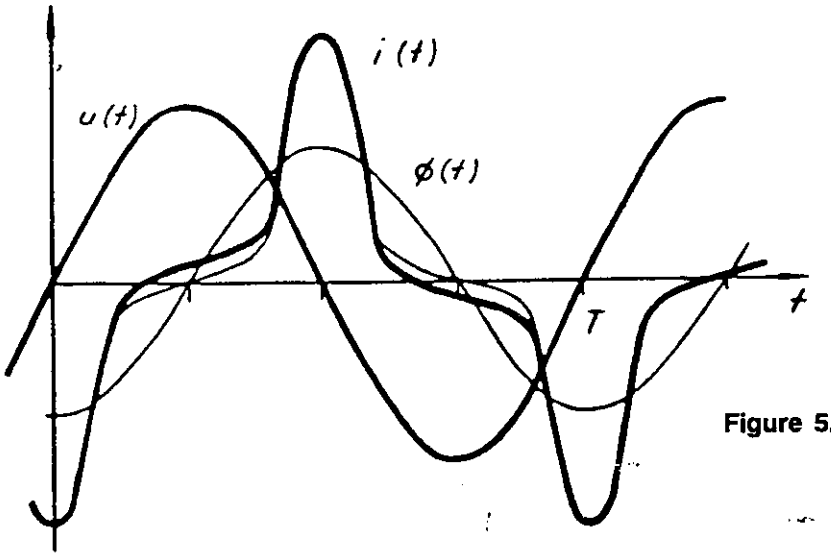

Figure 5.2.2 **Typical voltage, u(t), flux, ϕ(t), and current, i(t), relations in a transformer.**

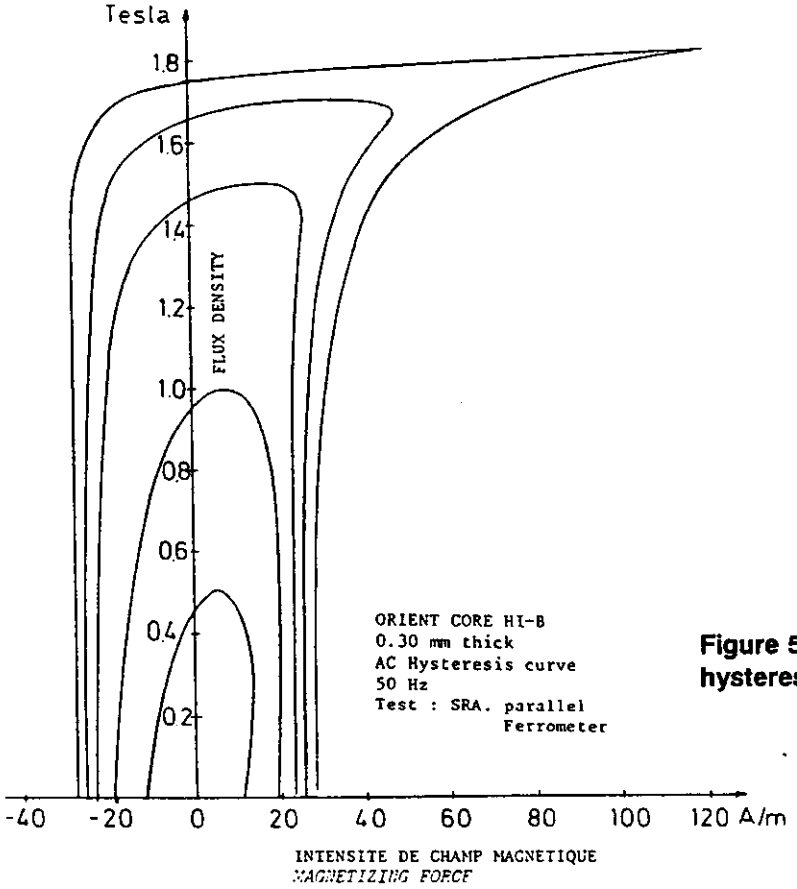

Figure 5.2.3 Example of power frequency hysteresis curves of modern core steel

Boyle has shown that it is possible to determine generalized characteristics sufficiently accurate to be used in overvoltage calculations. The characteristics are independent of transformer size and rated voltage from medium to ultra high voltages. The characteristic for CROS cores is valid for different grades of material from M3 through M7. A characteristic for HRS cores is judged to cover most older transformers with that type of core material.

Also the losses have an influence on the overvoltages at magnetizing current interruption. They are of two kinds:

- hysteresis losses
- eddy-current losses

The hysteresis losses per cycle are assumed to be basically frequency independent, while the eddy-current losses per cycle are proportional to the rate of change of the flux density. This is important when no-load current is interrupted. The current through the breaker can be assumed to be chopped instantaneously. The current through the transformer winding will then fall to zero along a hysteresis curve, which is dependent on the rate of change of the current fall and thus on the effective capacitance of the circuit to be interrupted.

5.2.6 Transformer capacitances

5.2.6.1 General

In each phenomenon occurring during the process of an interruption with current chopping, capacitances are involved. In the case of transformer switching one can distinguish between several parts that contributes differently to the effective capacitance involved in the interruption process:

a. The interwinding and intercoil capacitances of the transformer are distributed, often in a non-homogenious way, and are normally different for the different phases in a 3-phase transformer unit.

b. The bushing capacitance to earth can be regarded as a constant and lumped part C_b of the total transformer capacitance per phase.

c. The components in the connection between circuit breaker and transformer terminals (busbars, cables, current transformers, voltage transformers, busbar insulator etc.) have distributed capacitances to earth and/or between phases. The total value is known by measurement or calculation and may normally be represented by a lumped capacitance to earth, C_x. (The capacitances between the phases are neglected)

Because of the first contribution a sophisticated treatment of the chopping phenomena requires extensive modelling of the (three-phase) transformer primary coils, secondary coils and interconnecting couplings. This model should also include non-linear, voltage and frequency dependent, inductances and resistances. These models can only be handled by circumstantial computer programs. An example is the recent work of Langhammer [30].

Such complicated analysis are neither suitable nor necessary in most cases, where only an estimation is required of a total "effective" or "equivalent" capacitance per phase in parallel to an inductance representing the transformer.

This total equivalent transformer capacitance is supposed to be composed from three different contributions, see Figure 5.2.4.

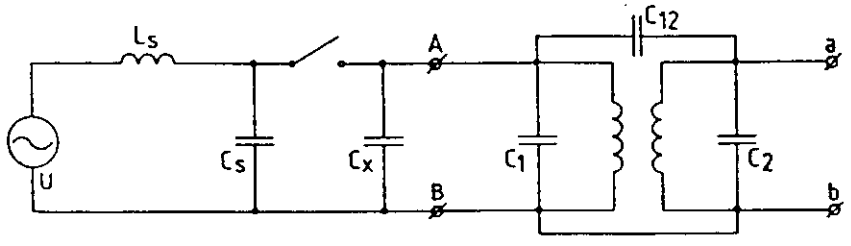

Figure 5.2.4 Simplified equivalent transformer capacitance circuit for chopping overvoltage calculation

C_1 is the capacitance of the primary side bushing increased with the representation of all winding capacitances to ground, C_2 is the same for the secondary side, C_{12} represents the effect of all capacitive couplings between two windings of the same phase. These capacitances are determined by low-

frequency or resonance measurements or simply taken as typical values from text books or other publications [7, 8, 9, 10].

Such a rough approach is often adequate because of two reasons:

- The constant part $C_b + C_x$ of the total capacitance is often as large as the effective coil capacitance. The larger this first part, the less critical is the exact determination of the equivalent transformer capacitance.

- The associated voltage and current transient phenomena are a function of the square root of the total capacitance.

5.2.6.2 Capacitance values for overvoltage calculations

For calculations of overvoltages after chopping the effective shunt capacitance of the transformer for rather low frequencies (less than a few kHz) has to be determined. This capacitance is given by:

$$C_t = C_x + C_1 + (\frac{N_2}{N_1})^2 C_2 + (1 \pm \frac{N_2}{N_1})^2 C_{12} \qquad (5.2.1)$$

where N_1 are primary turns, N_2 are secondary turns. The sign in the third term chosen for additive (+) and subtractive (-) phase to earth voltages. The third term can usually be neglected.

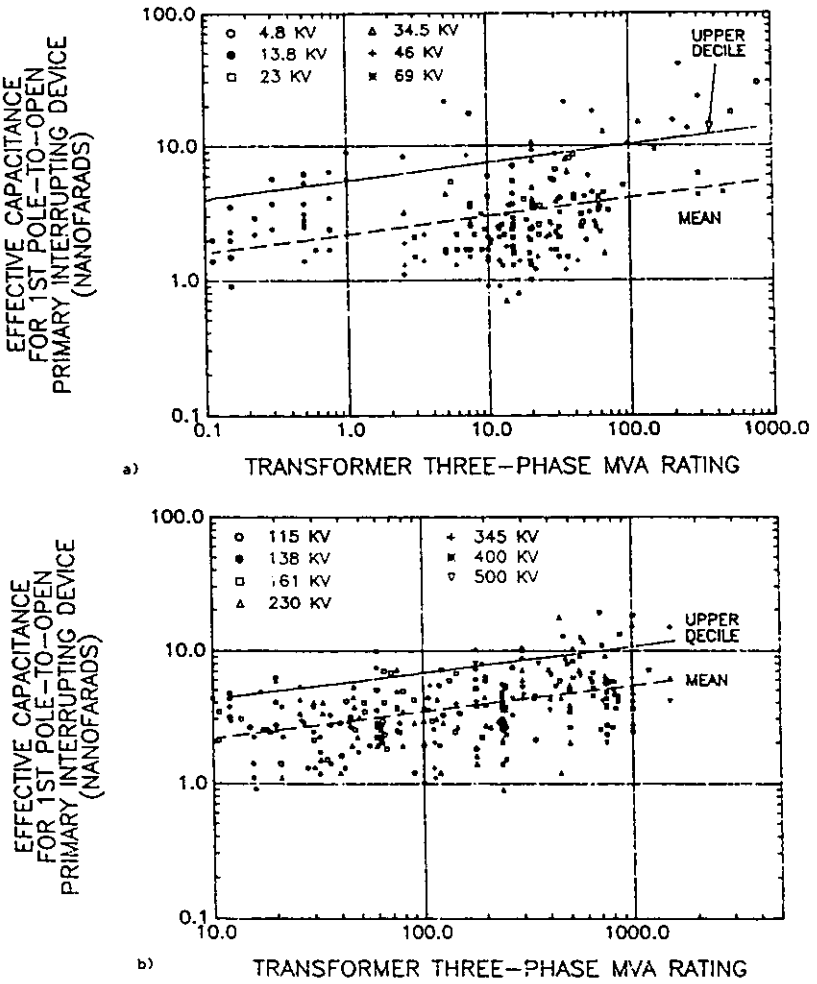

Figure 5.2.5 Effective transformer capacitance based on measured frequencies [9].
a) - system voltage 4.8 kV to 69 kV
b) - system voltage 115 kV to 500 kV

C_1 and C_2 are often taken as 1/3 of the total (measured) capacitance to earth, but in fact this factor is only theoretically accounted for the coils and assumes a linear voltage distribution along the coil. It should be larger if the bushings are a substantial part of it [7].

In Figure 5.2.5 capacitance values for a large number of transformers measured by low voltage injection methods are given. (Values from Tables in ref [9]). These values are thought to be representative in overvoltage calculations. The values are very scattered and there is little correlation between capacitance values and rated voltage.
Somewhat lower capacitance values are given in ref. [8] and ref. [34].

When the transformer is switched from the high voltage side the third and fourth term in eq. 5.2.1 can usually be neglected. In case the transformer is switched from the low voltage side the contribution from the H.V.-side capacitance is considerable and the third term must be taken into account but the fourth term can often be neglected.

A three-phase equivalent scheme is given in Figure 5.2.6 for the three-legged star-delta transformer. (Several other schemes with the same degree of validity exist).

Now C_x is not the only capacitance to earth per phase but also the delta-star transformed phase-to-phase capacitance has to be included. Single-phase equivalent circuit representation depends on the actual way of earthing and whether the 1st, 2nd or 3rd phase-to-clear is to be represented.

During first phase interruption (phase A) connections B and C must be regarded as being earthed directly (connected to D through the source side) for the transient oscillation. During second phase clearing only the last phase is earthed. These earth connections influence not only the effective capacitance C_1 in Eq. 5.2.1 but also the effective inductance in the single-phase representation.

Such influences are treated in detail for linear inductances in Appendix 4 and 5, also including D-connections.

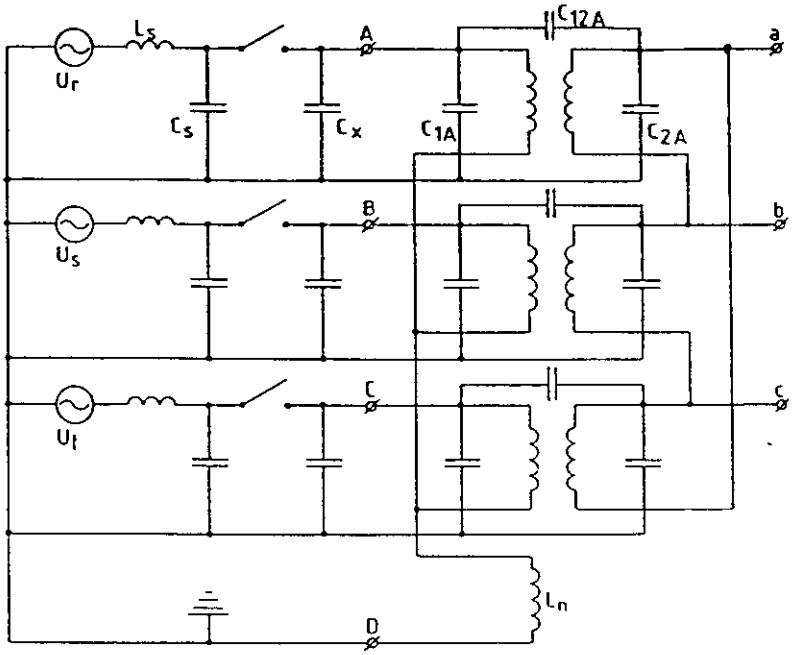

Figure 5.2.6 A three-phase equivalent scheme of a three-legged star-delta transformer.

L_n = 1/3(L_0 - L_1) = -M
L_0 = zero sequence inductance
L_1 = positive sequence inductance
M = mutual inductance, taken as positive

Note: Since L_n is usually negative, this equivalent scheme is not suitable in TNA studies and in some digital calculation programs. The implementation of this scheme in the EMTP-program and calculation of transient currents and voltages after interruption of linear inductances is given in ref. [31]. Representation of a comparable model in TNA studies is possible by means of an additional delta winding. More detailed representations can be derived by using the analogy between magnetic and electric networks as treated in ref. [33].

5.2.6.3 Capacitances for chopping level calculations

The instability and/or chopping level of the arc current is dependent on the effective capacitance parallel to the arc. See Chapter 2, Section 2.3 [13].

Since the instability oscillation usually has a frequency of > 100 kHz it is obviously the high frequency capacitance that must be regarded in chopping level determination.

This high frequency "input capacitance", C_i, is well known from surge voltage distribution theory and calculations. Methods for measuring and calculations of such capacitances are given in ref. [8].

If approximate h.f. values of C_1, C_2 and C_{12} are available the effective input capacitance can be estimated to

$$C_i = C_1 + \frac{C_2 \cdot C_{12}}{C_2 + C_{12}} \qquad (5.2.2)$$

When the transformer is switched at the H.V.-side, the value of C_i is 0.6 to 0.8 times the value for overvoltage calculation [8, 34], but this difference has only a marginal influence on the calculation result in most practical situations, for the same reasons as mentioned in 5.2.6.1.

The effective capacitance parallel to the arc is

$$C_p = C_s C_t / (C_s + C_t), \text{ with } C_t = C_x + C_i \qquad (5.2.3)$$

In most cases the capacitance on the supply side, C_s, is large in comparison with C_t, due to capacitances of the busbar, potential and current transformers, coupling capacitors, capacitor banks etc. Therefore, one can assume $C_p \approx C_t$ in most cases, especially as $C_p < C_t$ gives lower overvoltage.

5.2.6.4 Capacitance values at oscillations after reignition

The "second parallel oscillation", defined in ref. [13], is a h.f. phenomenon with a frequency of the same order as the instability oscillation. Therefore the same "input capacitance" as in 5.2.6.3 should be used for C_t.

"Main circuit oscillations" [13] are not to be expected in transformer switching because the small no-load current will normally be interrupted again (after the second parallel oscillation has died out or even during the oscillation).

5.3 Interruption of no-load currents

5.3.1 General

This section is concerned with a theoretical analysis of the generation of overvoltages due to the switching of unloaded transformers. Overvoltages created by chopping of steady-state no-load currents as well as inrush currents are studied.

5.3.2 Effective magnetic energy

The overvoltage generated at chopping magnetizing current is given by the release of magnetic energy during the change of magnetic status from the instant of current chopping to the zero passage of the

magnetizing current. The released energy is proportional to the area P in Figure 5.3.1, when chopping at $i_m = i_{ch}$ and a natural frequency oscillation close to the power frequency is assumed. In the Figure chopping at the peak value of a steady state current is illustrated.

In Figure 5.3.1 the return to current zero is assumed to follow the 50/60 Hz hysteresis curve. In actual operation the return will follow a curve dependent on the rate of decay of the flux density as shown in Figure 5.3.2 by curve b. The released energy is smaller than in Figure 5.3.1 since the decay in all practical cases is faster than 50/60 Hz.

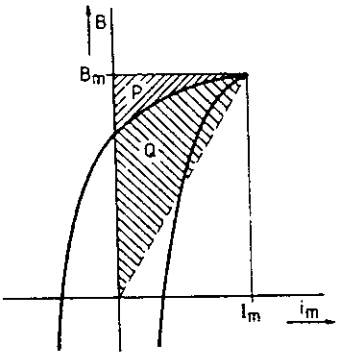

Figure 5.3.1
Chopping at peak no-load steady-state current.
Power frequency return.

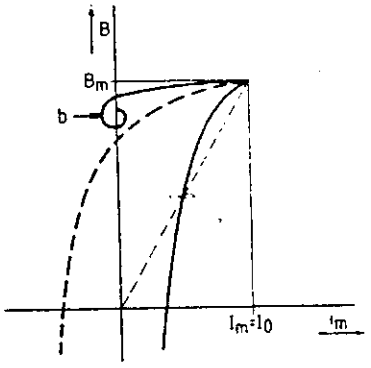

Figure 5.3.2
Chopping at peak no-load steady-state current. Return with a rate of decay > power frequency decay.

The case of chopping an inrush current is illustrated in Figure 5.3.3. The current may then be chopped at values higher than the peak steady state current when falling from saturation.

The released energy is again proportional to the surface area P (above the return curve b. Since the slope of the B-i_m curve in the saturation range is mainly determined by the air-cored inductance of the coil the area P in this range will increase more linearly with the chopping current. However, chopping of currents in the saturation region (B ≥ 2 T) are far above even the highest chopping level of any circuit-breaker.

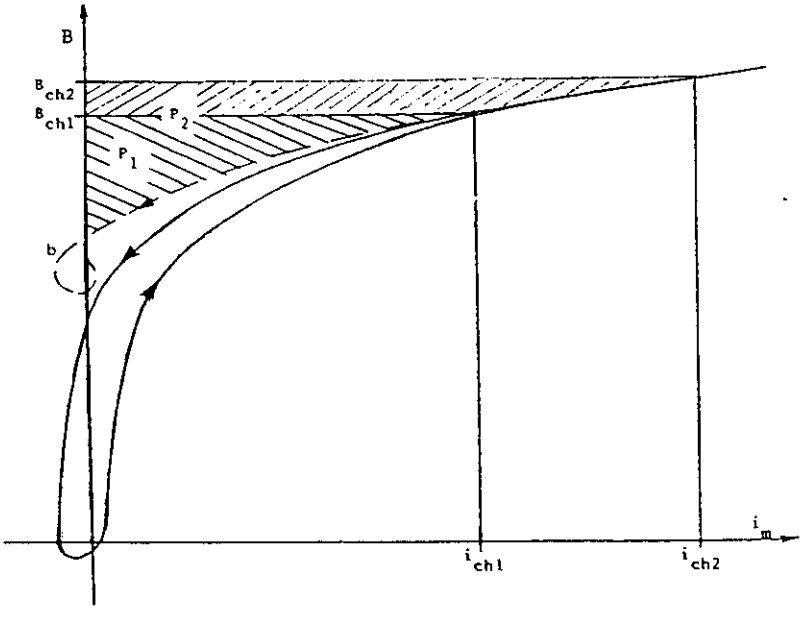

Figure 5.3.3 Released energy at inrush current chopping

We can now define the "magnetic efficiency", η (or "efficiency of release of magnetic energy") as

$$\eta = \frac{W_b}{W_{id}} = \frac{AreaP}{Area(P + Q)} \tag{5.3.1}$$

where W_b = released magnetic energy from the transformer when demagnetized from the point i_{ch}, B_{ch} along curve b.

W_{id} = stored magnetic energy in an ideal linear inductor with the same core area and number of turns, when $i_m = i_{ch}$ and $B = B_{ch}$.

W_{id} is represented by the area P + Q in Figure 5.3.1. Therefore:

$$W_{id} = \frac{1}{2} NAB_{ch} i_{ch} \tag{5.3.2}$$

where N = number of winding turns
A = crossectional area of the iron core

In the normal case of steady state excitation, the highest possible chopping current is the peak value of the magnetizing current, i_p. Therefore, when interrupting steady state currents:

$$i_{ch} \leq i_p \tag{5.3.3}$$

If an inrush current is interrupted, the circuit-breaker may chop the current at a higher value up to the max. chopping level of the breaker.

To quantify the decay of flux density the equivalent scheme of Figure 5.3.4 could be analyzed.

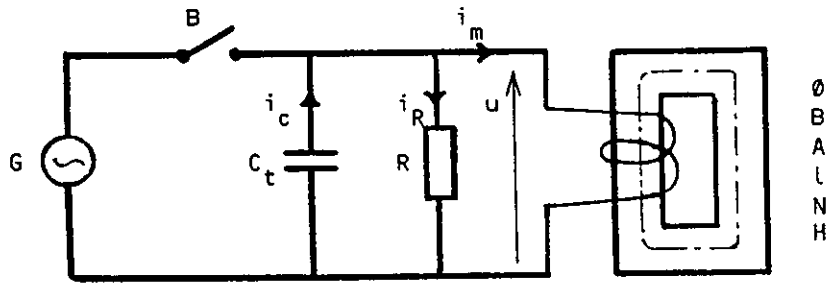

Figure 5.3.4 Equivalent scheme of an unloaded transformer.

The eddy current losses may be represented by a parallel resistance R (according to Appendix 1). With the transformer characteristics: flux = Θ, flux density = B, core area = A, magnetic path length = l, number of turns = N and current = i_m, the following equations can be set up:

$$i_c = i_R + i_m$$

$$N\frac{d\phi}{dt} + \frac{1}{C_t}\int i_c \cdot dt = 0$$

$$u = i_R R = N\frac{d\phi}{dt}$$

$$\phi = AB$$

$$H = \frac{N}{l} i_m$$

$$B = \mu_o \mu_r (i_m + I)H$$

where C_t = the equivalent parallel capacitance (discussed in 5.2.6.2) and
$\mu_r(i_m|\downarrow)$ = a non-linear, hysterical function of i_m.

From these equations the relation between B and i_m is derived:

$$\frac{d^2B}{dt^2} + \frac{1}{RC_t}\frac{dB}{dt} + \frac{i_m}{C_tNA} = 0$$

or

$$\frac{d^2B}{dt^2} + \frac{1}{RC_t}\frac{dB}{dt} + \frac{B}{\mu_o\mu_rN^2AC_t} = 0 \qquad (5.3.5)$$

If the coefficients of the above differential equation in the dependent variable B would be constant, the solution for B is known to be a damped sine function. It is, however, a differential equation with one variable coefficient $\frac{1}{\mu_o\mu_rN^2AC_t}$ since μ_r is here not a constant but a function of i_m, i.e.

$$\mu_r = \frac{1}{N\mu_o}\cdot\frac{dB}{di_m}$$

Thus the analogous expression for the angular frequency ω, i.e.:

$$\omega = \sqrt{\frac{1}{\mu_o\mu_rN^2AC_t}}$$

is varying with time. Therefore no defined frequency can be assigned to the chopping transient oscillation of a no-load transformer.

If dB/di_m is known by knowledge of the curve $B = f(i_m)$, the variation of the variable coefficient and thus also of the varying quasi-frequency as function of i_m is determined by the shape of this magnetization characteristic. The equation may then be solved numerically by approximating the B/i_m-curve by straight line segments.

Boyle has developed a practical way to estimate the overvoltage peak for modern transformers with cold-rolled grain-oriented steel cores as well as for transformers with hot-rolled steel cores in the following way (see Appendix 1):

a. Calculation of η dependent upon B_{ch} and an "effective frequency"

$$f_{eff} = \frac{1}{2\pi\sqrt{L_{eff}\cdot C_t}} \qquad (5.3.6)$$

with a specially defined "effective inductance"

$$L_{eff} = \beta NA\frac{B_{ch}}{i_{ch}} \qquad (5.3.7)$$

where $\beta = 0.15$ for CROS-cores *)
$\beta = 0.5$ for HRS-cores *)

Note: *) The factors 0.15 for CROS-cores and 0.5 for HRS-cores are more or less arbitrarily chosen. This does not influence the final results.

b. Equating the released magnetic energy with the increase in electric energy

$$\frac{1}{2}C_t u_m^2 = \frac{1}{2}\eta NAB_{ch}i_{ch} + \frac{1}{2}C_t u_o^2 \tag{5.3.8}$$

where u_m = peak chopping overvoltage
u_c = voltage across C_t immediately prior to chopping

Though the defined effective frequency has little physical meaning, because of the non-linearity of the problem (see above), it is a useful parameter for the representation of η (Fig. 5.3.5) and it may give an approximate indication of the voltage waveform up to the first peak. Boyle's calculation of η is based on an equivalent circuit consisting of a non-linear inductance in parallel with a resistor. The non-linear inductance represents with its $B(i_m)$ characteristic the falling branch of the hysteresis curve for the transformer. The resistor takes account of frequency dependent losses on the assumption that the ratio of hysteresis losses/eddy-current losses (frequency dependent losses) is 0.5/0.5 for CROS and 0.7/0.3 for HRS at power frequency. This assumption seems reasonable because higher eddy-current losses lead to higher damping and investigations indicate that eddy-current losses even dominate over hysteresis losses [14, 15, 16].

Additional resistive losses in the transformer and external damping are usually negligible in comparison.

$$u = U_N 2\sin\omega t_1 = NA\cdot\frac{dB}{dt}$$

NA in eq. 5.3.7 may be found from the steady-state conditions:
So

$$NA = \frac{u_o}{\omega_1 B_m} = \frac{U_N}{\omega_1 B_m} \tag{5.3.9}$$

where u_o = amplitude of the rated voltage
U_N = rated phase-to-earth voltage (r.m.s.)
B_m = maximum flux density at rated voltage
ω_1 = power angular frequency

The effective inductance can then be expressed as

$$L_{eff} = \beta\frac{u_o B_{ch}}{\omega_1 i_{ch} B_m} \tag{5.3.10}$$

where β = 0.15 is used for CROS-cores
β = 0.5 is used for HRS-cores

From L_{eff} and C_t the "effective frequency", f_{eff}, can now be calculated (eq. 5.3.6) and η determined from Figure 5.3.5.
The generated overvoltage can now be calculated from Eq. 5.3.8, which gives

$$u_m = \sqrt{u_c^2 + \frac{\eta NAB_{ch}i_{ch}}{C_t}} \tag{5.3.11}$$

With NA from eq. 5.3.9

$$k_a = \frac{u_m}{u_o} = \sqrt{\left(\frac{u_c}{u_a}\right)^2 + \frac{\eta i_{ch} B_{ch}}{u_o \omega_1 C_t B_m}} \qquad (5.3.12)$$

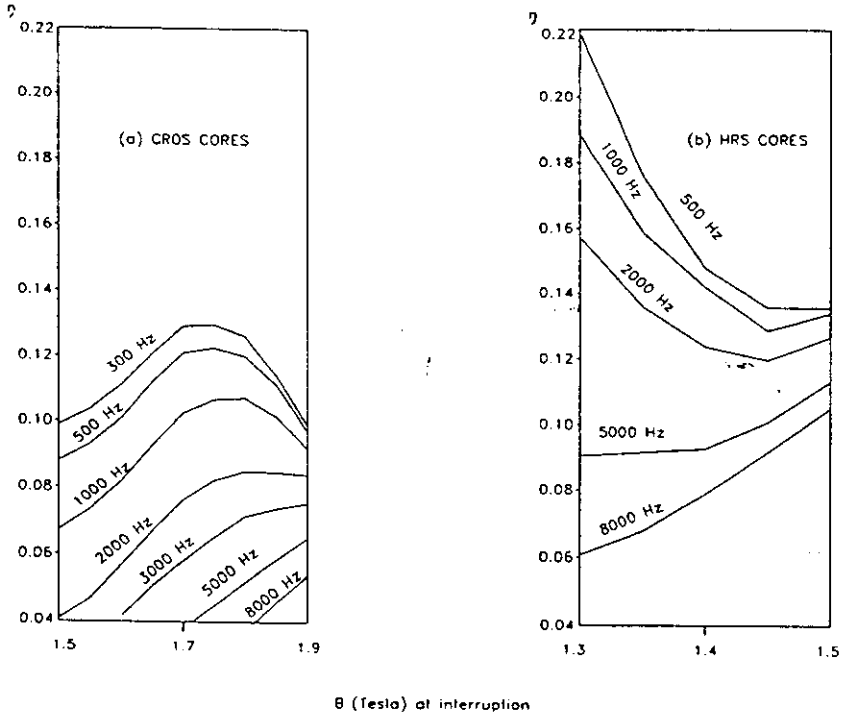

Figure 5.3.5 Efficiency of release of magnetic energy (η) for transformers.
a) Hysteresis/eddy-current loss at 50 Hz = 0.5/0.5, typical for CROS-cores
b) Hysteresis/eddy-current loss at 50 Hz = 0.7/0.3, typical for HRS-cores

In the further treatment we must now distinguish between the two principal cases:

- steady state current interruption
- inrush current interruption

5.3.3 Steady-state current interruption

A typical oscillogram from an interruption of steady-state current in an unloaded transformer with HRS-core is given in Figure 5.3.6.

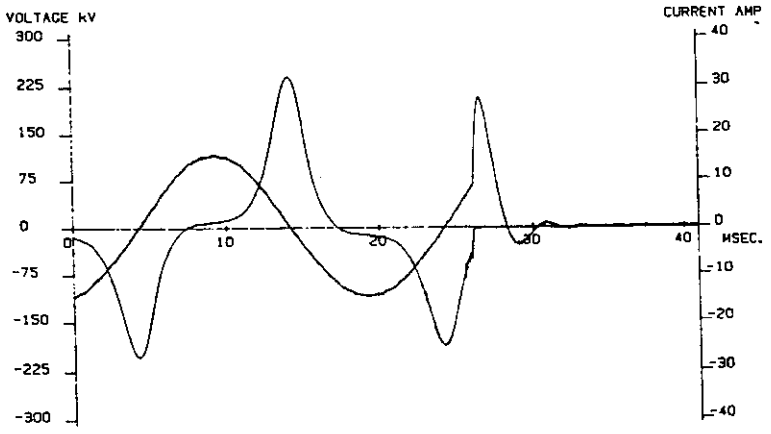

Figure 5.3.6 Interruption of steady-state current of a no-load transformer

For modern transformers with CROS-cores, the steady-state peak current is often less than the chopping level of the circuit-breakers. The current may therefore theoretically be chopped at its peak. Even though the experience shows that this is unlikely, we will assume this to occur in the following treatment of steady state current interruption since it would result in the highest overvoltages as shown in ref. [17].

To simplify the treatment we will study a single-phase case.

At or close to the current peak the voltage across the transformer terminals is close to zero, i.e., $u_c \approx 0$. Since further $B_{ch} = B_m$ and $i_{ch} = i_p$, eqs. 5.3.11 and 5.3.12 simplifies to:

$$u_m = \sqrt{\frac{\eta\, u_o\, i_{ch}}{\omega_1\, C_t}}$$

and

$$k_a = \sqrt{\frac{\eta\, i_p}{u_o\, \omega_1\, C_t}} \qquad (5.3.13)$$

with η from Figure 5.3.5 the overvoltage factor k_a can be calculated.

The peak magnetizing current can be expressed as a fraction of the rated current

$$i_p = \gamma\, i_m = \gamma\, \alpha \frac{P_N}{U_N} \qquad (5.3.14)$$

where $\gamma = i_p/I_m$ = form factor

α = ratio magnetizing current/rated current (both r.m.s. value)
P_N = rated power of single-phase transformer
$u_0 = U_N\sqrt{2}$ = rated crest voltage of single-phase transformer
I_m = r.m.s. value of magnetizing current

Eq. 5.3.13 can then be written as:

$$k_a = \sqrt{\frac{\eta\, \gamma\, I_m}{\omega_1\, C_t\, U_N\sqrt{2}}} = \sqrt{\frac{\eta\, \gamma\, \alpha\, P_N}{\omega_1\, \sqrt{2}\, C_t\, U_N^2}} \qquad (5.3.15)$$

Even though the design of the transformer has an influence on the form factor, one can assume the same form factor for a certain design flux density, B_m, i.e. γ = constant. Further in this case

$$\eta = f(f_{eff})$$

From Eqs. 5.3.6, 5.3.9, 5.3.10 and 5.3.14:

$$\eta = f\left(\frac{\omega_1 \gamma \alpha P_N}{\beta C_t U_N^2}\right) \qquad (5.3.16)$$

i.e. k_a is a function of the parameter:

$$\frac{\alpha P_N}{C_t U_N^2}$$

The curves in Figure 5.3.5 are derived for a power frequency of 50 Hz, but can also be used for 60 Hz. The difference (if any) will be negligible in view of other assumptions and approximations. (There are different opinions in the WG on how the power frequency influences the magnetic efficiency.)

The use of the parameter $\alpha\ P_N/(C_t\ U_N^2)$ was first suggested by Panek and Tuohy [18].
Panek and Tuohy calculated the chopping overvoltages by solving numerically the differential equation for the flux density based on eq. 5.3.5 and a dynamic H(B) curve

$$H = \frac{B}{\mu(B)} + a\frac{dB}{dt} \tag{5.3.17}$$

The first term on the right hand side of eq. 5.3.17 – the characteristic of non-linear inductance – was taken as

$$\mu(B) = \frac{B}{H} = \frac{(1 - b(B))^d}{c} \tag{5.3.18}$$

which is a fair approximation for the characteristics of CROS.

The second term represents the frequency dependent losses.

The constants a in eq. 5.3.17 and b, c and d in eq. 5.3.18 are empirical constants that can be obtained from steady-state BH measurements.

The result of calculations of chopping overvoltages (peak current chopping assumed) for transformers with B_m = 1.55 T and form factor γ = 2.5 has been reproduced in Figure 5.3.11. [18].

Eq. 5.3.17 leads to the same representation of frequency dependent losses by a resistor in the appropritate equivalent circuit as in Appendix 1.

There are several other calculation models representing the B–H characteristic of core steel that could be used in solving the differential equation describing the chopping process [19, 36]. The classical Langevin function ($B = B_{max} \cdot \coth k_1 H - 1/k_1 \cdot H$) as well as pure mathematical approximations can be used in established computer programs for differential equation solution.

5.3.4 Magnetizing inrush current interruption

Transformers are subject to high magnetizing inrush currents when energized. The level of inrush currents depends largely upon the point on wave of energization and the remanent flux in the core. The transformer core will be driven into a saturated condition where the effective inductance becomes extremly low in comparison with the steady-state magnetizing inductance and the inrush currents become very large.

The chopping current level is now determined by the characteristics of the switching device, and this case must therefore be treated differently from interruption of steady-state currents. Some circuit-breakers with very high chopping levels may – theoretically – produce high overvoltages.

The most onerous case can be shown to be interruption when the inrush current peaks are still much higher than the chopping level. In this case the initial voltage across the capacitance is close to the crest value of the applied voltage, i.e. $u_c \approx u_0 = U_N \sqrt{2}$. Eq. 5.3.12 then simplifies to

$$k_a = \frac{u_m}{u_o} = \sqrt{1 + \frac{\eta\, i_{ch} B_{ch}}{u_o \omega_1 C_t B_m}} \tag{5.3.19}$$

The η-value can be taken from Fig. 5.3.5 if B_{ch} and the equivalent frequency are known.

The equivalent frequency is as before given by

$$f_{eff} = \frac{1}{2\pi\sqrt{L_{eff}C_t}} \qquad (=5.3.6)$$

where L_{eff} as for steady state current may be approximated by

$$L_{eff} = \beta\frac{NAB_{ch}}{i_{ch}} = \beta\frac{u_o B_{ch}}{\omega_1 i_{ch} B_m} \qquad (5.3.10)$$

where β = 0.15 is used for CROS and β = 0.5 for HRS cores.

B_{ch} can be estimated from the chopping level and the magnetizing current at rated voltage by means of the curves in Appendix 1, Figures A1.3 and A1.4 for CROS and HRS cores respectively.

The curves show the flux density B as function of instantaneous current when falling from saturation. The curves also approximately represent cases with flux falling from lower levels, as long as the peak current is much larger than i_p (the peak current at steady state). The normalized current in the diagrams is referred to the r.m.s. value of the no-load current at a design flux density of B = 1.7 T.

For most circuit-breakers the chopping level is dependent on the capacitance in parallel with the circuit-breaker [4, 13]:

$$i_{ch} = \kappa V(n \cdot C_t) \qquad (5.3.20)$$

where n = number of series connected breaking units.
κ = chopping number for one breaking unit.

A recording from an inrush current interruption is shown in Figure 5.3.7.

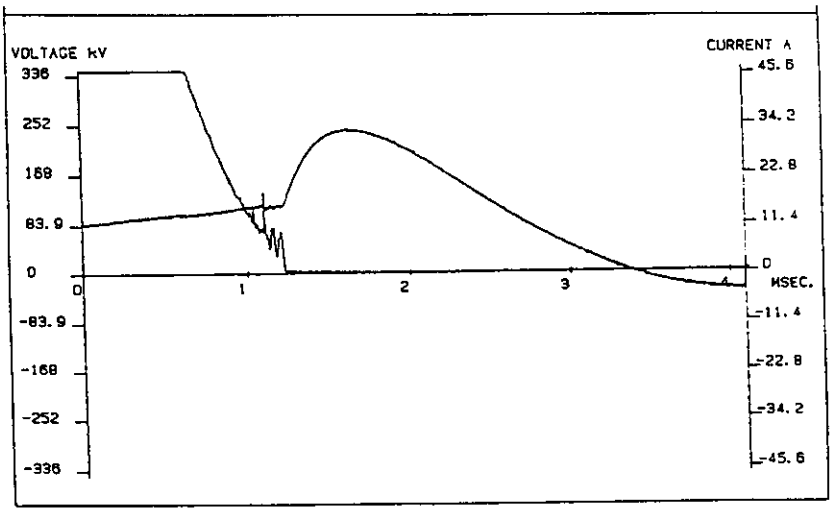

Figure 5.3.7 Example of no-load transformer inrush current interruption.

The value of the chopping number, κ, for a breaking unit is normally in the range $1 \cdot 10^4$ to $20 \cdot 10^4$. The relation in eq. 5.3.20 is not valid for vacuum circuit-breakers whose chopping level is only weakly dependent on the capacitance.

The value of C_p to be used is the effective high frequency capacitance treated in Clause 5.2.6.3.

Since the supply side capacitance usually is large we can often assume

$$C_p = C_t$$

which further gives a conservative estimation of the overvoltages.

The value of B_{ch} to be used can be derived from Figures A1.1, A1.3b and A1.4, if the normal r.m.s. excitation current at rated flux density, B_m, is known. The ratio of chopping level to normal excitation current gives the B_{ch}–value to be used both when calculating L_{eff} from eq. 5.3.10 and k_a from eq. 5.3.19, i.e.,

$$k_a = \frac{u_m}{u_o} = \sqrt{1 + \frac{\eta i_{ch} B_{ch}}{u_o \omega_1 C_t B_m}} = \sqrt{1 + \frac{\gamma \kappa \eta}{u_o \omega_1 C_t}} \qquad (5.3.21)$$

The curves in Figures A1.3b and A1.4 are based on rated flux densities of 1.7 T and 1.3 T respectively. The curves could anyway be used with an acceptable accuracy for other rated flux densities with the K_s–value based on the actual I_m–value.

5.3.5 Three-phase phenomena

Interphase effects in three-phase transformers where the phases are magnetically coupled by multi-leg cores or delta windings will make the interruption process much more complicated.

A wide variety of cases exist

- banks of single-phase units
- three-phase units
- autotransformers
- 2 or 3 winding transformer
- Y or D connections
- number of core-legs

all of which have to be treated differently.

Only cases with banks of single-phase units without mutual inductive coupling are covered by the above treatment of single-phase transformers. In a transformer with a three or five leg core or with a delta winding the phenomena are more complicated because of the mutual effects – each coil contributes magnetizing force to all the core legs. The situation is further complicated by the asymmetry of the magnetic circuit.

The overvoltages are likely to be less severe than in the single phase case because the energy in the magnetizing inductance will not be at a maximum in all three phases and this energy is discharged into the three phase capacitance circuit.

However, due to the mutual coupling between the phases there is always a risk to achieve an unfavourable superposition of voltages when the second and third phase is interrupted. This is illustrated by Fig 5.3.8 showing a HV side recording from a field test with a 400/120/21 kV, 400/400/125 MVA transformer under inrush conditions [37]. At the interruption a 1.3 kHz voltage oscillation is created due to the tertiary winding coupling (zero sequence system inherent frequency). This voltage oscillation is superimposed on the chopping overvoltage in the last phase to interrupt (B-phase), enhancing the overvoltage from some 1.7 p.u. to about 2.6 p.u. Phase A and C interrupt more or less simultaneously with a current chop of approximately 40 A. The chopping overvoltage in phase A is 1.9 p.u.

A computer simulation of this three-phase case has given a result that is very close to the recording. For comparison also a computation of an equivalent single-phase interruption was made. A substantially higher chopping overvoltage was achieved in spite of a lower chopping current

(20 A) used in the calculation. This indicates that a possible enhancement due to superposition, more than well may be compensated by the general reduction in three-phase operation as compared to the single phase case.

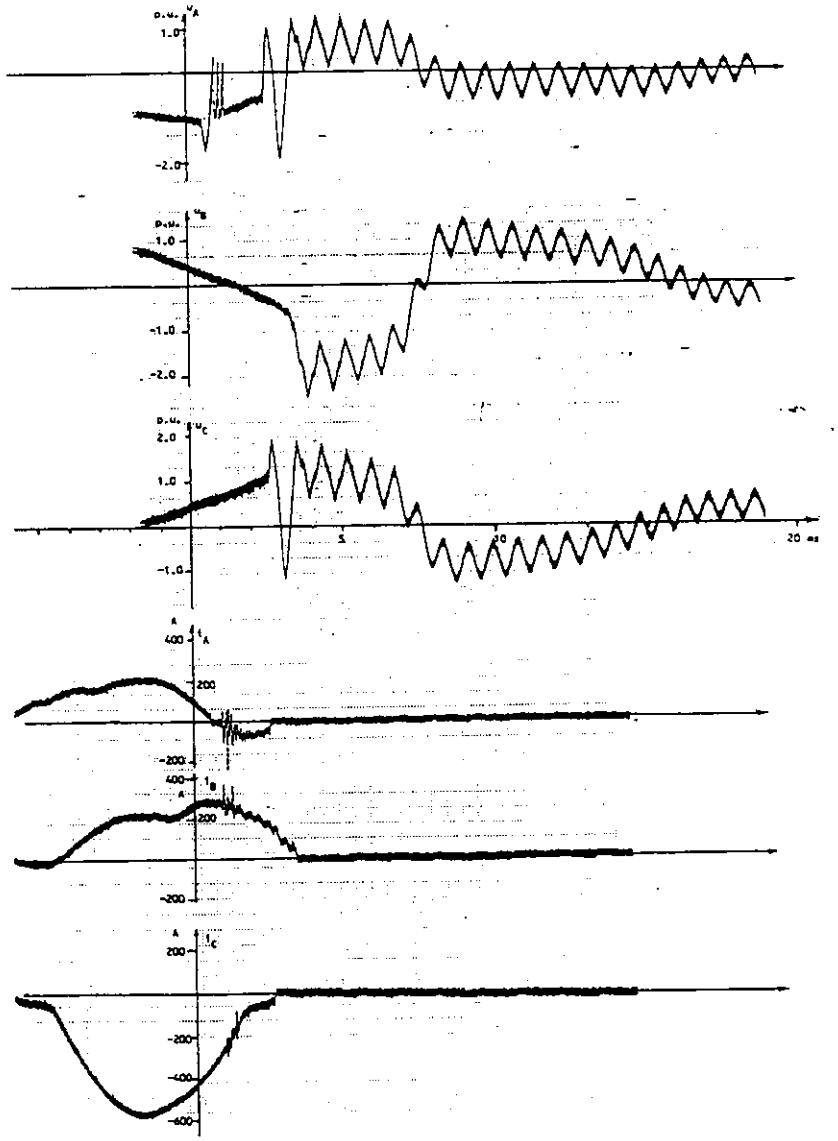

Figure 5.3.8 Inrush current interruption in 400 kV transformer. Field test [37].

A few theoretical studies of three-phase chopping have been made. Although considerable simplifications have been made, some general conclusions may be drawn.

5.3.5.1 Star-connected transformers with earthed neutral and delta secondary

A worst case study has been made by Boyle in Appendix 2. In a star connected transformer the most severe case would be when the second phase to clear chops at peak current provided that the first phase was interrupted 60 electrical degrees earlier. An overvoltage will then appear on the first phase to clear at the time of interruption of the second phase, which is the sum of the instantaneous value of the power frequency voltage present on that phase and an induced transient voltage approximately equal to the switching transient appearing in the second phase to clear. The maximum voltage on the first phase-to-clear would then be approximately

$$u = \frac{u_o\sqrt{3}}{2} + u_m \qquad (5.3.22)$$

where u_m is calculated from eq. 5.3.13 and
u_o is crest phase-to-earth voltage

or $k = 0.86 + ka$

where $k_a = u_m/u_o$.

The conditions required to create this worst case are:

- the second phase interrupts ≈ 3 ms after the first phase
- the second phase interrupts at peak current.

This is very unlikely and requires unusually large difference in contact opening of the breaker.

5.3.5.2 Delta connected transformers

For an unloaded three-phase bank of single-phase transformers connected in delta/star and supplied from delta side, the magnetic energy stored in one phase will be maximum when the current and flux density in its winding is at its peak value as is also the case in a star-connected transformer. In the steady state the currents in the other two windings at that moment will be very low because of the non-linear characteristic. Hence on simultaneous interruptions of the three phases the maximum energy is released when chopping at peak flux density in one winding. The energy is transferred to the effective capacitance across that winding. The inductance is high in the other two windings, therefore only a small energy transfer to the third capacitance takes place. The resulting overvoltage to earth will then be approximately half of the voltage across the winding, as can be seen from Figure 5.3.9.

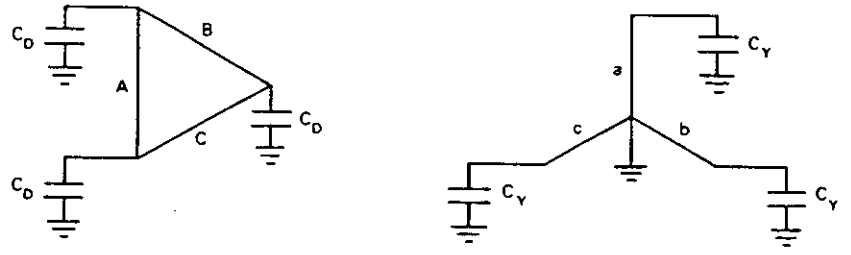

Figure 5.3.9 Capacitance distribution in a delta-star transformer (circuit valid for current chopping overvoltage calculations)

The effective capacitance across the delta winding will thus be

$$C_{eff} = \frac{C_p}{2} + \frac{3C_Y(N_1/N_2)^2}{2} \qquad (5.3.22)$$

and the maximum overvoltage to earth is now found from eq. 5.3.13:

$$u_m = \frac{1}{2}\sqrt{\frac{\eta u_o i_{ch}}{\omega_1 C_{eff}}} \qquad (5.3.24)$$

Also Panek et. al. [20] have studied the case of a D/Y bank consisting of three single-phase transformers switched on the D-side. In the study the eddy-current losses have been represented by a resistance:

$$R = \frac{N^2 A}{a \cdot l} \tag{5.3.25}$$

parallel with each winding ("a" is the constant in eq. 5.3.17 and *l* is the magnetic pathlength).

The maximum overvoltage to earth can be described by the curve A in Figure 5.3.10, which is principally the same as the curve for singlephase transformers in Figure 5.3.12. Panek et al. use the three-phase rated power and voltage to define what they call a normalized capacitance

$$\frac{C_t N^2 A}{l}$$

used as an independent variable. (This normalized capacitance is related to the chop parameter in Figure 5.3.12 by:

$$\frac{N^2 A}{l} = \frac{H_m \sqrt{2}}{B_m \omega_1 \gamma} \cdot \frac{U_N^2}{\alpha P_N} \tag{5.3.26}$$

where H_m, B_m and γ are design and material data.)

If instead a three-leg transformer is studied, the difference in magnetic path length and thus reluctance in the three phases has to be considered in calculations. This means that the phase currents are different.

Calculations for medium voltage transformers show that the maximum overvoltages are approximately the same as for the single-phase (or D-connected bank) case if simultaneous chopping in all three-phases is assumed [20]. This assumption should be acceptable when the chopping level is higher than the peak magnetizing current (a necessary condition to create maximum overvoltages). Curve B in Figure 5.3.10 shows the calculated maximum overvoltage for an actual transformer (1 MVA, 4.16 kV) in comparison with the D-connected bank (or a single-phase transformer).

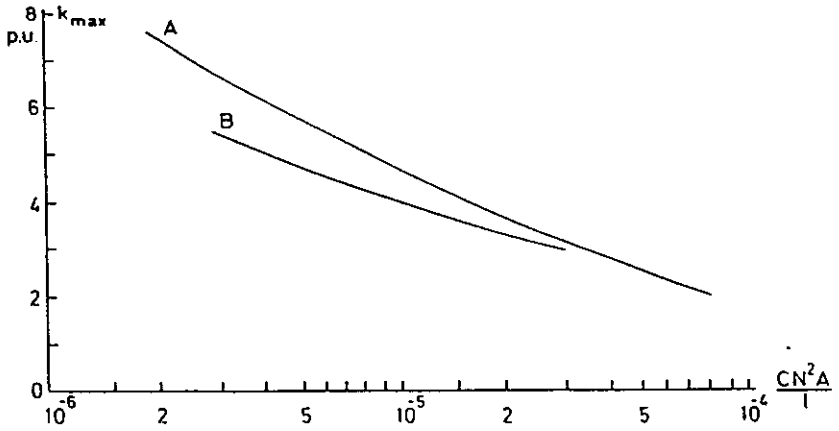

Figure 5.3.10 Maximum overvoltage as function of a normalized capacitance, $(C_t N^2 A)/l$. [20]
A: single-phase transformer and D-connected bank with peak current chopping
B: three-leg-core transformer with simultaneous chopping

It should be observed that the actual overvoltage factors in Figure 5.3.10 are from theoretical calculations on m.v. transformers. A number of conservative approximations have been made giving values which are too high compared to actual observations.

The main conclusion to be drawn from the studies is that three-phase transformer switching does not normally produce higher overvoltages than single-phase transformers and that the calculations based on

the single-phase model are approximately valid also for the three-phase case, at least as long as chopping in steady-state conditions are concerned.

It should be noted that when switching a transformer from the D-winding side the overvoltages in the clearing phases have opposite polarities which may give a certain risk of overstressing windings of conventionally protected transformers.

5.3.6 Reignition transients

Reignitions after the interruption of a small inductive current may either limit or enhance overvoltages (see Section 2.5 of Chapter 2). However, when the inductive load is an unloaded transformer a possible enhancement is very improbable. A considerable reduction due to reignitions has usually been observed [2, 7, 18, 29, 35] and the highest overvoltages have been recorded in tests without reignitions. A typical recording is shown in Figure 5.3.11.

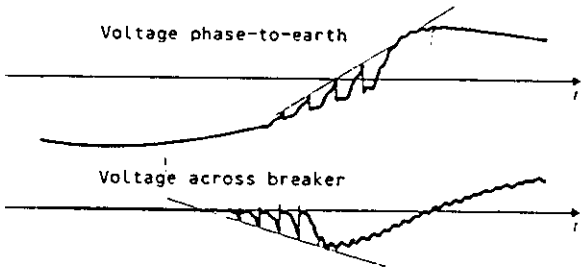

Figure 5.3.11 Measured voltage at interruption of no-load transformer current [2].

At interruption of steady state magnetizing current the cases shown in Figure 5.3.12 can in principle be achieved.

In cases 1 and 2 current chopping close to the current maximum is assumed. This gives the highest chopping overvoltage (overvoltage factor k_a). To achieve this case the breaker contact opening has to take place at or immediately prior to the current peak, otherwise the current would have been chopped earlier at a lower value. If the dielectric strength of the contact gap increases rapidly after the opening, either a clean chop without reignitions will result or a reignition during the rise to the suppression peak, case 1. The **highest overvoltage** will occur at a clean chop, i.e. the chopping overvoltage k_a, while the **maximum reignition transient** is created if the reignition occurs at the voltage peak. Without damping the reignition transient (peak-to-peak excursion) would then attain a value of 2 k_a. If damping and charge displacement (see Chapter 4 Clause 4.3.3.1) are taken into consideration a maximum swing of 1.5 ka could be anticipated. The overvoltage value (to earth) will anyway never exceed k_a.

If the breaker dielectric withstand increases slowly relative to the recovery voltage the chopping overvoltage may be considerably limited as demonstrated by case 2. At each reignition the energy of the load oscillation will decrease thereby reducing the actual maximum overvoltage to values below the prospective k_a-value. Several reignition transients (up to some dozen) may be produced, but their amplitudes are small. Especially older types of oil breakers with slow contact speed could behave as shown in case 2 [21]. It may then even happen that case 2 is followed by a train of reignitions during the recovery period as shown in case 4. But the amplitudes are always very small due to the limiting effect of the low voltage withstand of the contact gap [21].

If the breaker contact opening (and chopping) takes place near a current zero or if the chopping level is low compared to the magnetizing current, the supply side voltage will be high, up to the crest value. Then the cases 3 and 4 may then occur for breakers with fast and slow dielectric recovery respectively. In case 3 a reignition transient of about 2 p.u. would theoretically be possible without damping, but with damping a maximum of 1.5 p.u. may be expected. Case 4 may produce a train of reignition transients with

(20 A) used in the calculation. This indicates that a possible enhancement due to superposition, more than well may be compensated by the general reduction in three-phase operation as compared to the single phase case.

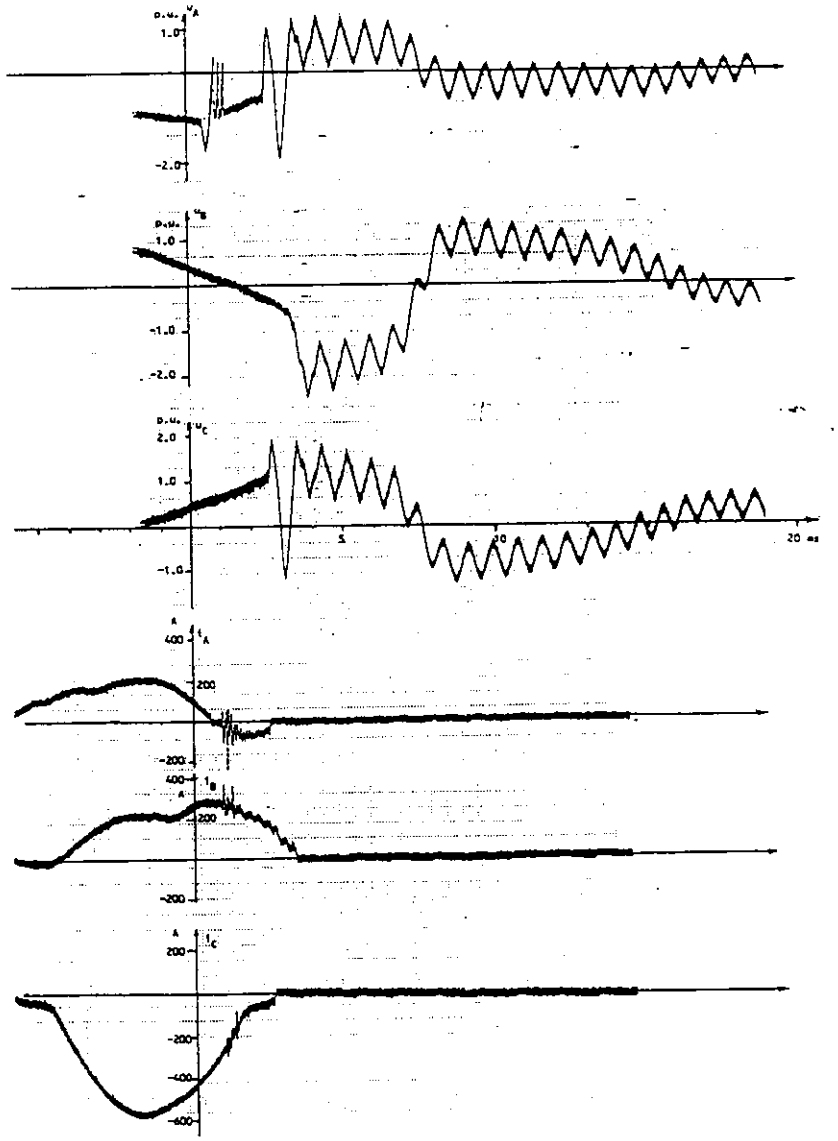

Figure 5.3.8 Inrush current interruption in 400 kV transformer. Field test [37].

A few theoretical studies of three-phase chopping have been made. Although considerable simplifications have been made, some general conclusions may be drawn.

5.3.5.1 Star-connected transformers with earthed neutral and delta secondary

A worst case study has been made by Boyle in Appendix 2. In a star connected transformer the most severe case would be when the second phase to clear chops at peak current provided that the first phase was interrupted 60 electrical degrees earlier. An overvoltage will then appear on the first phase to clear at the time of interruption of the second phase, which is the sum of the instantaneous value of the power frequency voltage present on that phase and an induced transient voltage approximately equal to the switching transient appearing in the second phase to clear. The maximum voltage on the first phase-to-clear would then be approximately

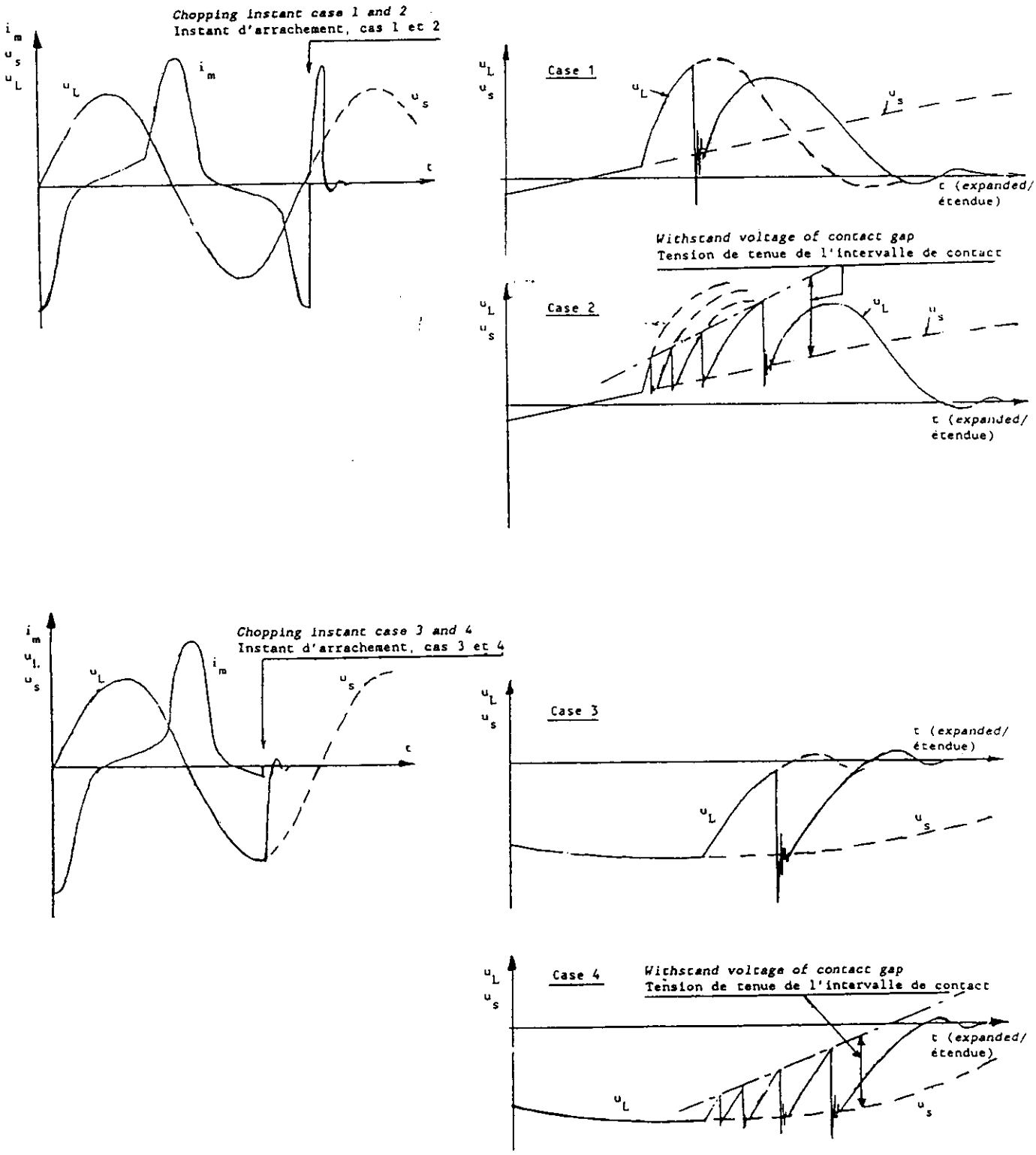

Figure 5.3.12 No-load transformer interruption with reignition.
Steady-state current interruption.

i_m = magnetizing current
u_s = supply side voltage
u_L = load side voltage
k_a = chopping overvoltage factor
u_r = peak-to-peak reignition transient.

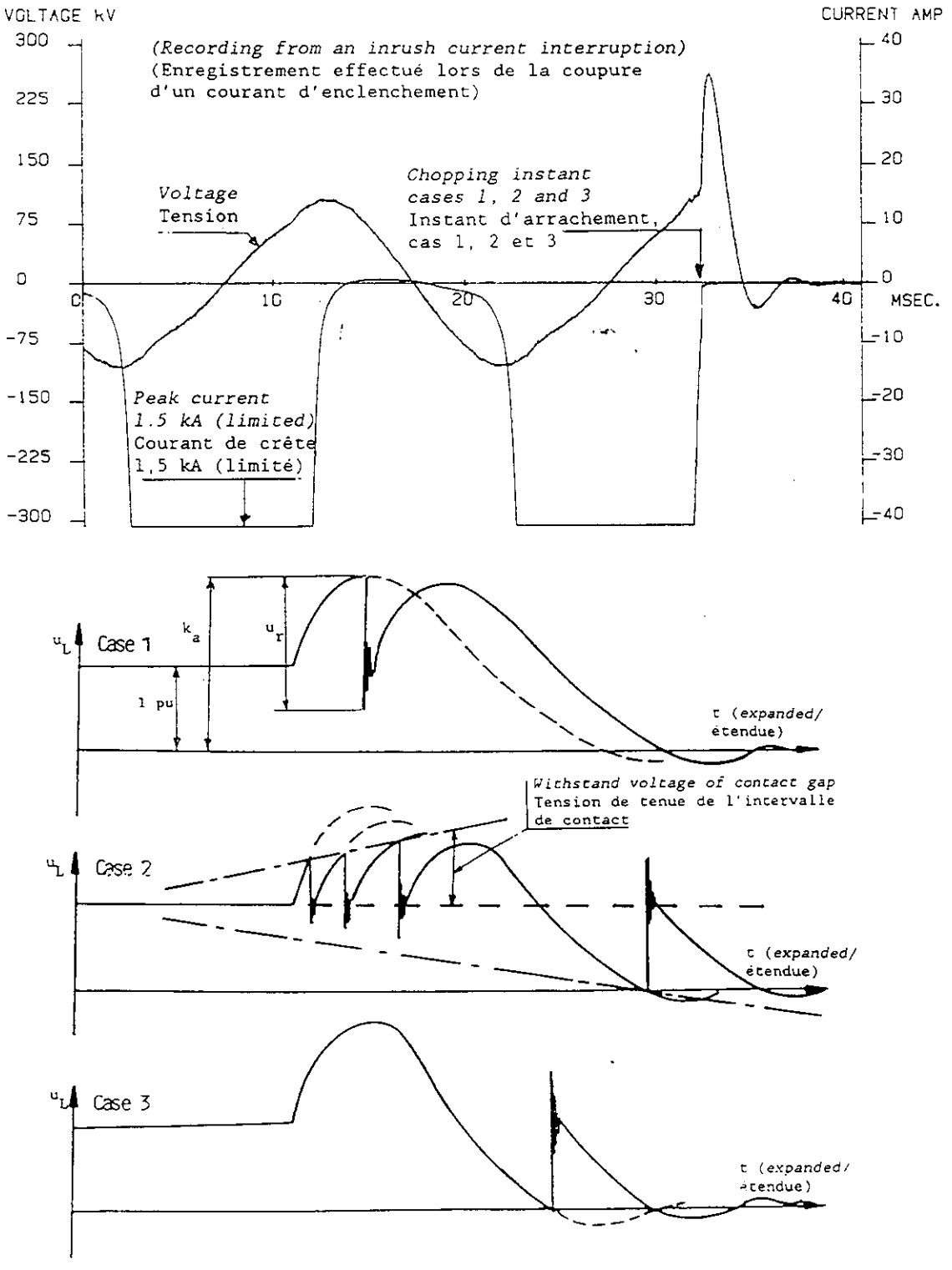

Figure 5.3.13 No-load transformer interruption with reignition. Inrush current interruption.

increasing amplitude up to 1.5 p.u. Neither the overvoltage value to earth nor the peak-to-peak excursion will thus exceed 1.5 p.u. in any case.

Even at inrush current interruption no enhanced overvoltages due to reignitions seem to be possible. Furthermore the reignition transients are expected to be less than 1.5 times k_a. Figure 5.3.13 illustrates this. Since the chopping level is normally much lower than the inrush current peak, the chopping takes place when the voltage is close to the voltage crest. The arcing time may be short or long and the dielectric strength of the contact gap may therefore attain any value. Reignitions may occur during the suppression peak, cases 1 and 2, or with recovery voltage across the breaker, case 3. In case 1 the peak-to-peak voltage excursion at the reignition is expected to be max 1.5 (k_a – 1) p.u.

Reignitions at recovery voltage either after a clean chopping, case 3, or after reignitions at the suppression peak, case 2, are expected to create overvoltages to earth of max 1.5 p.u. Even the excursion peak-to-peak of the reignition transients will not exceed 1.5 p.u.

Contrary to the reactor switching case, reignitions at interruption of no-load transformers cannot produce dangerous overvoltages.

Since transformers normally are tested by lightning impulse voltage, the transients generated at reignitions are deemed to be far from dangerous. Even repeated reignitions should be perfectly innocent due to the low amplitude. The repetition frequency is low and further not sufficiently constant to excite resonating overvoltages in the transformer winding.

5.3.7 Examples of calculation

To get a general knowledge on the maximum amplitude of overvoltages that could be expected when switching magnetizing currents, a few typical examples have been calculated. This will also illustrate the simple calculation procedure developed by Boyle described in Appendix 1.

In Table 5.3.1 the overvoltages at interruption of steady state magnetizing currents in a few typical transformers in the range 11 kV to 433 kV, have been calculated.

A total effective capacitance of 3 nF has been used in most calculations as this seems to be typical. See Figure 5.2.5.

It might be of some interest to compare the result with previous calculations made by the CIGRE Working Group WG 3.2. The main results of WG 3.2 are given in Appendix 3. Their calculations resulted in higher overvoltage factors due to an assumed higher value of the "magnetic efficiency", η_m [22].

For a number of transformers in the WG 3.2 study expected overvoltages have been calculated using Boyle's method. The values are presented in Figure 5.3.14 together with the values from Table 5.3.1. Further the calculated overvoltage curve of Panek and Tuohy [18] for peak current chopping at switching of single phase transformers has been inserted in Figure 5.3.14 for comparison.
The "chop parameter"

$$\frac{C_t U_N^2}{\alpha P_N}$$

is used as independent variable.

The correspondence of the two approaches – Panek's and Boyle's – is well illustrated. The calculation of the chop parameter seems to be a convenient way of getting a quick estimation of the maximum overvoltages to be anticipated when steady state no-load current is interrupted at the current peak (independent of the type of circuit-breaker as long as its chopping level is higher than the peak current).

Only a few values are above the Panek curve. As expected the single value for a transformer with HRS core is one of them.

Vacuum breakers behave different from other types in some respects, but should give *chopping overvoltages* of the same magnitude as other breakers. Ref. [29] compares result from a three-phase lab test with a vacuum breaker switching a 10 kV, 1600 kVA dry type transformer with calculated overvoltages according to the method of Boyle. For steady state current interruption the calculation gave conservative overvoltage values, while a few tests exceeded the theoretical max value (2.5 p.u.) due to repeated reignitions.

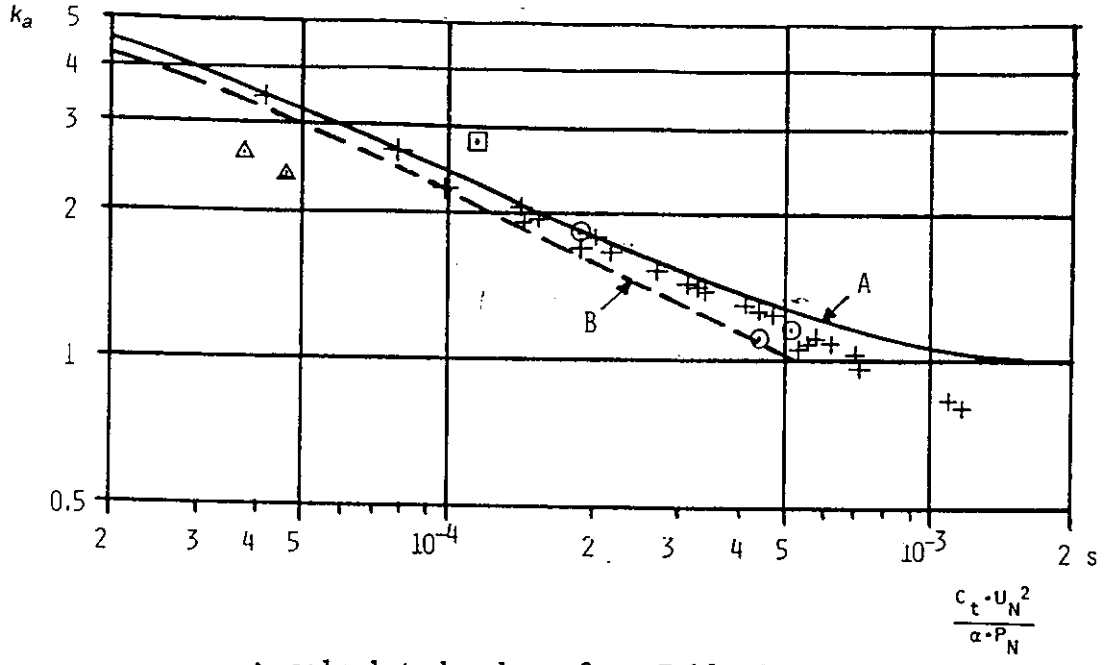

△ calculated values from Table 5.3.1, CROS cores, B_m = 1.5 T
⊙ calculated values from Table 5.3.1, CROS cores, B_m = 1.7 T
⊡ calculated value from Table 5.3.1, HRS core, B_m = 1.35 T
+ recalculated values for transformers in WG 3.2 study

Figure 5.3.14 Overvoltage factor for peak current chopping as function of
$\frac{C_t U_N^2}{\alpha P_N}$ from ref [18] (curve A) and Fig A1.9 of App. 1 (curve B)
compared with calculated values in Table 5.3.1 and Appendix 3.

A few cases of inrush current have also been studied. Here knowledge of the actual chopping level of the breaker is necessary (not only that it can chop at peak current). For modern breakers (except vacuum breakers) this level is conveniently expressed in the chopping number for one breaking unit, κ:

$$i_{ch} = \kappa n C_p = \kappa \sqrt{\frac{n C_s C_{th}}{C_s + C_{th}}}$$

where n = the number of breaking units in series and
C_{th} = the h.f. capacitance according to Clause 5.2.6.3, which determines the chopping current.

The value

$\kappa \cdot n = 10 \cdot 10^4$

has been used in the calculation. To illustrate the influence of κ also calculations have been made with

$\kappa \cdot n = 20 \cdot 10^4$

Table 5.3.1 Calculated overvoltages at interruption of steady-state no-load transformer currents.

Transformer, see note 1		A	B	C	D	E	F	G
Rated power, P_N	VA	$240 \cdot 10^6$	$240 \cdot 10^6$	$800 \cdot 10^6$	$20 \cdot 10^6$	$20 \cdot 10^6$	$1 \cdot 10^6$	$1 \cdot 10^6$
Rated voltage (switched side), U_N	V	$400 \cdot 10^3$	$132 \cdot 10^3$	$433 \cdot 10^3$	$132 \cdot 10^3$	$132 \cdot 10^3$	$11 \cdot 10^3$	$11 \cdot 10^3$
Crest voltage, $u_o = U_N \cdot \sqrt{2}/\sqrt{3}$	V	$327 \cdot 10^3$	$108 \cdot 10^3$	$353 \cdot 10^3$	$108 \cdot 10^3$	$108 \cdot 10^3$	$9 \cdot 10^3$	$9 \cdot 10^3$
Rated current, $I_N = \frac{P_N}{U_N \cdot \sqrt{3}}$	A	346	1050	1067	87.5	87.5	52	52
No-load current, r.m.s. value I_m	A	1.5	4.5	4.0	0.5	2.0	0.5	0.4
No-load current/rated current, $\alpha = \frac{I_m}{I}$	p.u.	0.0043	0.0043	0.0037	0.0057	0.023	0.0096	0.0077
" " " " , peak value, i_m	A	3.5	10.4	9.0	1.1	4.4	1.0	0.8
Chopping current, i_{ch}	A	3.5	10.4	9.0	1.1	4.4	1.0	0.8
Max flux density at rated voltage, B_m	T	1.7	1.7	1.7	1.6	1.35	1.5	1.5
Flux density at current chopping, B_{ch}	T	1.7	1.7	1.7	1.6	1.35	1.5	1.5
$L_{eff} = 0.15$ alt $0.5 \frac{u_o \cdot B_{ch}}{\omega \cdot i_{ch} \cdot B_m}$	H	44.6	4.96	18.7	47	39	4.3	5.4
Effective capacitance $C_t = C_x + C_1 + C_2(\frac{N_2}{N_1})^2$	F	$3.3 \cdot 10^{-9}$	$30.5 \cdot 10^{-9}$	$3 \cdot 10^{-9}$	$3 \cdot 10^{-9}$	$3 \cdot 10^{-9}$	$3 \cdot 10^{-9}$	$3 \cdot 10^{-9}$
Equivalent frequency, $f_{eff} = \frac{1}{2\pi \sqrt{L_{eff} \cdot C_t}}$	Hz	415	409	672	424	465	1.401	1.250
η from figure 5.3.4	p.u.	0.125	0.125	0.12	0.11	0.18	0.060	0.061
Max overvoltage $u_m = \sqrt{\frac{\eta \cdot u_o \cdot i_{ch}}{\omega \cdot C_t}}$	V	$371 \cdot 10^3$	$121 \cdot 10^3$	$636 \cdot 10^3$	$118 \cdot 10^3$	$301 \cdot 10^3$	$23.9 \cdot 10^3$	$21.6 \cdot 10^3$
$k = \frac{u_m}{u_o}$	p.u.	1.14	1.12	1.80	1.09	2.79	2.66	2.40
Chop parameter $\frac{C_t \cdot U_N^2}{\alpha \cdot P_N}$	s	$5.1 \cdot 10^{-4}$	$5.1 \cdot 10^{-4}$	$1.9 \cdot 10^{-4}$	$4.6 \cdot 10^{-4}$	$1.14 \cdot 10^{-4}$	$3.8 \cdot 10^{-5}$	$4.7 \cdot 10^{-5}$

Note (1) (all 50 Hz)

Transformer A 240 MVA 400/132 kV auto operating at rated volts, HV switched CROS
" B " " " LV switched "
" C 800 MVA 433/13.5 kV " " HV switched "
" D 20 MVA 132/33 kV double wound operating at rated volts, HV switched CROS
" E 20 MVA 132/33 kV " " HRS
" F 1 MVA 11/.433 kV dry type " " CROS
" G 1 MVA 11/.433 kV oil immersed " " CROS

Table 5.3.2 Calculated overvoltages at inrush current interruption for several chopping numbers and capacitance values.

Transformer, See note 2		A	A	A	A	B
Rated power, P_N	VA	$240 \cdot 10^6$	=	=	=	$240 \cdot 10^6$
Rated voltage (switched side), U_N	V	$400 \cdot 10^3$	=	=	=	$132 \cdot 10^3$
Crest voltage, $u_o = \frac{U_N \cdot \sqrt{2}}{\sqrt{3}}$	V	$327 \cdot 10^3$	=	=	=	$108 \cdot 10^3$
Rated current, $I_N = \frac{P_N}{U_N \cdot \sqrt{3}}$	A	346	=	=	=	1050
No-load current, r.m.s value, I_m	A	1.5	=	=	=	4.5
No-load current/rated current, $\alpha = \frac{I_m}{I_N}$	p.u.	0.0043	=	=	=	0.0043
- " - " - peak value, i_p	A	3.5	=	=	=	10.4
Chopping number, κ	$\frac{A}{\sqrt{F}}$	$10 \cdot 10^4$	$20 \cdot 10^4$	$10 \cdot 10^4$	$20 \cdot 10^4$	$10 \cdot 10^4$
- " - current, $i_{ch} = \kappa \sqrt{\frac{C_s \cdot C_{th}}{C_s + C_{th}}}$	A	6.7	13.4	4.8	9.6	6.7
i_{ch}/I_m	p.u.	4.46	8.93	3.2	6.4	1.5
Max flux density at rated voltage, B_m	T	1.7	=	=	=	1.7
Flux density at i_{ch}, B_{ch} from Figure A1.3	T	1.81	1.87	1.77	1.84	1.67
$L_{eff} = 0.15$ alt $0.5 \cdot \frac{u_o \cdot B_{ch}}{\omega \cdot i_{ch} \cdot B_m}$	H	24.8	12.8	33.9	17.6	7.6
Eff l.f. capacitance $C_t = C_x + C_1 + C_2(\frac{N_2}{N})^2$	F	$3.3 \cdot 10^{-9}$	=	=	=	$30.5 \cdot 10^{-9}$
Eff h.f. capacitance $C_{th} = 0.7 \cdot C_t$	F	-	-	$2.3 \cdot 10^{-9}$	=	-
Eff h.f. capacitance $C_{th} = C_x + C_1 + \frac{C_{12} \cdot C_2}{C_{12} + C_2}$	F	$4{,}5 \cdot 10^{-9}$	=	-	-	$4.5 \cdot 10^{-9}$
Equivalent frequency, $f_{eff} = \frac{1}{2\pi \sqrt{L_{eff} \cdot C_t}}$	Hz	556	774	476	669	331
η from Fig 5.3.5	p.u.	0.12	0.10	0.12	0.11	0.13
Max overvoltage $u_m = \sqrt{u_o^2 + \frac{u_o \cdot \eta \cdot i_{ch} \cdot B_{ch}}{\omega C_t \cdot B_m}}$	V	$614 \cdot 10^3$	$756 \cdot 10^3$	$544 \cdot 10^3$	$684 \cdot 10^3$	146
$k = \frac{u_m}{u_o}$	p.u.	1.88	2.31	1.66	2.09	1.35

Note 2: Transformer A 240 MVA 400/132 kV auto operating at rated voltage
HV switched

B 240 MVA 400/132 kV auto operating at rated voltage
LV switched

To show the relative insensitivity of the h.f. capacitance, C_{th}, on overvoltages, two different assumptions have been made

- $C_{th} = 0.7 \cdot C_t$ *according to Clause* 5.2.6.3
- $C_{th} = C_1 + \frac{C_2 C_{12}}{C_2 + C_{12}}$ *according to Eq.* 5.2.2

where $C_1 \approx C_2 \approx C_{12} \approx 3$ nF is assumed.

Since usually the supply side capacitance, C_s, is much larger than the transformer capacitance, the approximation

$$C_p \approx C_{th}$$

has been used.

The result of the calculation is given in Table 5.3.2.

The overvoltage values at inrush currents are – of course – higher than for steady-state, but for modern SF_6 puffer circuit-breakers with $\kappa \approx 10 \cdot 10^4$ or less for one breaking unit, overvoltage factors of less than 2.5 p.u. seem to be a realistic anticipation.

At medium voltage considerably higher overvoltages are anticipated. But also here the calculation method seems to give a conservative estimation of the maximum overvoltage. In ref. [29] a test with a dry type 10 kV transformer switched by a vacuum breaker is presented. Overvoltages calculated from the actual chopping current is shown to always exceed the measured voltage values, in many cases considerably, due to reignitions. Even repeated reignitions decreased the overvoltage considerably.

5.4. Operational experience and result of field tests

The operational experience shows that switching of unloaded transformers normally causes no problems irrespective of the switching device. Nevertheless, the switching case has been of some concern and a large number of tests – both in networks and in laboratories – have been performed and reported.

The working group has collected the published information from a lot of older field tests [23]. A brief summary of these tests together with more recent tests reported, has been made in Tables 5.4.1 and 5.4.2.

It must be observed that the tests have been made under extremely varying conditions of:

- type of circuit-breaker
- supply network
- earthing
- transformer size and design
- opening resistors (none, linear, non-linear)
- overvoltage limitation

When averaging overvoltage values in the Tables, those differences have been neglected. For details the reader is directed to the sources (given in Table 5.4.3).
From the analysis of published test results it is difficult to draw any definite conclusions whether conditions exist that may cause problems in no-load transformer switching. The material indicates that the overvoltage level is low irrespective of the type of switch, transformer type and network arrangements.

For high voltage breakers ($\geq$ 72 kV) overvoltages > 4 p.u. are observed only in rare cases of older tests. The mean values are usually below 2 p.u.

For medium voltage breakers somewhat higher overvoltages are occasionally recorded – as expected – but with average values generally below 2.5 p.u.. Medium-voltage switches will typically produce lower overvoltages, perhaps on the order of 1.5 p.u. or less, as shown in Table 5.4.2. The results to be expected, of course, will be dependent upon the type of switch employed; however, generally speaking, medium voltage switches do not chop currents to the same degree as circuit-breakers. If some chopping does occur, it very likely would be similar to that depicted in Figure 5.3.12, Case 3 and 4; therefore, the overvoltages to be expected will be low.

For both ranges the extreme values of voltages are recorded for transformers manufactured before 1953. It is then likely that the transformers tested are of older types with HRS cores. Further the measuring technique in those days were less advanced than today and the recorded values may suffer from inaccuracies – in both directions.

Table 5.4.1 Transformer no-load switching overvoltages at field tests with high voltage transformers

Type	Rated Voltage kV	Ref code	Year of test	Test location	No. of tests	Results Transient voltage to earth Mean (p.u.)	Max (p.u.)
AIRBL	80	H	1954	Net	120	1.27	2.3
"	80	B	1960	Net	30	2.17	3.6
"	110	B	1960	Net	35	1.49	2.57
"	123	N	1980	Net	3	–	1.0
"	150	B	1960	Net	60	1.74	3.3
"	"	A	<1953	Net	72	1.66	4.3
"	"	H	1980	Net	20	1.3	1.8
"	220	B	1960	Net	120	1.21	2.11
"	350	F	1954	–	–	1.3	1.7
"	380	B	1960	Net	5	1.37	1.7
"	400	P	1986	Net	22	2.2	2.7*
MINOIL	80	H	1954	Net	240	1.46	2.7
"	150	A	<1953	Net	51	2.02	4.7
OIL	75	H	1954	Net	480	1.19	1.9
"	123	N	1980	Net	3	–	1.0
"	138	J	1964	Net	4	1.28	1.86
"	150	A	<1953	Net	34	1.95	3.3
"	230	J	1964	Net	6	1.35	1.93
SF6	123	N	1980	Net	18	–	1.45
"	150	M	1981	Lab	22	1.3	1.7
"	275	K	1981	Net	24	–	1.1
"	420	N	1980	Net	3	–	1.0
"	500	K	1981	Net	12	–	1.1
SF6-HVS	230	J	1964	Net	12	1.02	1.24

Legend: AIRBL = Air blast circuit-breaker
MINOIL = Minimum oil circuit-breaker
OIL B = Oil circuit-breaker
SF6 = SF6 circuit-breaker
SF6-HVS = SF6 high voltage switch
MVS = Ablative type medium voltage switch

* = limited by arresters

For sources: See Table 5.4.3.

The only known problem area seems to be switching with vacuum circuitbreakers due to the possibility of voltage escalation and virtual current chopping [24, 25, 26]. Most problems have been reported from switching arc furnace transformers under load, but also no-load switching may produce excessive overvoltages especially under inrush conditions. Special care should be taken in cases with dry type transformers with low parallel effective capacitance [27, 29].

Table 5.4.2 Transformer no-load switching overvoltages at field tests with medium voltage transformers

Type	Rated Voltage kV	Ref code	Year of test	Test location	No. of tests	Results Transient voltage to earth Mean (p.u.)	Max (p.u.)
AIRBL	10	H	1954	Net	600	1.37	3.4
"	10	D	1974	Lab	40	1.1	1.4
"	11	A	<1953	Net	9	3.2	4.7
"	50	A	<1953	Net	13	2.0	2.8
"	60	E	1963	Lab	1	-	4.3
MINOIL	12	D	1974	Lab	40	1.2	1.9
"	60	I	1962	Lab	208	1.36	2.42
OIL B	20	M	1981	Lab	20	2.12	2.8
	45	A	<1953	Net	13	1.7	2.4
	50	A	<1953	Net	30	2.1	3.6
	60	A	<1953	Net	179	2.2	6.1
VACUUM	20	M	1981	Lab	20	1.6	2.6
	6	L	1981	Lab	360	-	3.1
	12	D	1974	Lab	40	1.5	2.4
SF6-HVS	69	J	1976	Lab	15	1.15	2.02
MVS	13-15	0	>1960	Lab	210	1.01	1.44
	23-25	0	>1960	Lab	208	1.02	1.53
	34-38	0	>1960	Lab	165	1.01	1.15

Legend: See Table 5.4.1; For sources: See Table 5.4.3.

Table 5.4.3 List of publications used as sources for Tables 5.4.1 and 5.4.2

Reference A: Berger, K. Ueberspannungen beim abschalten leerlaufender transf. Bull. Schweiz electrotech. Ver. Bd 44 (1953) No 9

Reference B: Baltensperger, P. Inductive current switching surges Brown Bovery Mitt. 47 (1960):4

Reference C: Leyman, B S. Tests and simulation of reactor loaded transformers C.E.R.L. RD/L/N 224/71

Reference D: Tiitola, T. Noload transf and artificial circuit switching Doc CIGRE 13-74(WG 13.02)07 IWD

Reference E: Verre, P. le. Overvoltages caused by breaking of small inductive currents at high voltages. Rev General de l'Ectricité, Fev. 1963

Reference F: Jancke – Sandstrom. Field testing of 380 kV circuit breaker
CIGRE Report 1954–106

Reference H: Poma – Richard. Contribution to the study of overvoltages when switching small currents
CIGRE Report 1954–118

Reference I: Berger – Vogelsanger. Overvoltages when switching no–load transformers
Internal Report

Reference J: From S & C Unpublished Data, Exhibit "A" – CIGRE 13–81(WG 13.02) 38 IWD

Reference K: S Matsumura, S Tominaga, K Yoshinaga (Japan). Small inductive current switching by puffertype SF6 gas circuit breakers. CIGRE Document 13–81(SC) 16

Reference L: F Battiwala, U Habedank, H H Schramm, R Kugler (Germany, F.R.). Comparison of different arc extinguishing systems with respect to interruption of small inductive currents CIGRE 13–81(SC)20 from Colloqium of CIGRE 13, Helsinki, Sept. 81

Reference M: G Aldrovandi, E Colombo, G Mazza, G Santagostino (Italy). Behaviour of MV and HV circuit breakers when switching no load transformers. CIGRE Document 13–81 (SC) 26

Reference N: H Patrunky, H J Sowade, B Stoesser, G Emberger, U Habedank, G Luxa, F Ritcher, H Schramm. Switching of transformers, reactors and long transmission lines. Field tests in German 420 kV networks. CIGRE Report 1980: 13–08

Reference 0: Unpublished data from S&C, Document CIGRE 13–87(WG 13.02)03 IWD

Reference P: Unpublished data from Imatra Power Company. CIGRE Document 13–86(WG13.02)19IWD

5.5 Interrupter testing for unloaded transformer switching

5.5.1 General

In testing for no–load transformer switching there are, basically, two methods used. One tests the circuit–breaker performance when interrupting current in a test transformer and the other when interrupting current in a linear reactor with added damping.

For circuit–breakers used on systems of 100 kV and above and for switching large transformers it is not practicable to use the actual transformer.

The use of a test station transformer is a doubtful substitute. A test station transformer would in general have ratings and characteristics that may be very different from the actual transformer. It may even have a different core material. A transformer with an HRS core can in no way be representative for a transformer with a CROS core.

Overvoltage levels due to chopping and reignitions generated while switching a test station transformer would have little relation to the levels achieved when switching an actual transformer in the field. Further, results may be entirely different in different test stations.

Alternatively a damped linear reactor circuit (or a reactor–loaded transformer) is sometimes used to simulate transformer switching. The overvoltages obtained are then dependent on the inductance of the test load, its natural damping and the damping provided by the added resistor. An actual no–load transformer interruption would appear as an overdamped response and could be approximated by a heavily damped reactor circuit provided that the actual transformer response is known. No general conclusions on the behaviour as a transformer switch could be drawn and the results achieved in such a test circuit cannot be used to predict overvoltages in actual installations.

5.5.2 Test recommendations

5.5.2.1 No-load current of transformers 72.5 kV and above

Experience indicates that when switching unloaded transformers under steady state conditions and at voltages not exceeding their rated voltage the overvoltages are usually well below the standard insulation levels (IEC 71-1). Tests are therefore not recommended to simulate this switching condition. Switching of the inrush magnetizing current of an unloaded transformer is an unlikely condition and no tests are recommended.

In case of doubt, it is possible to make approximate estimates of overvoltages by making the calculations given in Section 5.3. The values of chopping characteristics may be provided by some reactor current type tests described in Chapter 4.

5.5.2.2 No-load current of transformers below 72.5 kV

Generally tests are not required but in cases of doubt only testing in the field will allow full assessment of the ability of a circuit-breaker for that case. If field tests are not possible, three phase tests may be made in a laboratory using the actual transformer to be switched in service.

Testing of a circuit-breaker will generally not produce meaningful results unless the connection between the transformer and the circuit-breaker is the same as in the field (length, type of cable). The characteristics of the supply side must also be as closely as possible identical to the field conditions. Medium-voltage switches having a minimal current-chopping tendency may be tested in the laboratory to determine the interrupting capability of the switch.

Test series, measurements and evaluation of results may be the same as for reactor testing. However, equation 4.5.1 in Chapter 4, cannot be used for calculating the chopping current because L is no longer defined for deenergizing a transformer.

5.6 Limitation of overvoltages

The no-load switching of modern transformers does not normally require measures to limit switching overvoltages or even special care in the selection of a suitable circuit-breaker. If calculations according to the methods given in Section 5.3 should indicate that unacceptable overvoltages are anticipated, similar measures to limit overvoltages as applied in reactor switching , described in Chapter 4, section 4.4.3, can be used. Only situations when interruption of inrush currents with circuit-breakers having high chopping levels are involved (heavy duty air-blast breakers), may require protection measures. This particularly applies to phase-to-phase overvoltages stressing unprotected windings of delta connected transformers switched from the delta side.

5.7 Summarizing remarks

A substitute circuit to represent actual field no-load transformer switching cannot be realized. To get an acceptable test evidence on the magnitude of the overvoltages created at interruption of unloaded transformers, the only possibility is to test the actual switching device together with the actual transformer preferably in the actual network.

With a good knowledge of the characteristics of the transformer and the switch together with approximate network data, it seems to be possible to estimate an expected overvoltage level upon switching unloaded transformers under steady-state as well as inrush conditions.

The calculation model given in Section 5.3 is based on two groups of transformer core material:

- grain-oriented cold-rolled steel (CROS)
- hot-rolled steel (HRS)

Even though the magnetic characteristics can vary rather much within the groups, the results of the calculation model given are not very sensitive with regard to normal variations. E.g. the so-called

"superoriented" steel (HI-B) behaves in respect of overvoltage production very much like normal grain-oriented steel, at least in comparison with other approximations made to ease the calculation.

Other calculation models can be used. General differential equation solving programs can easily be used, but the accuracy of the result is dependent on the representation of the B-H characteristic of the actual transformer core. To get an estimation of the overvoltages to be anticipated for cases with peak current chopping it may be sufficient to calculate the chop parameter,

$$\frac{C_t U_N^2}{\alpha P_N}$$

from available data for the actual installation and to evaluate the maximum overvoltage from Figure 5.3.14.

The results of the calculations in Clause 5.3.7 should be regarded as estimations. Nevertheless, the results for a range of typical transformers, both high voltage and medium voltage, allows some conclusions to be drawn.

A. Modern transformers with grain-oriented steel cores generate very low overvoltages when switched under steady state conditions, even if current chopping occurs at the peak current.

   a) For high voltage transformers ($\geq$72 kV) the maximum overvoltages are generally less than 1.5 p.u. with maximum values less than 2.0 p.u. even in special cases (very high power, high magnetizing current).

   b) For medium voltage transformers the maximum overvoltages will normally be < 2.5 p.u. and in rare cases (dry-type transformers), < 4 p.u..

B. Switching devices with low chopping levels generate still lower overvoltages. E.g. with medium voltage switches, the overvoltages will normally be less than 1.2 p.u. with maximum values on the order of 1.5 p.u..

C. Switching under inrush condition may generate somewhat higher overvoltages. With modern h.v. circuit-breakers that have chopping numbers $\kappa = 20 \cdot 10^4$ or less (for one breaking unit) the probability to get more than 2.5 p.u. will be small. Only heavy duty air-blast circuit-breakers are expected to cause higher overvoltages.

D. Reignitions will not give rise to any increase in overvoltage magnitude. The peak-to-peak excursion will under all circumstances be below twice the chopping overvoltage value and in all practical cases less than 1.5 times the chopping overvoltage, k_a. This will not endanger the transformer insulation. Resonating overvoltages in the transformer winding cannot be excited since the rather few reignition transients that may occur, will not have a repetition frequency stable enough. The only case where voltage escalation due to repetitive reignitions can occur, is the switching of dry-type transformers with vacuum breakers or vacuum switches. But even in this case the excitation of resonating overvoltages seems to be very unlikely due to the statistical variation of the repetition frequency.

E. Modern transformers with CROS cores that have passed normal lightning impulse tests will without any doubt withstand all switching overvoltages when switched at no-load with modern circuit-breakers. H.V. transformers are almost always protected with surge arresters which give a further insurance. In the case of transformers connected directly to a gas insulated switchgear protection may be omitted. But even in this case no-load switching will be harmless since the chopping number of SF6-breakers is too low to create a dangerous situation even when switching under inrush conditions.

5.8 CONCLUSION

The current interruption of modern transformers in no-load conditions, with modern circuit-breakers or switches will usually give overvoltages below the insulation levels specified by the present standards. As a consequence, specific tests do not need to be recommended.

For the special cases with older types of transformers (HRS-cores) and/or heavy duty air-blast circuit-breakers which may result in higher overvoltages, tests cannot be recommended for the following reasons:

- A substitute test circuit to represent the no-load transformer can never give a reliable information about the actual overvoltages in the field.

- A test station transformer cannot be used since the result will be highly unreliable.

For these cases the overvoltages can be estimated with sufficient accuracy by the procedure described in this report, with the breaker chopping characteristics provided by reactor switching tests.

5.9 References in Chapter 5

1. CIGRE Working Group 12.07.
Resonance behaviour of high-voltage transformers.
CIGRE-report 12-14, 1984.

2. Möller K, et al.:
Beanspruchung grosser Transformatoren durch multiple Wiederzundungen.
Elektrizitätswirtschaft 85(1986):13, p. 478-482.

3. Colombo E., Santagostino G.:
Result of the enquiries on actual network conditions when switching magnetizing small inductive currents and on transformer and shunt reactor saturation characteristics.
Electra No. 94, May 1984.

5. Talukdar S.N. et al.:
On modelling transformer and reactor saturation characteristics for digital and analog studies.
IEEE Trans. PAS-94(1975) p. 612-621.

6. Gray N.:
Determination of the inherent characteristics of Power System Circuits.
Students Quarterly Journal, IEE, March 1970.

7. Greenwood, A.N.:
Electrical Transients in Power Systems New York. Wiley-Intersciences. 1971.

8. Bertula T., Palva V.:
Transformer Capacitances.
Sähkö Electricity in Finland, Vol. 39, October 1966.

9. Harner R.H. and Rodriguez J.:
Transient recovery voltages associated with power-system, three-phase transformer secondary faults.
IEEE 1972 Winter Meeting, paper No. T72 112-6.

10. Hammarlund, P.:
Transient Recovery Voltage Subsequent to Short-circuit Interruption with Special Reference to Swedish Power Systems. Transactions No. 189, I.V.A., Stockholm 1946.

14. Swift G.W.:
Power transformer core behaviour under transient conditions. IEEE Trans PAS-90(1971):5.

15. Brailsford F. and Fogg R.:
Anomalos iron losses in cold-reduced grain-oriented transformer steel.
Proc. IEE, Vol 111 No. 8, Aug. 1964.

16. Lavers J.D., Biringer P.P. and Hollitscher H.:
The effect of third harmonic flux distortion on the core losses in
thin magnetic steel laminations.
IEEE Trans. PAS-96(1977):6.

17. Staub, B.:
Modellversuche zur Ermittlung der maximal möglichen Ueberspannung beim Ausschalten Leerlaufenden Transformatoren.
Bull. SEV, Bd. 55 (1964):2, p. 43-51.

18. Tuohy, E.J., Panek, J.:
Chopping of transformer magnetizing currents Part I: Single phase transformers.
IEEE Trans. Vol. PAS-97 No. 1 Jan/Febr 78.

19. Bozorth, R.M.:
Ferromagnetism.
Van Norstrand, 1951.

20. Ihara, Panek, Tuohy:
Chopping of transformer magnetizing currents Part II: 3-phase transformers
IEEE Trans. Vol. PAS-102 No. 5, May 1983.

21. Young A.F.B.:
Some researches on current chopping in high-voltage circuit-breakers.
Proc. IEE, Vol. 100, Part II, No. 76, August 1953.

22. Thaler, R.:
Auswirkungen der modernen Transformatorbauweise auf die Transformator-SchaltUberspannungen.
Bull. SEV 56(1965):25, p. 1115-1117.

23. Dorn J. and van der Aa, J.:
List of investigations on interruption of inductive currents. Report No. EH 75-S89, T H Eindhoven 1975.

24. Panek, J., Fehrle, K.G.:
Overvoltage phenomena associated with virtual current chopping in three phase circuits.
IEEE Trans. PAS 94(1975):4, p. 1317-1325.

25. Pretorius, R.E.:
The suppression of internal overvoltage surges in industrial high voltage systems.
The Certified Engineer, 54(1981):7, p. 938-956.

26. Aldrovandi, G. et al.:
Behaviour of m.v. and h.v. circuit-breaker when switching no-load transformers.
CIGRE 13-81(SC)26 from Colloqium of CIGRE 13 in Helsinki, Sept. 81.

27. Ohashi, H. et al.:
Application of vacuum circuit-breaker to dry type transformer switching.
IEEE-report A 76 174-3, PES Winter Meeting & Tesla Symposium, New York, 1976.

28. Roguski, A.:
Voraussetzung der transienten Netzparameter auf der Grundlage durchgefUhrter Messungen.
Elektrie 30(1976):10, p. 526-529.

29. Van den Heuvel, W.M.C. et al:
Interruption of a dry-type transformer in no-load by vacuum circuit-breaker.
EUT-Report 83-E-141, (1983), Eindhoven University of Technology.

30. Langhammer, G.: Ueberspannungsentwicklung beim Abschalten induktiv belasteter Drehstromtransformatoren.
Thesis, MUnchen 1986.

31. Kalasek. V.K.I.: Comparison of an analytic study and EMTP-implementation of complicated three phase schemes for reactor interruption.
EUT-Report 88-E-204. Eindhoven University of Technology.

32. Bollen, M.H.J., Vaessen, P.T.M.:
Frequency spectra for admittances and voltage transfers measured on a three-phase power transformer,
EUT-Report 87-E-181 {1987}. Eindhoven University of Technology.

33. Cherry, E.C.: "The duality between interlinked electric and magnetic circuits and the formation of transformer equivalent circuits", Proc. Phys. Soc. (B) 62 (1949) p. 101-111.

34. IEEE Application Guide for Transient Recovery Voltages for AC High-Voltage Circuit Breakers Rated on a Symmetrical Current Basis
ANSI/IEEE C37.011-1979

35. Ananian, L.G. et al.: Field testing of voltage transients associated with vacuum breaker no-load switching of a power transformer in an industrial plant. IEEE Trans Ind Appl, Vol. IA-19, No 6, Nov/Dec 1983, p. 914-919.

36. Artemjev, D., Tihodeev N., Shur S.: Isolation of electrical networks.
Energy. Leningrad 1965. (In Russian)

37. CIGRE Document 13-86 (WG 13.02)19 IWD
Unpublished data from Imatra Power Company, Finland

Chapter 6:

SWITCHING OF REACTOR-LOADED TRANSFORMERS

6.1 Introduction

Reactive compensation with medium voltage three-phase reactors, connected to the transmission network through tertiary windings of three-phase EHV/HV interconnection or step-down transformers, or autotransformers, is quite common in many systems. This compensation arrangement is very often preferred, due to the switching and insulation advantages offered by MV reactors, in comparison with HV ones connected directly on the transmission line. MV reactors are normally switched at the MV side, through suitable medium voltage circuit-breakers or switches specified for that duty. This is covered by Chapter 4.

However, occasionally, the need may arise to disconnect the reactor from the HV side of the transformer, or autotransformer, and this is the case examined in this chapter. This case of interruption of small inductive currents is different from the direct reactor switching case, obviously due to the intervention of the transformer between the circuit-breaker and the reactor. The transformer modifies the interaction between the circuit-breaker and the reactor circuit, and complicates this three-phase switching phenomenon.

6.2 Typical network configurations and reactor and transformer characteristics.

The general layout and arrangement of connections etc is the same as described in Chapter 4 Sub-Clause:

- 4.2.1.2 for open-air substations
- 4.2.1.3 for metal-enclosed substations (GIS)

The power transformers used for connecting the reactors to the network, are usually step-down or interconnecting three-phase transformers of the transmission system, including a MV tertiary delta winding suitable for the connection of a reactor. This winding may be connected to earth through an earthing transformer or through surge control capacitors, externally connected to the transformer terminals.
The main characteristics of the EHV and HV transformers of the system are given in Chapter 5 (Sub-Clause 5.2.3).
The reactors loading the delta tertiary winding of the transformers may have a rated voltage ranging from 10 to 36 kV and a rated power in the 10-150 MVA range, according to an enquiry carried out by WG 13:02 [3].
The current on the HV side of the reactor-loaded transformer ranges from 50 to 300 A.
The reactors are either star connected with unearthed neutral, or delta connected. Some conditions with star-connected reactors having their neutral earthed and with an X_0/X_1 ratio equal to 1 have also been reported [3].
Examples of reactor data are given in Chapter 4 (Sub-Clause 4.3.1).

6.2.2 Transformer capacitances

Transformer capacitances are the most important characteristic of a transient transformer model. They are, however, difficult to determine due to their dependence on the frequency of oscillations and a lack of relevant data. The capacitance evaluation becomes more important due to the increased use of digital simulation, which requires a precise three-phase modelling of transformers for transient studies.

A treatment of transformer capacitances which should be adequate also for the requirements of this Chapter is comprised in Clause 5.2.6 of Chapter 5. It is used as the basic reference for this Chapter.

6.3 Single-phase switching phenomena

A study of the single phase switching case may give a basic understanding of reactor-loaded transformer switching and a comparison with the other cases treated in the previous chapters.

Figure 6.3.1 shows one possible equivalent representation of a single phase circuit with a reactor loaded transformer.

The basic phenomena of interruption and the circuit response can be outlined on the simplified lossless circuit diagram of Fig. 6.3.1. Prior to interruption, the current i_1 is flowing through the primary winding and the current i_2 is flowing through the secondary winding and the reactor.

Upon current chopping at the primary side, the power-frequency load current at the secondary side stops as well. This abrupt stop is equivalent to a current chopping in the secondary winding. The electromagnetic energy stored in the reactor inductance L, is transferred on the circuit capacitances C_2 and C_1 through the transformer windings.

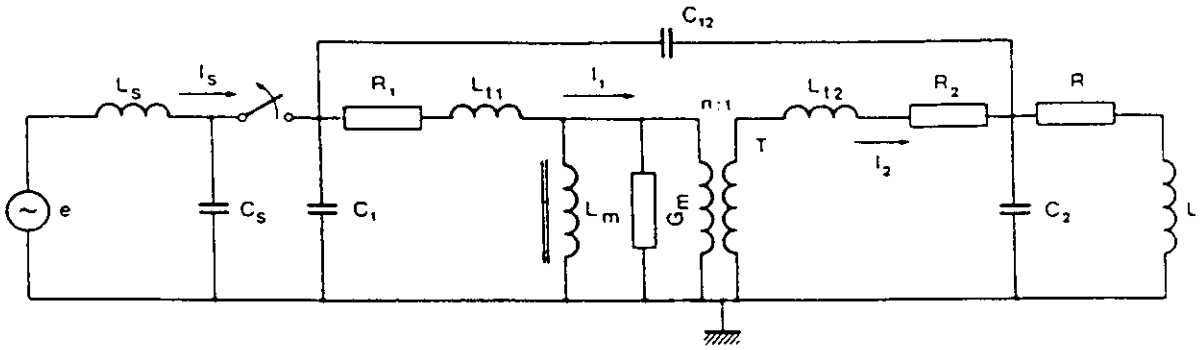

Fig 6.3.1. Single-phase circuit of a reactor-loaded transformer

L_{t1}, L_{t2} : leakage inductances of the transformer windings
R_1, R_2 : resistance of the transformer windings
L_m : non-linear magnetizing inductance
G_m : non-linear shunt loss conductance of the core
C_1, C_2 : primary and secondary winding capacitance to earth
C_{12} : interwinding capacitance
T : ideal transformer with ratio n:1
L_s, C_s : source side short-circuit impedance and capacitance
L, C, R : inductance, capacitance and resistance of the reactor, where the capacitance to earth, C, is included in C_2.

For an HV/MV transformer, C_2/n^2 is very small compared to C_1, therefore the energy is mainly transferred on C_1 and any chopping overvoltage is mainly governed by this capacitance and the relevant inductance. The chopping overvoltage can be calculated by referring all circuit inductances and the capacitances C_2 and C_{12} to the primary side, as in Fig. 6.3.2a.
C_2 and C_{12} can sometimes be neglected at this consideration resulting in the further simplified equivalent scheme in Fig. 6.3.2b.

Assuming that the energy upon chopping is mainly transferred to C_1 electromagnetically through the transformer windings, which seems reasonable at the actual oscillation frequencies of 1 to 5 kHz, the simple equivalent circuit in Fig. 6.3.2b, similar to the directly connected reactor treated in Chapter 4, can be used in calculating the chopping overvoltage. See also equations 2.3.18 and 2.3.19 of Chapter 2.

The overvoltage factor k_a is given by:

$$k_a = \sqrt{1 + \left(\frac{i_{ch}^2}{u_o}\right)\left(\frac{L_t + n^2 L}{C_1}\right)}$$

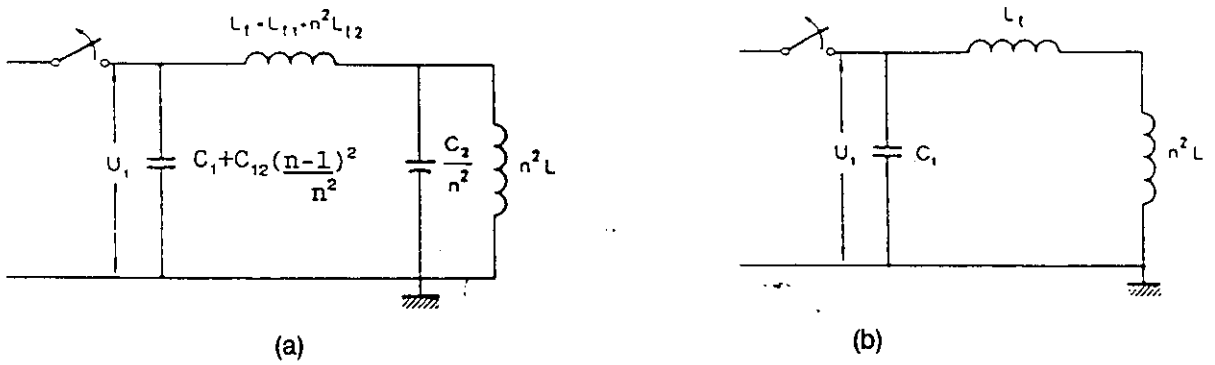

Fig. 6.3.2 Equivalent circuit referred to the primary side
(a): complete with C_2 and C_{12},
(b): neglecting C_2 and C_{12}

Voltage transients are transferred through the transformer from one winding to another in many cases capacitively. The capacitive voltage transfer of high-frequency transients, such as those of the "second parallel oscillation" (order of 100 to 500 kHz) is expressed as:

$$U_2 = \frac{C_{12}}{C_{12} + C_2} \cdot U_1$$

where C_{12} represents the effective coupling capacitance between the primary and secondary windings and C_2 the total capacitance of the secondary winding to core and ground. (These high frequency capacitances have values that are different from the low frequency values. See Chapter 5.) It is evident that C_{12} and C_2 are determined by the coil and core geometry and structure, so that the transferred voltage U_2 can represent a very significant fraction of the transient voltage U_1. The turns ratio takes no part in this voltage transfer. Such capacitively transferred surges are of very short duration because other attributes of the winding quickly come into play.

During the second parallel oscillation following a reignition, the circuit behaves approximately as the equivalent circuit in Fig. 6.3.3a.
Through this oscillation the voltage difference between both sides of the circuit-breaker is equalized.

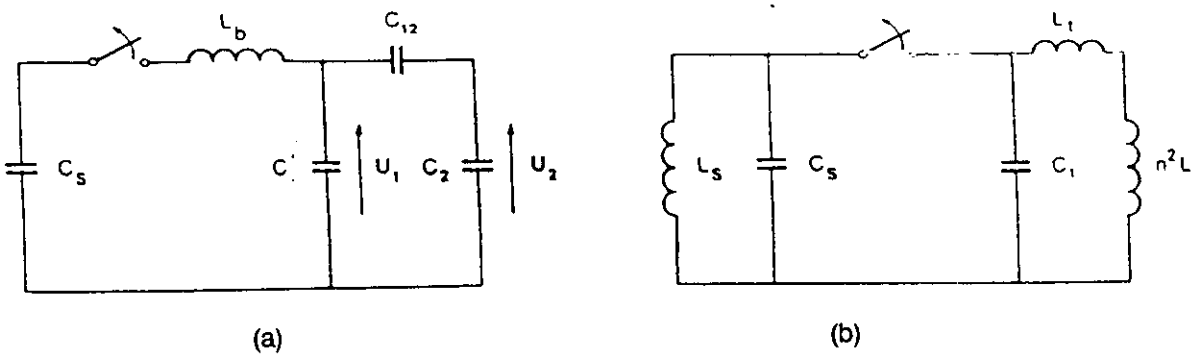

Figure 6.3.3 Equivalent circuit for different oscillation frequencies after a reignition:
(a) for very high frequency oscillations (second parallel oscillation)
(b) for medium frequency oscillations (main circuit oscillation)

In case that the frequency of the second parallel oscillation is close to one of the resonant frequencies of the transformer, a series resonance oscillatory circuit can be established between the capacitance C_{12} + C_2 and the reactance L_t of the transformer, which can give rise to an overvoltage in the transformer winding.

During the main circuit oscillation following after the decay of the second parallel oscillation, the equivalent circuit is described by Fig. 6.3.3b. The reactor inductance L, the transformer inductance L_t and the source inductance L_s are all involved. C_{12} and C_2/n^2 are disregarded in Fig. 6.3.3b since the effective capacitance C_2 of the MV side referred to the primary side is usually much lower than C_1.

6.4 Three-phase switching phenomena

Three-phase switching phenomena result from the coupling between
phases especially on the load side of the switching device. For the switching of reactor-loaded transformers the interphase coupling on the load side is considerably influenced by the winding connection of the transformer.

The typical case of a reactor-loaded transformer is a three-phase
transformer or autotransformer or a bank of single-phase transformers or autotransformers loaded with reactors on a delta connected tertiary winding, primary and secondary winding being star connected and at least the primary neutral being earthed. The delta connection of the tertiary leads to the characteristic inductive interphase coupling of this case.

The transformer together with the reactor may only be de-energized when the last voltage suorce is disconnected by switching off the primary (resp. secondary) side if the secondary (resp. primary) side has been disconnected before. The disconnected winding, as star connected, has no influence on the switching transients except through its capacitances. These may be taken into account by using resultant capacitances. So an equivalent circuit with only two windings may be considered. Fig. 6.4.1 includes such an equivalent circuit which is suitable for calculating chopping overvoltages related to the switching of reactor-loaded transformers. The representation of the transformer takes account of the short-circuit inductance of the transformer including zero-sequence inductance, earth capacitances and capacitance between the switched primary winding (1) and the reactorloaded winding (2). It corresponds to the single-phase equivalent circuit of fig. 6.3.2. For more detailed representation refer to [5] and [6].

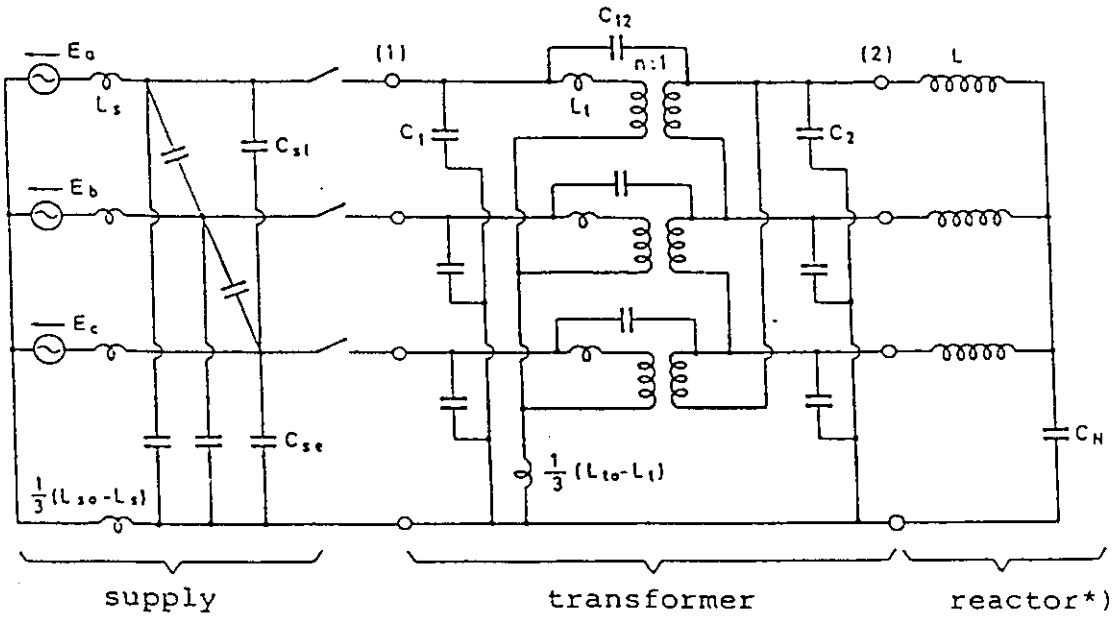

Figure 6.4.1 Three-phase circuit-diagram of a reactor-loaded transformer.
*) line-to-earth capacitances of the reactor transferred to transformer tertiary terminals.

If there is a long bus or line between the transformer and the reactor, this may lead to appreciable line-to-line capacitances which then should be taken into account.

The supply side and the reactor may be represented in the same manner as for the switching of direct-connected reactors, treated in Chapter 4.

The zero-sequence inductance of the transformer L_{to} is, due to the delta connection of the tertiary winding, even for three legged transformers approximately equal to the positive sequence inductance which is equal to the relevant short-circuit inductance L_t.

The interphase coupling inductance for the primary side terminals, with the tertiary side short-circuited, is $(L_{to}-L_t)/3$, which therefore is small. Nevertheless there is strong interphase coupling through the delta connected tertiary winding if the tertiary winding is not short-circuited but loaded with the reactor. The resultant interphase coupling inductance for the transformer reactor combination, as seen from the primary side terminals, is:

$$\frac{1}{3}L_1\left(\frac{L_o}{L_1} - 1\right) = \frac{1}{3}L_1(\alpha - 1)$$

where L_1 = the resultant positive-sequence inductance,
L_o = the appropriate zero-sequence inductance of the combination seen from the primary side terminals and
$\alpha = L_o/L_1$

The resultant zero-sequence inductance is equal to that of the transformer alone ($L_o = L_{to} \approx L_t$) whereas the resultant positive-sequence inductance is equal to the sum of the short-circuit inductance of the transformer and the inductance of the reactor (i.e. $L_1 = L_t + L'$,where $L' = L \cdot 3n^2$ is related to the primary side of the transformer). Due to the fact that normally the inductance of the reactor is several times the short-circuit inductance of the transformer the ratio $\alpha = L_o/L_1$ is rather small, a typical value being 0.1. This means strong coupling between phases.

Power frequency load-side line-to-earth voltages of the open poles are determined by this coupling and the recovery voltages influenced accordingly. Tables 6.4.1 and 6.4.2 show these voltages in p.u. for the limit value of $\alpha = 0$ and the typical value of $\alpha = 0.1$.

Of course not only power frequency voltages but also transients with moderate frequencies are transferred from one phase to the others through this coupling inductance. The TRV of open poles is influenced by transients caused by the interruption of later poles-to-clear including current chopping transients and main oscillation transients of reignitions. (See following Sub-clause 6.5 and especially Figs. 6.5.1 and 6.5.2 of this Sub-clause.)

The coupling inductance has significant influence upon chopping overvoltages and on the transfer of the chopping effects from one phase to other phases. This may be expressed by the resultant inductance as seen from the breaker terminals of the pole where the current is chopped and by the resultant coupling inductance between the terminals of that pole and the terminals of poles already open, if any. These inductances are shown in table 6.4.3 for the different poles-to-clear related to L_1, the positive-sequence inductance of the transformer/reactor combination.

In addition to the ideal value $\alpha = 0$ and the typical value $\alpha = 0.1$ also $\alpha = 1$ which represents the uncoupled case has been included.

Table 6.4.1: Per unit load-side line-to-earth power frequency voltages of open poles

	Number of poles open		
	1	2	3
$\alpha = 0$	1	1/2	-
$\alpha = 0.1$	0.75	0.43	-

Table 6.4.2: Pole-clearing-factor, i.e. p.u. power frequency recovery voltage for first, second and third pole-to-clear

	Pole to clear		
	1	2	3
$\alpha = 0$	0	√(3/2)	1
$\alpha = 0.1$	0.25	0.87	1

Table 6.4.3: Resultant inductances and resultant coupling inductances for the three poles-to-clear related to the positive sequence inductance of the transformer-reactor combination L_1.

α	Pole considered	Pole to clear		
		1	2	3
0	1	0	-1/2	-1/3
	2	-	1/2	-1/3
	3	-	-	2/3
0.1	1	0.25	-0.43	-0.30
	2	-	0.57	-0.30
	3	-	-	0.70
1	1	1	0	0
	2	-	1	0
	3	-	-	1

Due to the influence of capacitances these values are not a direct measure for chopping overvoltages with respect to a certain current chopped but they show rather well the influence of the coupling inductance on these voltages.

The capacitances influence the transients associated with the interruption essentially. Even if the simple representation of the transformer/reactor combination of Fig. 6.4.2 is used, chopping transients, except for the first pole-to-clear, generally will be double frequency ones whereas for independent phases (α = 1) and ideally coupled phases (α = 0) this representation leads for all poles-to-clear to single frequency transients.

For the first-pole-to-clear the circuit is a single frequency one, therefore the resultant surge impedance, i.e. the square root of the resultant inductance divided by the phase capacitance, determines the chopping overvoltage in that phase.

One of the most interesting effects of this type of interphase coupling is that for the ideal case (α = 0) the recovery voltage of the first pole-to-clear is zero (see table 6.4.2) and that current chopping in the first pole-to-clear does not give rise to any chopping overvoltage. The resultant inductance is zero (see table 6.4.3). It can be shown that, under this ideal condition, current chopping in the first pole-to-clear neither changes the currents in the reactor nor the total magnetic energy. Only during interruption of the second and third pole-to-clear there are non-zero recovery voltages and chopping overvoltages, if chopping occurs.

α = 0 means negligible zero-sequence inductance compared with the positive sequence inductance of the combination or, considering the delta connection of the tertiary winding, a transformer short-circuit inductance that is negligible compared with the inductance of the reactor.

For the typical case of α = 0.1 the power frequency recovery voltage is 0.25 p.u. and the resultant inductance 0.25 L_1.
Compared to the uncoupled case with a resultant inductance of 1 p.u. relatively low chopping overvoltages will result.

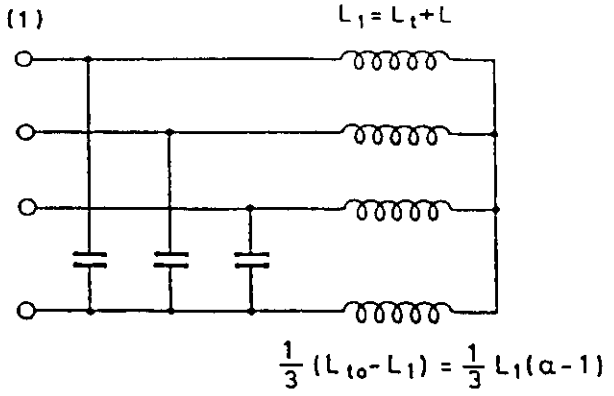

Figure 6.4.2 Simplified representation of transformer-reactor combination
(L' = inductance of the reactor related to the primary side of the transformer)

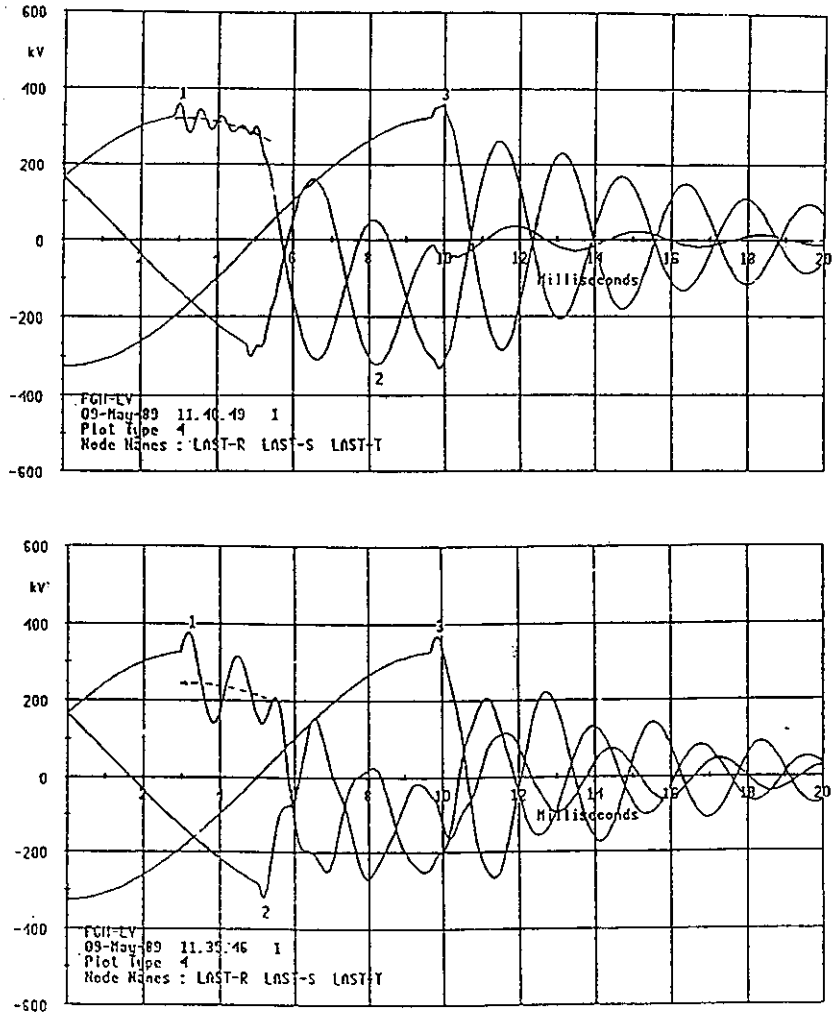

Figure 6.4.3: Calculated line-to-earth voltages during interruption of a 400 kV reactor-loaded transformer on the basis of the substitute circuit of Fig 6.4.2 with current chopping.
a) $\alpha = 0.01$ representing a case near the limit case of $\alpha = 0$
b) $\alpha = 0.1$ representing the typical case.
The hatched lines show the course of the power frequency recovery voltage of the first pole-to-clear.

If the capacitive transfer of overvoltages to the tertiary side is not considered or of no concern, e.g. due to special capacitors connected to the tertiary terminals, and C_1 is large enough compared to C_{12}, then C_{12} may be neglected. C_2 may be transferred to the primary side if L_t is much smaller than L.

The equivalent circuit of the transformer/reactor combination may then be simplified representing only the primary terminals as shown in Fig. 6.4.2.

This equivalent circuit is identical with that used for the switching of earthed reactors with $L_0/L_1 = X_0/X_1 \neq 1$ (see Chapter 4, table 4.3.3) with the special characteristic that L_0/L_1 is of the order of 0.1. In Appendix 4 and 5 interphase coupling and the resulting three-phase switching phenomena during reactor switching are thoroughly dealt with. The results may be used also for the primary side of the transformer when switching reactor-loaded transformers. Fig. 6.4.3 shows line-to-earth voltages during interruption of a 400 kV reactor-loaded transformer calculated on the basis of the substitute circuit of fig. 6.4.2. The influence of α especially on the TRV of the first pole-to-clear may be observed.

6.5 Reignition phenomena

Overvoltage phenomena associated with reignitions during the switching of reactor-loaded transformers can be expected to be similar to that associated with the switching of direct-connected reactors. The conditions described in Chapter 4, Sub-clause 4.3.3, will be generally applicable to reactor-loaded transformers. The circuit elements controlling the high-frequency transients associated with reignitions are approximately the same for both circuits. The overvoltage magnitudes and frequencies generated by a given circuit-breaker at a particular system voltage and load current therefore should be essentially the same.

In the typical configuration for a reactor-loaded transformer with a delta-connected tertiary treated in section 6.4, a reignition on one phase may be coupled through the delta-tertiary winding into the other two primary phases. The interaction between the phases will be even more complicated than for the directly connected reactor treated in Sub-clause 4.3.4 of Chapter 4. The interaction between phases will be somewhat similar to that noted for Case 3 in Table 4.3.3, wherein there will be a transfer of both chopping overvoltages and reignition transients.

To illustrate the complexity, a recording from a field test conducted on a large 275 kV autotransformer with a 30 MVA tertiary-connected reactor is presented in Figure 6.5.1. Two reignitions are observed on the blue phase, the last pole to clear. The rapid changes in voltage resulted in significant voltage changes also on the red and yellow phases causing a protective gap breakdown in the red phase [9].

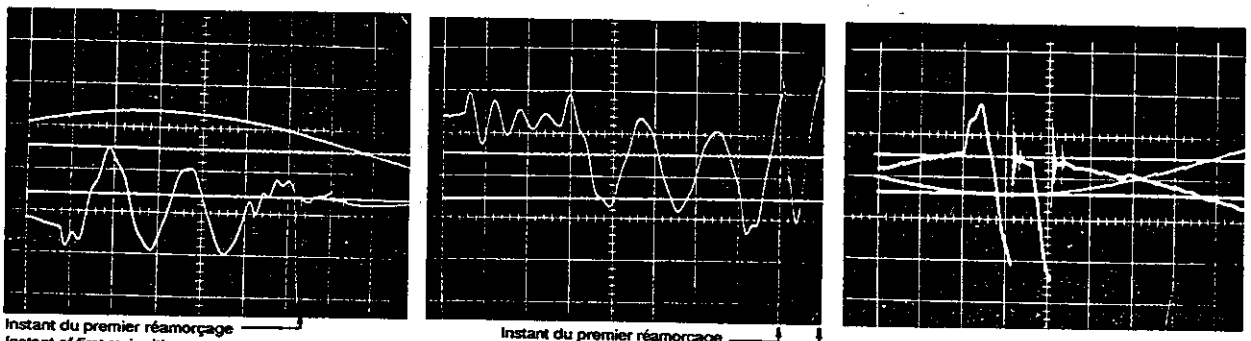

(a) Tension côté charge de la phase rouge
Red phase load side voltage

Courbe sup./ *U.B.* : 257 kV/div.
Courbe inf./ *L.B.* : 258 kV/div.
Base de temps/ *T.B.* : 1 ms/div.

(b) Tension côté charge de la phase jaune
Yellow phase load side voltage

Courbe sup./ *U.B.* : 261 kV/div.
Courbe inf./ *L.B.* : 250 kV/div.
Base de temps/ *T.B.* : 1 ms/div.

(c) Tension côté charge de la phase bleue
Blue phase load side voltage

Courbe sup./ *U.B.* : 263 kV/div.
Courbe inf./ *L.B.* : 261 kV/div.
Base de temps/ *T.B.* : 1 ms/div.

Dernier pôle à couper/ *Last pole to clear*

Note. Time bases are not coincident

Figure 6.5.1 Interphase coupling effects following a circuit-breaker reignition.
Field test record – 275 kV autotransformer with 30 MVA tertiary- connected reactor.

A transient network analyzer (TNA) study was performed, using a model of the field test circuit, to determine the sensitivity of overvoltage magnitudes to different circuit parameters and to examine the various mechanisms of overvoltage production observed in the field test. Figure 6.5.2 shows oscillograms from the TNA study similar to those obtained during the field test. Point A represents the start of the recovery transient for the third pole-to-clear as reflected in the second pole-to-clear recovery transient. This transient was coupled and added to the existing transient up until the time of reignition, Point B, in the last pole to clear.

In (a) a reignition at the suppression peak is modelled and in (c) a reignition occurs at the recovery peak. The voltage transients in the second pole-to-clear due to a reignition in the third pole are completely different in the two cases. To explain this it was investigated what happened if no recovery voltage transients were imposed on the second pole from the third pole.

If the third pole is not clearing (or if no coupling exits between the second and third pole) the second pole-to-clear voltage would have been as shown in (b) and (d). At the instant of the reignition in the third pole, the second pole-to-clear voltage would thus have been at Point C as shown in (b) and (d), if the third pole had not cleared. Upon reignition of the third pole at Point C, therefore, the voltage on the second pole-to-clear will collapse toward a voltage represented by Point C. The reignition therefore results in a step change in voltage from Point B to Point C. An overshoot follows the step change in voltage on the second pole and produces the peak positive or negative overvoltage as shown in (a) and (c) respectively.

The shape of the transient overvoltage in the second pole-to-clear is thus extremely dependent on the reignition in the third pole-to-clear, not only on whether a reignition occurs or not, but also on the instant of the reignition.

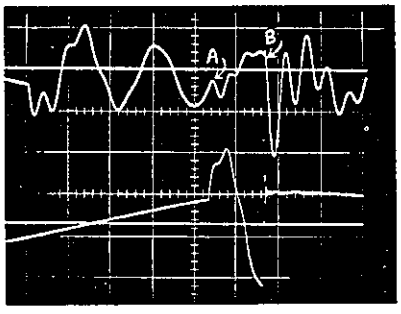

(a) Second and third pole-to-clear voltages with a reignition in the third pole-to-clear at suppression peak voltage

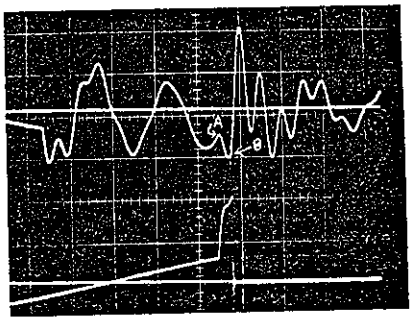

(c) Second and third pole-to-clear voltages with a reignition in the third pole-to-clear at recovery peak voltage

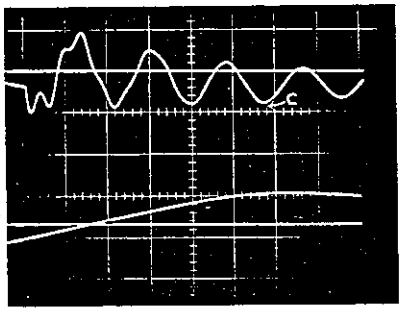

(b) Second pole-to-clear voltage with no coupled transients from last pole clearance

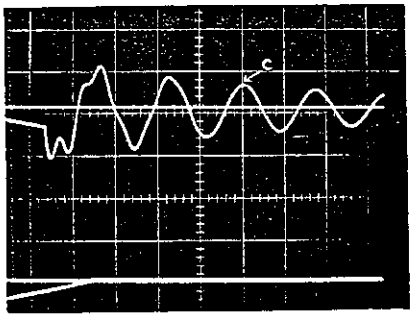

(d) Second pole-to-clear voltage with no coupled transients from last pole clearance

Upper beam: Second pole-to-clear, 1 div = 1.35 p.u.
Lower beam: Third pole-to-clear, 1 div = 1.35 p.u.
Timebase = 1 ms/div.

Figure 6.5.2 Interphase coupling effects following a circuit-breaker reignition.
TNA study – 275 kV autotransformer with 30 MVA tertiary-connected reactor.

The results of the field tests and the TNA study indicates the extreme difficulty to predict maximum overvoltages without a very exact modeling of the actual situation. The recovery characteristic of the circuit-breaker must be known very accurately to give correct reignition instants in a simulation.
Also the stochastic nature of the voltage withstand of the contact gap should be taken into account to correspond to an actual application.

The magnitude of the coupled overvoltage will be influenced significantly by the following factors:

a. The point in time at which the reignition occurs.

b. The natural frequencies and damping of the second and third pole clearing transients.

c. The magnitudes of the chopping induced overvoltages; that is, higher chopping voltages will result in higher coupled overvoltages. .

d. The relative points in time of current chopping on the second and third poles.

The variation in these factors would give widely differing results in practice. It may be concluded, however, that the maximum overvoltages in the switching of the reactor-loaded transformers are no longer determined by the maximum chopping induced overvoltages but by the coupled overvoltages following a reignition.

6.6 Test Results

Available data on the switching of reactor-loaded transformers are minimal since direct-connected reactors are typically employed at the higher voltages. Also, reactors connected to the medium-voltage tertiary winding of a large autotransformer are typically directly switched at the medium voltage. A few field and laboratory tests, however, have been performed.

Field tests were conducted on a 275 kV autotransformer with medium-voltage reactors connected on a delta-tertiary winding of the transformer. The transformer and either a 30 MVAR reactor or a 60 MVAR reactor was switched [9].
A summary of these test results appears in Table 6.6.1.

Table 6.6.1 Peak overvoltages caused by switching a 275 kV autotransformer with a 30 MVA and 60 MVA tertiary connected reactor [9]

Taille du réacteur *Reactor size* MVA	Valeur *Value*	SURTENSION CRETE / *PEAK OVERVOLTAGE* (1)							
		1er pôle/ *1st pole*		2ème pôle/ *2nd pole*		3ème pôle/ *3rd pole*		Résumé/ *Summary*	
		Us PU	Um PU	Us PU	Um PU	Us PU	Um PU	Us PU	Um PU
30 (5)	Moy. *Mean*	1.43	1.72	1.42	2.04	1.99	1.25	1.61	1.67
	Max.	1.77	2.27 (4)	1.70	2.93 (4)	2.64 (4)	2.52	2.64 (4)	2.93
60 (6)	Moy. *Mean*	1.47	1.63	1.55	1.00	1.78	1.13	1.60	1.25
	Max.	1.73	2.34	2.22	1.00	2.14	2.50	2.22	2.50

U_s = suppression peak voltage to earth
U_m = maximum overvoltage to earth

(1) nominal system voltage 270 kV
(2) values for first, second and third poles to open
(3) values for all three poles
(4) gap breakdown occurred at maximum voltage
(5) 54 test operations
(6) 12 test operations

The following general conclusions were drawn from these tests:

a. Switching the 30 MVAR reactor produced higher overvoltages on the primary than switching the 60 MVAR reactor.

b. Circuit-breaker reignitions resulted in overvoltages on the adjacent primary phase which exceeded overvoltages due to current chopping.

c. The overvoltage potential for a reactor-loaded transformer is at least as great as that for direct-connected reactors of a similar size.

In another field test, a 400/120/21 kV, 400/400/125 MVA transformer loaded with a 21 kV, 63 MVA reactor was switched on the primary side [10]. The maximum overvoltage to ground produced was 2.6 per unit. The maximum overvoltage obtained upon simultaneous switching of two 63 MVA reactors was on the same order of magnitude. Arresters were installed on the high-voltage side of the transformer; therefore, the maximum overvoltages may have been limited. The test oscillograms clearly show the interaction between the phases during switching.

6.7 Limitation of overvoltages

The overvoltages produced at switching of a reactor-loaded transformer appear on both sides of the transformer, stressing as well the HV winding and the MV windings of the transformer and the reactor.

The phenomena can be expected to be similar to those associated with the direct switching of reactors and the characteristics given in Chapter 4, Section 4.4 for the overvoltage levels and the means to limit overvoltages will be generally applicable to reactor-loaded transformers. However, it may be necessary to protect additionally on the MV side.

6.8 Testing

6.8.1. Laboratory tests

Laboratory tests may be performed either to obtain general information about the switching device, or with the objective of reproducing the conditions in a specific reactor-loaded transformer installation as closely as possible. It is recognized that it would be extremely difficult to use a laboratory circuit to simulate the transformer and reactor. Therefore the actual transformer and reactor should be used. But even then it may be doubted that the behaviour of the circuit at reignitions in the circuit-breaker will be reproducible from test station to test station. The maximum overvoltages observed at such tests may therefore be significantly different in different test stations.

If tests are performed with the aim to determine circuit-breaker characteristics for calculation purposes, the general requirements set forth in Chapter 4, Clause 4.4.4, should be taken into account.

6.8.2. Field Tests

A field test in the actual network seems to be the only way to achieve full assessment of the performance of a switching device for a specific installation of a reactor loaded transformer.

Care must be taken that the circuit is not noticeably modified by the measuring equipment used. The capacitance of the voltage dividers must be low compared to the capacitances of the circuit. Furthermore, care must be taken that the circuit will not be substantially changed by an abnormal connection of the supply network (the substation) and by protective devices.

For an outline of the test series and measurements, refer to Clause 4.5.4 of Chapter 4. In addition to these tests, it might also be valuable to perform some closing tests to determine the severity of the switching transients upon closing for the actual installation.

6.9 Conclusive remarks

The switching of a reactor-loaded transformer, as far as the development of transient voltages are concerned, is basically similar to that of a directly switched reactor and the same general conclusions as in Chapter 4, section 4.6, are mostly valid. It is also here necessary to distinguish between chopping and reignition overvoltages.

6.9.1. Chopping overvoltages.

The chopping overvoltages appearing on the primary side of the transformer will most likely correspond to switching of a directly connected reactor with differences in effective capacitances and inductances taken into account. In the typical case of a tertiary delta connected reactor the chopping overvoltages of the first phase-to-clear will be lower than in the corresponding case with a directly switched reactor. For the second and third pole a certain reduction of the suppression peak may also exist, but due to the strong inductive interphase coupling the second and third phase to clear will be subject to transfer of chopping transients (with typical frequencies of some kHz) from the previously clearing phases. These transferred transients may be superimposed on the overvoltages created by chopping in the actual phase in an unpredictable way. However, no significant increase of the maximum level is expected. The overvoltages can be referred to the reactor side through the transformer ratio.

6.9.2. Reignition overvoltages

As shown in section 6.5 reignitions may drastically influence the interruption process, in the same way as for a directly connected reactor with strong interphase coupling as described in Chapter 4, Clause 4.3.3 and thoroughly treated in Appendix 4 and 5. By the inductive coupling the main circuit oscillation (5 to 20 kHz) following a reignition is transferred to the other phases and by the capacitive coupling the high frequency transients like the "second parallel oscillation" are transferred (see Chapter 2).
The latter may attain relatively high values, depending on the capacitance configuration of the transformer.

Repeated reignitions may give rise to resonance conditions when some resonant frequency of the transformer winding is excited. However, to create dangerous oscillation amplitudes a rather stable repetition frequency is required, and it is most unlikely that such a condition will be fulfilled [11].

6.9.3 Validity of testing

Laboratory tests intended to be representative of network conditions are not recommended due to the difficulty of achieving an equivalent laboratory circuit. The possibility to make a simple and straightforward prediction of maximum overvoltages based on any tests except in the actual circuit, must be regarded as very remote.
From tests with directly connected reactors e. g. in the substitute test circuits described in Chapter 4, it may be possible to evaluate circuit-breaker characteristics to be used in detailed modelling in a computer.

6.9.4 Application considerations

The minimal information available from actual field tests indicates an overvoltage level comparable to the one at direct reactor switching. There is a possibility, however, of creating higher, and in some cases dangerous, overvoltages due to the interaction between the phases. The switching of reactor loaded transformers normally is not practiced and should be avoided as far as possible. Reactor switching should preferably be performed by medium voltage circuit-breakers between the transformer and the reactor. When switching on the high voltage side is unavoidable appropriate protection means, such as surge arresters, should be applied.

6.10 References in Chapter 6

[3] "Results of the enquires on actual network conditions when switching magnetizing and small inductive currents and on transformer and shunt reactor saturation characteristics", E. Colombo and G. Santagostino. Electra No 94, May 1984.

[5] "Transformer models in the simulation of electromagnetic transients" H.W. Dommel, 5th PSCC, Cambridge, England, Sept. 1975.

[6] "Digital approach of three-phase interruption of a reactor-loaded transformer", B.C. Papadias, G.C. Theodossiou, Colloqium of CIGRE 13, Helsinki, Sept. 1981.

[9] "275 KV switching of a supergrid Transformer Having a Reactor Loaded Tertiary - The Results of Live Testing and a Transient Network Analyser Study" - CEGB Laboratory Note No. RD/L/N 224/71 - Central Electricity Research Laboratories.

[10] "Overvoltages on power transformer disconnection". Test report by Imatra Power Company (unpublished) 1986-10-20, CIGRE 13-86(WG-13.02)19IWD

[11] "Oscillatory switching voltages and relevant response of HV power transformers", W. Stein, et.al., CIGRE report 12-03, 1984.

APPENDIX 1

CURRENT CHOPPING OVERVOLTAGES FOLLOWING THE INTERRUPTION OF TRANSFORMER NO-LOAD CURRENT

by D. Boyle

A1.1 Introduction

This appendix aims to explain the phenomena observed when interrupting the no-load current of transformers neglecting reignitions. The interruption of steady magnetizing current and of transient inrush current is considered. An empirical method of calculating chopping overvoltages is described.

The paper forms a theoretical background for recommendations relating to the application and testing of switches and circuit-breakers for the transformer switching duty.

The range of transformers considered is from medium voltage power transformers switched at 3.3 kV to the highest ratings of generator and transmission transformers.

Main consideration is given to modern power transformers having cold rolled oriented steel cores (CROS) but responses from older transformers using hot rolled steel (HRS) are also given.

A1.2 Transformer Characteristics

In estimating overvoltages caused by the interruption of transformer no-load current, it is useful to consider the magnetic energy stored by the transformer and transferred to the effective capacitances during the interruption process. The effective capacitances are discussed in Chapter 5, Clause 5.2.6.

The transformer core losses per cycle may be separated into two components; non-frequency dependent (hysteresis loss) and frequency dependent (eddy loss). The frequency dependent losses will be referred to as eddy losses although they are not, strictly, all eddy losses [A1, A2, A3]

Much data has been collected [A4] and examination of this encourages the use of normalized data in the assessment of overvoltages following interruption. General considerations of magnetization curves and losses can give consistent results throughout the range of transformers.

An initial problem is that the information available on magnetization characteristics is usually expressed in terms of r.m.s. voltage and r.m.s. current. The characteristics for a number of transformers are shown in Figure A1.1.

The no-load current for a transformer is non-sinusoidal for a sinusoidal applied voltage, and a knowledge of the r.m.s. current is not directly useful. A method such as that described by Talukdar et al [A5] with some modification as described below has been used to derive the instantaneous current, i_m, given in Figures A1.3 and A1.4 from a knowledge of the r.m.s. current I_mm to maximum flux density, B_m. The I_m/B_m characteristic as given in Figure A1.1 may be obtained from transformer manufacturers. If the characteristic up to B_m = 1.9 T is known by measurements, this will normally provide sufficient information to permit the calculation of overvoltages for the range of possible chopping levels of circuit-breakers. If it is necessary to extend the range of instantaneous current values to a higher level of saturation, a knowledge of the air-cored inductance of a transformer winding will permit interpolation between the maximum measured I_m/B_m to the point at which saturation is assumed to be complete, considered here to be at 2.05 T. Beyond this point the dB/di_m gradient is constant.

The model used is a parallel connection of a non-linear inductance and a resistance representing no-load loss. See Figure A1.8. The instantaneous current, i_m, may be calculated from the measured values of the no-load r.m.s. currents for a series of ascending values of B_m. The no-load current is considered to have two components; i_L = the inductive component, and i_R = the hysteresis part of the resistive

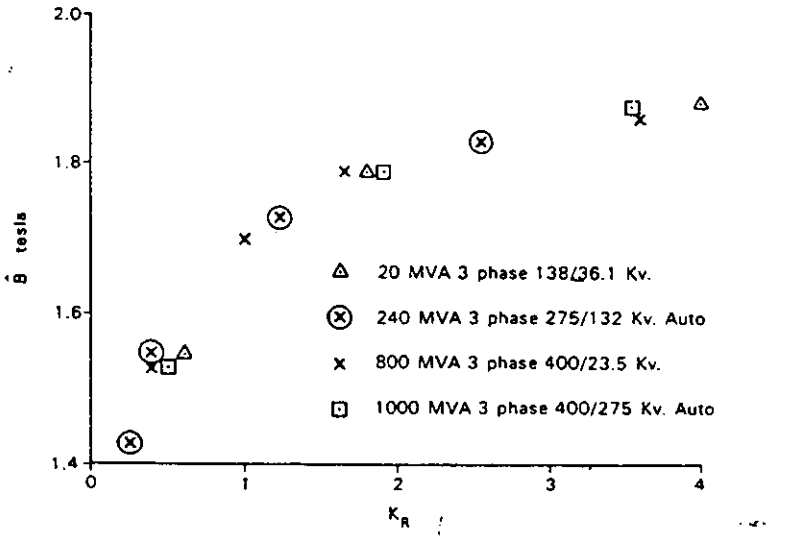

$$K_R = \frac{I_m \text{ for excitation to B}}{I_m \text{ for excitation to 1.7 T}}$$

Figure A1.1 Flux density vs r.m.s. magnetizing current for transformers with CROS cores

component. The hysteresis loss is assumed to be 50 % of the total loss as discussed later. For a given B_m we can assume that

$$B = B_m.\sin\Theta(t)$$

where $\Theta(t)$ is the phase angle.

Then $i_R = \hat{i}_R.\cos\Theta(t)$

where $\hat{i}_R = 0.5.\sqrt{2}.P/U$
U = phase voltage associated with B_m
P = losses per phase

$i_L(B_m)$ is considered to be a series of straight line sections between successive values of B_m, starting from $i_L = 0$ at $B_m = 0$.

If we define the flux density for $i_m = 0$ on the falling excitation curve as B_{rem} and the corresponding phase angle as Θ_{rem}, i.e. $B_{rem} = B_m.\sin\Theta_{rem}$ (see Figure A1.2), we can obtain the first value of i_L as:

$$i_L = \hat{i}_R.\cos\Theta_{rem}$$

The unknown values of i_L corresponding to the successive peaks of B_m are then calculated using the previous known value of i_L and the r.m.s. value of I_m corresponding to the new value of B_m by a method such as that described in Ref. /A5/.

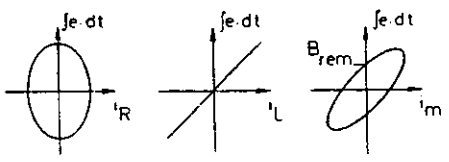

Figure A1.2 First step of calculation

The method is modified by calculation of a new value of i_R and a new value of B_{rem} for each successive value of B_m. For $B = B_m$ we have

$$\hat{i}_R = P_N.0.5.\sqrt{2}/U_N$$

where U_N is the r.m.s. phase-to-earth voltage
P_N is the single-phase power loss associated with B_m

B_{rem} can be estimated with sufficient accuracy from d.c. hysteresis curves for the material used. There is some error in this assessment but the error is small and the results of chopping overvoltage calculations are not very sensitive to this error.

Power losses per phase for a typical transformer are shown in Figure A1.5 for CROS and HRS. From data available from core steel manufacturers typical d.c. hysteresis curves for appropriate peak flux densities are shown in Figure A1.6.

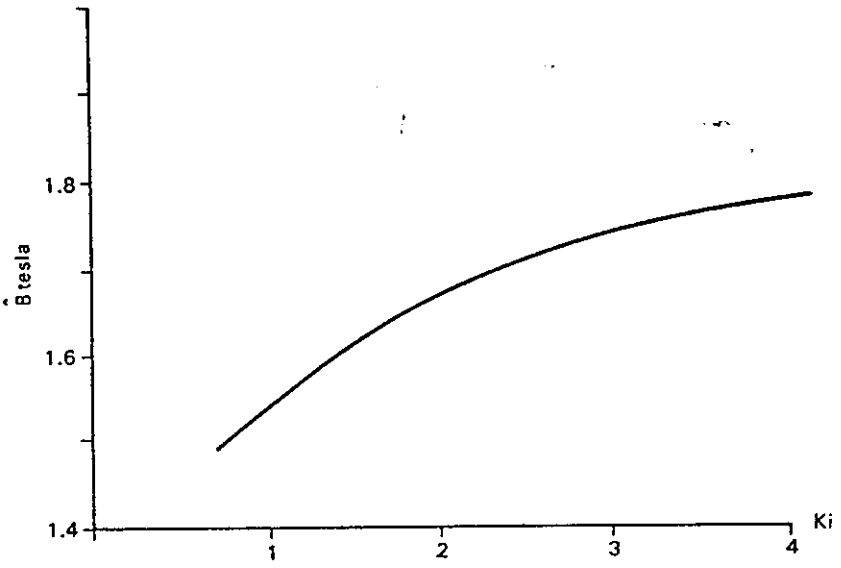

(a) Peak current factor (K_i) for steady-state a.c. excitation to $\hat{B}$

$K_i = \hat{i}/I_m$, where $\hat{i}$ is the peak current at $\hat{B}$ and
I_m is the r.m.s. value of no-load current at $\hat{B}$ = 1.7 T

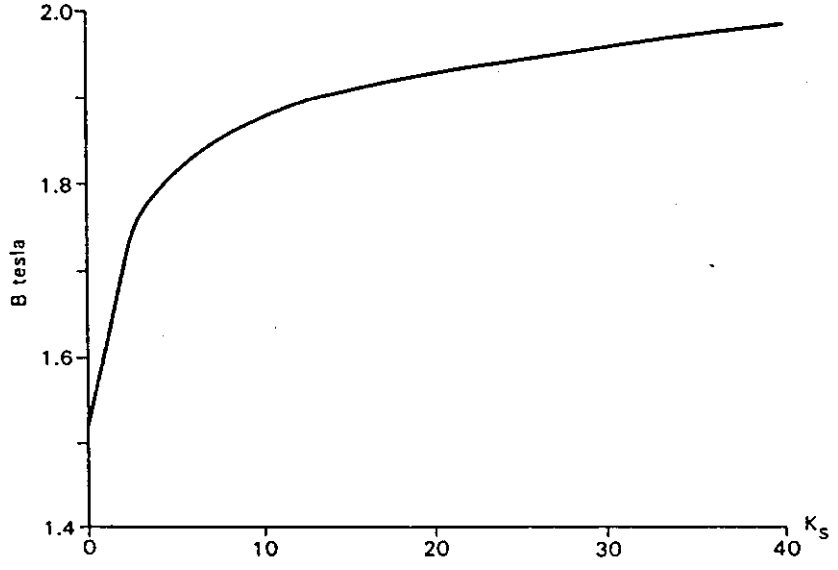

(b) Current factor (K_S) for excitation falling from saturation

$K_S = i/I_m$, where i is the instantaneous current value corresponding to the instantaneous value of B.
I_m is the r.m.s. value of no-load current at $\hat{B}$ = 1.7 T

Figure A1.3 B vs i for CROS cores

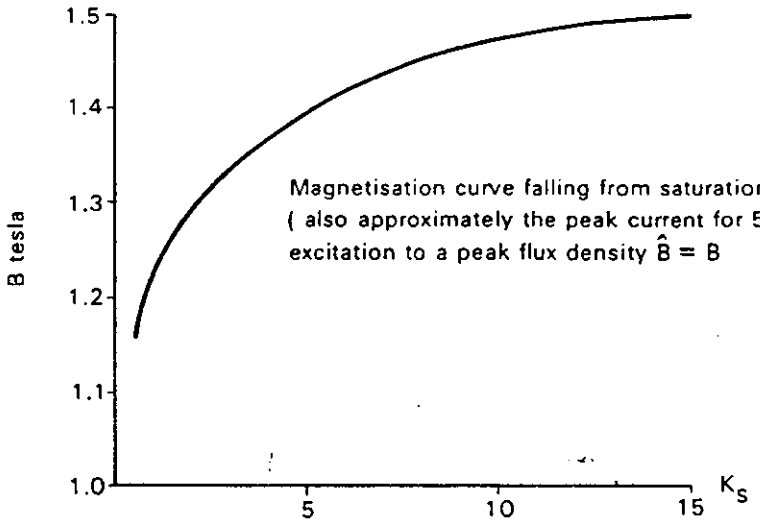

$$K_S = \frac{i_m}{I_m} = \frac{\text{instantaneous value of current}}{\text{r.m.s value of no-load current for excitation to B = 1.3 T}}$$

Figure A1.4 B vs i for HRS cores

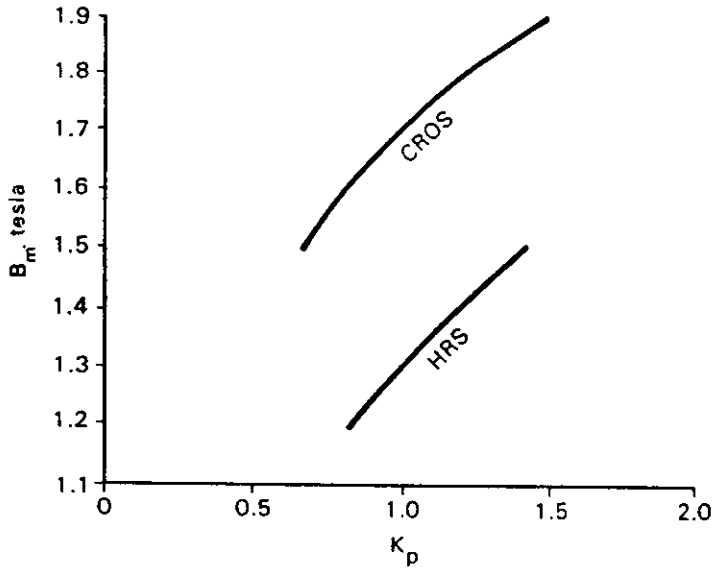

$$K_p = \frac{\text{loss at peak flux density } B_m}{\text{loss at peak flux density 1.7 T (CROS) or 1.3 T (HRS)}}$$

Figure A1.5 Total losses versus B_m for HRS and CROS cores at 50 Hz

The CROS curve in Figure A1.5 is a characteristic of a grade of oriented steel similar to 30M5 and this characteristic has been assumed in the subsequent calculations. Variations in the core steel characteristics for the range of materials currently in use will only slightly change the numerical results in this paper. Similarly the HRS characteristics used are for a typical grade of hot rolled core steel.

The total no-load losses of a transformer are usually known. Information on the distribution of the total loss between eddy loss (frequency dependent) and hysteresis (non-frequency dependent) loss is not readily available for transformers over the range of excitations of interest in this paper. Ref. [A1] suggests that by extrapolating the curve of total loss versus frequency, for frequencies between 25 Hz and 100 Hz, back to zero frequency an effective non-frequency dependent loss of 50 to 60 per cent of the total loss at 50 Hz can be obtained for CROS cores excited in the direction of orientation.

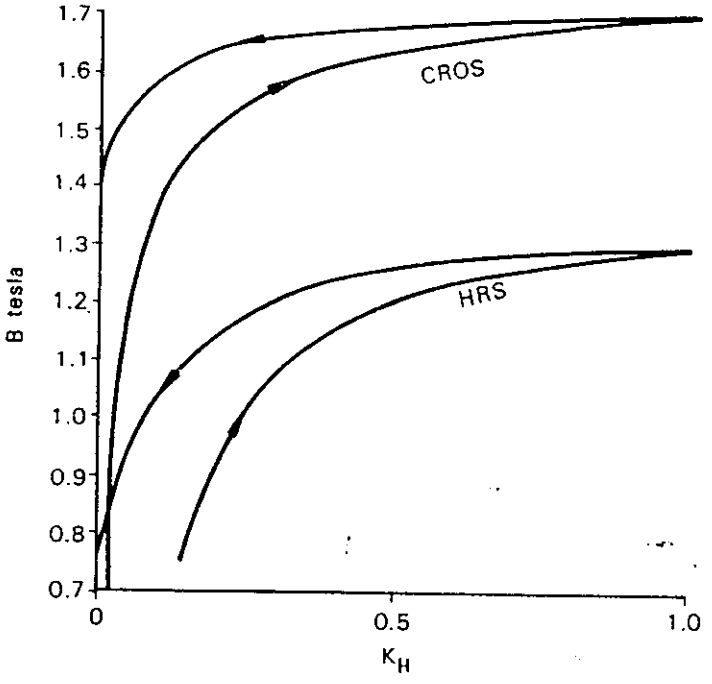

$$K_H = \frac{i_m \text{ at B Tesla}}{i_m \text{ at B = 1.7 T (for CROS) or 1.3 T (for HRS)}}$$

Note: i_m at 1.7 T for CROS ≠ i_m at 1.3 T for HRS

Figure A1.6 Typical d.c. hysteresis curves for CROS and HRS cores

Other publications [A2] suggest a somewhat higher frequency dependent share of the losses. Therefore, the calculations in this paper are done primarily with a ratio of frequency dependent to total losses of 0.5 for CROS cores. A higher proportion of frequency dependent losses will give lower overvoltages. To indicate the sensitivity of the results to this parameter some calculations are done with a ratio of 0.3. Results of the calculations are shown in Figure A1.9.

A1.3 Transformer model for interruption overvoltages

For the purpose of assessing peak overvoltages on interruption without reignition we are interested in the variation of no-load current from its value at interruption to the point at which it changes sign at zero current during which period the magnetic energy is transferred into the circuit capacitance.

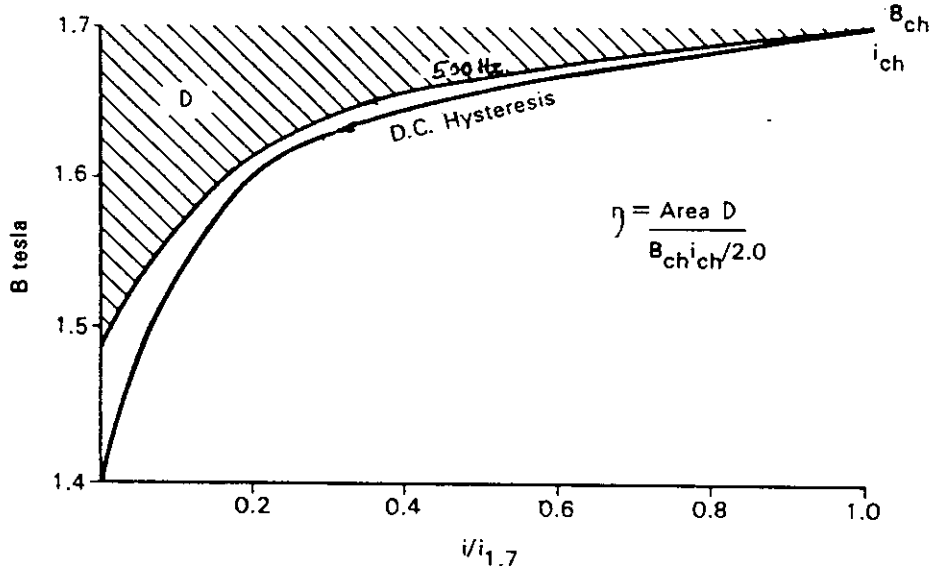

Figure A1.7 Transformer no-load current for falling flux

The B/i curve following interruption will depend upon the rate of change of current. Figure A1.7 shows d.c. hysteresis in comparison with a 500 Hz excitation curve. The maximum energy transferred for example at 500 Hz to the circuit shunt capacitance will be proportional to the shaded area in Figure A1.7. It is useful to define the energy released in terms of an efficiency of release of energy, η. In this paper η is given a special definition. It is defined as the ratio of the energy released to the total energy contained in a lossless linear inductance having a current i_{ch}, flux density B_{ch}, core area and number of turns equal to that of the transformer.

When no-load current is interrupted, the current will fall to zero along a curve (i vs B), which is determined by the inductance, the non-frequency dependent loss and the frequency dependent, 'eddy-current loss'. If the characteristic, flux density (B) versus current (i), between the point of interruption and zero current is considered to be along the d.c. hysteresis curve (non-frequency dependent) (Figure A.1.7), this can be modelled by a non-linear inductance in the region of interest.

$$i(t) = f(B) = f(k \int u dt + B_{ch})$$

This has a characteristic similar to an inductance, L,

where $i(t) = (1/L) \int u dt + i_{ch}$

The characteristic non-frequency dependent loss and pure magnetizing current may therefore be modelled as a non-linear inductance, L_i.

The circuit of a single-phase transformer coil and its effective parallel capacitance, C_t, may then be represented by a parallel combination of
$R - L_i - C_t$, Figure A1.8, where L_i is the non-linear function of the volts-time integral (magnetic flux) mentioned above. For the purposes of assessing chopping overvoltages it is necessary to consider the magnetizing characteristic of a transformer from the point of interruption to the point where i_m in Figure A1.8 becomes zero. R represents eddy current losses and may be taken as the resistance giving an eddy current loss of 0.5 times the total 50 Hz losses.

Thus

$$R = \frac{U_N^2}{0.5 P_L}$$

where U_N is the rated phase-to-earth voltage and
P_L is the loss per phase at 50 Hz

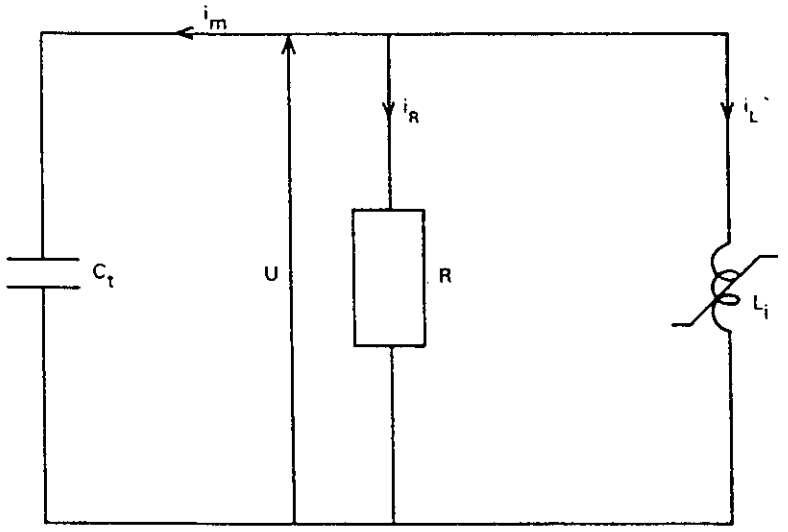

Figure A1.8 Transformer equivalent circuit

For the falling hysteresis curve

$L_f = NA(dB/di)$

where N is number of turns and
A is crossectional area of core

NA may be obtained from the manufacturer or derived from

$$NA = \frac{U_N\sqrt{2}}{\omega B_N}$$

where B_N is the peak flux density corresponding to U_N.

The model has a frequency dependent eddy-current loss characteristic /A3/, and has good accuracy from the point of interruption to the point of zero current and peak voltage, though the accuracy would be less in the following time interval.

The model may be used to calculate the peak voltages obtained for the interruption of a specified transformer. Alternatively, it may be used to derive a set of curves giving values of η for different values of capacitance and different points of current interruption, using the normalized characteristics discussed in Section A1.2.

The calculations can easily be done on a computer to produce the results shown in Figure 5.3.5 of the main report.

Since L_f is non-linear, the RLC circuit calculations have been done by a step-by-step trapezoidal integration method

u_1, u_2 = voltages at start and end of interval Δt respectively

i_{m1}, i_{m2} = capacitor currents at start and end of interval Δt respectively

i_{L1}, 1_{L2} = inductor currents at start and end of interval Δt respectively

i_{m2} at the end of an interval Δt may be obtained as $1_{m2} = (i_{L2} + u_2/R)$

Therefore $i_{m2} = -[i_{L1} + \Delta t(u_2 + u_1)/2L_f + u_2/R]$

but $i_{L1} = -[i_{m1} + u_1/R]$

Therefore $i_{m2} = -[\Delta t(u_2 + u_1)/2L_f + u_2/R - i_{m1} - u_1/R]$ Eq. (A1.1)

where suffix 2 indicates values at the end of Δt and suffix 1 indicates values at the start of Δt.

Since $u_2 = u_1 + \Delta t(i_{m2} + i_{m1})/(2C_t)$

we have also

$$i_{m2} = (u_2 - u_1)\, 2C_t/\Delta t - i_{m1} \qquad \text{Eq. (A1.2)}$$

Therefore combining equations A1.1 and A1.2 gives

$$u_2 = [u_1(2C_t/\Delta t - \Delta t/2L_f + 1/R) + 2\, i_{m1}]/(2C_t/\Delta t + \Delta t/2L_f + 1/R)$$

To a close approximation the value of L_f is given by

$$L_f = NA\ (dB/di_L)_I$$

where $(dB/di_L)_i$ is the slope of the linear section "i" of the hysteresis characteristic.

The characteristic may conveniently be divided into linear steps having small intervals of current. The number of steps may be as large as desired.

Then $$B_2 = B_1 + \frac{\Delta t(u_2 + u_1)}{2NA}$$

where B_1 and B_2 are flux densities at the start and end of interval Δt respectively.

Thus in the interval Δt:

$$L_i = NA(B_2 - B_1)/(i_{L2} - i_{L1})$$

L_i can be determined by an iterative procedure but it is sufficiently accurate to consider L_i as the value obtained from the previously calculated time step currents and flux densities provided that the time step is small. An iterative procedure then need only be used for the first time step of the calculation.

Using this procedure until $i_m = 0$, an efficiency can be calculated as defined in Figure A1.7, i.e.

$$\eta = \frac{2D}{B_{ch} \cdot i_{ch}} \quad \text{(from Figure A1.7)}$$

where $$D = \sum_{i=i_{ch}}^{i=0} \frac{(i_2 + i_1)\cdot(B_2 - B_1)}{2}$$

Figure 5.3.5.a shows values of η for cores having cold reduced oriented steel (CROS), which has been commonly used for power transformers for 25–30 years. Figure 5.3.5.b gives η for hot rolled steel (HRS) cores, which was commonly used in transformer manufacture up to the late 1950s and may exist in some transformers still in service. Other core materials have been introduced in recent years, and for them the same principles may be used to calculate overvoltages following interruption provided that the appropriate core steel characteristics are used.

η is a function of the frequency dependent loss and can be related to an effective frequency $f_{eff} = 1/(2\pi\sqrt{L_e C_t})$ where C_t is the effective capacitance across the winding and L_e may be related to the B/i curve in the interval between interruption and the first current zero in the winding.

E.g. $L_e = NA\cdot(B_{ch} - B_{rem})/i_{ch}$, where B_{rem} is the flux density at zero current on a 50 Hz magnetisation curve falling from B_{ch}, i_{ch}.

B_{rem} would be approximately 0.85 B_{ch} for a typical CROS transformer.
(The value for an HRS core would be approximately 0.5)

Therefore $L_e = 0.15\ NA\ B_{ch}/i_{ch}$ (CROS)
$L_e = 0.5\ NA\ B_{ch}/i_{ch}$ (HRS)

Note that this is an arbitrary definition of L_e which is simply a constant for a particular transformer winding interrupted at B_{ch} and the constant 0.15 (or 0.5) is used solely to relate η to a meaningful frequency which gives an indication of the order of the frequency obtained during the part of the process between interruption and the appearance of the maximum chopping voltage. The essential values of the curves given in Figure 5.3.5 would be unaltered by a different choice of this constant. All the frequencies assigned to the set of curves would
merely be changed by a constant term.

A1.4 Chopping overvoltages in a single-phase transformer

A1.4.1 Steady-state current interruption

At steady-state current interruption the highest possible overvoltages are produced when chopping at peak current. The maximum overvoltages will then be (see Clause 5.3.3, eq. 5.3.15, of the main report):

$$k_a = \sqrt{\frac{\eta\,\gamma\,\alpha\,P_N}{\sqrt{2}\;U_N^2\omega_1 C_t}} = f\left\{\frac{U_N^2 C_t \omega_1}{P_N\,\alpha}\;;\;\eta\,\gamma\right\}$$

where $\gamma = \frac{i_p}{I_m}$ = form factor

U_N = rated voltage of single-phase transformer (r.m.s. value)
α = ratio magnetizing current/rated current (both r.m.s. value)
P_N = rated power of single-phase transformer
$u_o = U_N\sqrt{2}$ = rated crest voltage of single-phase transformer
I_m = r.m.s. value of magnetizing current
$\omega_1 = 2\pi f_1$ = angular power frequency
C_t = effective parallel capacitance
η = magnetic efficiency (from Figure 5.3.4)

The overvoltage factor is thus a function of the parameters

$$\frac{U_N^2 C_t\, f_1}{P_N \alpha} \quad \textit{and} \quad \eta\,\gamma$$

of which the first one is determined by the rated quantities of the transformer and the second by the B/H characteristic of the core.

The form factor $\gamma = i_p/I_m$ is dependent on the shape of the B/i characteristic and hence on the peak flux density at interruption. The B/i characteristic shape has been found to be substantially the same for a given core material type over the whole of the range of transformers under consideration.

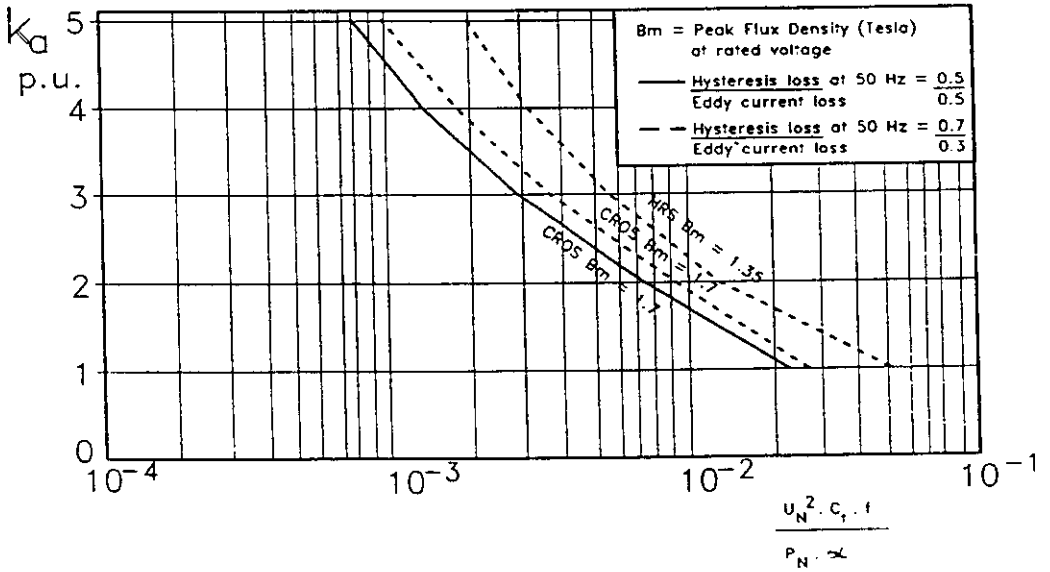

Figure A1.9 Interruption of single-phase transformer no-load current at peak value during steady-state excitation

Figure A1.9 gives the peak overvoltage (phase-to-earth) versus the parameter $(f \cdot U_N^2 \cdot C_1)/(P_N \cdot \alpha)$ for interruptions at the peak of the no-load current during a steady state a.c. excitation. Values are given for transformers with CROS cores having a peak flux density of 1.7 T and transformers with HRS cores having a peak flux density of 1.35 T at rated voltage. The ratio of eddy-current loss to the total loss at 50 Hz for these transformers is assumed to be 0.5 and 0.3 respectively as discussed in Section A1.2. An additional curve is given where this ratio is 0.3 for transformers with CROS cores and a peak flux density of 1.7 T at rated voltage.

Note: The rather high theoretical overvoltages indicated from the Figure are very improbable in actual operation due to low probability of current chopping at the peak value. Further if such a chop should occur it must be at short contact gap and therefore most likely limited by reignitions.

A1.4.2 Inrush current interruption

Transformer no-load currents may also be interrupted immediately after energization, either by maloperation of equipment or by the appearance of a fault on one phase at the time of energization. In this situation the possible inrush currents are large, up to several times the rated full load current of the transformer and a significant transient may persist for tens of seconds in large transformers. It is necessary to estimate the possible level of current which may be chopped by the circuit breaker. Calculations can then be done similar to those used for steady-state calculations.
The overvoltage factor will be (see Clause 5.3 of Chapter 5):

$$k_a = \sqrt{\left(\frac{u_c}{u_0}\right)^2 + \frac{\eta\, i_{ch} B_{ch}}{u_0 \omega_1 C_1 B_m}}$$

where $u_c \approx u_0$ when the peak current is much higher than the breaker chopping level, i_{ch}.

In Figure A1.10 examples of calculation of overvoltages are given for transformers with CROS cores. Curve A is the same as the steady-state curve in Figure A1.9, which means current peak chopping at B = 1.7 T and 0.5 eddy current/hysteresis loss ratio. Chopping currents are of the order 1 A to 10 A. To chop at B = 1.8 T the chopping level must be about three times as high, which seems possible at least for low magnetizing currents, while for B = 1.9 T the chopping level must be about 100 times the peak current at 1.7 T. Such extreme chopping levels are not realistic.

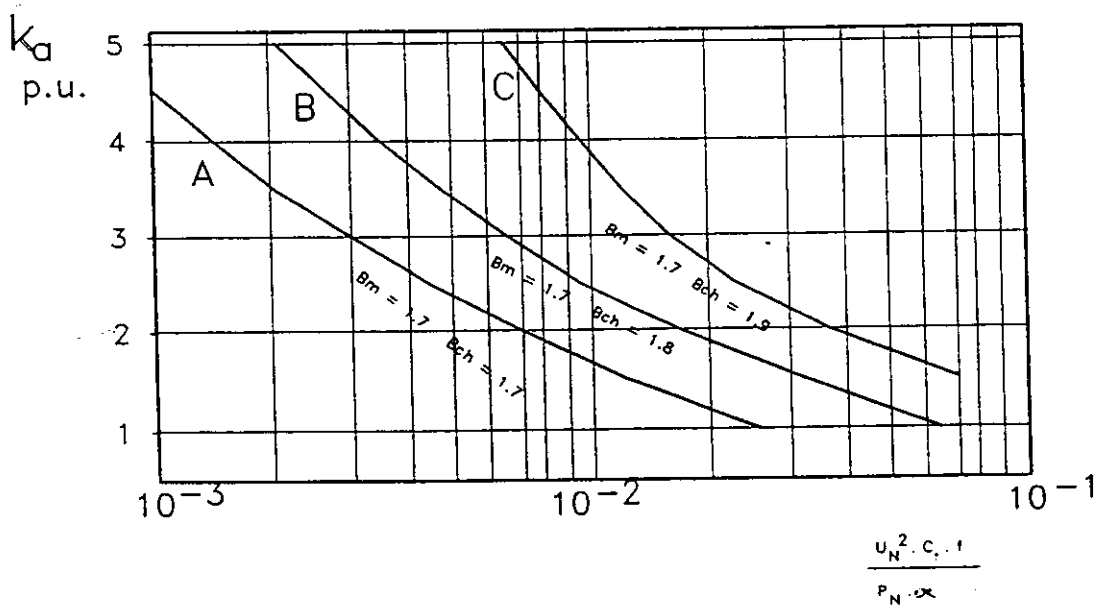

Figure A1.10 **Interruption of single-phase transformer no-load current during inrush conditions**

A1.5 References in Appendix 1

A1. Brailsford F., Fogg R.:
Anomalous iron losses in Cold Reduced Grain Oriented Transformer Steel.
Proc. IEE., Vol. 111, No. 8, August 1964.

A2. Lavers J.D., Biringer P.P., Hollitscher H.: The Effect of third harmonic flux distortion on the core losses in thin magnetic steel laminations.
IEEE Trans., Vol. PAS-96, No. 6, Nov/Dec 1977.

A3. Swift G.W.:
Power transformer core behaviour under transient conditions. IEEE Trans. Paper 71 TP 88-PWR, 1971.

A4. Colombo E., Santagostino G.:
Results of the enquiries on actual network conditions when switching magnetising and small inductive currents and on transformer and shunt saturation characteristics. Electra No. 94, May 1984.

A5. Talukdar S.N., Dickson J.K., Dugan R.C., Sprinzen M.J., Lenda C.J.:
On Modelling transformer and reactor saturation characteristics for digital and analog studies.
IEEE Trans., PAS-94(1975) p. 612-621.

APPENDIX 2

THREE-PHASE TRANSFORMERS

by D. Boyle

Interphase effects in three-phase transformers where the phases are magnetically coupled by multi-limb cores or delta windings will modify the responses obtained at no-load current-interruption. There is some possibility of an increase in overvoltage.

(a) Star connected transformers with earthed neutral

Considering the interruption of currents in a star connected transformer with a delta tertiary winding, Figure A2.1(a). The 132 kV winding and the delta are shown but not the secondary winding, for simplicity. The most severe case would be a second phase to clear at peak current in that phase. An overvoltage will appear on the already opened first phase to clear which is the sum of the instantaneous value of power frequency voltage present on that phase at the time of interruption of the second phase and an induced transient voltage approximately equal to the switching transient voltage appearing on the second phase to clear. Figure A2.1 shows the result of a computer calculation which illustrates this. It should be noted that no-load currents of a three-phase transformer with interphase coupling will exhibit subsidiary peaks and this is evident in the shape of the current on phase A which falls after interruption of phase B before rising again to a peak at 5 ms.

It can be seen that the maximum voltage on the first phase will be approximately $U_N\sqrt{3}/2 + U_{ch}$ where U_N is the peak of the 50 Hz induced voltage and U_{ch} is the peak transient voltage on the second phase to clear. This is, however, an unlikely condition requiring chopping of the second phase current at 3 ms or later after the first phase and then requiring a chopping at peak current on the second phase.

Figure A2.2 shows a calculated response for single-phase transformer of the same rating for comparison. The single phase case shows a higher chopping overvoltage than the three-phase case.

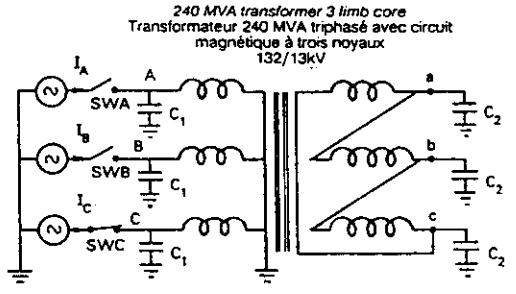

(a) *Circuit diagram/circuit*

Leakage reactance = 31% on rating
Résistance de fuite = 31% du nominal
C_1 = 10 nF ; C_2 = 40 nF
SWA opens at 5 ms ; SWB opens at 1.67 ms ; SWC remains closed
L'interrupteur SWA s'ouvre à 5 ms ; l'interrupteur SWB s'ouvre à 1,67 ms ; l'interrupteur SWC reste fermé.

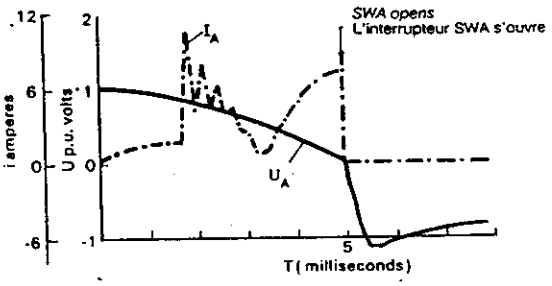

(b) *Voltage to earth at A (U_A) and SWA current (I_A)*
Tension à la terre en A (U_A) et courant traversant SWA (I_A)

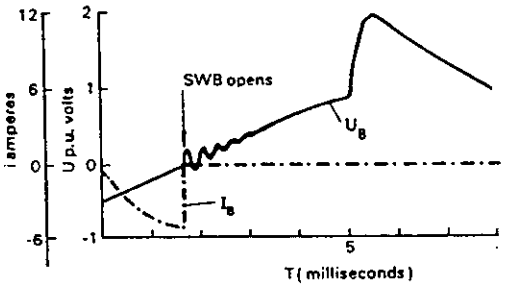

(c) *Voltage to earth at B (U_B) and SWB current (I_B)*
Tension à la terre en B (U_B) et courant traversant SWB (I_B)

Figure A2.1 Three-phase transformer current interruption (1st and 2nd pole-to-clear only shown)

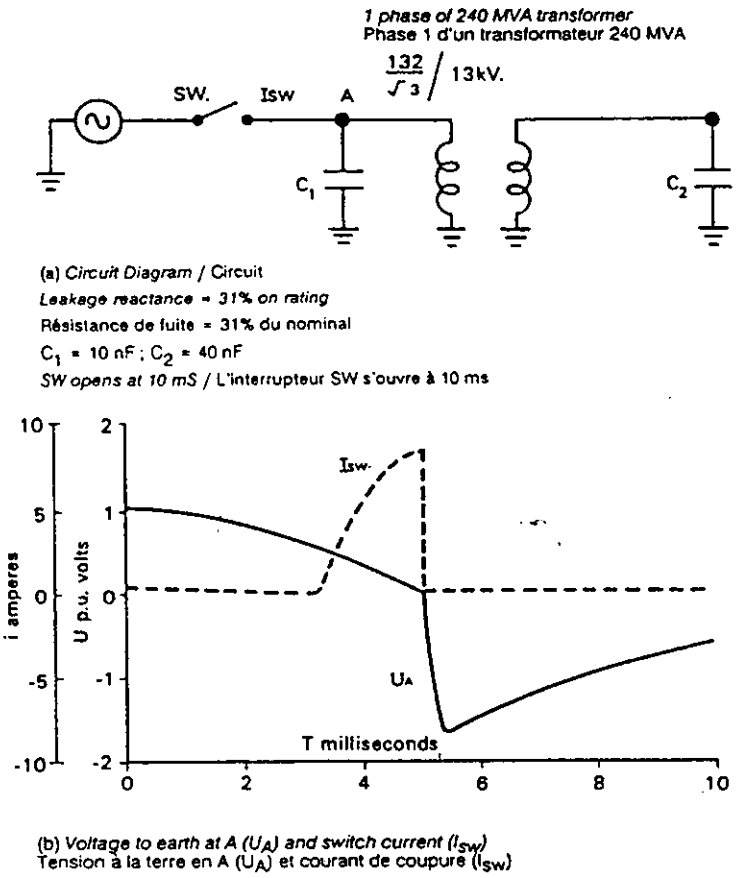

Figure A2.2 Single-phase transformer current interruptions (no interphase coupling)

(b) Delta connected transformers

For an unloaded three-phase bank consisting of 3 single-phase transformers connected in delta/star and supplied from the delta side, the maximum magnetic energy will be stored in the three-phase transformer when the current and flux density in one winding is at its peak value. In the steady state the currents in the other two windings at that moment will be very low because of the non-linear characteristic. For example, in a transformer having a peak flux density of 1.7 tesla in one limb of a CROS core the other phases will have instantaneous values of flux density of 0.85 tesla at that moment when energized from a balanced supply voltage. Examination of Figure A1.6 of Appendix 1 indicates that the current in the latter two windings would be only of the order of 3 % of the value in the first winding. It may thus be presumed, with an insignificantly small error, that the current in the two lines connected to the winding carrying the large current is the same as the current in that winding.

Hence on simultaneous interruptions of the three windings the energy released will be that stored in the winding at peak flux density and will be transferred to the effective capacitance across that winding. The resulting overvoltage can then be estimated by the method described in Section 5.3 bearing in mind that the voltage to earth will be half the calculated voltage across the winding as stated in Section 4.

If the transformer has a single multi-limb core the shape of the steady state magnetizing current curve is more complicated due to interphase coupling through the core. This can be studied if required by computer calculations on a full model of the transformer. But the overvoltages will not be significantly different from those obtained by use of the parameters discussed in Section 5.3.

APPENDIX 3

RESULTS OF A PREVIOUS CIGRE STUDY

Former CIGRE Working Group No. 3.2 made a study of no-load transformer switching overvoltages in 1967. See ref [A6] below and [22] of Chapter 5. They used a magnetic efficiency, η_m, defined as the ratio of released energy to actually stored energy at peak magnetizing current. (This η_m is thus different from the η used in this report which is related to the energy stored in a linear inductance with the same core area and number of turns.)

The overvoltages was then calculated from:

$$\frac{1}{2}Cu_m^2 = \eta_m W_m$$

where

$$W_m = \frac{1}{2}L(I_m\sqrt{2})^2 = \frac{U_m I_m}{\omega\sqrt{3}}$$

I_m = r.m.s. magnetizing current (peak value/$\sqrt{2}$)
U_N = rated voltage (phase-to-phase)
C = parallel capacitance

Maximum overvoltages at steady-state current switching are produced when peak current is chopped, giving:

$$k_{max} = \sqrt{\frac{\eta_m I_m \sqrt{3}}{\omega C U_N}}$$

This is identical to the expressions in Clause 5.3.3 if the form factor is set to $\gamma = \sqrt{2}$ in eq. 5.3.15. and observing that U_N here is phase-to-phase voltage.

WG No. 3.2 calculated expected maximum overvoltages for transformers from three different manufacturers. The results are given in Figure A.3.1. All the transformers had CROS cores with a characteristic approximately equal to the one used in Appendix 1.

The value of η_m used in the calculations was η_m = 0.2 to 0.4, which thus is higher than the η-values obtained from Figure 5.3.5. as expected due to the difference in definitions.

For some of the transformers (Nos 1 to 25) data have been available to permit calculation with the method proposed in this report assuming a form factor
δ = 2.5. Recalculating the maximum overvoltages using the curves in Figure 5.3.5 gives lower overvoltages than the values in Figure A.3.1. with a factor 0.7 to 0.9, in spite of the form factor probably being on the high side. This may partly be due to that eddy current losses was not taken into account in the WG 3.2 calculations.

The new recalculated overvoltage factors as function of the chop parameter i.e.:

$$k_a = f\left(\frac{C_t U_N^2}{\alpha P_N}\right)$$

have been inserted into Figure 5.3.11.

The values fit well with the Panek and Boyle curves and support the conclusion that dangerous overvoltages cannot be generated at interruption of no-load steady-state current.

It should be observed that no external capacitance (C_x) has been taken into account in the calculations, therefore actual overvoltages in the field could be expected to be still lower.

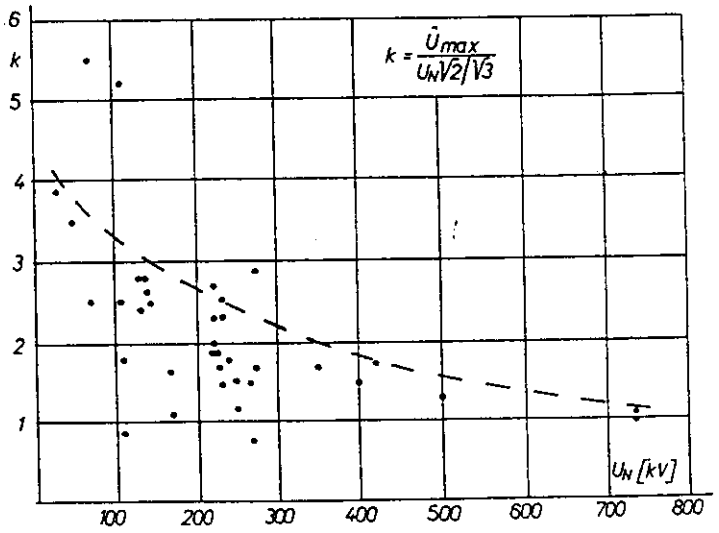

Figure A3.1 Max overvoltage factors when interrupting transformer magnetizing current (From CIGRE-report 1968: 13-01)

Reference:

A6. CIGRE SC 13 (Meyer, Baltensperger): Progress report of Study Committee No. 3 (High-voltage circuit-breakers), CIGRE-report 1968:13-01.

Appendix 4

INTERACTION BETWEEN PHASES IN THREE-PHASE REACTOR SWITCHING

Part 1: Grounded reactors

by

W.M.C. VAN DEN HEUVEL and B.C. PAPADIAS

ABSTRACT

Interruption phenomena after current chopping in three-phase reactor circuits are complicated by the interaction between the separate phases. This interaction is due to capacitive and/or inductive interphase couplings. At the moment of second and third pole clearance the transients in the foregoing interrupted phases are often not yet damped out. This fact complicates the picture furthermore.

This first Part I (Appendix 4) gives a summary of the occurring phenomena and a general treatment of single-phase and three-phase star-connected inductances with solid or low-impedance inductive grounding of the neutral.

Capacitive as well as inductive couplings are studied. Attention is paid to the possible maxima in the recovery voltages. This part ends with a compilation of all initial conditions and recovery voltage expressions to ease calculation of the possible occurring overvoltages.

A second part, Part II (Appendix 5), deals with ungrounded, star- or delta-connected inductances.

A4.1 INTRODUCTION

It is well known that interruption of small inductive currents can introduce high overvoltages due to chopping of the current before or after its natural zero. A vast amount of literature is published on this subject, see e.g. the list of references to Chapters 1 to 6. Most of the fundamental work is directed to single phase circuits for obvious reasons: current chopping, overvoltages and reignition phenomena are extremely complicated. Three-phase interactions confuse the issue still more and make it less approachable for numerical evidence.

But practical circuits nearly always are three-phase networks. Therefore not only testing but also calculation of overvoltages in inductive current interruption should be directed to three phases.

This Appendix collects the theoretical work already done in this specific field and aims to give a general treatment of the interactions in disconnecting networks containing three-phase reactors. Capacitive as well as inductive couplings are involved and a low damping is assumed. Therefore the results are also applicable to stalled motors. Interruption of transformers in no-load has the same theoretical backgrounds but overvoltages are considerably lower due to the complicated damping by iron losses [3, 4, Appendix 1].

This part covers reactors with grounded neutral. In the second part (Appendix 5) ungrounded inductances in star or delta connection will be dealt with.

A4.1.1 Current chopping level

The chopping level in vacuum circuit-breakers is mainly determined by the kind of contact material. It is of the order of 5 to 10 A and there is only a weak dependency on the capacitance which can be seen in parallel to the breaker [6].
In other breakers the main reason for current chopping is arc instability due to the negative slope of the i(u) - characteristic of the circuit-breaker arc. Here the chopping levels reach between one and some tens of amps. This level depends on the arc extinguishing medium and mechanism and also on the circuitry around the breaker.

Especially C_p, the capacitance seen in parallel to the breaker, may have an essential influence. A number of authors [6, 7, 8, 9] published a linear relationship between the chopping current i_0 and the square root of C_p:

$$i_0 = \kappa\sqrt{C_p} \qquad \text{(A4.1.1)}$$

Practical κ-values vary from 1.10^4 (for certain medium voltage SF_6-breakers) to 20.10^4 (for some VHV breakers), see Chapter 2.

A4.1.2 Survey of phenomena in a single phase circuit

A survey of idealized chopping phenomena occurring in a single phase circuit with considerable damping is given in Figure A4.1.1. No reignitions are indicated here.The expression for the TRV (= transient recovery voltage) is the same as for the three phase reactor with grounded neutral without any coupling, as treated in section A4.4.1, equation (A4.4.4). In this case the highest overvoltage across the inductive load is the suppression peak arising directly after current chopping. The highest voltage across the breaker contacts is the recovery peak after polarity change of the TRV.

If a reignition occurs a main frequency current may start to flow again following the same steady-state loop as before. The transition to this state proceeds via one or more h.f. oscillations, superimposed upon the initial rate of rise of the current [16]. The most important h.f. transient is the "second parallel oscillation" through which the source side and load side capacitances (C_s, C_g and C_l) balance their charges through their series inductances. Its frequency is typically of the order of (some) hundred kHz.

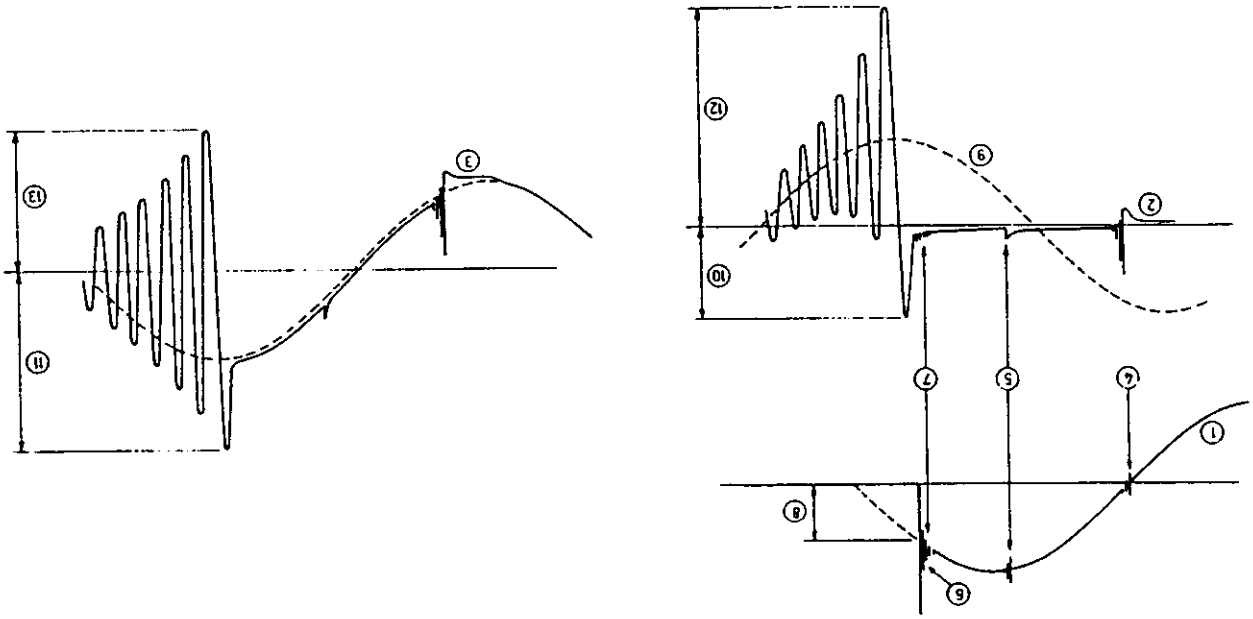

Figure A4.1.1 Survey of chopping phenomena in a single-phase circuit

1 current to interrupt
2 voltage across circuit-breaker (c.b.)
3 voltage across inductive load
4 failed interruption due to short contact distance
5 influence of arc voltage
6/7 instability oscillation leading to current chopping
8 chopping level
9 main voltage
10/11 first max. across c.b./ind. load - "suppression peak"
12/13 second max. across c.b./ind.load - "recovery peak"

Reignitions may occur during voltage rise to the suppression peak as well as to the recovery peak. In the first case they reduce the overvoltage in the network because the reignited current has the same polarity as before and will normally be chopped again at a lower level (Figure A4.1.2). Reignition in the second case may cause a new current loop followed by new chopping and an overvoltage across the load which may be higher than before, even if no chopping occurred at all, see Figure A4.1.3. In both cases the transient h.f. oscillating current immediately following a reignition may be interrupted by the breaker in one of its current zeros. Thereafter new voltage rise and reignition is possible. Repeated reignitions during increasing current-to-interrupt may occur at successively higher voltages. This phenomenon is called voltage escalation [10, 11, 17].

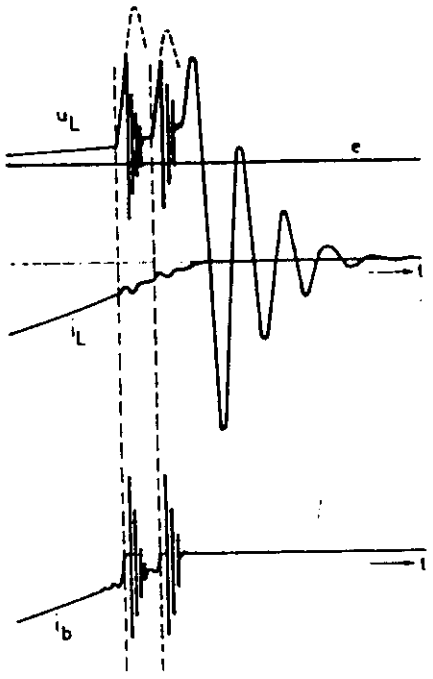

Figure A4.1.2
Reignitions before suppression peak not leading to new current flow

U_L voltage across the terminals,
i_L current through inductive load
e main voltage
i_b current through breaker

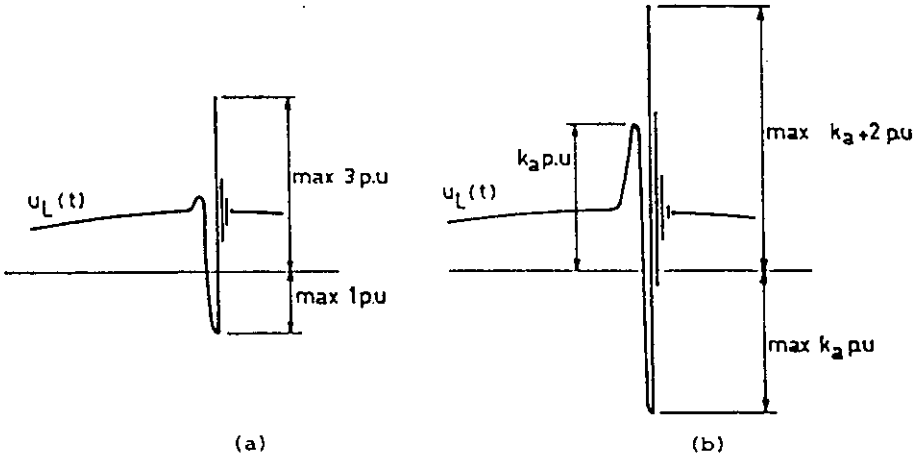

Figure A4.1.3 Maximum reignition voltages without (a) and with (b) current chopping

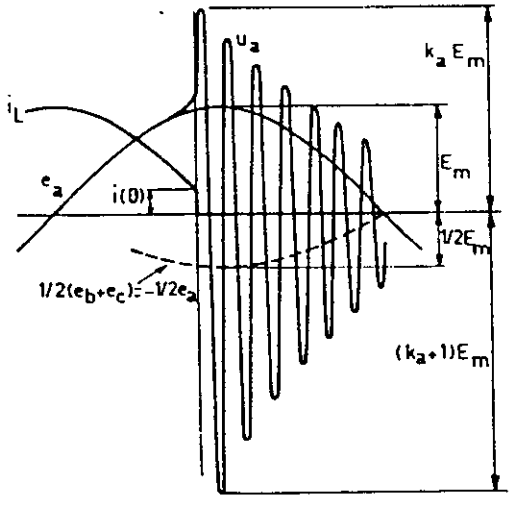

Figure A4.1.4
Recovery voltage after first pole clearance
Ungrounded neutral

A4.1.3. Additional phenomena in three-phase circuits

In three-phase circuits the calculation of TRV's is much more complicated because of the greater number of circuit elements, the inductive and/or capacitive interphase couplings and the different initial conditions. Moreover there are some additional phenomena which are not observed in single phase networks:

a) A current chopping in the first phase to interrupt, followed by a reignition at a high value of the suppression peak, introduces a h.f. oscillating current as in the single phase case. All capacitive and inductive elements of the circuitry in the direct vicinity of the circuit-breaker are involved in the energy exchange of this oscillation. So in the three-phase condition a part of the current may flow through the other breaker poles, causing a h.f. oscillation superimposed on the momentary main frequency current through these poles. The resulting current may pass zero and consequently be interrupted although a relatively higher current is flowing through the inductive load. This phenomenon is called virtual current chopping [12, 13]. Up to now it was only observed in vacuum breakers at very short contact distance.

b) The h.f. oscillation after a reignition in the last phase to interrupt is also fed from the capacitances of the three phases. Therefore h.f. voltages may be generated in the other phases superimposed on the momentary value of the TRV in these phases. This momentary value may even be a high recovery peak viz. in case of an unearthed reactor. This reignition transfer of overvoltages was treated in more detail in Chapter 2. See also [14].

c) After interruption of the first phase of an ungrounded load the potential of the star connection jumps to the half sum of the second and third phase voltage. Therefore the TRV between the entrance of the first disconnected load and ground does not oscillate around zero, as in Figure A4.1.1., but around $1/2(e_2 + e_3)$ as given in Figure A4.1.4. Now the recovery peak is the highest overvoltage to the circuit-breaker as well as to the load terminal. Mathematical expressions were given in [14]. A similar effect will be observed in a non-solidly grounded load but the main frequency component in the TRV will be smaller. Inductive coupling between phases will cause an opposite consequence; see section A4.4.3.1 and A4.4.4.1.

d) After clearance of the second and third pole in the case of ungrounded load the interrupted circuit is completely disconnected from earth except by its ground-capacitances. Therefore a d.c. potential to ground may be left in this circuit. It was shown that a high d.c. potential can be caused by non-simultaneous current chopping in the second and third phase [14].

Calculations of the transient recovery voltages and more details on the additional three-phase phenomena are given in clause A4.4 and Part II (Appendix 5). Many of the treated effects are depending on the reactor characteristics and the way of grounding of the neutral.

A4.2. REACTOR CHARACTERISTICS

Due to the interaction between phases in three-phase interruption of a reactor the recovery voltage and other transients are affected by both the type of the core and the winding connections of the inductive three-phase circuit. The reactor windings are commonly star connected, with grounded or ungrounded neutral.

When star connected reactors with independent phases (five-legged or shell-type cores) have solidly earthed neutrals, interruption of each phase can be considered separately, provided line-to-line capacitances are small compared to line-to-ground capacitances.

Reactors connected through a tertiary m.v. winding of a transformer are often unearthed.

A4.2.1. Reactors with earthed neutral

Directly connected shunt reactors in high voltage networks are usually covered by cases 1 and 2 of Table A4.2.1.

In the case of $X_0/X_1 = 1$, the independence of the phase magnetic circuits calls for negligible inductive interaction between phases, so that the mutual inductance $M \approx 0$ and $L_0 \approx L_1$. The three-phase interruption can usually be treated as three successive interruptions, provided that the capacitive interphase coupling is also negligible. This may not be always the case for a bank of three single phase reactors, since there may still exist a small capacitive coupling between the connections of the phases, but its influence could be disregarded (section A4.4.1.).

In a 5-legged reactor, or a shell-type reactor a certain inductive coupling between phases may exist. Energy transfer between phases may then take place, although there is no evidence that such an energy transfer has resulted in an appreciable increase of the overvoltages. All experience gained so far support the view that this case may be treated as three consecutive single phase interruptions (section A4.4.1).

The case of $X_0/X_1 \neq 1$ is commonly met in three-legged reactors. The inductive coupling is considerable now with a typical value of M of the order of 2/7 L, or 2/3 L_0, so that $X_0/X_1 \approx 0{,}3$. (M is taken as positive). Examples of interphase influences are given in Figures A4.4.14, A4.4.20 and A4.4.21.

A4.2.2. Unearthed reactors

In some cases the reactors are not earthed, or not solidly earthed at their neutral. This is particularly true for the m.v. reactors connected through tertiary windings of high voltage transformers or autotransformers, where the reactor neutrals are often left unearthed to avoid the flow of zero-sequence fault currents. In that case the ratio X_0/X_1 is practically infinite, although in fact there is always an indirect neutral earthing through the reactor capacitance to ground.

Due to the intense interaction effects appearing in unearthed reactors, the whole pattern of switching phenomena becomes still more complicated than previously. The detailed treatment of these phenomena is the main objective of Part II (Appendix 5).

Table A4.2.1 Typical reactor characteristics and interaction phenomena

Impedance ratio	Reactor type	Possible interaction	
		First order influence	Second order influence
CASE 1: $\frac{X_o}{X_1} = 1$	Earthed reactors no capacitive coupling i Single phase reactor ii 5-legged reactor iii Shell type reactor		a) Transfer of reignition transients b) Transfer of chopping overvoltages
CASE 2 $\frac{X_o}{X_1} = 1$ $\frac{X_o}{X_1} \neq 1$	Earthed reactor As case 1 but with capacitive interphase coupling i 3-legged reactors ii Reactor earthed neutral ("4-legged reactors")	a) Transfer of chopping overvoltages	b) Transfer of reignition transients
CASE 3 $\frac{X_o}{X_1} = \infty$	Unearthed reactors Any type of core	a) Transfer of chopping overvoltages b) Transfer of reignition transients	Common d.c. voltage shift

Independent of the reactor connection, current chopping in each consecutive phase will initiate transient oscillations. For iron–core reactors the frequency is typically a few kHz, while it may reach 50 kHz for air–core reactors. For each interrupting case in turn an equivalent parallel RLC–circuit may be defined which can be used for simulation of the interruption process. The components R, L and C of such equivalent circuits can be obtained from corresponding positive and zero sequence values for the reactor. Frequency dependence must also be considered. The positive–sequence values of the inductance at a frequency of a few kHz will typically be 5–10 per cent lower than the corresponding power frequency values. This will probably also be true for the zero–sequence values. A good approximation may thus be obtained by use of the power frequency values. Positive and zero sequence power frequency capacitance and resistance values are generally not known.

Neutral grounding and the core type of three–phase reactors determine the interaction between phases. This asymmetry is characterized by the ratio X_0/X_1, of the zero sequence to positive–sequence reactance of the reactor circuit, which is in general equal or less than unity for directly earthed and very large (practically infinite) for unearthed reactors. There also exist some reactors equipped with a zero–sequence fourth winding, connected between neutral and ground, with the purpose of increasing the zero–sequence impedance. In this case, the ratio X_0/X_1 varies usually between 1 and 2.

The typical reactor cases are tabulated in Table A4.2.1, with the associated interaction phenomena.

A4.3. ANALYTIC FORMULATION

All calculations in the next clauses are directed to a three–phase reactor circuit with grounded neutral (Clause A4.4) or isolated neutral (Part II, Appendix 5). In all TRV–calculations the following simplifications were accepted:

– The circuit is perfectly symmetrical in all its elements;

– The source side may be represented by an ideal three–phase voltage source in star connection with solidly grounded neutral;

– All dampings are neglected;

– The reactor is represented by three star–connected linear inductances with or without magnetic interphase couplings and with capacitances to ground;

– The connection between circuit–breaker and reactor is represented by lumped capacitances. Their inductances are included in the reactor representation;

– The average arc voltage is at least one order of magnitude smaller than the main voltage. Therefore its influence on the magnitude of the current–to–interrupt is negligible;

– All transient–oscillation frequencies are high compared to the main frequency.

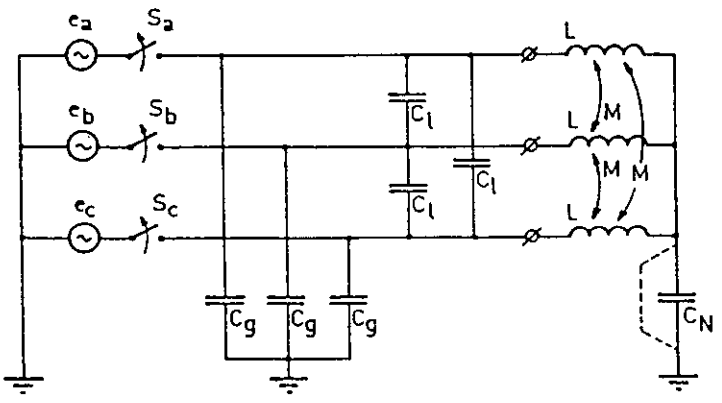

Figure A4.3.1 General representation of the three phase symmetrical reactor circuit

$e_{a,b,c}$: main voltages
$S_{a,b,c}$: c.b. poles
C_g, C_l : line–to–ground, line–to–line capacitance of the reactor and the connection between c.b. and load
C_N: neutral to ground capacitance
L: total inductance of each single–phase reactor
M: mutual inductance between to reactors

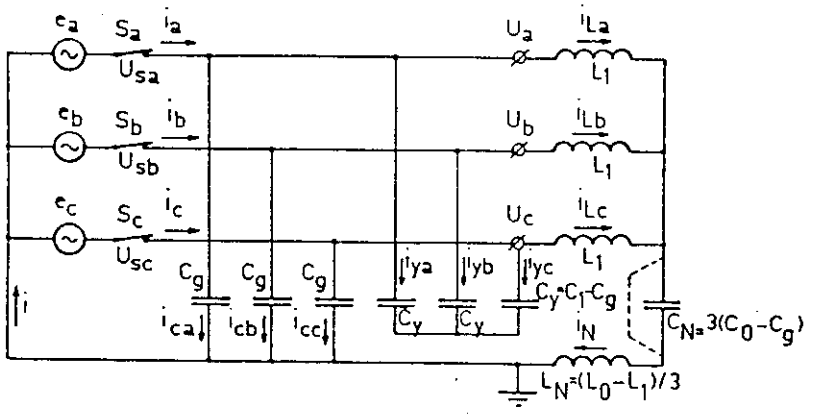

Figure A4.3.2 General representation with transferred components

As Figure A4.3.1, with transferred (positive and zero sequence) components

$u_{a,b,c}$ are the voltages between the reactor terminal and ground

$C_1 = C_g + 3C_\ell$; $C_0 = 1/3\ C_N$; $L_0 = L-2M$; $L_1 = L+M$ (M is taken as positive)

The general representation of this model circuit is given in Figure A4.3.1. Depending on the configuration under consideration the indicated elements have zero or finite values.

Expressing the circuit parameters in terms of their positive and zero-sequence components the model circuit of Figure A4.3.2 is obtained. For very short line connections the reactor ground capacitances are dominating. Then $C_1 = C_g = 1/3\ C_N$ and $C_0 = 2C_g$ may be introduced. Line-to-line capacitances may be neglected in this situation.

If cables are used for the connection between breaker and reactor, then $C_N << C_g$. Belt type cables have line-to-line capacitance with $C_\ell \approx 1/3\ C_g$. So $C_1 \approx 2\ C_0$. Shielded type cables have no capacitive coupling: $C_1 \approx C_0$. Neutral-to-ground capacitance C_N may be shorted by low-impedance grounding of the neutral.

For single-phase reactors M = 0, so $L_1 = L_0 = L$. Shell-type and 5-legged reactors have some mutual inductance but here also $L_1 = L_0 = L$ in first approximation.

Reactors on 3-legged iron cores with their relatively long air gaps have a zero sequence impedance which may not be neglected: $L_0 \approx 0.3\ L_1$. So only in the case of a 3-legged reactor with ungrounded neutral the impedance Z_N consists of C_N and $L_N = 1/3\ (L_0 - L_1)$ in series. In this case C_N will be rejected by grounding the neutral ($C_N = \infty$) and then only L_N is left. In all other cases $L_N \approx 0$.

All currents and voltages in the following chapters are taken positive in the direction indicated in Figure A4.3.2. All TRV's u_a, u_b and u_c are voltages against earth.

Calculation methods using Laplace-transformation and symmetrical impedance components are amply treated by Slamecka et al [15].

A4.4. REACTORS WITH GROUNDED NEUTRAL ($C_N = \infty$)

A4.4.1. No capacitive or inductive coupling

($C_1 = 0$; $C_0 = C_1 = C_g = C$; $M = 0$; $L_1 = L$; $L_N = 0$)

A4.4.1.1. Recovery voltage after current chopping without reignition

Three solidly grounded reactors without any interphase coupling represent the most simple case. Each phase can essentially be regarded as a single phase inductive load with its parallel capacitance (Fig A4.4.1). Interruptions succeed each 60 el. degrees. They may be followed by reignitions until the contact gap is sufficiently large. There is experimental evidence that the overvoltages due to chopping grow higher with increasing contact distance [7]. So the highest overvoltages are to be expected in the last phase to interrupt.

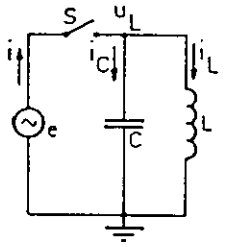

Figure A4.4.1 Single-phase representation of grounded reactor without interphase coupling

In Figure A4.4.1 a source phase voltage

$$e = E_m \cos(\omega t + \phi)$$

will drive a current $i = I_m \sin(\omega t + \phi)$ through the breaker S. Here

$$I_m = \frac{E_m}{\omega L}(1 - \omega^2 LC) \qquad \text{(A4.4.1)}$$

Further $i_L = I_{mL} \sin(\omega t + \phi)$ and $I_{mL} = E_m/\omega L$, because the arc voltage is neglected.
At t = 0 the current will chop at a momentary value

$$i(0) = I_0 \sin\phi \approx I_{mL}\sin\phi = I_L(0) \qquad \text{(A4.4.2)}$$

while the main voltage is

$$e(0) = E_0 = E_m \cos\phi \approx u_L(0) \qquad \text{(A4.4.3)}$$

After chopping u_L develops as

$$u_L(t) = e^{-\frac{t}{\tau}} U_m \cos(\omega_t t + \psi) \qquad \text{(A4.4.4)}$$

with

$$U_m = \sqrt{[u_L(0)]^2 + [i_L(0)\,\omega_t L]^2} \qquad \text{(A4.4.5)}$$

$$\sin\psi = \frac{i_L(0)\,\omega_t L}{U_m} \quad \textit{and} \quad \cos\psi = \frac{u_L(0)}{U_m} \qquad \text{A4.4.6)}$$

$$\omega_t^2 \approx \frac{1}{LC} \qquad \text{(A4.4.7)}$$

Here $1/\tau$ is introduced as the actual damping factor of the LC-circuit at its natural frequency. This damping is very small for shunt reactors. So after a time $t = \psi/\omega_t$ the recovery voltage has practically attained to its first maximum, *the suppression peak*, provided current chopping appears before natural current zero.

This case is the most frequently occurring by far. It is illustrated in Figure A4.1.1 and Figure A4.4.2a. Because i_L (0) and E_0 have opposite signs, ψ in eq. (A4.4.4) is a negative angle.

Current chopping after natural zero i illustrated in Figure A4.4.2b. Now ψ is a positive angle and there will be no suppression peak.

With the help of eqs. (A4.4.1) to (A4.4.3) equation (A4.4.5) can be transferred into an expression for the theoretically maximum overvoltage per unit, k_a, (the amplitude of the phase voltage E_m being 1.0 p.u.).

$$k_a = \frac{U_m}{E_m} = \sqrt{1 + \frac{3[i_L(0)]^2}{2\omega CQ}} \quad p.\ u. \tag{A4.4.8}$$

Here $Q = 3\ E_m I_m/2$ which can be taken as the total power of the three-phase reactor, because $\omega L << 1/\omega C$.

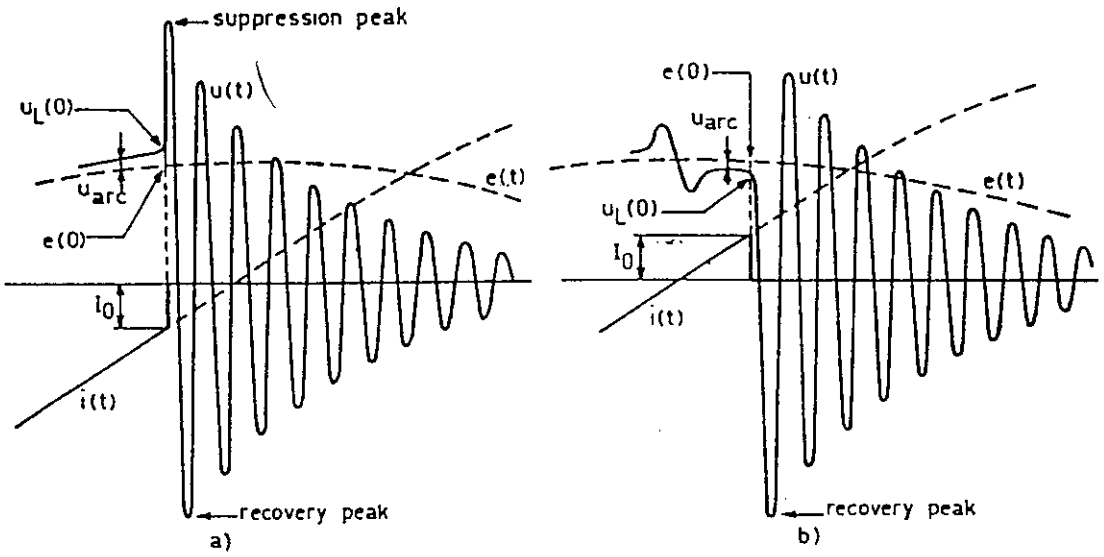

Figure A4.4.2 Current chopping before (a) and after (b) natural current zero

The overvoltage factor k_a is plotted as a function of the chopping level for a number of C and Q-values in Figures A4.4.3 to A4.4.6. Moreover $k_a = f(QC)$ is given in Figures A4.4.7 and A4.4.8 for a number of chopping levels.

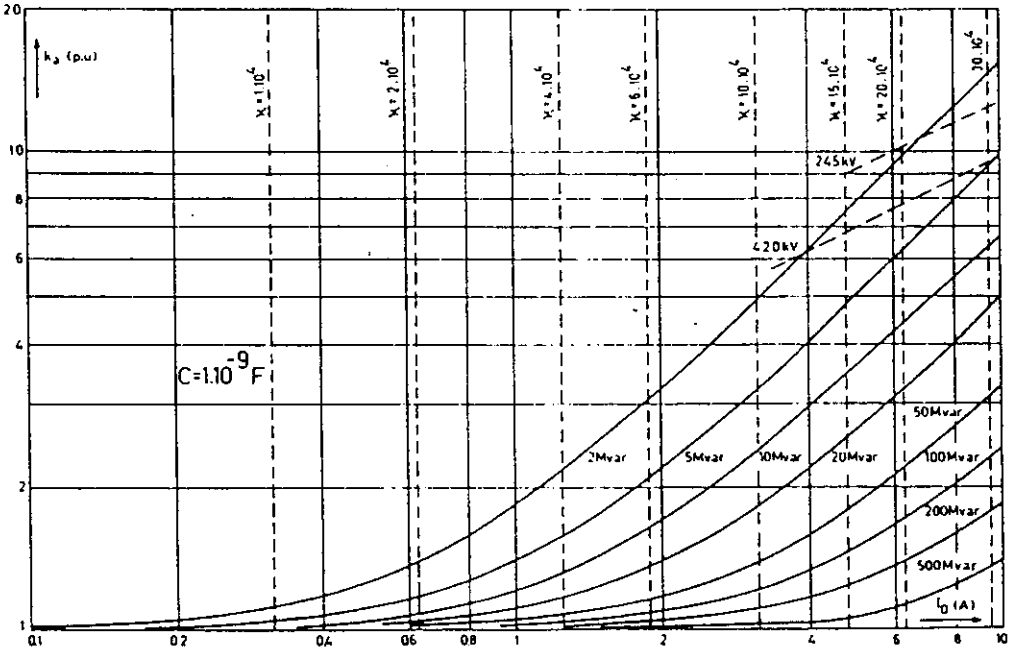

Figure A4.4.3 Overvoltage factor k_a as a function of the chopping current I_0 for three-phase inductive load from 2 to 500 Mvar and an effective parallel capacitance of 10^{-9} F. (Without reignitions)

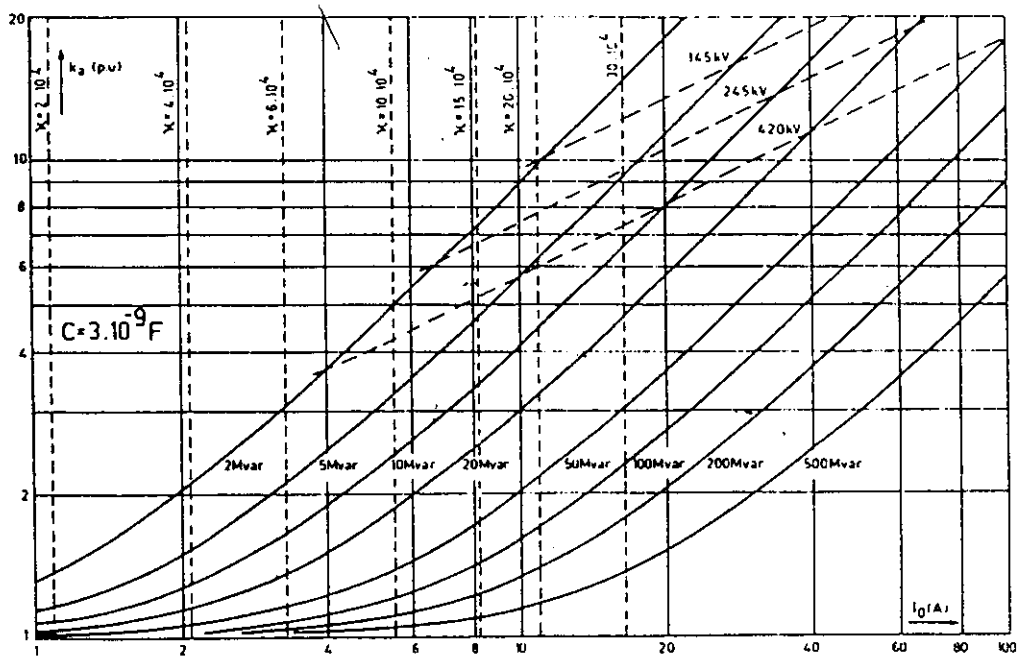

Figure A4.4.4 **Overvoltage factor k_a as a function of the chopping current I_0 for three-phase inductive load from 2 to 500 Mvar and an effective parallel capacitance of $3 \cdot 10^{-9}$ F. (Without reignitions)**

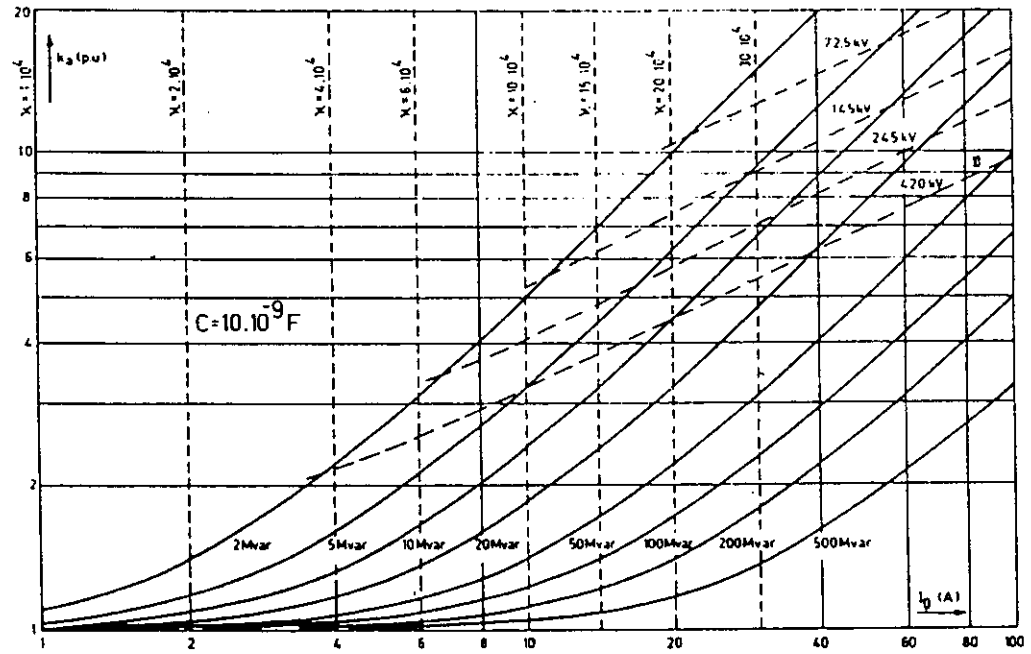

Figure A4.4.5 **Overvoltage factor k_a as a function of the chopping current I_0 for three-phase inductive load from 2 to 500 Mvar and an effective parallel capacitance of $10 \cdot 10^{-9}$ F. (Without reignitions)**

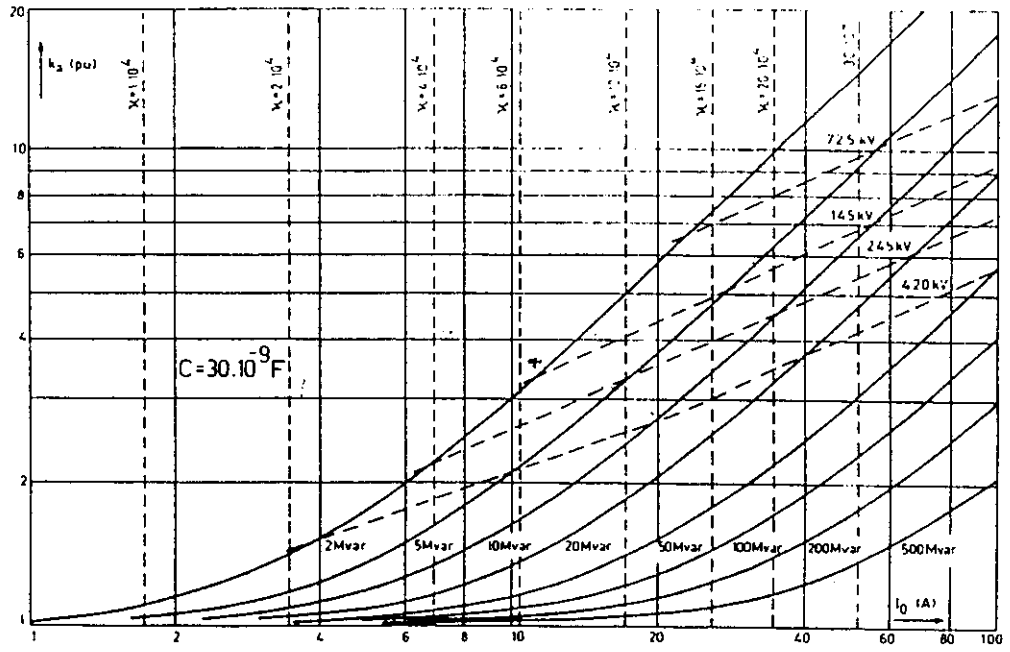

Figure A4.4.6 **Overvoltage factor k_a as a function of the chopping current I_0 for three-phase inductive load from 2 to 500 Mvar and an effective parallel capacitance of $30 \cdot 10^{-9}$ F. (Without reignitions)**

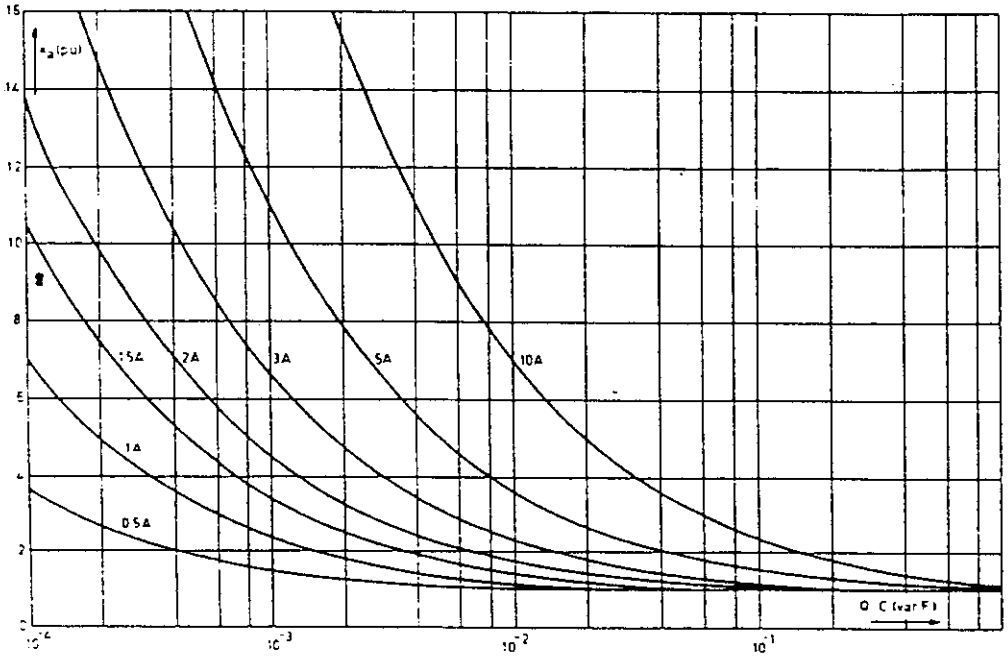

Figure A4.4.7 **Overvoltage factor k_a versus Q·C for chopping currents from 0.5 to 10 A.**

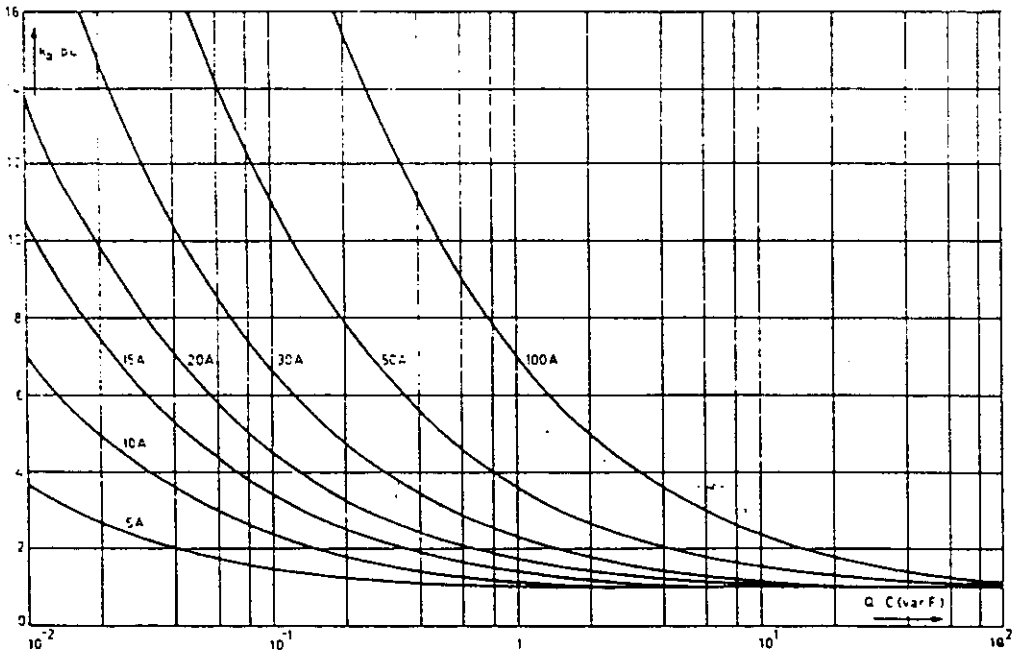

Figure A4.4.8 Overvoltage factor k_a versus Q·C for chopping currents from 5 to 100 A.

Some dotted lines in Figures A4.4.3 to A4.4.6 show line voltage levels where the current amplitudes are equal to the indicated current: $I_m = I_0$. So higher chopping currents cannot occur for these line voltages under steady-state conditions.

For those circuits and breakers in which eq. (A4.1.1) holds the chopping tendency of the breaker can be characterized by the "chopping-number" κ:

$$\kappa = \frac{I_0}{\sqrt{C_p}} \qquad \text{(A4.4.9)}$$

In case of a stiff source (Figure A4.4.1) the parallel capacitance C_p is equal to C.

Relevant κ-value lines are indicated in Figures A4.4.3 to A4.4.6. Theoretical overvoltage factors as a function of κ-values are plotted in Figure A4.4.9 with Q as a parameter, using:

$$k_a = \sqrt{1 + \frac{3\kappa^2}{2\omega Q}} \qquad \text{(A4.4.10)}$$

Foregoing considerations give rise to some remarks:

- From eq. (A4.4.10) and Figure A4.4.9 it can be seen that not the incidental chopping value I_0 nor the parallel capacitance C are governing the overvoltages. In first approach it is only the chopping tendency (κ) together with the power of the inductive load (Q).

- Figures A4.4.3 to A4.4.6 indicate clearly in which situations high overvoltages will certainly not be generated by current chopping. They cannot be used to predict whether extremely high overvoltages will really occur because many breakers tend to smooth out such extremes by reignitions. On the other side, high overvoltages due to reignitions may occur, even without current chopping (Figures A4.1.2 and A4.1.3).

- In Figures A4.4.3 to A4.4.9 a main frequency of 50 Hz was taken. All curves may be used for 60 Hz networks when instead of the real Q a reduced power Q = 5/6 Q. is taken into account.

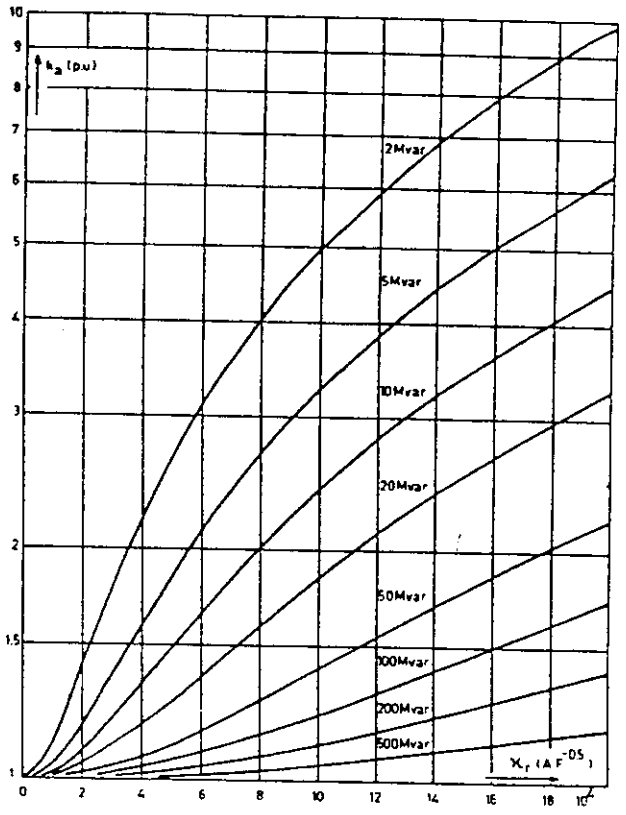

Figure A4.4.9 Overvoltage factor k_a versus chopping number κ for uncoupled reactors without reignitions

- Figure A4.4.9 cannot be used for vacuum breakers because expression eq.(A4.1.1) does not hold for these apparatus.

- The results A4.4.4) to (A4.4.7) are exact and independent of the magnitude of the arc voltage and the capacitive current. In general

$$u_{arc} < 1 \qquad and \qquad \frac{I_C}{I_L} = \frac{\omega^2}{\omega_t^2} < 1$$

will be valid. Therefore equations (A4.4.5) and (A4.4.7) may also be written as:

$$U_m = \sqrt{E_0^2 + (I_0 \omega_t L)^2}$$

$$\sin\psi = \frac{I_0 \omega_t L}{U_m} \qquad and \qquad E_0 = E_m \cos\phi \tag{A4.4.11}$$

In the next sections these simplifications will be maintained, so $u_L(0) = E_0$ and $i_L(0) = i(0)$ will be taken. Calculations of u_L and i_L in case of non-negligible arc voltage can be found in the work of Slamecka et al. [15].

- Usually the chopping level is much lower than the current amplitude: $I_0 << I_m$. In these cases $|E_0|=E_m$ is a justified approximation, but care must be taken for the right sign. In normal cases it is opposite to I_0, so ψ is a negative angle.

- Equation (A4.4.5), giving the recovery voltage amplitude (damping being neglected), may directly be derived from the energy equation

$$\frac{1}{2}Cu_L(0)^2 + \frac{1}{2}Li_L(0)^2 = \frac{1}{2}CU_m^2$$

In more complicated three-phase circuits the expressions for the recovery voltages are more complex and often have a double-frequency mode. But each individual h.f. oscillation amplitude keeps a same form as (A4.4.5):

$$U_{ampl} = \sqrt{x_1^2 + x_2^2}$$

where x_1 is an expression consisting in initial capacitor charge voltages and x_2 is a function of initial currents through the inductances.

– Although damping is neglected in the calculations a term $\varepsilon^{-t/\tau}$ is added in eq. (A4.4.4) to count for the decrease in amplitude during the oscillation time. In fact the actual damping is a complex function governed by the frequency dependent resistance of L and the iron losses. It may be represented by a resistor R in series and/or one in parallel to L. But because of its low value ($R << \omega_t L$) and the variation of its magnitude over the frequency range such a precise representation has little sense. The more practical way of determining an average damping factor $1/\tau$ from the decay of the TRV–amplitudes and so neglect the resistances in the calculation has proved to be justified by experimental evidence and is followed in this paper.

– In eq. (A4.4.6) $\sin\psi$ as well as $\cos\psi$ are defined because ψ may have any value between zero and 2π. This is of special importance when calculating second and third phase interruption transients. For sake of simplicity in the next sections the angles ψ will only be specified by their sin–value.

Note: A κ–value for a multi–unit circuit–breaker is not the same as for its single unit. Their relation is treated in Chapter 2, sub–clause 2.3.4.

A4.4.1.2. Tertiary connected reactors

If the reactor is not connected to an infinite bus but to a tertiary winding of a high–voltage transformer there is no difference in the expressions for the recovery voltage and all foregoing expressions are operative. But in general the occurring chopping currents I_0 and consequently the overvoltages will be lower in this case. The reasons are:

– medium voltage circuit–breakers have often lower chopping levels than the high voltage breakers (or, in other words, they have a lower κ–value):

– the source side transformer has a relatively high series impedance and low impedance to ground to the h.f.–instability oscillation. Therefore the source side capacitance to ground, C_s is also active in the instability phenomena leading to current chopping. Seen from the breaker terminals this C_s is in series connection with C. So C_p in equation (A4.4.9) is now

$$C_p = CC_s/(C + C_s) \qquad \text{(A4.4.12)}$$

Now a reduced κ–value, κ_r must be introduced in equation (A4.4.10):

$$k_a = \sqrt{1 + \frac{3\kappa_r^2}{2\omega Q_L}} \quad \textit{with} \quad \kappa_r = \kappa\sqrt{\frac{C_s}{C_s + C}} \qquad \text{(A4.4.13)}$$

Applying this lower κ_r–value instead of the real κ of the circuit–breaker justifies the use of all curves as before.

There is also a slight distinction in the recovery voltage across the circuit–breaker. Now this voltage is not only governed by the difference between main voltage and $u_L(t)$ but also by the short lasting h.f.–oscillation of the source side transformer. The result is a high initial rate–of–rise of the TRV with a small amplitude giving somewhat more tendency to reduce overvoltages by thermal reignitions.

A4.4.2. With grounded neutral and capacitive coupling solely

($C_N = \infty$; $C_0 = C_g$; $C_1 = C_g + 3C_\ell$; $M = 0$; $L_N = 0$; $L_1 = L$)

As before interruptions succeed each 60 degrees in sequence a – c –b until the first pole clears. Now the capacitive interphase coupling may influence the transient behaviour, especially after second and third pole clearing. Each time a higher overvoltage than before is possible because the total amount of energy left in the interrupted circuit increases with each pole.

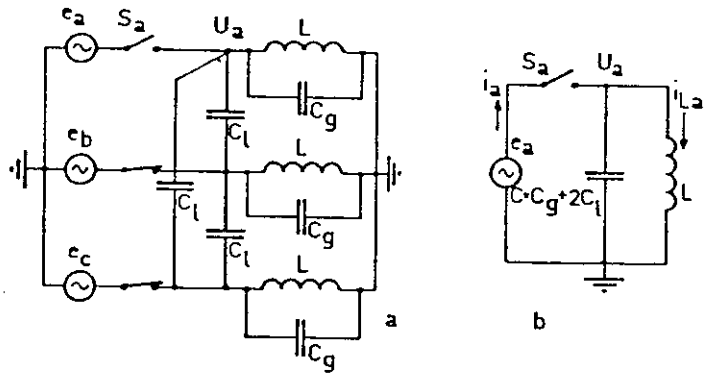

Figure A4.4.10
Capacitively coupled reactors, first phase interruption
a) complete circuit
b) reduced circuit

A4.4.2.1 First phase interruption (phase "a")

Let phase "a" be first interrupted as indicated in Figure A4.4.10a. The source voltages e_b and e_c will not introduce a notable main frequency component in the interrupted phase a, because $\omega L << 1/\omega C_\ell$. Taking furthermore into account that phases "b" and "c" are shorted for h.f. transients the reduced circuit of Figure A4.4.10b is left.

Therefore all results of current chopping in the first phase will be the same as before (section 4.1) provided now $C = C_g + 2C_\ell$ is taken. Introducing for the phase voltage

$$e_a = E_m \cos(\omega t + \phi)$$

gives

$$i_a = I_m \sin(\omega t + \phi) \quad \text{with} \quad I_m = E_m/\omega L$$

The initial conditions are (1) : $u_a(10) = E_m \cos\phi$, $i_a(10) = I_m \sin\phi$.
The recovery voltage after chopping can be written as:

$$u_a(t) = e^{-t/\tau_2}\, U_{m12} \cos(\omega_2 t + \psi_{12}) \tag{A4.4.15}$$

with

$$U_{m12} = \sqrt{\{[u_a(10)]^2 + [i_a(10)\,\omega_2 L]^2\}} \tag{A4.4.16}$$

$$\sin\psi_{12} = \frac{i_a(10)\,\omega_2 L}{U_{m12}}$$

$$\omega_2^2 = 1/\{L(C_g + 2C_\ell)\}$$

Again $1/\tau_2$ is the actual damping factor of the involved LC-circuit at its natural frequency ω_2.

A4.4.2.2. Second phase interruption (phase "c")

After approximately 60 degrees the second pole (in phase "c") will also interrupt by chopping. Now Figure A4.3.1 is reduced to the circuit of Figure A4.4.11a. As before the influence of the remaining main frequency voltage (e_b) is negligible. For the h.f. transients Figure A4.4.11a may therefore be further reduced to Figure A4.4.11b.

Changing now to a new time coordinate t' where $t' = t - t_1$ and t_1 is the time passed between first and second pole clearance, one can write:

$e_c = E_m \cos(\omega t' + \phi_3)$; $i_c = I_m \sin(\omega t' + \phi_3)$ where $\phi_3 = \phi - 180°$

The initial conditions in the interrupted phase "c" are: $u_c(20) = E_m \cos\phi_3$; $i_c(20) = I_m \sin\phi_3$.

At this moment the transient oscillation in the first interrupted phase "a" may still have a sizable voltage and/or current amplitude:

---

(1) The subjunction (10) is used instead of (0) to indicate the initial conditions at the moment of first pole interruption. Later on (20) and (30) are used for the voltage and currents at the moment of second and third pole interruption respectively.

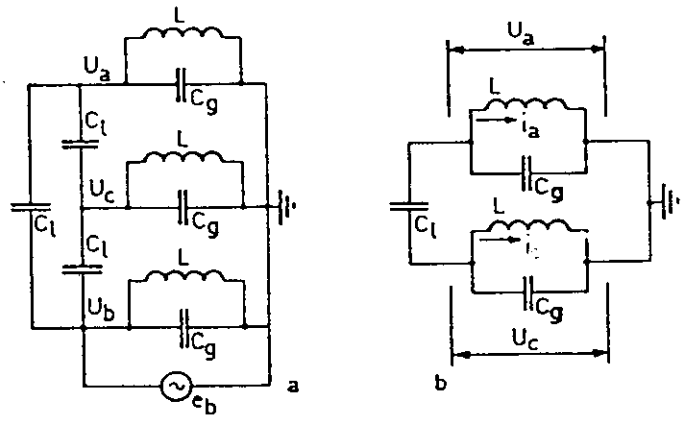

Figure A4.4.11 Capacitively coupled reactors, second phase interruption
a) complete circuit
b) reduced circuit

$$u_a(20) = (U_{m12} \cos \omega_2 t_1) \exp(-t_1/\tau_2) = \sigma_2 U_{m12} \cos \omega_2 t_1 \qquad \text{(A4.4.17)}$$

$$i_a(20) = \left(\frac{U_{m12}}{\omega_2 L} \sin \omega_2 t_1\right) \exp(-t_1/\tau_2) = \frac{\sigma_2 U_{m12}}{\omega_2 L} \sin \omega_2 t_1 \qquad \text{(A4.4.18)}$$

$$t_1 \cong T/6 \qquad \sigma_2 = \exp(-t_1/\tau_2)$$

These values also appear as initial conditions in the transients after second pole interruption.

The recovery voltages are now:

$$u_a(t) = \varepsilon^{-t'/\tau_1} U_{m21} \cos(\omega_1 t' + \psi_{21}) + \varepsilon^{-t'/\tau_3} U_{m23} \cos(\omega_3 t' + \psi_{23}) \qquad \text{(A4.4.19)}$$

$$u_c(t) = \varepsilon^{-t'/\tau_1} U_{m21} \cos(\omega_1 t' + \psi_{21}) - \varepsilon^{-t'/\tau_3} U_{m23} \cos(\omega_3 t' + \psi_{23}) \qquad \text{(A4.4.20)}$$

with

$$U_{m21} = \sqrt{[A_1^2 + A_2^2]} \qquad U_{m23} = \sqrt{[B_1^2 + B_2^2]}$$

$$A_1 = 1/2\ \{u_a(20) + u_c(20)\} \qquad B_1 = 1/2\ \{u_a(20) - u_c(20)\}$$

$$A_2 = 1/2\ \omega_1 L\ \{i_a(20) + i_c(20)\} \qquad B_2 = 1/2\ \omega_3 L\ \{i_a(20) - i_c(20)\}$$

$$\sin \psi_{21} = A_2/U_{m21} \qquad \sin \psi_{23} = B_2/U_{m23}$$

$$\omega_1^2 = 1/\{L(C_g + C_l)\} \qquad \omega_3^2 = 1/\{L(C_g + 3C_l)\}$$

Line–to–line voltages $u_a - u_b$, $u_b - u_c$ and $u_c - u_a$ are easy to determine from (A4.4.19), (A4.4.20) and $u_b(t) = e_b(t)$.

The expressions (A4.4.19) and (A4.4.20) show that after interruption in the second phase a double frequency oscillation occurs which has principally the same shape in both phases. The only difference is a 180 degrees phase shift between the lower frequency (ω_3) components.

The highest overvoltage which possibly may occur in one of the two phases is:

$$(u_a)_{max} = (u_c)_{max} = U_{m21} + U_{m23}$$

Using $k_1 = U_{m12}/E_m$ = overvoltage factor after the first phase interruption

$$\sigma_2 = \varepsilon^{-T/6\tau_2} \ ; \ k_{21} = \alpha k_1 \ ; \ \beta = \omega_2 t_1 + \psi_{21},$$

the initial conditions can be written as

$$u_a(20) = k_{21} E_m \cos \beta \ ; \ u_c(20) \cong E_m$$

$$i_a(20) = k_{21} \frac{E_m}{\omega_2 L} \sin \beta \ ; \ i_c(20) \cong i_a(10)$$

Now

$$k_1 = \sqrt{[1 + \{\frac{i_a(10)\,\omega_2 L}{E_m}\}^2]}$$

and the possible overvoltage factor after second phase interruption is

$$k_2 = 1/2\ \{[(1 + k_{21}\cos\beta)^2 + \left(\frac{\omega_1}{\omega_2}\right)^2 (k_{21}\sin\beta - \sqrt{k_1^2 - 1})^2]^{1/2} + \\ + [(1 - k_{21}\cos\beta)^2 + \left(\frac{\omega_3}{\omega_2}\right)^2 (k_{21}\sin\beta + \sqrt{k_1^2 - 1})^2]^{1/2}\} \qquad \text{(A4.4.21)}$$

In Figure A4.4.12 k_2 is plotted as a function of β for several values k_1 and k_{21}, using $\omega_1/\omega_2 = 1{,}1$ and $\omega_3/\omega_2 = 0{,}92$. From such plots it can be seen that possible overvoltages after second phase interruption are higher than after first phase interruption: $k_2 > k_1$ except for a small part around $\beta = 100°$. But there is only little chance that the theoretically maximum $U_{m21} + U_{m23}$ occurs instantaneously after current chopping. So the actual maximum is usually (much) lower than the theoretical value, due to the damping. A typical example with $k_2 = 2$ and $k_{21} = 1$ is treated in section A4.4.1.5.

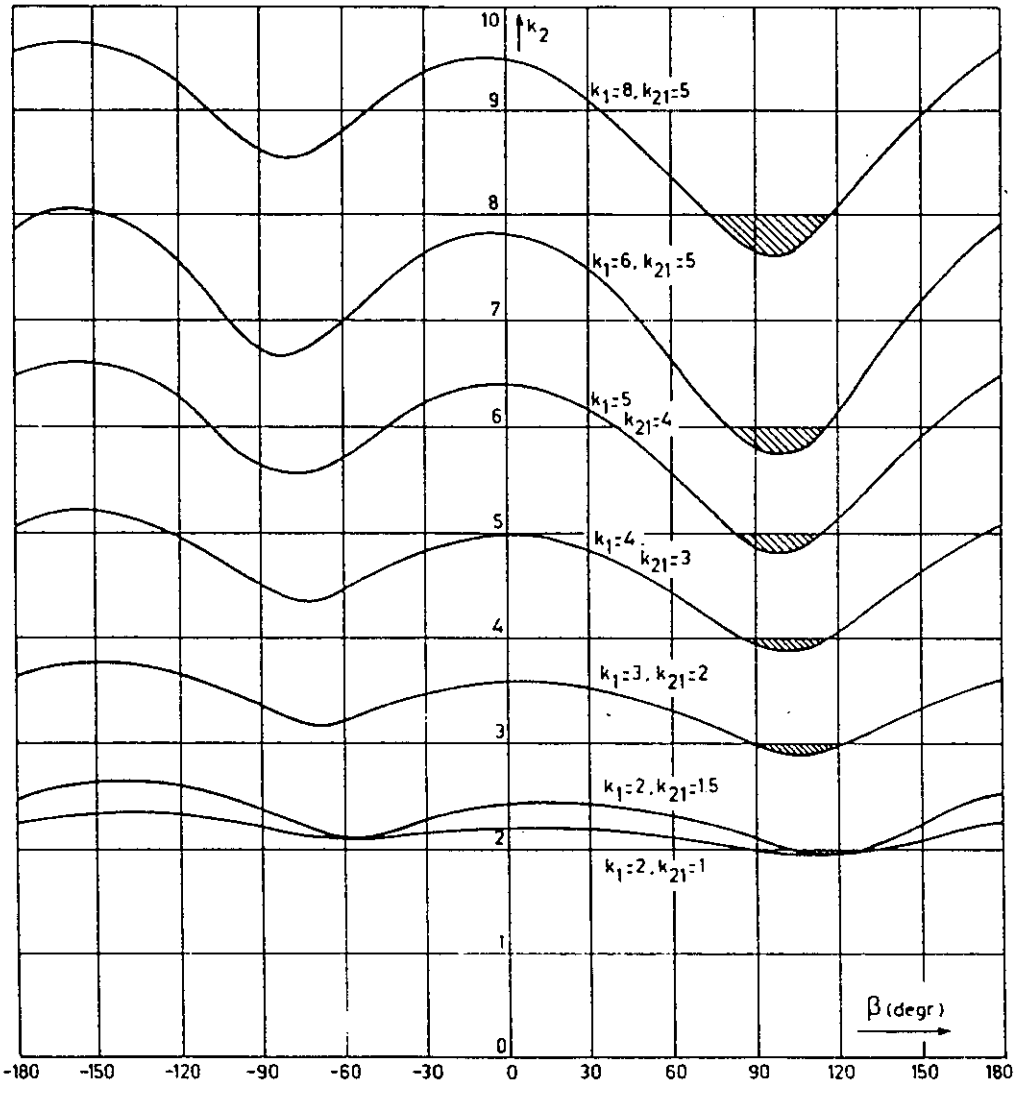

Figure A4.4.12 Examples of maximum overvoltage factors after second phase interruption (k_2) versus angle β of the first phase transient at t = t(20)

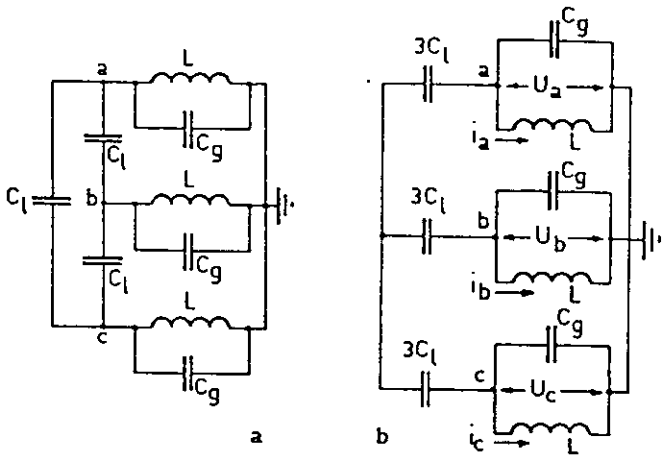

Figure A4.4.13 Capacitively coupled reactors, third phase interruption;
a) complete circuit
b) reduced circuit

A4.4.2.3. Third phase interruption (phase "b")

Again 60 degrees after the second pole the third pole will interrupt in phase "b". Now transients will develop in a circuit according to Figure A4.4.13a which can be transferred in Figure A4.4.13b by delta–star transformation.

Now $e_b = E_m \cos(\omega t'' + \phi_2)$ and $i_b = I_m \sin(\omega t'' + \phi_2)$ when $t'' = t - t_2$ and t_2 is the time interval between first and third pole interruption, $\phi_2 \approx \phi$.

So the initial conditions in the interrupted phase "b" are

$$u_b(30) = E_m \cos \phi_2$$

$$i_b(30) = I_m \sin \phi_2$$

At t" = 0 the transient oscillation in phases "a" and "c" may still be present, causing initial conditions

$$u_a(30) = \sigma_1 U_{m21} \cos\beta_1 + \sigma_3 U_{m23} \cos\beta_3 \qquad \text{(A4.4.22)}$$

$$u_c(30) = \sigma_1 U_{m21} \cos\beta_1 - \sigma_3 U_{m23} \cos\beta_3$$

$$i_a(30) = \frac{\sigma_1 U_{m21}}{\omega_1 L} \sin\beta_1 + \sigma_3 \frac{U_{m23}}{\omega_3 L} \sin\beta_3 \qquad \text{(A4.4.23)}$$

$$i_c(30) = \frac{\sigma_1 U_{m21}}{\omega_1 L} \sin\beta_1 - \sigma_3 \frac{U_{m23}}{\omega_3 L} \sin\beta_3$$

where

$$\sigma_1 = \varepsilon^{-T/6\tau_0} \quad ; \quad \sigma_3 = \varepsilon^{-T/6\tau_3}$$

$$\beta_1 = \omega_1 (t_2 - t_1) + \psi_{21} \quad ; \quad \beta_3 = \omega_3 (t_2 - t_1) + \psi_{23}$$

so

$$\frac{\beta_1 - \psi_{21}}{\beta_3 - \psi_{23}} = \frac{\omega_1}{\omega_3}$$

As a result of all these starting conditions the recovery voltages in the three phases are:

$$u_a(t) = \varepsilon^{-t''/\tau_0} U_{m30} \cos(\omega_0 t'' + \psi_{30}) + \varepsilon^{-t''/\tau_3} U_{ma33} \cos(\omega_3 t'' + \psi_{a33}) \qquad \text{(A4.4.24)}$$

$$u_b(t) = \varepsilon^{-t''/\tau_0} U_{m30} \cos(\omega_0 t'' + \psi_{30}) + \varepsilon^{-t''/\tau_3} U_{mb33} \cos(\omega_3 t'' + \psi_{b33}) \qquad \text{(A4.4.25)}$$

$$u_c(t) = \varepsilon^{-t''/\tau_0} U_{m30} \cos(\omega_0 t'' + \psi_{30}) + \varepsilon^{-t''/\tau_3} U_{mc33} \cos(\omega_3 t'' + \psi_{c33}) \qquad \text{(A4.4.26)}$$

with

$$U_{m30} = \sqrt{[D_1^2 + D_2^2]} \qquad U_{mb33} = \sqrt{[F_1^2 + F_2^2]}$$

$$D_1 = u_s(0) \qquad F_1 = u_b(30) - u_s(0)$$

$$D_2 = \omega_0 L\, i_s(0) \qquad F_2 = \omega_3 L\, [i_b(30) - i_s(0)]$$

$$\sin\psi_{30} = D_2/U_{m30} \qquad \sin\psi_{b33} = F_2/U_{mb33}$$

$$U_{ma33} = \sqrt{[E_1^2 + E_2^2]} \qquad U_{mc33} = \sqrt{[G_1^2 + G_2^2]}$$

$$E_1 = u_a(30) - u_s(0) \qquad G_1 = u_c(30) - u_s(0)$$

$$E_2 = \omega_3 L\, [i_a(30) - i_s(0)] \qquad G_2 = \omega_3 L\, [i_c(30) - i_s(0)]$$

$$\sin\psi_{a33} = E_2/U_{ma33} \qquad \sin\psi_{c33} = G_2/U_{mc33}$$

$$u_s(0) = \frac{1}{3}[u_a(30) + u_b(30) + u_c(30)]$$

$$i_s(0) = \frac{1}{3}[i_a(30) + i_b(30) + i_c(30)]$$

$$\omega_0^2 = 1/LC_g \qquad \omega_3^2 = 1/[L(C_g + 3C_\ell)]$$

So after interruption of the third phase a double-frequency oscillation is generated in all three of the phases but with a specific shape in each phase. Depending on magnitudes and polarities of the several initial conditions high overvoltages are possible in each phase. In the first as well as in the second phase higher overvoltages than after their interruption are often observed. Due to the long period without current flow a reignition in these phases is unlikely. Furthermore the chopping current in the last pole-to-interrupt is usually the highest one. For these reasons the third pole interruption represents the most severe burden to the interrupted network in case of cable connected reactors with line-to-line capacitances.

In other configurations some line-to-line capacitances will also be present. But if $C_\ell << C_g$ all frequencies ω_0, ω_1, ω_2 and ω_3 are nearly the same and the recovery voltages are very near to those treated in section A4.4.1.

For small values C_ℓ and C_g all frequencies ω_0 to ω_3 may be so high that they are practically damped out within 60 degrees.

A4.4.2.4. Reignition transfer through capacitive coupling

As stated before (section A4.1.2) a "second parallel oscillation" will arise after a reignition, involving C_g, C_ℓ and the (small) inductances of the circuit-breaker connections. In the case of first or second pole interruption the current crossing C_ℓ will flow through at least one more breaker arc. This may cause virtual current chopping (see section A4.1.3a).

Especially after virtual current chopping virulent voltage escalation due to repetitive reignitions is possible (section A4.1.2).

If the second parallel oscillation is generated by a reignition in the last interrupted breaker pole it appears across the other two poles and reactors as a h.f. voltage, superimposed on the momentary values of their recovery voltage. This phenomenon is more severe in case of ungrounded reactors, because there a high recovery voltage arises simultaneously in the second and third phase. Therefore it is treated in part II (Appendix 5).
Reignitions after second or third pole interruption will cause oscillations of the same kind as described in A4.4.2, involving all inductances and capacitances in the circuit. The oscillating current may be interrupted around its first current zero. Then the oscillation voltage has just changed polarity and is at its maximum. This maximum appears as the new initial condition in the TRV-expressions. It may be much higher than before. Thus the new overvoltages described by equations (A4.4.33) and (A4.4.34) or by (A4.4.37) to (A4.4.39) start with higher voltage conditions in the reignited phase than was the first time. In this way reignitions may lead to high overvoltages even without any essential current chopping.

A4.4.2.5 Examples of TRVs in capacitively coupled reactors with solidly grounded neutral

As an example a reactor-bank of 30 Mvar without inductive coupling, connected to a 36 kV, 50 Hz network is chosen.

A circuit-breaker is supposed to interrupt the reactors in phase sequence a-c-b, causing an overvoltage of 2 p.u. in the first phase (k_a = 2, κ = 14.10^4, see Figure A4.4.9).

Figure A4.4.14, No. 1 gives the TRV occurring in the three phases when the connection to the circuit-breaker consists of a three-phase cable with total line-to-ground capacitance C_g = 10 nF and line-to-line capacitance C_ℓ = 3 nF.

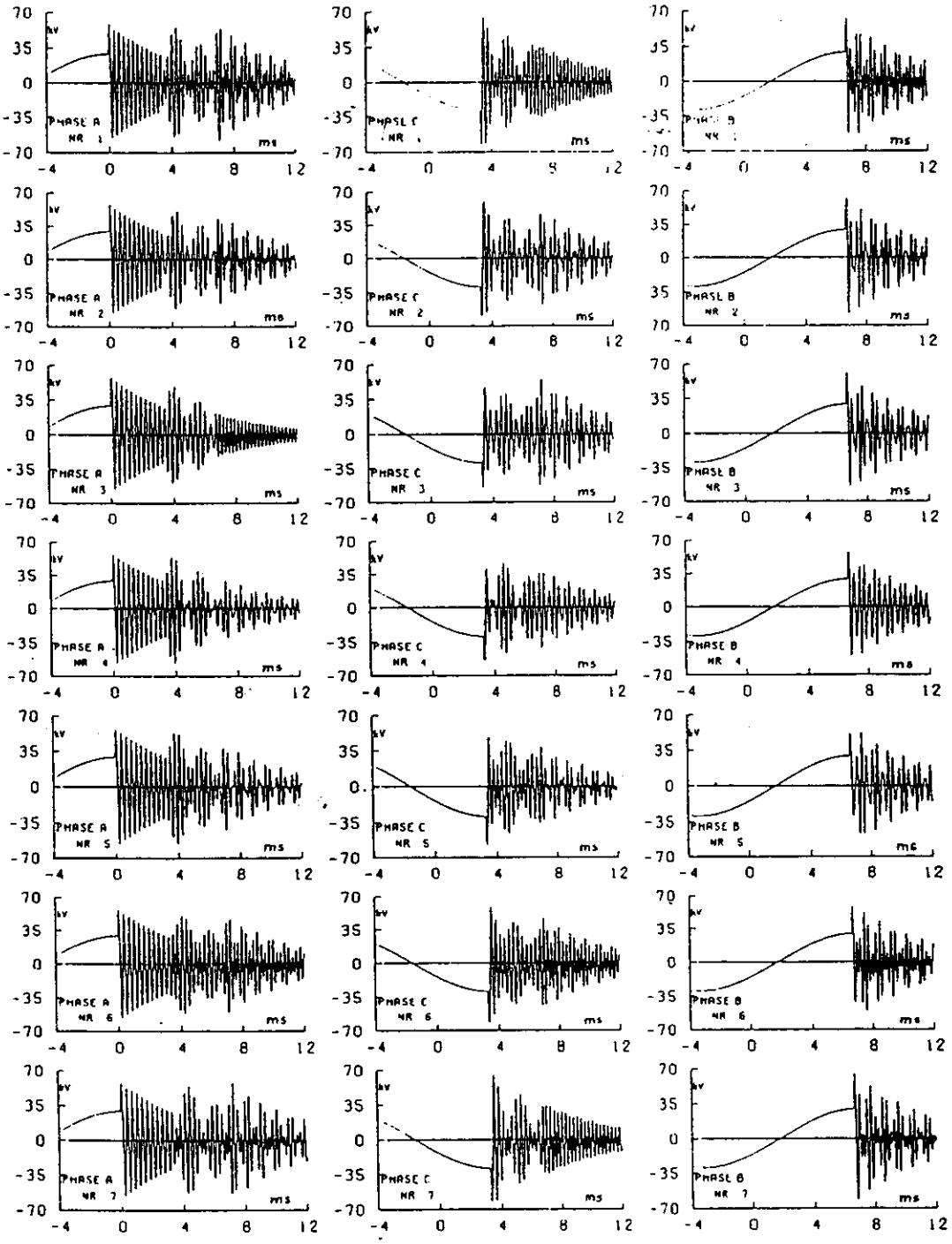

Figure A4.4.14 Examples of recovery voltages during interruption of a reactor bank with capacitive coupling solely. Data are given in the text.

Developing frequencies are f_2 = 3 390 Hz, f_1 = 3 760 Hz, f_3 = 3 110 Hz and f_0 = 4 290 Hz, eqs. (A4.4.16), (A4.4.20) and (A4.4.26).

With I_m = 680 A and $\omega_2 = 21.3.10^3$ s $^{-1}$ a chopping current I_0 = (–) 17,4 A is found (eq. (A4.4.16)). From i_a (10) = $I_0 = I_m \sin \phi$ the phase angle at the moment of current chopping appears to be ϕ = (–) 1,46°

To find comparable sets of TRV–patterns, k_a = 2 was maintained and C_g and C_ℓ were raised in steps of ΔC_g = 0,34 nF and ΔC_ℓ = 0,10 nF respectively. So the number of complete oscillation loops in the time interval t_1 = 1/6 T changes in 6 steps (Figure A4.4.14, Nos 1 to 7) from n = 11.3 to n = 10.3. This causes a 60 degrees phase shift in the initial conditions at t (20) for each step. During the same time I_0 changes somewhat (from 17.4 to 19.0 A) as well as the developing frequencies do.

The time constant τ was taken $4{,}8.10^{-3}$ s for all TRV's. This gives a damping of 50 per cent in 1/6 T.

Figure A4.4.14 clearly shows the complexity of the TRV–patterns. But in this rather typical example no excessive overvoltages arise due to transfer of chopping voltages. Only a few peaks higher than 2 p.u. are observed (e.g. no. 1, phases b and c) but an analysis of the numerical data does not show more than 2.3 p.u. as a maximum. This is in agreement with the calculated values from eq. (A4.4.21) plotted in figure A4.4.12 for $k_1 = k_a = 2$ and k_{21} = 1 (due to 50 per cent damping).

Higher overvoltages might occur in case of lower reactive power Q, higher chopping current I_0 (and thus a higher k–value) or smaller damping $1/\tau$ or due to reignition(s).

Note: The variation of C_g and C_ℓ only causes a total 360 degrees phase shift in the initial conditions at t(20). The double frequency oscillation occurring between t (20) and t (30) makes the variation of the initial conditions at t (30) less systematically. The calculation of possible TRV's for a practical situation in the field should rather be performed by varying the chopping current over its statistical range with constant C_g and C_ℓ. In this specific case a variation over 5 A would cause a total phase shift of only 36 degrees at t(20). Then the highest overvoltages are related to the highest chopping current.

A4.4.3. With grounded neutral and inductive coupling solely

($C_N = \infty$; $C_\ell = 0$; $C_g = C_0 = C_1$; $M \neq 0$; $L_1 = L + M$; $L_0 = L - 2M$; $L_N = \frac{1}{3}(L_0 - L_1)$)

Again interruptions and reignitions will succeed in sequence a–c–b until the first pole clears. After interruption of the second and third pole, energy transfer from the earlier interrupted phase(s) through the inductive coupling will also in this case influence the TRV's.

All expressions for the recovery voltages will basically have the same form as the foregoing chapter with one single exception: After interruption of the first and second phase a main frequency voltage component will be induced in the switched–off phase(s) adding a main frequency component to its TRV.

Because of this clear similarity, in this and the next chapter only the reduced scheme and the results will be given, all based on the general representation of Figures A4.3.1 and A4.3.2. Initial conditions are only stated as far as they deviate from the corresponding foregoing situations.

Results are applicable to reactors on three–legged iron cores and, more general, to all star connected inductances which are grounded through a reactor (L_N). An example is treated in section A4.4.5, Figure A4.4.22.

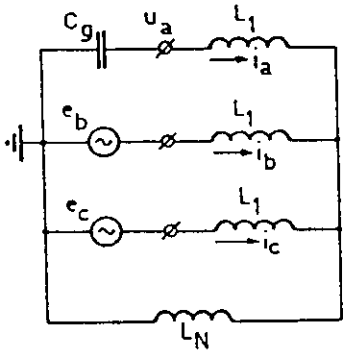

Figure A4.4.15 Inductively coupled reactors. Reduced scheme for first phase interruption

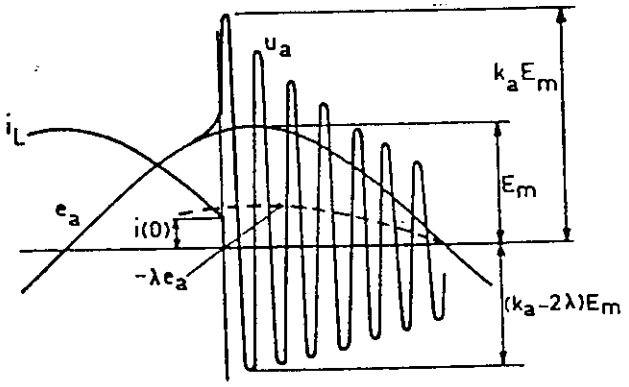

Figure A4.4.16 Influence of inductive coupling (λe_a) on the TRV after first phase interruption.

A4.4.3.1. First phase interruption (phase "a")

Figure A4.4.15 gives the reduced scheme. Phase voltage and initial conditions being similar to those in section A4.4.2.1, the expression for the transient recovery voltage is now:

$$u_a(t) = -\lambda e_a(t) + \varepsilon^{-t/\tau_7} U_{m17} \cos(\omega_7 t + \psi_{17}) \qquad \text{(A4.4.27)}$$

with

$$U_{m17} = \sqrt{\left\{\left[\frac{L_1 + 3L_N}{L_1 + 2L_N} u_a(10)\right]^2 + \left[\frac{i_a(10)}{\omega_7 C_g}\right]^2\right\}}$$

or

$$U_{m17} = (1 + \lambda)\sqrt{\{[u_a(10)]^2 + [i_a(10)\,\omega_7 L_1]^2\}} \qquad \text{(A4.4.28)}$$

$$\omega_7^2 = \frac{L_1 + 2L_N}{L_1 C_g (L_1 + 3L_N)} \qquad \sin\psi_{17} = \frac{(1 + \lambda)\, i_a(10)\, \omega_7 L_1}{U_{m17}}$$

$$\lambda = \frac{L_N}{L_1 + 2L_N}$$

As stated before (clause A4.3) the zero sequence inductance of reactors on three-legged iron cores is approx. $L_0 \approx 0.3\ L_1$.

Because $L_N = 1/3\ (L_0 - L_1)$, the main frequency component in $u_a(t)$ will then be $0.44e_a$, so $\lambda = -0.44$.

The amplitude of the TRV is much smaller than in a non-inductive coupled situation (section A4.4.3.2), see Figure A4.4.16 as an example.

Some other specific configurations may directly be deduced from (A4.4.27):

- in ungrounded reactor banks L_N in Figure A4.4.15 becomes almost infinite, so, $\lambda = 0.5$ and the TRV oscillates around $-1/2\ e_a = 1/2\ (e_b + e_c)$ (see section A4.1.3c and part II, Appendix 5).

- an "ideal" coupled reactor bank or transformer would have $L_0 = 0$ and $L_N = -1/3\ L_1 = -M$. This would give $\lambda = -1$ and eq. (A4.4.27) shows that there would be no transient recovery voltage at all after first pole clearance.

- inductive coupling introduces negative λ-values. An uncoupled grounding impedance L_N causes a positive λ-value. Taking $\lambda = 0$ the non-inductive coupled, directly grounded situation (section A4.4.2.1) is found again.

A4.4.3.2 Second phase interruption (phase "c")

The reduced scheme is Figure A4.4.17. The phase voltages again are written as:

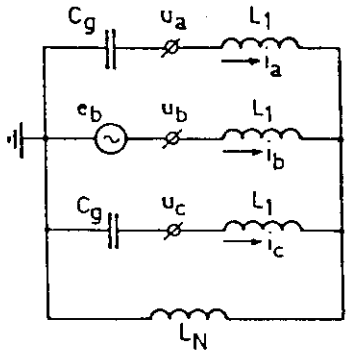

Figure A4.4.17 Inductively coupled reactors . Reduced scheme for second phase interruption.

$$e_a = E_m \cos(\omega t + \phi)$$

$$e_b = E_m \cos(\omega t'' + \phi_2)$$

$$e_c = E_m \cos(\omega t' + \phi_3)$$

$$t' = t - t_1$$

$$t'' = t - t_2$$

$$\phi_2 \cong \phi$$

If again the moment of current chopping in the second phase is chosen t' = 0 and the initial voltages u_b and u_c are:

$$u_b(20) = E_m \cos(\phi_3 + 120^\circ) \qquad \text{(A4.4.29)}$$

$$u_c(20) = E_m \cos\phi_3$$

Initial values $u_a(20)$ and $i_a(20)$ are found from A4.4.27 as before (see eqs. (A4.4.17) and (A4.4.18)) and using

$$-e_a(20) = u_b(20) + u_c(20)$$

(The main frequency component in $i_a(20)$ is negligible.)
So

$$u_a(20) = \lambda\{u_b(20) + u_c(20)\} + \sigma_7 U_{m17} \cos\omega_7 t_1 \qquad \text{(A4.4.30)}$$

$$i_a(20) = \sigma_7 \omega_7 C_g U_{m17} \sin\omega_7 t_1 \qquad \text{(A4.4.31)}$$

with $\lambda = \dfrac{L_N}{L_1 + 2L_N}$ and $\sigma_7 = \varepsilon^{-t_1/\tau_7}$

Now $t_1 \neq T/6$ and $\phi_3 \neq \phi - 180^\circ$ (unlike capacitive coupling solely).

Due to voltage induction from the other phases, the currents i_b and i_c will not have a 90 degrees phase shift to the voltage but may be written as:

$$i_b(t) = \frac{E_m\sqrt{1-\lambda+\lambda^2}}{\omega L_1}\sin(\omega t' + \phi_3 + \phi_0 + 120^\circ)$$

$$i_c(t) = \frac{E_m\sqrt{1-\lambda+\lambda^2}}{\omega L_1}\sin(\omega t' + \phi_3 - \phi_3) \qquad \text{(A4.4.32)}$$

$$\text{where } \tan\phi_0 = \frac{\lambda\sqrt{3}}{2-\lambda} \qquad \text{(see also Figure A4.4.18)}$$

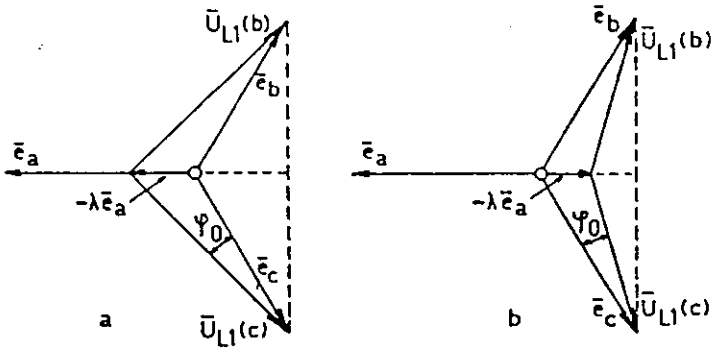

Figure A4.4.18 Voltage across L_1 after first phase interruption

a) for inductively coupled reactors $\lambda < 0$, $\phi_0 < 0$

b) with external grounding inductance; $\lambda > 0$, $\phi_0 > 0$

Note that in case of inductive coupling the second phase will interrupt after $60 + \phi_0$ degrees, which is earlier than before, because $\phi_0 < 0$.

So the initial current (= chopping current) is

$$i_c(20) = -\frac{E_m\sqrt{1-\lambda+\lambda^2}}{\omega L_1}\sin(\phi_3 - \phi_0 - 180^\circ) = -i_a(10)$$

which defines ϕ_3 and t_1.

Recovery voltages are:

$$u_a(t) = \nu e_b + \varepsilon^{-t'/\tau_6} U_{m26}\cos(\omega_6 t' + \psi_{26}) + \varepsilon^{-t'/\tau_4} U_{m24}\cos(\omega_4 t' + \psi_{24}) \quad \text{(A4.4.33)}$$

$$u_c(t) = \nu e_b + \varepsilon^{-t'/\tau_6} U_{m26}\cos(\omega_6 t' + \psi_{26}) - \varepsilon^{-t'/\tau_4} U_{m24}\cos(\omega_4 t' + \psi_{24}) \quad \text{(A4.4.34)}$$

with

$$U_{m26} = \sqrt{(H_1^2 + H_2^2)} \qquad \sin\psi_{26} = H_2/U_{m26}$$

$$H_1 = \frac{1}{2}\{u_a(20) + u_c(20)\} - \nu e_b(t_1)$$

$$H_2 = \frac{1}{2\omega_6 C_g}\{i_a(20) + i_c(20)\} - \frac{\nu e_b'(t_1)}{\omega_6} \qquad \omega_6^2 = \frac{1}{L_1 C_g}\left(\frac{L_N + L_1}{3L_N + L_1}\right)$$

$$U_{m24} = \sqrt{(J_1^2 + J_2^2)} \qquad \sin\psi_{24} = J_2/U_{m24}$$

$$J_1 = \frac{1}{2}\{u_a(20) - u_c(20)\}$$

$$J_2 = \frac{1}{2\omega_4 C_g}\{i_a(20) - i_c(20)\} \qquad \omega_4^2 = \frac{1}{L_1 C_g}$$

$$\nu = \frac{L_N}{L_1 + L_N}$$

As before there is a main frequency component in the TRV which is now $\nu e_b(t)$. Taking again the three-legged core reactor with $L_0 = 0.3L_1$ as an example, $\nu = -0{,}3$ and the component νe_b, having $0.3E_m$ as a maximum, will not contribute essentially to the overvoltage. The angle $\phi_0 \approx -17.3^\circ$ and for $I_0 << I_m$: $\phi_0 \approx \phi_3$.

So $\nu e_b(20) = \nu E_m \cos(\omega t' + \phi_3 = 120^\circ)$ at $t' = 0 \approx 0.06\ E_m$

This example shows that the main frequency component has no influence on the first maximum after current chopping. Then it also does not appear in H_1 and H_2.

What is left in formula's (A4.4.33) and (A4.4.34) is exactly the same as (A4.4.19) and (A4.4.20).

Therefore the remarks on possibly increasing of overvoltages due to energy transfer from the first interrupted phase as made in section A4.4.2.2 apply here as well. But since the overvoltage after first phase interruption is reduced by the main frequency component, the TRV's after second pole clearing may be lower than with capacitive coupling solely.

A4.4.3.3 Third phase interruption (phase "b")

Starting again with

$$e_b = E_m \cos(\omega t' + \phi_2)$$

the initial conditions in phase "b" are

$$e_b(30) = E_m \cos\phi_2 \cong E_m$$

$$i_b(30) = E_m \sin \phi_2 / \omega(L_1 + L_N)$$

Now this phase will interrupt $60 - \phi_0$ degrees after phase "c", so the foregoing transients are damped out further than without inductive coupling, as $\phi_0 < 0$.

Further initial conditions are

$$u_a(30) = \nu e_b(30) + \sigma_{26} U_{m26} \cos\beta_1 + \sigma_{24} U_{m24} \cos\beta_2$$

$$u_c(30) = \nu e_b(30) + \sigma_{26} U_{m26} \cos\beta_1 - \sigma_{24} U_{m24} \cos\beta_2 \qquad \text{(A4.4.35)}$$

$$i_a(30) = \sigma_{26} U_{m26} \omega_{26} C_g \sin\beta_1 + \sigma_{24} U_{m24} \omega_{26} C_g \sin\beta_2$$

$$i_c(30) = \sigma_{26} U_{m26} \omega_{26} C_g \sin\beta_1 - \sigma_{24} U_{m24} \omega_{26} C_g \sin\beta_2 \qquad \text{(A4.4.36)}$$

with

$$\sigma_{26} = \exp\{(t_1 - t_2)/\tau_6\} \qquad \sigma_{24} = \exp\{(t_1 - t_2)/\tau_6\}$$

$$\beta_1 = \omega_6 (t_2 - t_1) + \psi_{26} \qquad \beta_2 = \omega_4 (t_2 - t_1) + \psi_{24}$$

$$t_2 \cong \frac{1}{3} T$$

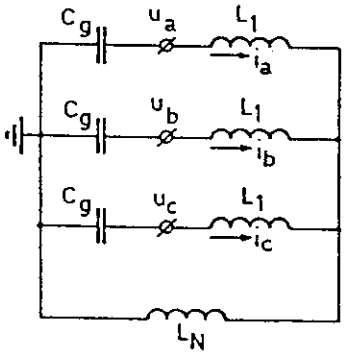

Figure A4.4.19 Inductively coupled reactors. Reduced scheme for third phase interruption.

Recovery voltages in the three phases are:

$$u_a(t) = \varepsilon^{-t''/\tau_5} U_{m35} \cos(\omega_5 t + \psi_{35}) + \varepsilon^{-t''/\tau_4} U_{ma34} \cos(\omega_4 t + \psi_{a34}) \qquad \text{(A4.4.37)}$$

$$u_b(t) = \varepsilon^{-t''/\tau_5} U_{m35} \cos(\omega_5 t + \psi_{35}) + \varepsilon^{-t''/\tau_4} U_{mb34} \cos(\omega_4 t + \psi_{b34}) \qquad \text{(A4.4.38)}$$

$$u_c(t) = \varepsilon^{-t''/\tau_5} U_{m35} \cos(\omega_5 t + \psi_{35}) + \varepsilon^{-t''/\tau_4} U_{mc34} \cos(\omega_4 t + \psi_{c34}) \qquad \text{(A4.4.39)}$$

with

$$U_{m35} = \sqrt{[K_1^2 + K_2^2]} \qquad U_{mb34} = \sqrt{[N_1^2 + N_2^2]}$$

$$K_1 = u_s(0) \qquad N_1 = u_b(30) - u_s(0)$$

$$K_2 = \frac{i_s(0)}{\omega_5 C_g} \qquad N_2 = \frac{i_b(30) - i_s(0)}{\omega_4 C_g}$$

$$\sin \psi_{35} = K_2/U_{m35} \qquad \sin \psi_{b34} = N_2/U_{mb34}$$

$$U_{ma34} = \sqrt{[M_1^2 + M_2^2]} \qquad U_{mc34} = \sqrt{[p_1^2 + p_2^2]}$$

$$M_1 = u_a(30) - u_s(0) \qquad P_1 = u_c(30) - u_s(0)$$

$$M_2 = \frac{i_a(30) - i_s(0)}{\omega_4 C_g} \qquad P_2 = \frac{i_c(30) - i_s(0)}{\omega_4 C_g}$$

$$\sin \psi_{a34} = M_2/U_{ma34} \qquad \sin \psi_{c34} = P_2/U_{mc}34$$

$$u_s(0) = \frac{1}{3}[u_a(30) + u_b(30) + u_c(30)] \qquad \omega_4^2 = 1/L_1 C_g$$

$$i_s(0) = \frac{1}{3}[i_a(30) + i_b(30) + i_c(30)] \qquad \omega_5^2 = 1/C_g(L_1 + 3L_N)$$

Comparing these results with the foregoing (eqs. A4.4.24 to A4.4.26) shows exactly the same formula's as in case of capacitive couplings. The only difference (besides numerical values) exists in the initial conditions: The somewhat longer damping time makes them less severe but the main frequency component may balance this effect.

Therefore all remarks on shape and amplitude as made in section A4.4.2.3 will also apply here.

A4.4.3.4. Reignition transfer through inductive coupling

Without any capacitive coupling the "second parallel oscillation" is not expected to penetrate into other phases because its frequency is much too high. So virtual current chopping due to the inductive coupling is not to be expected. However, Damstra [11] reported that virtual current chopping even is possible through the small mutual inductances between the conductors connecting the breaker to the supply network and the load. All other remarks on reignition transfer as made in section A4.4.2.4. will also apply here.

A4.4.4. With grounded neutral, inductive and capacitive coupling

($C_N = \infty$; $C_\ell \neq 0$; $C_g = C_0$; $C_1 = C_g + 3C_\ell$; $L_1 = L + M$; $L_0 = L - 2M$; $L_N = \frac{1}{3}(L_0 - L_1)$)

The case of combined inductive and capacitive coupling has no essential new aspects compared to what is said in clauses A4.4.2 and A4.4.3. All expressions for TRV's and initial conditions have exactly the same form as in clause A4.4.3, only the capacitor values in the voltage amplitudes and frequencies differ.

Therefore there is no fundamental reason for higher overvoltages due to the extra capacitive coupling. But compared to inductive coupling solely, all frequencies are smaller due to the larger capacitances and this effects also smaller damping constants $1/\tau$. So the initial conditions from the foregoing transients may be larger at the moment of second and third pole clearance and this may result in higher overvoltages.

Because the expressions for combined inductive and capacitive coupling cover also all foregoing results they are given here in a complete and general form. The more specific expressions of clauses A4.4.1, A4.4.2 and A4.4.3 may be found by introducing adequate zero values for C_ℓ and/or L_N, as are indicated under the clause headings.

A4.4.4.1. Compiled expressions for TRV's in switching three-phase inductances with grounded neutral (Scheme Figure A4.3.1.; $C_N = \infty$).

System voltages

$$e_a(t) = E_m \cos(\omega t + \phi)$$
$$e_b(t) = E_m \cos(\omega t + \phi - 120^\circ)$$
$$e_c(t) = E_m \cos(\omega t + \phi - 240^\circ)$$

Symmetrical currents

$$i_a(t) = I_{m3} \sin(\omega t + \phi) \text{ etc.}$$

$$I_{m3} = E_m/\omega L_1$$

$$\omega = \textit{main frequency} = 2\pi/T;$$

A4.4.4.1.1 First pole clearance at t = 0; pole "a".

Initial conditions: $u_a(10) = E_m \cos\phi$

Chopping current: $i_a(10) = I_{m3} \sin\phi = I_0$

This chopping level is also accepted in second and third pole interruption.

Recovery voltage:

$$\boxed{u_a(t) = -\lambda e_a(t) + \epsilon^{-t/\tau_j} U_{1j} \cos(\omega_j t + \psi_{1j})}$$

$$u_{1j} = (1+\lambda)\sqrt{(P_1^2 + P_2^2)} \qquad \sin\psi_{1j} = (1+\lambda) P_2/U_{1j}$$

$$P_1 = u_a(10) \qquad \omega_j^2 = \frac{2L_N + L_1}{L_1 (C_g + 2C_0)(3L_N + L_1)}$$

$$P_2 = i_a(10)\,\omega_j L_1 \qquad \lambda = L_N/(L_1 + 2L_N)$$

$$1/\tau_j = \textit{damping factor of } \omega_j - \textit{circuit.}$$

(Note: $\sin\Psi_{ij}$ is negative in case of current chopping before current zero. λ is negative in case of inductive coupling through three-legged cores.)

A4.4.4.1.2 Second pole clearance at t = t_1, pole "c"

Two-phase currents for $0 < t < t_1$:

$$i_b = I_{m2} \sin(\omega t + \phi - 120^\circ + \phi_0)$$
$$i_c = I_{m2} \sin(\omega t + \phi - 240^\circ - \phi_0)$$

$$\sin(\omega t_1 + \phi - 60^\circ - \phi_0) = \frac{I_{m3}}{I_{m2}} \sin\phi \qquad \phi_0 = \tan^{-1}\left\{\frac{\lambda\sqrt{3}}{2-\lambda}\right\} \textit{ (this defines } t_1\textit{)}$$

$$I_{m2} = \{\sqrt{(1 - \lambda + \lambda^2)}\}\, I_{m3}$$

Initial conditions:

$$u_a(20) = \lambda\{u_b(20) + u_c(20)\} + \sigma_j U_{1j} \cos\beta$$
$$u_b(20) = E_m \cos(\omega t_1 + \phi - 120^\circ)$$
$$u_c(20) = E_m \cos(\omega t_1 + \phi - 240^\circ)$$

$$i_a(20) = \sigma_j\,\omega_j\,(C_g + 2C_\ell)\,U_{1j}\sin\beta$$

$$i_b(20) = I_{m2}\sin(\omega t_1 + \phi - 120^\circ + \phi_0)$$

$$i_c(20) = I_{m2}\sin(\omega t_1 + \phi - 240^\circ - \varphi_0) = \Big\}\ \textit{chopping current}$$

$$= -I_{m2}\sin(\omega t_1 + \varphi - 60^\circ - \phi_0) \simeq i_a(10)$$

$$\sigma_j = \exp.(-t_1/\tau_j) \qquad \beta = \omega_j t_1 + \psi_{1_j}$$

β = phase angle in u_a and t_a at $t = t_1$. By varying β between -180° and $+180^\circ$ all possible TRV's are obtained.

$$t_1 = \left\{\frac{I_{m3} - I_{m2}}{I_{m2}}\,\phi + 60^\circ + \phi_0\right\}\frac{T}{360^\circ}\ \text{si}\ \textit{if}\ I_0 \ll I_m$$

Recovery voltages ($t' = t - t_1$)

$$u_a(t) = \nu\,e_b(t) + \varepsilon^{-t'/\tau k}\,U_{2k}\cos(\omega_k t' + \psi_{2k}) + \varepsilon^{-t'/\tau n}\,U_{2n}\cos(\omega_n t' + \psi_{2n})$$

$$u_c(t) = \nu\,e_b(t) + \varepsilon^{-t'/\tau k}\,U_{2k}\cos(\omega_k t' + \psi_{2k}) - \varepsilon^{-t'/\tau n}\,U_{2n}\cos(\omega_n t' + \psi_{2n})$$

$$U_{2k} = \sqrt{(Q_1^2 + Q_2^2)}\ ;\ \sin\psi_{2k} = Q_2/U_{2k} \qquad U_{2n} = \sqrt{(R_1^2 + R_2^2)}\ ;\ \sin\psi_{2n} = R_2/U_{2n}$$

$$Q_1 = \frac{1}{2}\{u_a(20) + u_c(20)\} - \nu\,e_b(t_1) \qquad R_1 = \frac{1}{2}\{u_a(20) - u_c(20)\}$$

$$Q_2 = \frac{1}{2}\,\frac{i_a(20) + i_c(20)}{\omega_k(C_g + C_\ell)} + \frac{\nu\,e_b'(t_1)}{\omega_k} \qquad R_2 = \frac{1}{2}\{i_a(20) - i_c(20)\}\,\omega_n L_1$$

$$\omega_k^2 = \frac{L_N + L_1}{L_1(C_g + C_\ell)(3L_N + L_1)} \qquad \nu = \frac{L_N}{L_1 + L_N} \qquad \omega_n^2 = \frac{1}{L_1(C_g + 3C_\ell)}$$

$$e_b'(t_1) = -E_m\,.\,\omega\sin(\omega t_1 + \phi - 120^\circ)$$

A4.4.4.1.3 Third pole clearance at $t = t_2$; pole "b"

Single phase current for $t_1 < t < t_2$:

$$i_b = I_{m1}\ \sin\ (\omega t + \phi - 120^\circ)$$

$$t_2 \simeq \frac{1}{3}T$$

$$I_{m1} = I_{m3}\left(\frac{L_1}{L_1 + L_N}\right)$$

Initial conditions:

$$u_a(30) = \nu\,u_b(30) + \sigma_k\,U_{2k}\cos\beta_1 + \sigma_n\,U_{2n}\cos\beta_2$$

$$u_b(30) = E_m\cos(\omega t_2 + \phi - 120^\circ)$$

$$u_c(30) = \nu\,u_b(30) + \sigma_k\,U_{2k}\cos\beta_1 - \sigma_n\,U_{2n}\cos\beta_2$$

$$i_a(30) = \sigma_k\,\omega_k(C_g + C_\ell)\,U_{2k}\sin\beta_1 + \sigma_n\,\omega_n(C_g + 3C_\ell)\,U_{2n}\sin\beta_2$$

$$i_b(30) = I_{m1}\sin(\omega t_2 + \phi - 120^\circ) = \Big\}\ \textit{chopping current}$$

$$i_c(30) = \sigma_k\,\omega_k(C_g + C_\ell)\,U_{2k}\sin\beta_1 - \sigma_n\,\omega_n(C_g + 3C_\ell)\,U_{2n}\sin\beta_2$$

$$\sigma_k = \exp.\{(t_1 - t_2)/\tau_k\} \qquad \beta_1 = \omega_k(t_2 - t_1) + \psi_{2k}$$

$$\sigma_n = \exp.\{(t_1 - t_2)/\tau_k\} \qquad \beta_2 = \omega_n(t_2 - t_1) + \psi_{2k}$$

β_1, β_2 are phase angles in $u_a(30)$, $i_a(30)$ and $u_c(30)$, $i_c(30)$ respectively.

Recovery voltages ($t'' = t - t_2$)

$$u_a(t) = \varepsilon^{-t''/\tau_m} U_{3m} \cos(\omega_m t'' + \psi_{3m}) + \varepsilon^{-t''/\tau_n} U_{a3n} \cos(\omega_n t'' + \psi_{a3n})$$

$$u_b(t) = \varepsilon^{-t''/\tau_m} U_{3m} \cos(\omega_m t'' + \psi_{3m}) + \varepsilon^{-t''/\tau_n} U_{b3n} \cos(\omega_n t'' + \psi_{b3n})$$

$$u_c(t) = \varepsilon^{-t''/\tau_m} U_{3m} \cos(\omega_m t'' + \psi_{3m}) + \varepsilon^{-t''/\tau_n} U_{c3n} \cos(\omega_n t'' + \psi_{c3n})$$

$$U_{3m} = \sqrt{(S_1^2 + S_2^2)} \qquad U_{b3n} = \sqrt{(V_1^2 + V_2^2)}$$

$$S_1 = u_s(0) \qquad V_1 = u_b(30) - u_s(0)$$

$$S_2 = \frac{i_s(0)}{\omega_m C_g} \qquad V_2 = \{i_b(30) - i_s(0)\}\,\omega_n L_1$$

$$\sin\psi_{3m} = S_2/U_{3m} \qquad \sin\psi_{b3n} = V_2/U_{b3n}$$

$$U_{a3n} = \sqrt{(T_1^2 + T_2^2)} \qquad U_{c3n} = \sqrt{(W_1^2 + W_2^2)}$$

$$T_1 = u_a(30) - u_s(0) \qquad W_1 = u_c(30) - u_s(0)$$

$$T_2 = \{i_a(30) - i_s(0)\}\omega_n L_1 \qquad W_2 = \{i_c(30) - i_s(0)\}\,\omega_n L_1$$

$$\sin\psi_{a3n} = T_2/U_{a3n} \qquad \sin\psi_{c3n} = W_2/U_{c3n}$$

$$u_s(0) = \frac{1}{3}\{u_a(30) + u_b(30) + u_c(30)\}$$

$$i_s(0) = \frac{1}{3}\{i_a(30) + u_b(30) + i_c(30)\}$$

$$\omega_m^2 = \frac{1}{C_g(L_1 + 3L_N)} \qquad \omega_n^2 = \frac{1}{L_1(C_g + 3C_\ell)}$$

$u_a(10)$ and $u_b(30)$ may be taken E_m except for small I_m ($I_m < 3I_0$); $u_c(20)$ may be taken E_m except for small I_m or for inductively coupled reactors. See last remark of section A4.4.1.1. for all angles ψ.

A4.4.4.2. Examples of TRV's in inductively coupled reactors with solidly grounded neutral

To find comparable graphs to Figure A4.4.14 the same power, voltage, frequency, overvoltage factor and time constant were taken: 30 Mvar, 36 kV, 50 Hz, $k_a = 2$, $\tau = 4.8.10^{-3}$s. Further $L_0 = 0.3\ L_1$, so $3\ L_N = -0.7L_1$.

Figure A4.4.20 is with and Figure A4.4.21 is without capacitive coupling. Both cases start with $C_g = 10$nF in the set no. 1, where again $C_\ell = 3$nF in Figure A4.4.20.

Developing frequencies are $f_{j,k,n,m}$ = 4520, 6010, 3110 and 7820 Hz (Figure A4.4.20) and $f_{j,k,n,m}$ = 5720, 6850, 4290 and 7820 Hz (Figure A4.4.21) respectively.

Chapping currents are $I_0 = (-)$ 19.5 A in Figure A4.4.20 and $I_0 = (-)$ 15.4 A in Figure A4.4.21. The time interval t_1 was $t_1 = 2.39$ ms, in both cases.

As before the next 6 oscillograms show the TRV's each time after a further 60 degrees phase shift in initial conditions at t(20). In Figure A4.4.20 the steps are $\Delta C_g = 0.35$ nF and $\Delta C_\ell = 0.10$ nF. In Figure A4.4.21 C_g is varied in steps $\Delta C_g = 0.293$ nF.

These oscillograms are still more complex than without inductive coupling. The reasons for this are the main frequency components in phases "a" and "c" after first and second pole clearance, and the larger differences than before between ω_k and ω_n and between ω_m and ω_a.

The maximum overvoltages are a little more than 2 p.u. but even somewhat lower than with capacitive coupling solely. Overvoltages higher than the recovery peak are principally possible.

Figure A4.4.22 is an enlargement of Figure A4.4.20, phase "a", no. 4, to show the combined effect of the multi-frequency components in more details.

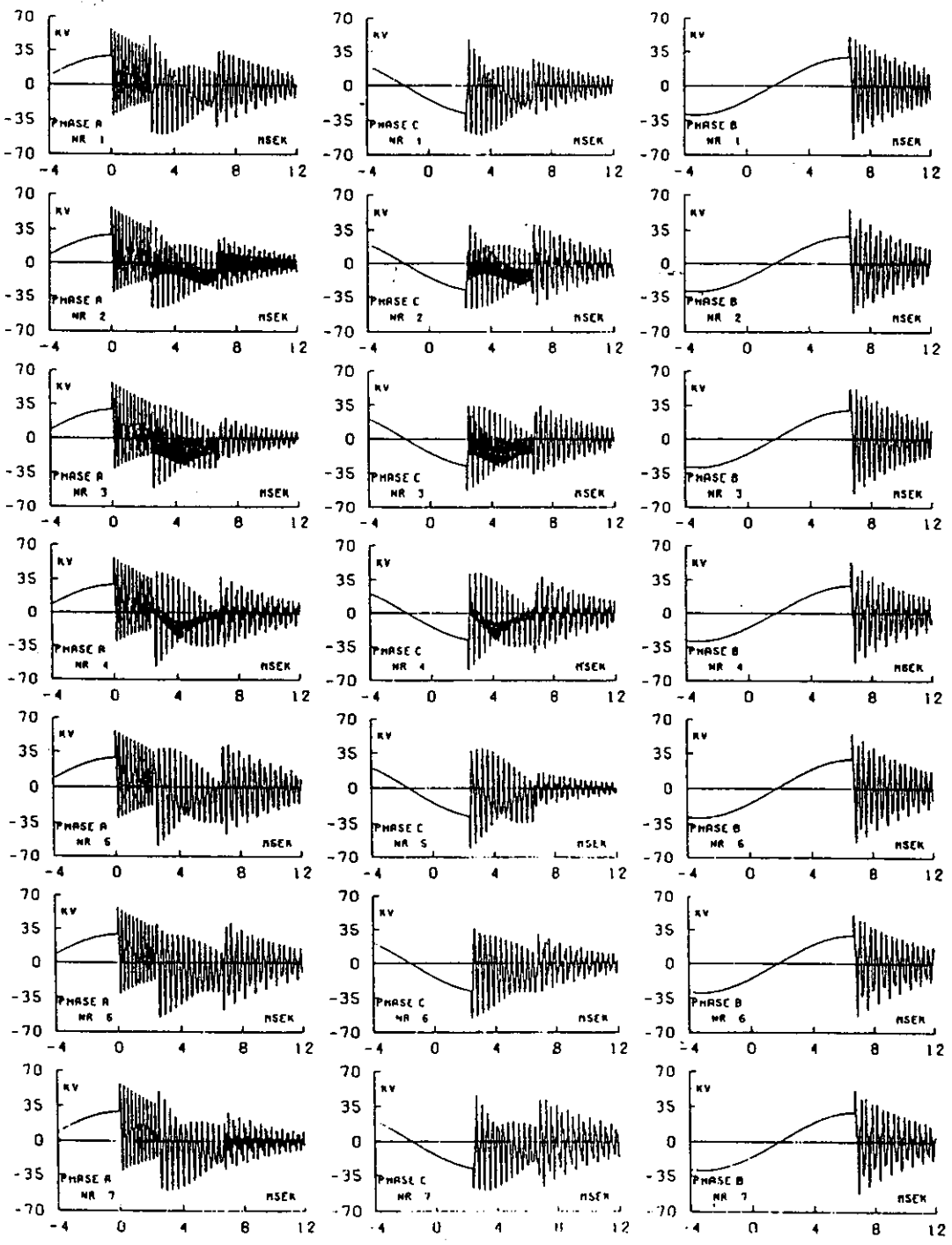

Figure A4.4.20 Examples of TRV's during interruption of reactors with inductive and capacitive coupling.(For data see text)

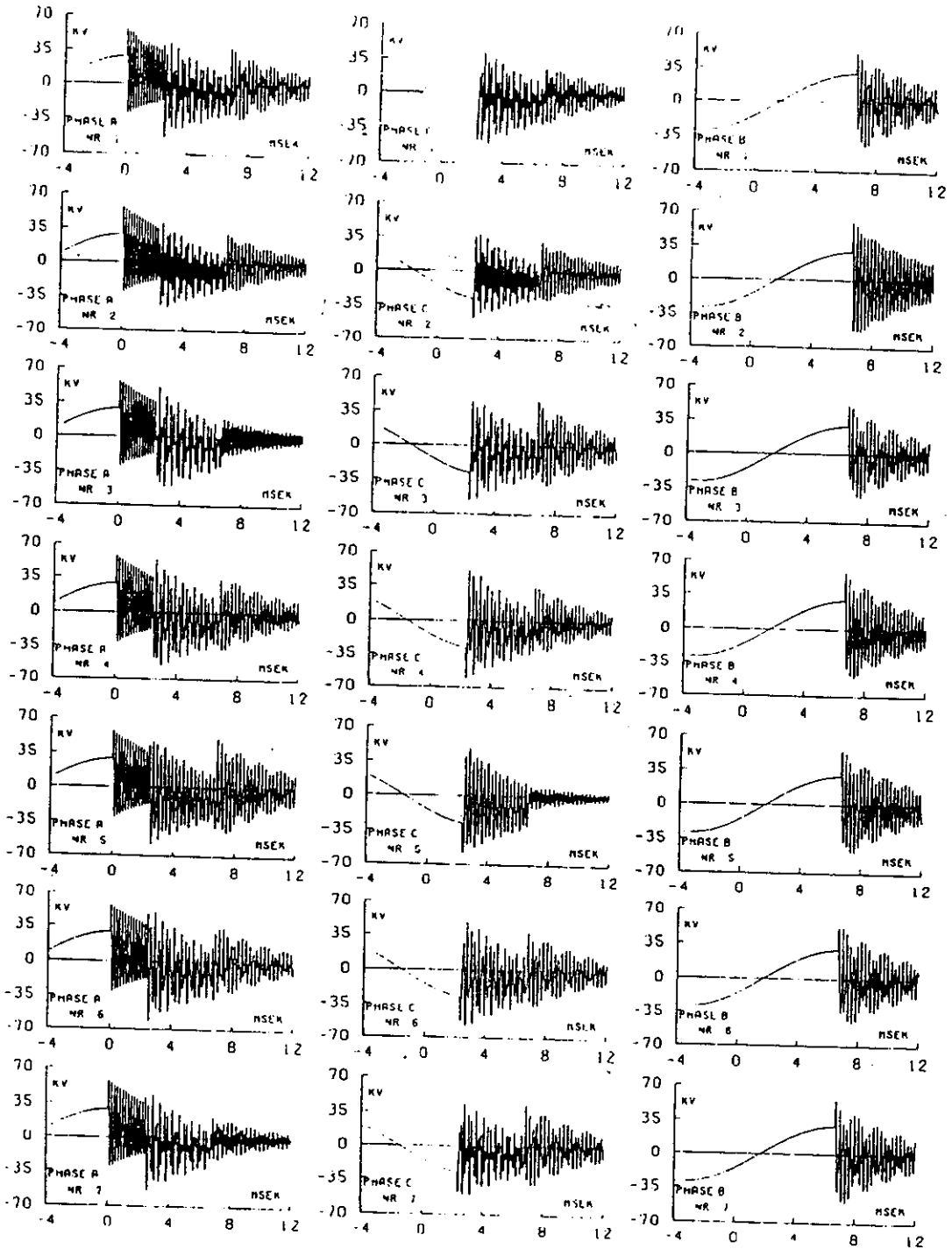

Figure A4.4.21 Examples of TRV's during interruption of reactors with inductive coupling solely. (For data see text)

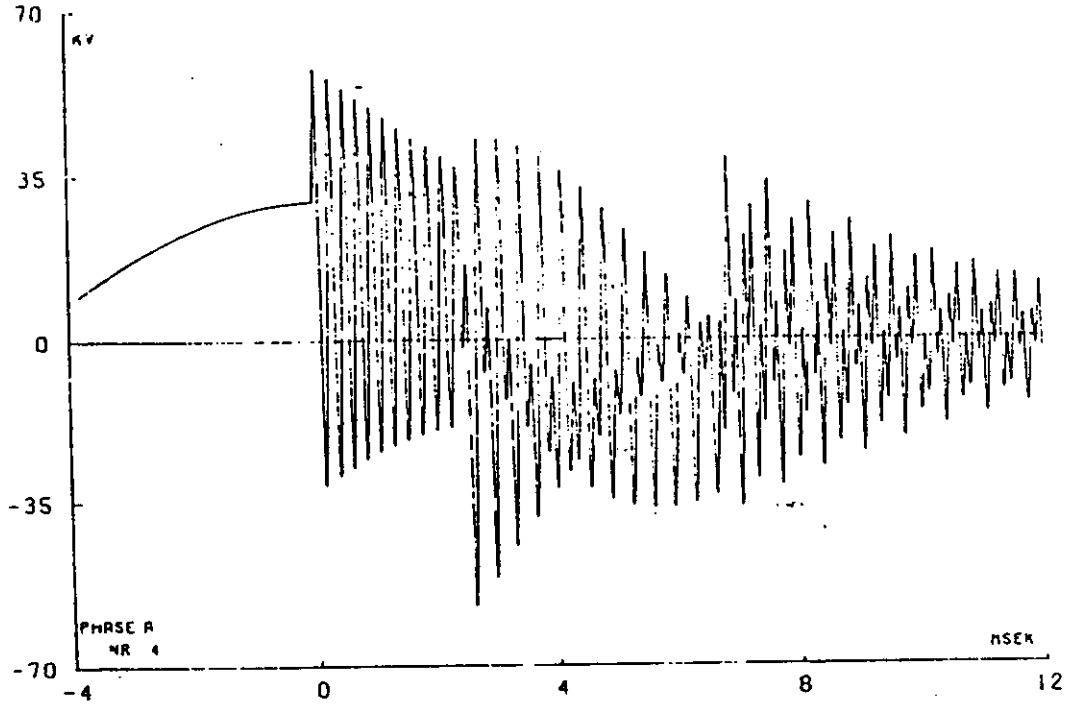

Figure A4.4.22 Enlargement of graph No. 4, phase "a" of Figure A4.4.20.

A4.5. CONCLUSIONS

The inductive and capacitive couplings between phases complicate the whole interruption procedure of three-phase reactors, mainly affecting the recovery voltages of all phases, in both magnitude and frequency of oscillation. The interaction between phases is twofold. At first, the recovery voltage of the first phase to clear is influenced by the presence of the other two phases. Then, each successive interruption of any other phase reforms the shape of the recovery voltage of the previously interrupted phases.

The relevant expressions of recovery voltages allow for estimation of the respective contribution in each case.

A4.6. ACKNOWLEDGEMENTS

The authors wish to thank Dr. V.K.I. Kalasek for preparing the computer plots of Figures A4.4.14, A4.4.20, A4.4.21 and A4.4.22.

A4.7 REFERENCES IN APPENDIX 4

[3] E.J. Tuohy, J. Panek. – Chopping of transformer magnetizing currents, Part I: Single phase transformers, IEEE-Trans. PAS-97 (1978), p. 261-268.

[4] S. Ihara, J. Panek, E.J. Tuohy. – Chopping of transformer magnetizing currents, Part II: Three-phase transformers. To be published in IEEE-Trans. PAS.

[6] M. Murano et al. – Current chopping phenomena of medium voltage circuit breakers, IEEE Trans. PAS-96 (1977), p. 143-149.

[7] G.E. Gardner, R.J. Urwin. – Arc instability and current chopping in an air-blast interrupter, Proc. IEE 124 (1977), p. 619-627.

[8] G.C. Damstra. – Current chopping and overvoltages in relation to system parameters, CIGRE Paper, 120, (1964).

[9] S. Berneryd et al. – Switching of shunt reactors. Comparison between field and laboratory tests, CIGRE Paper 13–04 (1976).

[10] M. Murano et al. – Voltage escalation in interrupting inductive currents by vacuum switches, IEEE Trans. PAS–93 (1974), p. 264–271.

[11] G.C. Damstra. – Virtual chopping phenomena on switching three–phase inductive circuits, CIGRE Coll. SC13, Helsinki (1981), Report 13–81 (SC) 21.

[12] M. Muran et al. – Three–phase simultaneous interruption in interrupting inductive current using vacuum switches, IEEE Trans. PAS–93, (1974), p. 272–280.

[13] J. Panek, K.G. Fehrle. – Overvoltage phenomena associated with virtual current chopping in three phase circuits. IEEE Trans. PAS–94 (1975), p. 1317–1325.

[14] W.M.C. van den Heuvel. – Overvoltages after current chopping in a three–phase inductive circuit with isolated neutral, IEEE Trans. PAS–100 (1981), p. 4795–4801.

[15] E. Slamecka, W. Waterschek. – Schaltvorgänge in Hoch – und Niederspannungsnetzen, Book, Siemens Aktiengesellschaft Berlin and Munich, (1972).

[16] W.M.C. van den Heuvel. – Interruption of small inductive currents in a.c. circuits. Thesis Eindhoven (1966).

[17] P. le Verre. – Les surtensions lors de la coupure de faible courants inductifs en haute tension, Revue Générale de l'Electricité 72 (1963), p. 91–109.

Appendix 5

INTERACTION BETWEEN PHASES IN THREE-PHASE REACTOR SWITCHING

Part II: Ungrounded Reactors

by

W.M.C. VAN DEN HEUVEL and B.C. PAPADIAS

ABSTRACT

The second part of the Paper treats the phenomena associated with the interruption procedure in three-phase reactors with ungrounded neutral, in star or delta connection. The circuit reaction and the relevant electrical phenomena in this case are much more complicated, compared to the switching of grounded reactors examined in Part I (Appendix 4).

The Paper follows the same steps as in Part I, examining successively the interruption of each phase with all kind of interphase coupling, i.e. with no coupling at all, capacitive interphase coupling only, inductive coupling only and both inductive and capacitive coupling. The emphasis in each case is given to the derivation and interpretation of analytical expressions for the chopping and transfer transient recovery voltages, which are the important factors of the switching procedure and also an evidence of the interaction between phases.

Attention is also paid to the DC-potential-to-ground due to non-simultaneous current chopping and to worst-case calculation of overvoltages.

A5.1. INTRODUCTION

In a first Paper (Appendix 4) on current chopping in three-phase inductive circuits a general summary of the phenomena occurring was given. Thereafter single-phase and three-phase star-connected inductances with solid or low-impedance inductive grounding of the neutral were treated.

This Paper continues with ungrounded reactors in star or delta connection with or without interphase coupling.

A5.1.1. Simplifications and equivalent scheme

All calculations are based on the same simplifications as presumed in Part I, clause A4.3. Also the same general representation of the reactor circuit will be applied again (Fig A5.1.1). Positive voltage and current directions are, as before, indicated in the transferred components diagram of Figure A5.1.2.

In the phenomena treated in this Part II the neutral to ground capacitance C_N is not shorted by an earth connection. Therefore the transients in ungrounded reactors may be still more complicated than in the grounded cases, especially in star connected reactors on 3-legged iron cores, where $L_N \neq 0$ as well as $C_N \neq 0$.

A5.1.2. Delta-connected reactors

Delta-connected reactors have no neutral-to-ground capacitances. Therefore their representation can be simplified from Figure A5.1.3 to Figure A5.1.4 by delta-star transformation. In this equivalent scheme the currents through the transferred inductances L_1 are the real line currents, in contrast with the original delta-circuit currents.

Figure A5.1.4 may be regarded as a special case of Figure A5.1.2 viz with $L_N = \infty$. Therefore all results from Part I may be applied, provided the justified values for the circuit elements are introduced.

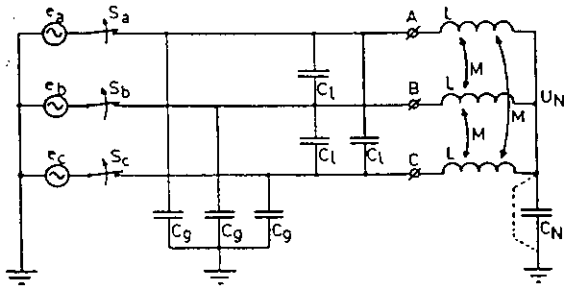

Figure A5.1.1 General representation of the three-phase symmetrical reactor circuit in star-connection

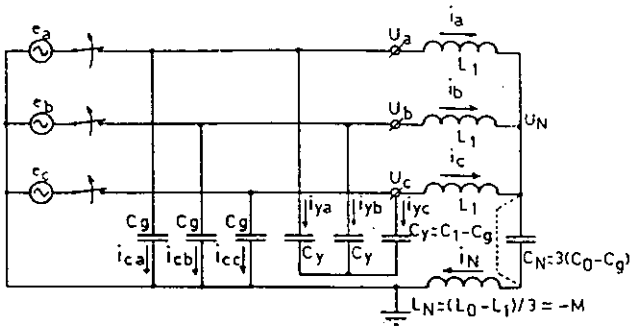

Figure A5.1.2 As Figure A5.1.1 with transferred (positive and zero-sequence components

$C_1 = C_g + 3C_\ell$; $C_0 = C_g + \frac{1}{3}C_N$; $L_0 = L - 2M$; $L_1 = L + M$
(M is taken as positive)

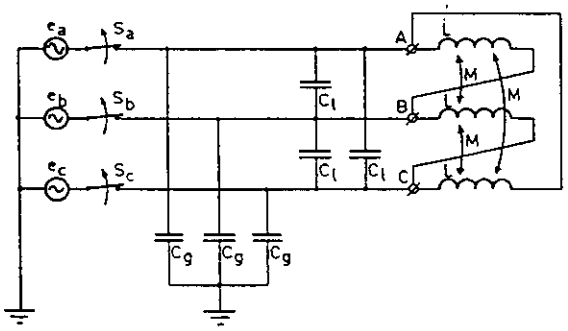

Figure A5.1.3 General representation of the three-phase symmetrical reactor circuit in delta connection

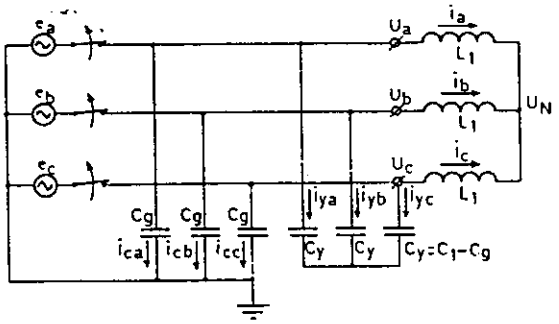

Figure A5.1.4 As Figure A5.1.3 with transferred components

$L_1 = \frac{1}{3}(L + M)$; $C_1 = C_g + C_\ell$

It is often more convenient to regard Figure A5.1.4 as a special case of Figure A5.1.2 viz with $C_N = 0$. This is done in the Sections A5.2.1.2 and A5.2.3.1. The same scheme can be used for calculation of overvoltages in circuits with long connections between circuit-breaker and inductances, when the normal sequence capacitance C_1 is much larger than the neutral-to-ground capacitance C_N.

A5.1.3. System voltages, currents and initial conditions

As before (see A4.4.4.1 of part I) system voltages are:

$$\begin{aligned} e_a(t) &= E_m \cos(\omega t + \phi) \\ e_b(t) &= E_m \cos(\omega t + \phi - 120^o) \\ e_c(t) &= E_m \cos(\omega t + \phi - 240^o) \end{aligned} \qquad (A5.1.1)$$

Symmetrical currents are:

$$i_a(t) = I_{m3} \sin(\omega t + \phi) \quad etc.$$
$$I_{m3} = E_m/\omega L$$
ω = main frequency = $2\pi/T$.

First pole clearance occurs at t = t(10) = 0; pole "a" (see Fig. A5.1.5 for time-coordinates). After that the transient voltage-to-ground $u_a(t)$ will consist of one or more h.f.-components superimposed on a main frequency contribution of - 1/2 $e_a(t)$, see Figure A5.1.6 and Figure A4.1.4 of Part I.

Therefore the recovery peak after first pole clearance will be approximately 1 p.u. higher as compared with the cases with grounded neutral.

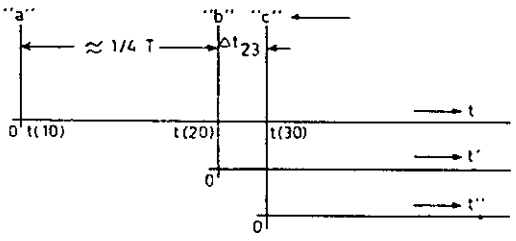

Figure A5.1.5 Time-coordinates

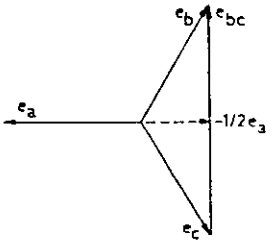

Figure A5.1.6 Voltage system

Initial conditions for first pole clearance are:

$$u_a(10) = E_m \cos \phi$$
$$i_a(10) = I_{m3} \sin \phi = I_0 \text{ (chopping current)}$$

The same chopping level will be accepted in the second and third pole interruption. In general $I_0 \ll I_{m3}$ and cos $\phi \approx 1$, where $\phi < 0$.

After first pole interruption the remaining line voltage is:

$$e_{bc}(t) = E_m \sqrt{3} \sin(\omega t + \phi) \approx - I_{m2} \cos\omega t \qquad \text{(A5.1.2)}$$

so

$$i_b(t) = - i_c(t) = -I_{m2} \cos(\omega t + \phi) \approx I_{m2} \cos\omega t \qquad \text{(A5.1.3)}$$

$$I_{m2} = E_m \sqrt{3}/2\omega L_1$$

At about 90 degrees after interruption of phase "a" the current through the other two phases approaches zero and will chop. Now the two arcs are never in exactly the same condition.
This is not only because of statistical variations, but also because the residual of the transient current in the a-phase will partly take its way through the two other phases, where $i_b \approx - i_c$. So the phase currents i_b and i_c will alternately and by turns be increased and decreased by a same part of i_a and this will influence their moment of chopping. But if one current, say i_b, at t =(20) is forced to zero, i_c can only flow back through the circuit capacitances and will also chop at t(30), a small time delay Δt_{23} after t(20).

For simultaneous current chopping ($\Delta t_{23} = 0$) the initial conditions are:

$u_a(30)$ = remnant of the first phase transient voltage $u_a(t)$ after 1/4 T.
$u_b(30) = \frac{1}{2}E_m\sqrt{3} \cos\phi' \approx \frac{1}{2}E_m\sqrt{3}$
$u_c(30) = -\frac{1}{2}E_m\sqrt{3} \cos\phi' \approx -\frac{1}{2}E_m\sqrt{3}$

$i_a(30)$ = remnant of first phase transient current after 1/4 T.
$i_b(30) = I_{m2} \sin\phi' = I_0$
$i_c(30) = -I_{m2} \sin \phi' = -I_0$

so

$$\frac{\sin\phi'}{\sin\phi} = \frac{2}{3}\sqrt{3} \qquad \text{(A5.1.4)}$$

Although the quality factor of reactor circuits generally high $u_a(t)$ will be damped out by far at t(30). So the average charge voltage of the three phases

$$u_s(0) = \frac{1}{3}[u(30) + u_b(30) + u_c(30)$$

is small after simultaneous chopping.

During non-simultaneous chopping the transient in phase "b" will start at t(20). Then it is possible that $u_b(t)$ has already approached its maximum at t(30) and in that case $u_s(0)$ may have a substantial value. This means that

all transients are superimposed on a relatively high d.c.–potential to earth from which $u_s(0)$ is the main component, (see e.g. eq. (A5.2.9)).

For this reason a worst case calculation of transient overvoltages must involve a critical time delay Δt_{23} between t(20) and t(30).

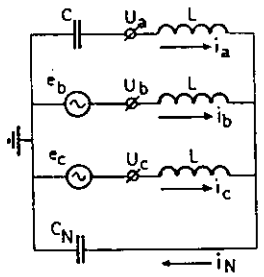

Figure A5. 2.1 Equivalent scheme for first phase interruption of ungrounded reactors. No interphase coupling.

A5.2. REACTORS WITHOUT INTERPHASE COUPLING

($C_N = \infty$; $C_\ell = 0$; $C_1 = C_g = C$; $M = 0$; $L_1 = L$; $L_N = 0$)

Even without any interphase coupling, current chopping in ungrounded reactors will introduce higher and often more complicated overvoltages than in the grounded state.

A5.2.1. First phase interruption (phase "a")

After contact separation of the breaker poles current interruption followed by recovery voltage and reignitions succeed each other every 60° until the first pole clears. Assuming this is phase "a" the reduced scheme of Fig. A5.2.1 will be valid and the next phenomena will occur:

At the instant of current chopping the source voltage e_a will almost have its crest value E_m, see section A5.1.3. Prior to clearing of any phase, the voltage to ground u_N of the reactor ungrounded neutral is at zero, due to the circuit and voltage symmetries and accordingly $i_N = 0$. After clearing of phase "a" the neutral moves away from ground potential through a transient oscillation towards the midpoint of the line voltages e_{bc}, so that u_N will take a final value equal to $-1/2\ e_a(t)$. The potential oscillation of point N presumed energy transfer through the phase and neutral connection inductances and capacitances L_1, C and C_N.

The energy trapped in L_1 and C will oscillate between L_1 and the capacitance C of phase "a", through the other two phases and the source neutral. The voltage u_a, developing across this capacitance will determine the recovery voltage of the clearing phase. The voltages u_b and u_c, at the other two phases, are held fixed by the source voltages e_b and e_c, whereas the currents i_b and i_c will undergo transient oscillations.

Phase voltages and initial conditions are given in section A5.1.3. Current chopping occurs at t = t(10) = 0. The expression for the transient recovery voltage between phase "a" and earth is:

$$u_a(t) = -\frac{1}{2}\,e_a(t) + \varepsilon^{\prime\prime\prime\prime 11}\,U_{m11}\cos(\omega_{11}t + \psi_{11}) + \varepsilon^{\prime\prime\prime 12}\,U_{m12}\cos(\omega_{12}t + \psi_{12}) \qquad \text{(A5.2.1)}$$

with

$$U_{m11} = \alpha\sqrt{[A_1^2 + A_2^2]} \qquad U_{m12} = \beta\sqrt{[B_1^2 + B_2^2]}$$

$$A_1 = u_a(10) \qquad B_1 = u_a(10)$$

$$A_2 = i_a(10)\,\omega_{11}L_1 \qquad B_2 = i_a(10)\,\omega_{12}L_1$$

$$\sin\psi_{11} = \alpha A_2/U_{m11} \qquad \sin\psi_{12} = \beta B_2/U_{m12}$$

$$\alpha = 1/2\left\{1 + \frac{1 - C^*}{(1 + C^*)\,D^*}\right\}\left(\frac{\omega_o}{\omega_{11}}\right)^2 \qquad \beta = 1/2\left\{1 - \frac{1 - C^*}{(1 + C^*)\,D^*}\right\}\left(\frac{\omega_o}{\omega_{12}}\right)^2$$

$$\beta = 1.5 - \alpha$$

$$C^* = \frac{C_N}{3C} \qquad D^* = \sqrt{\left\{1 - \frac{8C^*}{3(1 + C^*)^2}\right\}}$$

$C = C_s + 2C_t$ but C_t is taken zero (no interphase coupling).

$$\omega_o^2 = \frac{1}{L_1C}\,; \quad \omega_{11}^2 = \frac{1 + C^*}{2C^*}(1 - D^*)\,\omega_o^2\,; \quad \omega_{12}^2 = \frac{1 + C^*}{2C^*}(1 + D^*)\,\omega_o^2$$

Even after the first phase interruption a double frequency oscillation occurs, superimposed on the main voltage component $- 1/2\ e_a(t)$.

As before $1/\tau_{11}$ and $1/\tau_{12}$ are simplified representations of the relevant damping factors. Very short or long connections between c.b. and reactors give a simplification.

A5.2.1.1. Short connections between c.b. and reactors

Each reactor leg may now be represented by a line pi-section with the total capacitance to ground of each leg ($2C_g$) equally divided between the two leg ends. So the ungrounded reactor neutral is in fact connected to ground through $C_N = 3C_g$.

Then in eq. (A5.2.1):

$$C^* = 1 \qquad D^* = \frac{1}{3}\sqrt{3}$$

$$\alpha = \frac{3}{4}\left(1 + \frac{1}{3}\sqrt{3}\right) \simeq 1.18 \qquad \beta = \frac{3}{4}\left(1 - \frac{1}{3}\sqrt{3}\right) \simeq 0.32$$

$$\omega_{11}^2 = \omega_o^2\left(1 - \frac{1}{3}\sqrt{3}\right) \simeq 0.42\ \omega_o^2 \qquad \omega_{12}^2 = \omega_o^2\left(1 + \frac{1}{3}\sqrt{3}\right) = 1.58\ \omega_o^2$$

The transient recovery voltage is still a double frequency phenomenon. Examples are given in Figure A5.6.1. The maximum overvoltage will be smaller in the next case.

A5.2.1.2. Long connections between c.b. and reactors or delta connected reactors

If $C_N \ll C$ the frequency ω_{12} is high and its amplitude U_{m12} is very small.

Putting $C_N \to 0$ in eq. (A5.2.1) leads to $C^* \to 0$; $D^* \to 1$; $a \to 3/2$; $\beta \to 0$; $\omega^2_{11} \to 2/3\ \omega^2_0$; $\omega^2_{12} \to \infty$.

So eq. A5.2.1 reduces to :

$$\boxed{u_o(t) = -\frac{1}{2}e_o(t) + \varepsilon^{-t/\tau_{10}}\ U_{m10}\cos(\omega_{10}t + \psi_{10})} \qquad \text{(A5.2.2)}$$

where now

$$U_{m10} = \frac{3}{2}\sqrt{\{E_1^2 + E_2^2\}}.$$

$$E_1 = u_o(10) \qquad \omega_{10}^2 = \frac{2}{3L_1C}$$

$$E_2 = i_o(10)\ \omega_{10}L_1 \qquad \sin\psi_{10} = \frac{3}{2}E_2/U_{m10}$$

The same result will be found from eq. (A4.4.27) of Part I by letting $L_N \to \infty$. It is illustrated by Figure A4.1.4 of Part I.

If $E_2 = 0$ this equation (2.2) is the well-known expression for the first pole recovery voltage during a three-phase fault clearing.

A5.2.1.3. Short connections versus long connections

The question when a connection may be regarded as being long depends on the influence of the ratio of C and C_N on the occurring frequencies and especially on their amplitude U_{m11} and U_{m12} in equation (A5.2.1).

In Figure A5.2.2 the ratios ω_{11}/ω_0 and ω_{12}/ω_0 and the amplitude factors α and β are plotted as a function of C^*. It may be concluded that the ω_{12}-component with its amplitude factor β has no significance for $C^* \leq 0.3$.

In general a connection may be regarded as being long when the total capacitance $C = C_g + 2C_\ell$ is at least of the same order of magnitude as the neutral-to-ground capacitance C_N. Typical characteristics of reactors and their connections are collected in [5] and briefly summarized in Chapter 4.

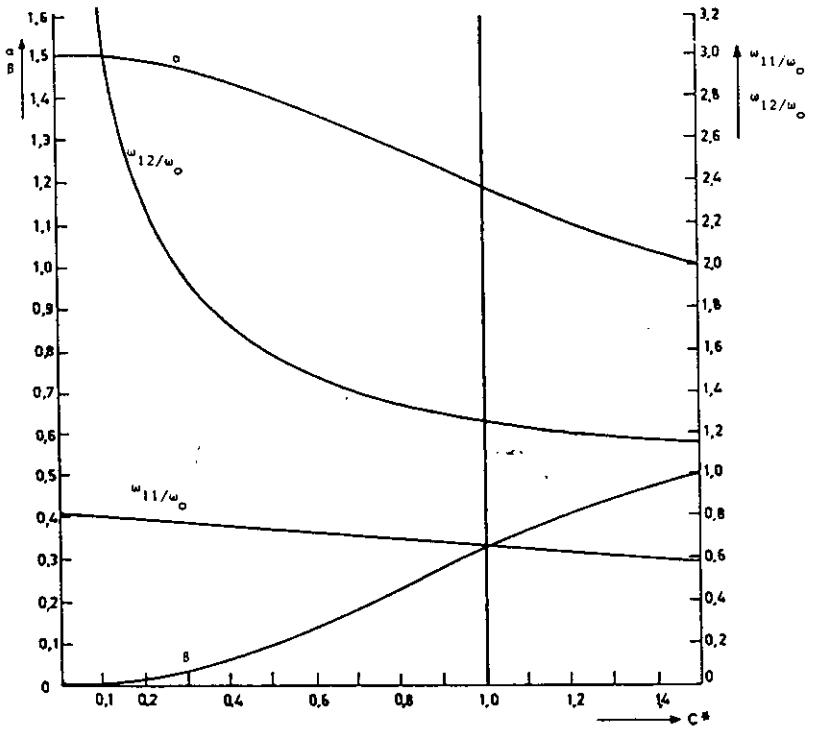

Figure A5.2.2 Example of frequency ratios and amplitude factors after first-phase interruption as a function of $C^* = C_N/3C$.

Calculations of overvoltages with eq. (A5.2.2) and thus neglecting the term with frequency ω_{12} will never yield too low results, provided $C/C_N > 1/3$.

Then the main transient frequency tends to $\omega_{11} = \sqrt{(2/3)} \cdot \omega_0$. This will even stronger apply when inductive coupling is present.

A5.2.2. Reignition after first pole clearance

By combining the Figures A4.1.3 and A4.1.4 of Part I, it will be clear that a reignition in the c.b. during the recovery peak may give an extremely high overvoltage. Theoretically it even may approach $k_a + 3$ p.u.

Such high values will seldom be attained in practical situations. The reason is not only the damping but also the fact that the source side is not at all "stiff" for the occurring h.f.-second parallel oscillation, which is of the order of 100 kHz or more, see Chapter 2. This may illustrated by Figure A5.2.3 which represents a single phase equivalent scheme for Figure A5.2.1 completed with some adequate source side elements.

Here $L'' \ll L_s$. The second parallel oscillation circuit is $C_g - C_s - L''$, through the reignited c.b.-pole S_a. Its current is:

$$i_{p2} = \frac{u_{C_s}(0) - u_a(0)}{\omega_{2p}^2 L''} \qquad \text{(A5.2.3)}$$

with $\omega_{2p}^2 = (C_g + C_s)/L''C_gC_s$

and $u_{Cs}(0) = E_m;\ u_a(0) = -(k_a + 1)E_m$

the expression for $u_a(t)$ after a reignition is found to be:

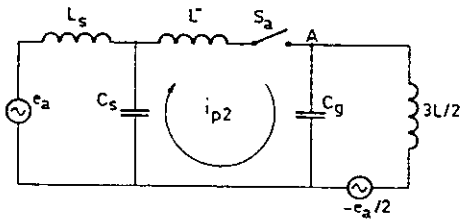

Figure A5.2.3 Equivalent circuit for second parallel oscillation after first pole interruption followed by a reignition.

$$u_a(t) = E_m \left\{ -(k_a + 1) - (k_a + 2)\frac{C_s}{C_s + C_g}\cos\omega_{2p}t \right\}$$

The maximum overvoltage will occur at $\omega_{2p} = \pi$ and this peak may theoretically reach to:

$$k_{max} = \frac{u_{a\,max}}{E_m} = \beta\,(k_a + 2) + 1 \qquad with \quad \beta = \frac{C_s - C_g}{C_s + C_g} \qquad \text{(A5.2.4)}$$

Only for $C_s \gg C_g$, (thus for a stiff source) and no damping, $\beta = 1$ and the theoretical maximum of $(k_a + 3)$ p.u. is attained.

If $C_s \approx C_g$, $\beta = 0$ and there will even be no reignition overvoltage at all. A normal value seems to be $\beta \approx 0{,}5$ according to Chapter 4.

This observation illustrates the significance of large and lumped capacitances in front of the c.b., such as are proposed by CIGRE Working Group 13.02 in the motor test scheme, Figure 3.7.2 of Chapter 3.

If C_s and L' are not lumped but distributed elements the occurring second parallel oscillation may be a more than single frequency phenomena which may reduce β to a lower value than given by eq. (A5.2.4).

It should finally be repeated here that also k_a itself is reduced if $C_s \gg C_g$ is not valid, see eq. (A4.4.13) of Part I.

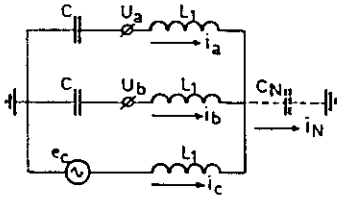

Figure A5.2.4 Equivalent scheme for second phase interruption. No interphase coupling.

A5.2.3. Second phase interruption (phase "b")

The equivalent scheme is Figure A5.2.4 when "c" is the second pole to clear. This will happen approximately 90 degrees after phase "a" at $t = t(20) \approx 1/4$ T.

Initial conditions $u_a(20)$ and $i_a(20)$ follow from eq. (2.1) or (2.2).

Further

$$u_b(20) = -u_c(20) = E_m \cos(\phi - 30°) \simeq 1/2\sqrt{3}\,E_m \cos\phi$$
$$i_b(20) = I_{m2} \sin\phi$$
$$i_c(20) = -I_{m2} \sin\phi$$
$$I_{m2} = E_m \sqrt{3/(2\,\omega L)}$$
$$e_c(t) = E_m \cos(\omega t + \phi - 240°)$$

or with the new coordinate t', starting at t(20), so t' = t – t(20):

$$e_c(t) = - E_m \cos(\omega t + 30^o)$$

The transient oscillations after interruption of the second pole will only develop during the short interval Δt_{23} = t(30) – t(20) and will determine the inial conditions for the third phase clearance.

We will restrict to two cases:

– A5.2.3.1. Delta connected reactors or star connected reactors with long feeders ($C \gg C_N$)

– A5.2.3.2. Star connected reactors with short feeding lines ($C_N \approx 3C_g$) respectively.

A5.2.3.1. Long connections between c.b. and reactors, $C_N \to 0$

When $C_N \to 0$ is taken in Figure A5.2.4, the transient voltages after interruption are:

$$u_a(t') = e_c(t) + U_{m20} \cos(\omega_o t' + \psi_{20}) + U_{m22} \cos(\omega_2 t' + \psi_{22}) \quad \text{(A5.2.5)}$$

$$u_b(t') = e_c(t) - U_{m20} \cos(\omega_o t' + \psi_{20}) + U_{m22} \cos(\omega_2 t' + \psi_{22}) \quad \text{(A5.2.6)}$$

(damping is neglected because of the small period Δt_{23}).

$$U_{m20} = \frac{1}{2}\sqrt{\{D_1^2 + D_2^2\}} \qquad U_{m22} = \frac{1}{2}\sqrt{\{F_1^2 + F_2^2\}}$$

$$D_1 = u_a(20) - u_b(20) \qquad F_1 = u_a(20 + u_b(20) - 2\,u_c(20) = 3\,u_b(20) + u_a(20)$$

$$D_2 = \frac{i_a(20) - i_b(20)}{\omega_o C} \qquad F_2 = \frac{i_a(20) + i_b(20)}{\omega_o C}$$

$$\sin \psi_{20} = D_2/2\,U_{m20} \qquad \sin \psi_{22} = F_2/2\,U_{m22}$$

$$\omega_o^2 = 1/L_1 C \qquad \omega_2^2 = 1/3\,L_1 C \qquad \omega_2 \simeq 0.58\,\omega_o.$$

As an example the equations (A5.2.5) and (A5.2.6) are plotted in Figure A5.2.5 for the first 100 μsec., using the same reactor–bank and chopping current as in section A4.4.2.5. of Part I: Q = 30 Mvar, line voltage = 36 kV, frequency = 50 Hz, $\kappa = 14.10^4$. Furthermore C = 2500 pF is taken. A damping of 75 percent in 1/4 T is presumed and accordingly $i_a(20) = -1.7$ A, $u_a(20) = 0$ is chosen.

In this example u_b has increased to > 62 kV after 25 μsec. and u_a is still rising. If the current in the third pole interrupts at Δt_{23} = 30 μsec. the average charge voltage $u_s(0) \approx 0.67$ p.u.

Substantially higher values of u_b, $u_s(0)$ and also u_a would be attained if Δt_{23} is of the order of 100 μsec, but such long intervals between t(20) and t(30) are not very likely to occur.

A5.2.3.2. Short connections between c.b. and reactors, $C_N \approx 3C$

When $C_N \approx 3C$ is taken in Figure A5.2.4, the transient oscillations contain three different frequencies:

$$u_a(t) = e_c(t) + U_{m20} \cos(\omega_o t' + \psi_{20}) + U_{m21} \cos(\omega_{21} t' + \psi_{21}) + U_{m22} \cos(\omega_{22} t' + \psi_{22}) \quad \text{(A5.2.7)}$$

$$u_b(t) = e_c(t) - U_{m20} \cos(\omega_o t' + \psi_{20}) + U_{m21} \cos(\omega_{21} t' + \psi_{21}) + U_{m22} \cos(\omega_{22} t' + \psi_{22}) \quad \text{(A5.2.8)}$$

$$U_{m20} = \frac{1}{2}\sqrt{\{D_1^2 + D_2^2\}} \qquad U_{m21} = \frac{1}{4}\sqrt{\{H_1^2 + H_2^2\}} \qquad U_{m22} = \frac{1}{4}\sqrt{\{J_1^2 + J_2^2\}}$$

$$D_1 = u_a(20) - u_b(20) \qquad \sin \psi_{20} = \frac{D_2}{2\,U_{m20}}$$

$$D_2 = \frac{\{i_a(20) - i_b(20)\}}{\omega_o C}$$

$$H_1 = u_a(20) + u_b(20) - 2(1 + \sqrt{1{,}5})\,u_c(20)$$

$$H_2 = \frac{i_a(20) + i_b(20)}{\omega_{21} C} \qquad \sin \psi_{21} = \frac{H_2}{4\,U_{m21}}$$

$$J_1 = u_a(20) + u_b(20) - 2(1 - \sqrt{1,5})\, u_c(20)$$

$$J_2 = \frac{i_a(20) + i_b(20)}{\omega_{22} C} \qquad \sin \psi_{22} = \frac{J_2}{4\, U_{m22}}$$

$$\omega_0^2 = \frac{1}{L_1 C} \qquad \omega_{21}^2 = |1 - \sqrt{(2/3)}|\, \omega_0^2 \qquad \omega_{22}^2 = |1 + \sqrt{(2/3)}|\, \omega_0^2$$

$$\omega_{21} \simeq 0{,}43\, \omega_0 \qquad \omega_{22} \simeq 1{,}35\, \omega_0$$

$i_N(20)$ is taken zero because $e_a(t) = 0$ and $i_a(20) = 0$.

The component U_{m20} with frequency ω_0 is the same as for long connections.

Summation of the two components with frequencies ω_{21} and ω_{22} can at most give the same amplitude as U_{m22} in eqs. (A5.2.5) and (A5.2.6). Voltages calculations by eqs. (A5.2.5) and (A5.2.6) will be safe for both cases and thus for all cases between $C_N = 0$ and $C_N = 3C$.

Reignitions during the short period Δt_{23} are not very likely to occur.

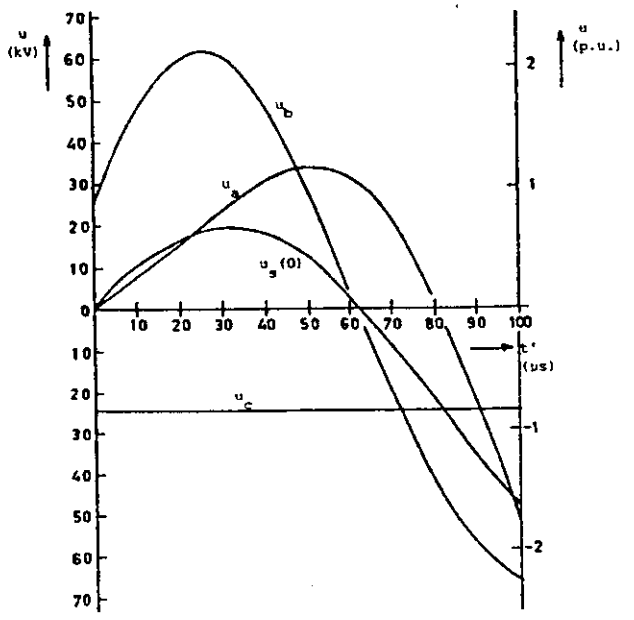

Figure A5.2.5 Example of developing voltages between second and third-phase interruption

A5.2.4 Third phase interruption (phase "c")

For short connections C_N may not be neglected now and Figure A5.2.6 gives the equivalent scheme. Current chopping occurs at t =t(30) and the new time coordinate is t" = t - t(30).
Initial conditions $u_a(30)$, $i_a(30)$, $u_b(30)$ and $i_b(30)$ can be calculated from (2.5) and (2.6) using $t' = t_2 - t_1$.

Further

$$i_c(30) \approx i_c(20) = -I_{m2} \sin\phi'$$
$$u_c(30) \approx u_c(20) \approx -\tfrac{1}{2} E_m \sqrt{3}$$

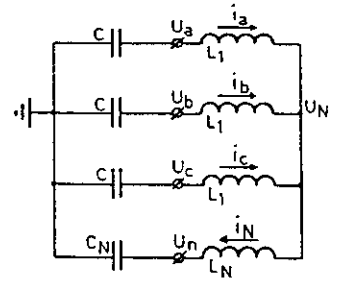

Figure A5.2.6 Third phase interruption. No interphase coupling.

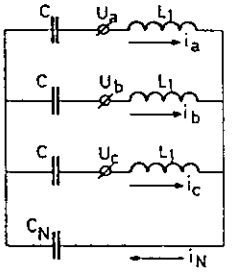

Figure A5.2.7 As Figure A5.2.6 but with inductive coupling.

If inductive coupling is present this will not introduce new aspects. Therefore this case will be involved here: Figure A5.2.7.

After complete interruption the actual energies will divide and oscillate in three modes:

a. The normal sequence mode oscillation in the three equal L_1 – C circuits causes a voltage across each capacitance with frequency

$$\omega = \frac{1}{\sqrt{L_1 C}}$$

This oscillation is stimulated by the difference between the initial phase voltages and currents in the relevant phase and the average of the initial conditions over the three phases.

b. The zero sequence mode–oscillation develops through the series circuit of $C_N - L_N - 1/3\ L_1 - 3C$ and thus has a frequency

$$\omega_3 = \sqrt{\frac{1}{L_N + \frac{1}{3}L_1}\left(\frac{3C_N C}{C_N + 3C}\right)} = \sqrt{\frac{C_0}{L_0 C_N C}}$$

This oscillation is generated by the averaged initial conditions in the L_1C–circuit and the initial conditions in the C_N–circuit.

Only the portion $C_N/(3C + C_N) = C_N/3C_0$ of the occurring voltage will appear across the phase capacitances C and thus between the phase terminal and ground, but the reactor coils will be loaded with the total voltage.

c. The present charges in the four "parallel" capacitors will be averaged, causing a dc–level–to–ground U_{dc}. Its magnitude follows from:

$$(3C + C_N)\ U_{dc} = C[u_a(30) + u_b(30) + u_c(30)] + C_N u_N(30)$$

The complete set of transient voltages between coil terminals and ground is:

$$u_j(t'') = U_{dc} + \varepsilon^{-t''/\tau_3}\ U_{m33} \cos(\omega_3 t'' + \psi_3) + \varepsilon^{-t''/\tau_1}\ U_{mj31} \cos(\omega_0 t'' + \psi_{j1}) \qquad \text{(A5.2.9)}$$

$$j = a, b, c.$$

with

$$U_{dc} = \frac{C}{C_0}\, u_s(0) + \frac{C_N}{3C_0}\, u_n(30) \qquad \text{(A5.2.10)}$$

$$u_{m33} = \gamma \sqrt{\{K_1^2 + K_2^2\}} \qquad \sin\psi_3 = \gamma K_2 / U_{m33}$$

$$K_1 = u_s(0) - u_n(30) \qquad K_2 = i_s(0)\ \omega_3 L_0$$

$$\gamma = C_N/3C_0$$

$$U_{mj31} = \sqrt{\{K_{ju}^2 + K_{ji}^2\}} \qquad \sin\psi_{j1} = K_{ji}/U_{mj31}$$

$$K_{ju} = u_j(30) - u_s(0) \qquad K_{ji} = \{i_j(30) - i_s(0)\}\ \omega_0 L_1$$

$$u_s(0) = \frac{1}{3}\{u_a(30) + u_b(30) + u_c(30)\}$$

$$i_s(0) = \frac{1}{3}\{i_a(30) + i_b(30) + i_c(30)\} = \frac{1}{3}\, i_N$$

$C_0 = \frac{1}{3} C_N + C =$ *zero sequence capacitance*

$L_0 = 3L_N + L_1 =$ *zero sequence inductance*

(Voltages across the windings of each separate coil have the same expressions but now $U_{dc} = 0$ and $\gamma = 1$)

Obviously the h.f. transients are now superimposed on the d.c.–potential to earth U_{dc} given by eq. (A5.2.10). This d.c.–level may disappear very slowly in a well–insulated ungrounded system.

The amplitude U_{m33} is small if $C > C_N$. For $C \gg C_N$ there only remains a single frequency transient of frequency ω_0 and then $U_{dc} = u_s(0)$.

It is shown in section A5.1.3 that $u_s(0) \approx 0$ after simultaneous current chopping. However, as demonstrated in section A5.2.3, $u_s(0)$ may reach a substantial value due to non-simultaneous chopping. Experimentally d.c.-levels of > 2 p.u. are measured in the motor test scheme as proposed by Working Group 13.02, see Chapter 3. This case is treated in more detail in [6].

As far as the authors know there are no experimental data available on d.c.-levels when switching shunt reactors.

A5.2.5. Worst-case calculation

It is clear that in this last phase interruption all electric and magnetic energies, stored at t(30), are involved. All these energies contribute to the amplitudes K, adding or subtracting, depending on the sign of initial current and voltages. Combinations leading to extremely high amplitudes are possible and may appear together with a relatively high d.c.-level.

In worst-case calculation the first and the last phase interruption must be compared, the latter being based on the maximum value of U_{dc}.

For "long connections" combining of (A5.2.5), (A5.2.6) and (A5.2.12) yields:

$$U_{dc} = u_s(10) = e_c(t) + 2U_{m22}\cos(\omega_2 t' + \phi_{22})$$

In the short interval Δ_{23}, $e_c(t) = -u_b(20) \approx \frac{1}{2}E_m\sqrt{3}$. Therefore the d.c.-level is max. for $\omega_2\Delta t_{23} = -\psi_{22}(+\pi)$, (where always $-\psi > 0$), or, for the first maximum:

$$(\Delta t_{23})_{max} = \frac{1}{\omega_2}\arctan\left|\frac{F_2}{F_1}\right| \qquad \text{(A5.2.11)}$$

It can further be shown that U_{m22} will become maximum when $i_a(t')$ is at its maximum and has the same sign as the current in the second-pole-to-interrupt (then $u_a(t') = 0$). If $i_a(20) = \sigma i_a(10) = \sigma I_0$ (so σ is the damping factor over $t' \approx 1/4T$ of the network frequency ω) the time-to-maximum U_{dc} can be calculated from

$$(\Delta t_{23})_{max} = \frac{1}{\omega_2}\arctan\left[\frac{2(1+\sigma)\kappa}{6\omega Q}\right] \qquad \text{(A5.2.12)}$$

So, if this interval $(\Delta t_{23})_{max} = t(30) - t(20)$ is accepted together with $i_a(20) = \sigma I_0$ the d.c.-level is

$$U_{dc} \approx -\tfrac{1}{2}E_m\sqrt{3} + \tfrac{1}{3}\sqrt{(F_1^2 + F_2^2)}$$

and all initial conditions at t(30) may be calculated, using eq. (A5.2.5) and (A5.2.6). Maximum possible overvoltages follow from (A5.2.9).

For very short connections the results may be somewhat too high.

A5.2.6. Reignition after third pole clearance

During a reignition in one phase, say phase "c", at t(40) the voltage across the relevant capacitor, u_c, swings in a second parallel oscillation. After half a period, at t(50), it may reach its maximum which is now opposite to the original value (Fig. A4.1.3 of part I, taking into account section A5.2.2).

Such a reignition in one phase is often not followed by a reignition in a second phase. Therefore the second parallel oscillation-current must be interrupted again. This may happen in its first or a following uneven current zero.

Then the transient voltages as given by (A5.2.9) start again, but now $u_b(50)$ and $u_c(50)$ will have the same polarity and possibly a high instantaneous value. Therefore the new d.c.-level may again be higher than before,

especially when also $u_a(50)$ has the same polarity as the two other phases.

Thus the result of a reignition may be a higher transient overvoltage superimposed on a higher d.c.–level. This effect is illustrated in Figure 4.3.12 of Chapter 4.

A5.3. REACTORS WITH CAPACITIVE INTERPHASE COUPLING

($C_N \neq \infty$; $C_1 = C_g + 3C_\ell$; $M = 0$; $L_1 = L$; $L_N = 0$)

A capacitive interphase coupling may be due to winding capacitances and/or to phase–to phase capacitances between the conductors of the connections.

A5.3.1. Interruption of the first phase

For first phase interruption eq. A5.2.1. is still valid provided $C = C_g + 2C_\ell$ is introduced.

A connection between c.b. and reactor may be regarded as being long when the reactor bank is delta–connected or when $C_g + 2C_\ell$ is at least of the order of C_N. In that case eq. A5.2.1 tends to eq. A5.2.2.

A5.3.2. Second phase interruption

For long connections the equations (A5.2.5) and (A5.2.6) are available, provided

$C = C_g + 3C_\ell$ is introduced in ω_0 and D_2

$C = C_g + C_\ell$ is introduced in ω_2 and F_2

For short connections the same procedure will give acceptable results which may be somewhat too high.

A5.3.3. Third phase interruption

All results and remarks in section (A5.2.4) are correct when

$C = C_g + 3C$ is introduced in ω_0;

$C = C_g$ is introduced in ω_3, C_0 and U_{dc}.

Examples are given in Figure 6.2.

A5.3.4. Reignitions

What is stated before on reignitions in section A5.2.2 and A5.2.6 will also hold for reactors with capacitive interphase coupling. In section A5.2.2 now C_g must again be replaced by $C_g + 2C_\psi$.

A reignition after interruption of the third pole will introduce a second parallel oscillation in which not only the reignited phase (say "c") is involved, but, through the interphase capacitances C_ψ, also the two other phases ("a" and "b"). Therefore a voltage peak with second parallel oscillation frequency will be superimposed on the instantaneous voltage in the non–reignited phases.

The instantaneous voltage in one of these phases may be high when this extra pulse is added and this can easily start a reignition in the c.b. pole or even a break–down in the circuit–to–interrupt. This effect is demonstrated in the oscillogram Figure 4.3.11 in Chapter 4. It is treated in more detail in [6].

A5.4. REACTORS WITH INDUCTIVE COUPLING SOLELY. LONG CONNECTIONS

[$C_N \neq \infty$; $C_\ell = 0$; $C_1 = C_g = C$; $L_1 = L + M$ (D–conn.: $L_1 = (L + M)/3$) ; $L_0 = L - 2M$; $L_N = (L_0 - L_1)/3$]

This case may correspond to a three–phase reactor circuit, with inductive coupling between phases, but with negligible interphase capacitance, compared to the capacitance between each phase and ground. The three–phase reactor circuit is represented by its measurable positive and zero–sequence inductances and capacitances, taking care of the interphase coupling, as shown in Figure A5.1.2.

Again the cases of "long" and "short" connection between c.b. and reactor-bank may be distinguished. "Long connections", (including all delta connected reactors) mean that the neutral-to-ground capacitance C_N is relatively small. The expressions for overvoltages in the three phases are extremely extensive and non-transparent. But the higher frequency component in which C_N is involved is small. Application of eqs. (A5.2.2), (A5.2.5) and (A5.2.6) gives safe results (somewhat higher than the realistic values to be expected) for the first and second phase-to-interrupt.

With the same restriction the last phase-interruption may be handled with eqs. (A5.2.9) and (A5.2.10) without the component of frequency ω_3, so taking $U_{m33} = 0$ (for $\gamma \rightarrow 0$).

The case of "short connections" will be treated here. Again each reactor leg is represented by a line pi-section with the capacitances to ground of each leg ($2C_g$) equally divided between the two legs. Thus the ungrounded neutral is in fact connected to the ground circuit through a capacitance $C_N = 3C_g$. In this case, $C_0 = 2C_g = 2C$ and $C_N = (3/2)C_0 = 3C$.

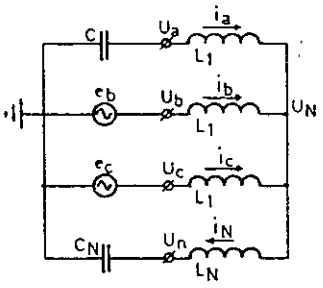

Figure A5.4.1 First phase interruption, inductive coupling

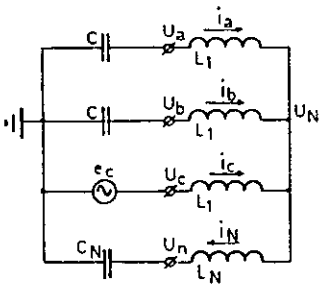

Figure A5.4.2 Second phase interruption, inductive coupling

A5.4.1. Short connections, first phase interruption (phase "a")

The physical behaviour is again as described in Section A5.2.1. But now the results are more complicated because the inductive coupling, represented by the (negative) inductance L_N, is also involved in the transient oscillations. Figure A5.4.1 gives the reduced scheme.

Phase voltages and initial conditions are given in section A5.1.3. The expression for the transient recovery voltage between phase "a" and earth is:

$$u_0(t) = -\frac{1}{2}\, e_a(t) + e^{-t/\tau_{11}}\, U_{m11} \cos(\omega_{11} t + \psi_{11}) + e^{-t/\tau_{12}}\, U_{m12} \cos(\omega_{12} t + \psi_{12}) \qquad \text{(A5.4.1)}$$

with

$$U_{m11} = \alpha \sqrt{\{A_1^2 + A_2^2\}} \qquad U_{m12} = \beta \sqrt{\{B_1^2 + B_2^2\}}$$

$$A_1 = u_a(10) \qquad B_1 = u_a(10)$$

$$A_2 = i_a(10)\, \omega_{11} L_1 \qquad B_2 = i_a(10)\, \omega_{12} L_1$$

$$\sin \psi_{11} = \alpha A_2 / U_{m11} \qquad \sin \psi_{12} = \beta B_2 / U_{m12}$$

$$\alpha = \frac{1}{2}\left(1 + \frac{1 - L^*}{(2 + L^*)\, D^*}\right)\left(\frac{\omega_o}{\omega_{11}}\right)^2 \qquad \beta = \frac{1}{2}\left(1 - \frac{1 - L^*}{(2 + L^*)\, D^*}\right)\left(\frac{\omega_o}{\omega_{12}}\right)^2$$

$$\beta = 1{,}5 - \alpha$$

$$L^* = \frac{L_o}{L_1} \qquad D^* = \sqrt{\left\{1 - \frac{6\, L^*}{(2 + L^*)^2}\right\}}$$

$$L_o = L_1 + 3\, L_N = \text{zero sequence inductance}$$

$$\omega_o^2 = \frac{1}{L_1 C} \qquad \omega_{11}^2 = \frac{L^* + 2}{3\, L^*}(1 - D^*)\, \omega_o^2 \qquad \omega_{12}^2 = \frac{L^* + 2}{3\, L^*}(1 + D^*)\, \omega_o^2$$

Again the transient recovery voltage is a double frequency oscillation with frequencies ω_{11} and ω_{12}, superimposed on a cosine term of amplitude (-) 1/2 E_m and system frequency ω.

Normally L^* is of the order of 1/3, which makes $D^* \approx 0.8$, $\omega_{11} \approx 0.7\omega_0$; $\omega_{12} \approx 2\omega_0$; $\alpha \approx 1.42$; $\beta \approx 0.08$.

Even in case of short connections the amplitude of the contribution with the highest frequency (U_{m12}) is small and neglecting this component by taking $\alpha = 1.5$, $\beta = 0$ will not give serious mistakes in amplitude. The transient oscillation after first phase interruption is not far from single frequency phenomenon under conditions given here, see for example Figure A5.6.3.

A5.4.2. Second phase interruption (phase "b")

Figure A5.4.2 represents the equivalent scheme. Initial conditions agree with those of section A5.2.3. Analytical expressions for the voltages $u_a(t')$ and $u_b(t')$ during the small period Δt_{23} contain $e_c(t)$ and triple-frequency transients. The expressions of the amplitudes and frequencies of oscillations are very complicated functions of all the initial conditions and L's and C's indicating strong interactions between phases of the three-phase circuit.

Calculations using equations (A5.2.5) and (A5.2.6) as described in section A5.2.5 may satisfy practical demands for possible initial conditions at t(30).

A5.4.3. Third phase interruption (phase "c")

This case is already treated in section A5.2.4 (Fig. A5.2.7). Expressions for the transient voltages are eqs. (A5.2.9) and (A5.2.10). In this instance, where $C_N = 3C_g$, the amplitude factor $\gamma = 1/2$ and $U_{dc} = 1/2\ \{u_s(0) + u_n(0)\}$.

So the d.c. level U_{dc} is only half as high as in case of $C_N \ll C$. All further remarks made in sections A5.2.4 and A5.2.5 will hold here.

A5.5. REACTORS WITH BOTH INDUCTIVE AND CAPACITIVE COUPLING

$[C_N \neq \infty\ ;\ C_1 = C_g + 3C_\ell\ ;\ M \approx 0\ ;\ L_1 = L + M\ ;$ (D-conn.: $L_1 = (L + M)/3)\ ;\ L_N = (L_0 - L_1)/3]$

Now all elements of Figure 1.2 are involved in the transients.

A5.5.1. First phase interruption

Despite the more complicated circuit the transient voltage after first phase interruption still has the same form as before: eq. (A5.2.1) or (A5.4.1). The two occurring frequencies are:

$$\omega_{11}^2 = \frac{(2L^* + 1)C^* + 3}{6L^*C^*}(1 - D^*)\,\omega_o^2 \qquad \textit{and} \qquad \text{(A5.5.1)}$$

$$\omega_{12}^2 = \frac{(2L^* + 1)C^* + 3}{6L^*C^*}(1 + D^*)\,\omega_o^2\ ; \qquad \text{(A5.5.2)}$$

where

$$D^* = \sqrt{\left[1 - \frac{24L^*C^*}{\{(2L^* + 1)C^* + 3\}^2}\right]} \qquad \text{(A5.5.3)}$$

$$\omega_o^2 = \frac{1}{L_1 C} \qquad L^* = \frac{L_o}{L_1} \qquad C^* = \frac{C_N}{3C} \qquad C = C_g + 2C_\ell$$

The amplitude factors α and β contain complicated relations of the present L's and C's and are in particular dependent on the two frequencies ω_{11} and ω_{12}; see for example eqs. (A5.2.1) and (A5.4.1) for special solutions. In most cases of inductive as well as capacitive coupling β is so small that no influence of the higher frequency component is perceptible.

A5.5.2. Second phase interruption

The remarks made in section A5.4.2 will also apply here.

A5.5.3. Third phase interruption

Principally the same two frequencies and DC-level as described in section A5.2.4 will hold now (see eq. (A5.2.9) and eq. (A5.2.10)). The inductive coupling keeps the same influence as given there. The capacitive coupling C_ℓ is only involved in the "normal sequence mode" oscillation. This means that $C = C_g + 3C_\ell$ must be introduced

in ω_0, where $C = C_g$ holds for C_0, ω_3 and U_{dc}.

Determination of $(\Delta t_{23})_{max}$ and $(U_{dc})_{max}$ may again be carried out as described in section (A5.2.5).

A5.6. EXAMPLES OF RECOVERY VOLTAGES IN UNGROUNDED REACTORS

In Part I (Appendix 4) all oscillograms were computed and plotted directly from the analytic expressions and given ratings. In this chapter all oscillograms were calculated with the EMTP-program only based on the given circuitry and ratings. Results of the two methods were compared for several circuits and showed to give the same results.

The EMTP-program offers an easy and swift method to tackle the problem even without any knowledge of mathematical results. Much care must be taken, however, to choose sufficiently small integration steps.

(A chopping level I_0 will be reached a time $\Delta t = I_0/(\omega\hat{\imath})$ before current zero. So an accuracy of 5% percent in I_0 requires an integration step $t_i \leq 0.05\ I_0/(\omega\hat{\imath})$. For an amplitude $\hat{\imath} = 1000$ A, main frequency 50 Hz and chopping current $I_0 = 10$ A, this step width is $t_i \leq 1.6$ µs).

This fact, together with the rigid structure of the EMTP-program makes long calculation times inevitable, especially when a worst-case situation must be determined.

To find comparable graphs to results in Part I the same data of the reactors and the c.b. were chosen. Time constant of damping is determined by a resistor R in parallel to the reactor coils. All data of circuit elements, calculated amplitude factors and frequencies are collected in Table A5.1.

Figure A5.6.1 represents the case of ungrounded reactors without any coupling and with short connection. Figure A5.6.1, No 1 gives the recovery voltages occurring at the terminals of the three inductances when short connections with the c.b. exist. Terminal-to-ground capacitance $C_g = 3$ nF and neutral-to-ground capacitance $C_N = 9$ nF (so $C^* = 1$) are chosen. Then from eq. A4.4.9 (Part I): $I_0 = \kappa\sqrt{C_{par}}$ and $C_{par} = C_g$ a chopping current $I_0 = 7{,}67$ A is found. This current is also accepted for the next two phases.

Table A5.1

Type de couplage et figure *Type of coupling and Figure*	Données du circuit *Circuit data*					Cour. haché *Chopp. curr.*	Coupure première phase *First phase clearance*				Coupure dernière phase *Last phase clearance*		
	C_g nF	C_ℓ nF	L mH	M mH	R MΩ	I_o A	α	β	f_{11} Hz	f_{12} Hz	f_o Hz	γ	f_3 Hz
Pas de couplage *Non-coupled* $C^* = 1$; $L^* = 1$ Fig. 6.1	3	0	138	0	0,53	7,67	1,18	0,32	5080	9820	7820	0,5	11660
Couplage capacitif par câble triphasé *Capacitively coupled through 3-phase cable* $C^* = 0{,}1875$; $L^* = 1$ Fig. 6.2	10	3	138	0	0,16	17,7	1,486 ≈ 1,5	0,014	2680	8090	3110	0,23	9400
Couplage inductif par 3 noyaux *Inductively coupled through 3-legged core* $C^* = 1$; $L^* = 0{,}3$ Fig. 6.3	3	0	105,8	32,2	0,53	7,67	1,432	0,068	5420	16820	7820	0,5	11660
Couplage capacitif et inductif *Capacitively and inductively coupled* $C^* = 0{,}1875$; $L^* = 0{,}3$ Fig. 6.4	10	3	105,8	32,2	0,16	17,7	≈ 1,5	≈0	2675	14730	3110	0,23	9400

To change the initial conditions at the moment of second pole interruption the number of complete oscillation of ω_{11} between t(10) and t(20) was changed from n = 28.3 to n = 27.3 in 6 equal steps of 60 degrees by variation of C_g and C_N, keeping $C^* = 1$ and $\kappa = 14.10^4$. Thus all frequencies and the chopping level were changed somewhat per step. Results are given in the plots Figure A5.6.1, numbers 2 to 7.

The procedure followed here defines only the initial conditions at t(20) roughly. The sequence of the interrupting phases (b–c or c–b) is not known beforehand since the moments of interruption t(20) and t(30) will follow automatically when the required chopping levels in the relevant phases are obtained. The occurring DC–levels are therefore determined by the casual voltage and current conditions at t(30) and thus a worst–case will not necessarily be present.

The above procedure was also followed in the next three examples. In Figure A5.6.2 a capacitive coupling is added to the reactors through a three–phase cable with a line–to–ground capacitance of 7 nF and line–to–line capacitance of 3 nF. In Figure A5.6.3 the reactors are considered as being inductively coupled through M = 32.2 mH (giving $L_0/L_1 = 0.3$; in Figure A5.6.4 capacitive as well as inductive coupling is accepted, maintaining the same C^* and L^* – values as in Figure A5.6.2 and A5.6.3. Capacitive coupling increases the capacitance–to–ground at the c.b.–terminal to $C_{par} = C_g + 2C_\ell$ and this will increase the current chopping level to $I_0 = (-)17.7$ A.

The examples given here show clearly the complexity of the TRV–patterns when relatively short connections between c.b. and reactors exist: Figures A5.6.1 and A5.6.3. These patterns turn into simple mono–frequency oscillations in case of "long" connections: Figures A5.6.2 and A5.6.4.

All oscillograms show the influence of the first–phase–to–clear basic voltage – $e_a(t)$ and a DC–level which varies in dependency of casual initial conditions.

The highest overvoltages in these typical examples are collected in Table A5.2.

Table A5.2

Fig.	Max. (kV)	Nr./Phase	Min. (kV)	Nr./Phase
6.1	82,7	3 B	- 85,2	7 C
6.2	88,3	3 B	- 87,6	1 A
6.3	81,0	3 B	- 81,9	4 A
6.4	86,3	3 B	- 88,9	5 A

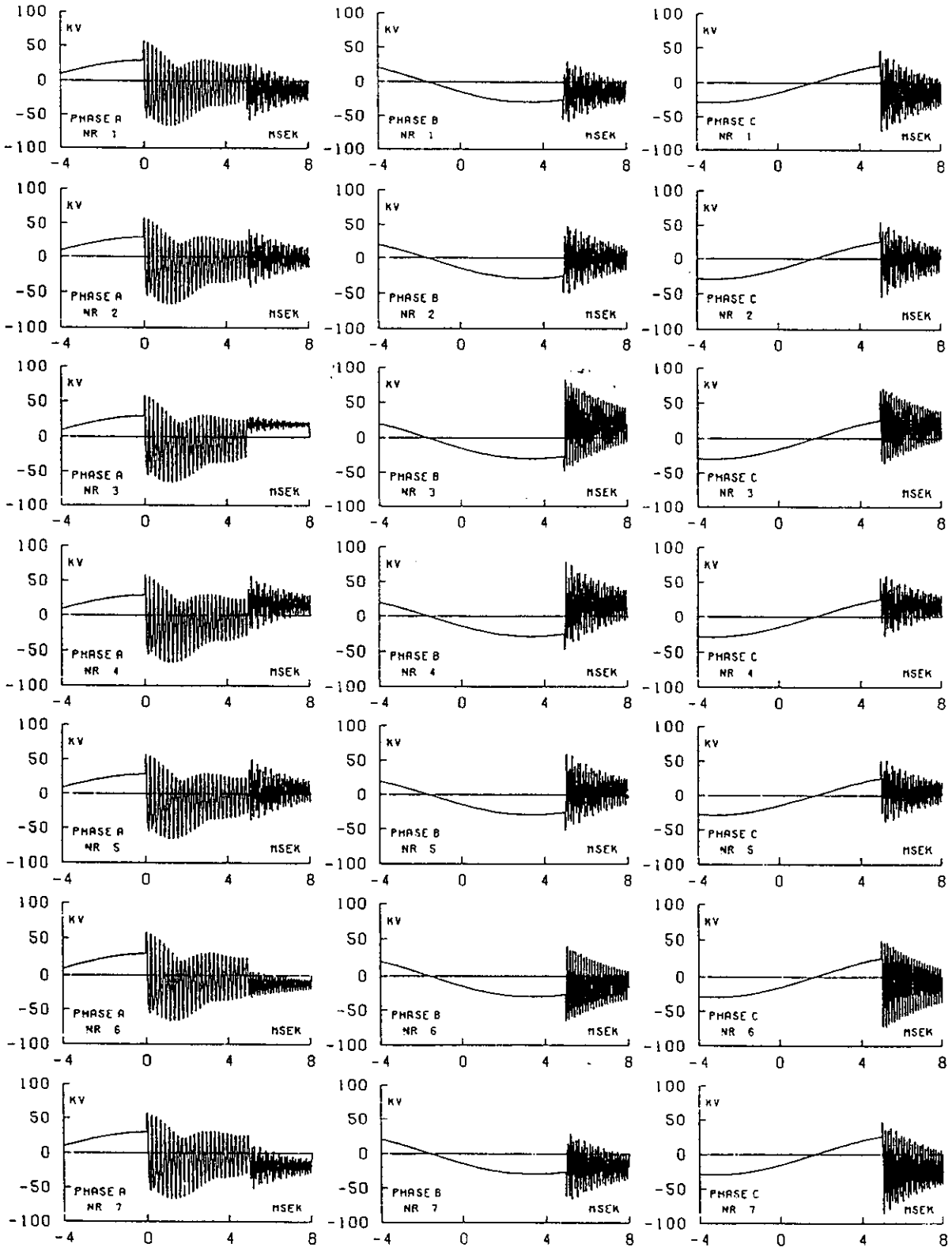

Figure A5.6.1 Non-coupled reactors. See Table A5.6.1 for circuit data.

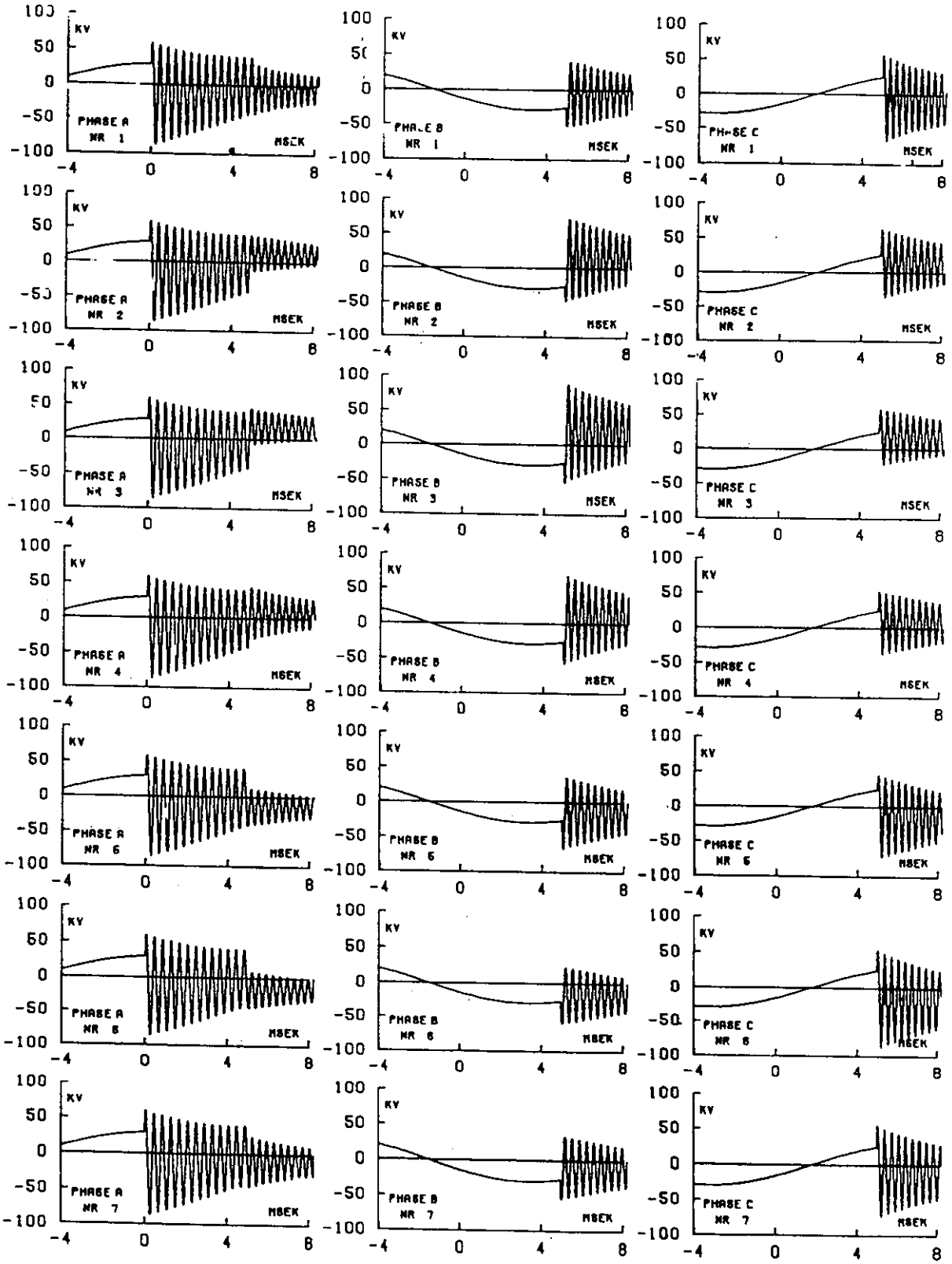

Figure A5.6.2 Capacitively coupled reactors. See Table A5.6.1 for circuit data.

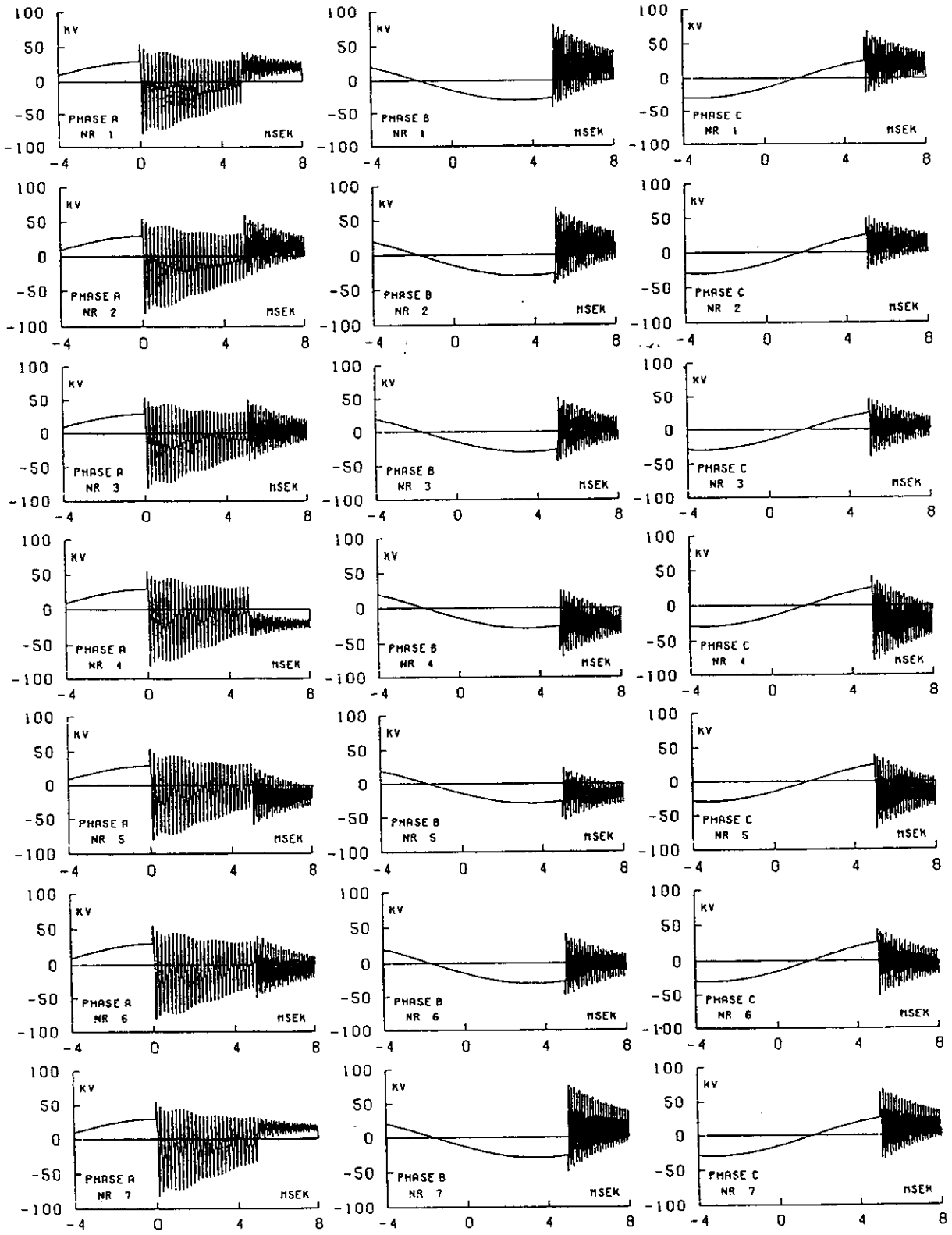

Figure A5.6.3 Inductively coupled reactors. See Table A5.6.1 for circuit data.

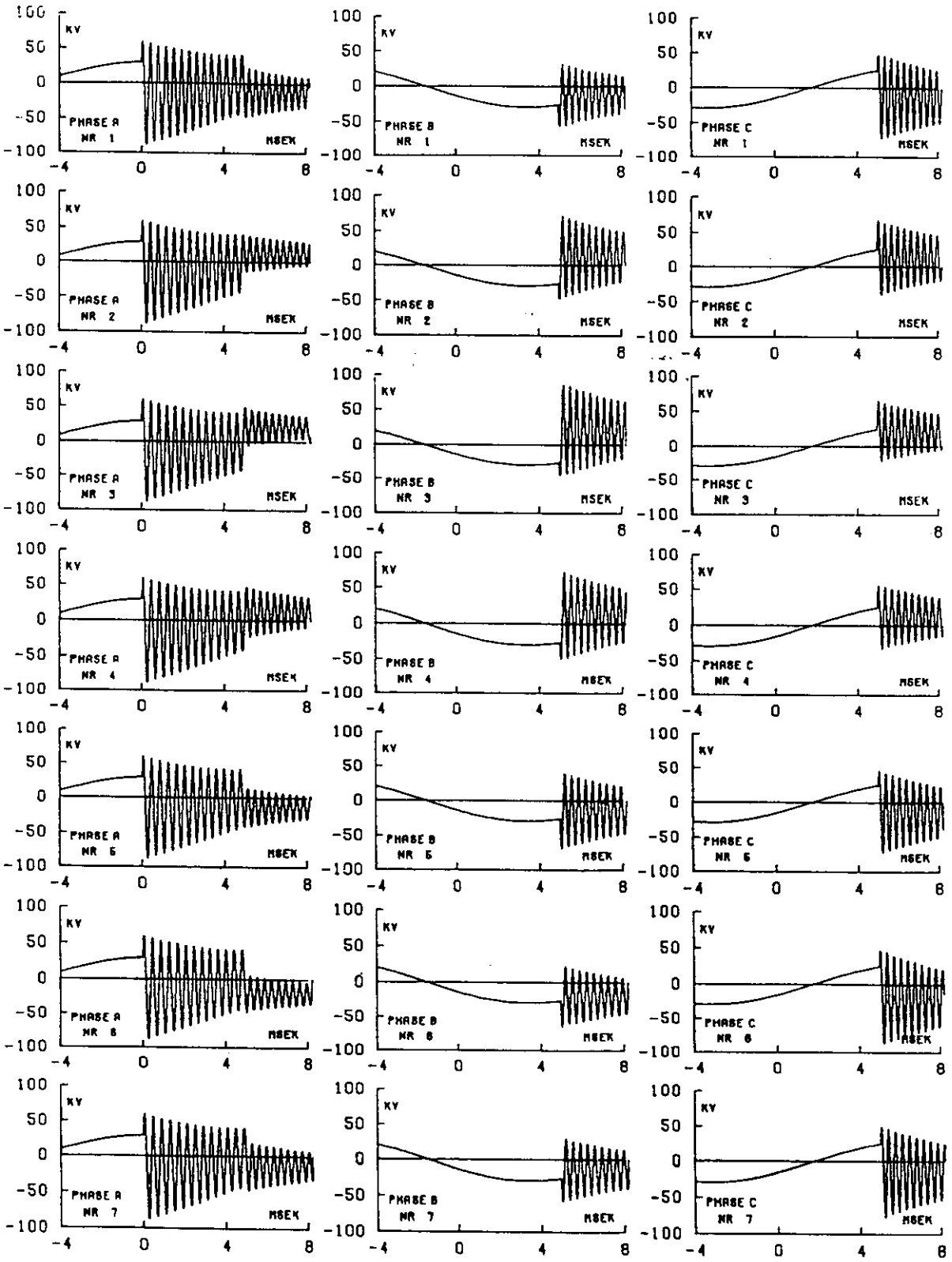

Figure A5.6.4 Capacitively and inductively coupled reactors. See Table A5.6.1 for circuit data.

A5.7. CONCLUSIONS

The phenomena of interaction between phases during the switching of three–phase reactors are more complicated in the case of ungrounded reactors, as compared with the grounded ones. The lack of neutral grounding in star–connected reactors provides a degree of interaction between phases even without any interphase coupling, to make the interaction stronger and more complicated when inductive interphase coupling is also considered. This is obvious from the complexity of the coefficients of the voltage terms and the composition of the oscillation frequencies as well, which both imply a multitude of circuit paths of the involved transients during the evolution of the phenomena.

Capacitive interphase coupling through C_ℓ will also complicate the analytical results of voltage calculations. But in effect this kind of coupling reduces the amplitudes of the contributions of higher frequencies. As a result the transient oscillation seems to be reduced to a single frequency phenomena which strongly facilitates its calculation.

The same observation will follow from application of large capacitances to ground C_g in relation to the neutral–to–ground capacitance C_N. In general ungrounded reactors will produce single frequency transients when $C_g + 2C_\ell \geq C_N$. In that case inductive coupling has no significant influence on the occurring transients.

The case of delta–connected reactors presents no particular problem and can easily be reduced to the simpler case of ungrounded reactor, non–coupled or with capacitive interphase coupling only.

In ungrounded reactors current chopping will generally generate higher overvoltages than in the grounded case. One reason is the first–pole–to–clear basic voltage of – 0.5 p.u. on which the transients are super–imposed. The other reason is the DC–voltage–to–ground at the reactor–terminals after third–pole–clearance. Worst–case calculation should involve and compare both effects.

It has to be repeated here that overvoltages due to current chopping can only develop in relatively small reactors together with circuit–breakers with high chopping–numbers. Voltage escalation effects due to reignitions are often more dominant and may occur even without any noticeable chopping level.

When interrupting large currents, di/dt before current zero may be so high, that an instability–oscillation cannot develop completely in the available time–before–zero. In that case no overvoltage due to current chopping can occur.

From the other side the transients treated in this paper are not only restricted to reactor banks but are also relevant for interruption of locked h.v.–motors and inductively loaded transformers. The complicated patterns of oscillations occurring in such cases might be better understood by the given analytic expressions and the examples of Clause 6.

A5.8. ACKNOWLEDGEMENT

The authors wish to thank Dr. V.K.I. Kalasek for preparing the computer plots of chapter 6 with help of the THE–Burroughs version M35 of the EMTP–program.

A5.REFERENCES IN APPENDIX 5.

[5] E. Colombo et G. Santagostino. – Results of the enquiries on actual network conditions when switching magnetizing and small inductive currents and on transformer and shunt reactor saturation characteristics. No 94 (1984) p. 35–53.

[6] W.M.C van den Heuvel. – Overvoltages after current chopping in a three–phase inductive circuit with isolated neutral, IEEE Trans. PAS–100, 1981, p. 4795–4801.

Le CIGRÉ a apporté le plus grand soin à la réalisation de cette brochure thématique numérique afin de vous fournir une information complète et fiable.

Cependant, le CIGRÉ ne pourra en aucun cas être tenu responsable des préjudices ou dommages de quelque nature que ce soit pouvant résulter d'une mauvaise utilisation des informations contenues dans cette brochure.

Publié par le CIGRÉ
21, rue d'Artois
FR-75 008 PARIS
Tél. : +33 1 53 89 12 90
Fax : +33 1 53 89 12 99

The greatest care has been taken by CIGRE to produce this digital technical brochure so as to provide you with full and reliable information.

However, CIGRE could in any case be held responsible for any damage resulting from any misuse of the information contained therein.

Published by CIGRE
21, rue d'Artois
FR-75 008 PARIS
Tel : +33 1 53 89 12 90
Fax : +33 1 53 89 12 99